Pollinator behaviour and the evolutionary genetics of petal surface texture in the Solanaceae

Katrina Alcorn

Department of Plant Sciences

University of Cambridge

A thesis submitted for the degree of

Doctor of Philosophy

April 2013

Declaration

This dissertation is the result of my own work and includes nothing which is the outcome of work done in collaboration except where specifically indicated in the text.

The work presented in Chapter 7 has been published in the journal *Functional Ecology* as 'Flower movement increases pollinator preference for flowers with better grip' (Alcorn, Whitney & Glover 2012).

The experiments in Chapter 8 were performed in collaboration with a rotation student, Felicity Bedford (University of Cambridge, feb39@cam.ac.uk).

Katrina Alcorn, 12th April 2013

Acknowledgements

This work would not have been possible without the support I have received from those around me. I especially thank my supervisor Beverley Glover for her intellectual and personal guidance. I also thank her for her patience, understanding and gentle coaxing. I thank her for believing we could get here in the end.

I thank Murphy Thomas, Mathew Box, and Ruben Alvarez-Fernandez for guiding me through the steep learning curve of molecular biology. I thank Heather Whitney for teaching me everything I know about bees, and for her support and encouragement. I thank Alison Reed for her extraordinary ability to understand, commiserate with and help me through stress, anxiety and general crazies. I thank Lin Taylor, Cecilia Martinez-Perez and Emily Bailes for their support and hugs and patience. I thank Edwige Moyroud and Samuel Brockington for their help and guidance. I thank Matthew Dorling for all his help, support and commiseration, as well as for dealing with my seemingly endless supply of horribly spiky *Solanum* plants taking over his greenhouses.

I thank my family, my grandma and grandpa, Pauline and Arthur Spurgeon, for their constant support, faith and encouragement. My dad, Douglas Alcorn, for all his support and love, and his excitement in all my research. Angela and Derek Gray for being my surrogate grandparents in this country and providing love, support and encouragement. My mum, Judith Alcorn, for never ceasing to make me feel like I am amazing and awesome, and for always believing I was capable of anything.

Julia Davies and David Hanke provided pastoral support through a period of personal crisis and for this I thank them.

Finally, thankyou to my partner Thomas for his determination to learn to deal with everything I can throw at him, for his amazing support, and his seemingly inexhaustible love.

Abstract

Conical cells in the petal epidermis are a common trait across the angiosperms, and influence pollinator behaviour and pollination success. This work explores two key aspects of conical cell evolution: firstly, why conical cells are so prevalent across many diverse species, and secondly, why some species have lost conical petal cells.

Using *Petunia* flowers to test bee preferences under conditions of motion, we investigate whether the tactile advantage of conical petal cells on complicated flowers can also benefit simple flowers with low inherent tactile difficulty. We find that flower movement increases bee preference for conical-celled flowers. Since motion increases flower attractiveness, a tactile benefit under motion may explain why conical cells have persisted throughout evolution across many diverse flower morphologies.

The major focus of this work is an exploration of conical cell loss using the buzz-pollinated genus *Solanum*. Phylogenetic, molecular developmental and bee behavioural approaches were used to develop an integrated understanding of the frequency, mechanisms and possible causes of conical cell losses. We provide evidence of multiple independent losses of conical petal cells in *Solanum*. We find that two of these losses have occurred through similar molecular means, that of a change in the expression patterns of regulatory Subgroup 9A (Mixta-Like) R2R3 MYB genes. Bumblebee behavioural experiments show that bees do not display a preference in favour of either conical- or flat-celled flowers while buzz pollinating. These results show that conical cells are a trait under more than a single simple selective pressure, as bumblebee preferences in *Petunia*, and previously shown in *Antirrhinum*, differ from those identified by this study in the buzz-pollinated genus *Solanum*.

These results help expand our understanding of the complex pressures that can act on a single multifunctional trait, as well as providing evidence for the repeatability of evolution on a molecular level.

Table of Contents

Chapter 2. Methods 17

List of Abbreviations

cDNA	complementary deoxyribonucleic acid
cPCR	colony PCR
dH20	deionised water
dNTP	deoxyribonucleic triphosphate
IPTG	isopropyl thiogalactoside
GTR	general time-reversible
LB	Luria–Betrani (medium)
LiCl	lithium chloride
MYB	a family of transcription factors named for myeloblastosis
NaAc	sodium acetate
ndhF	NADH dehydrogenase complex, subunit F
mya	million years ago
R2R3	repeats 2 and 3 of the MYB DNA–binding domain
PIPES	piperazine-N,N′-bis(2-ethanesulfonic acid)
PCR	polymerase chain reaction
RACE	rapid amplification of cDNA ends
RT–PCR	reverse transcriptase PCR
SDS	sodium dodecyl sulfate
TAE	Tris acetate EDTA
TBE	Tris borate EDTA
TrnT-F	*trnT* to *trnF* non-coding chloroplast DNA region
X–gal	5-bromo-4-chloro-3-indolyl-β-D-galactopyranoside
U	enzyme activity units
waxy	granule-bound starch synthase (also called GBSSI)

List of Figures

List of Tables

Chapter 1. Introduction

1.1 Overview

1.1.1 Angiosperm diversity and plant reproduction

The inherently sessile nature of plant life creates a challenge to the exchange of gametes between spatially separated individuals within a species, a challenge that the angiosperm lineage of plants has resolved with the evolution of the flower. Using attractants and rewards surrounding the reproductive organs, flowers serve as a mechanism to recruit animals as vectors for the transfer of pollen. Of all land plants, the angiosperms are the single most species-rich lineage (Crepet & Niklas 2009; Fiz-Palacios *et al.* 2011). The flower strongly influences this diversity, as equally diverse pollinators can drive the evolution of novel floral features through pollinator-mediated selection, leading to reproductive isolation and speciation (Van der Niet & Johnson 2012). Innovations in flower shape, colour, size, reward and scent may all be acted on under pollinator-mediated selection, as may the texture of the petals. This project is focused on the evolution of a petal surface textural feature, the presence of conical or papillate cells in the petal epidermis.

1.1.2 Conical petal epidermal cells

Conical (or papillate) cells in the petal epidermis are a common trait, present in the majority of extant petaloid flowering plants (Kay, Daoud & Stirton 1981; Christensen & Hansen 1998). The molecular genetic control of conical cell development has been studied most thoroughly in *Antirrhinum majus*. Under the control of an R2R3 MYB

transcription factor called *MIXTA*, conical cells form during flower development as outgrowths of epidermal cells after these cells cease dividing (Noda *et al.* 1994; Martin *et al.* 2002; Perez-Rodriguez *et al.* 2005; Baumann *et al.* 2007). Conical cells increase a plant's reproductive success compared to flat-celled mutants (Glover & Martin 1998) by influencing pollinator preference through a tactile benefit of increased grip (Whitney *et al.* 2009a, 2011a). They may also influence flower colour, temperature and wettability (Noda *et al.* 1994; Rands & Whitney 2008; Whitney *et al.* 2011b; a). Conical petal cells are present in many species from the earliest diverging lineages of the extant angiosperms, such as *Amborella trichopoda* (Amborellales) and *Cabomba caroliniana* (Nymphales) (Alison Reed, unpublished), and they occur across widely divergent species in almost all families across the angiosperm phylogeny (Kay, Daoud & Stirton 1981; Christensen & Hansen 1998). This suggests that conical cells may have arisen not long after the evolution of the first flowers, around 130 million years ago (Sun 1998; Sun *et al.* 2002; Sun *et al,* 2011; Soltis & Soltis 2004), and have remained an important part of plant-pollinator interactions to the present day.

Conical cells are a multifunctional trait that influence flower colour, temperature, shape, wettability and grip. Of these, grip appears to have the strongest influence on pollinator preference, particularly when flower handling is exceptionally difficult such as for a complicated flower like *Antirrhinum majus* (Glover & Martin 1998; Whitney *et al.* 2009a, 2011a). Most flowers, however, do not present such difficult challenges to foraging pollinators. There is also no link between angle of flower presentation and presence of conical cells in species surveyed across the angiosperms (Rands, Glover & Whitney 2011), and as yet no generalisable explanation has been demonstrated for the prevalence of conical cells amongst the wide range of species with flowers that are simple for a pollinator to handle. In addition, little is known about why and how conical petal cells are sometimes lost. Such losses are surprising given the many advantages that conical cells can confer on a plant.

This PhD aims to address these gaps firstly by testing potential evolutionary pressures on conical petal cells by investigating the effects of grip on pollinator preference in the simple flower of *Petunia*; and secondly by identifying the causes of evolutionary loss of conical petal cells through a study of pollinator preferences and molecular changes responsible for losses of this trait in the genus *Solanum*.

1.2 PLANT DEVELOPMENT

This project focuses on the formation of conical cells, which occurs during plant development under the control of the transcription factor encoded by the *MIXTA* gene. Plant development and growth occur through cell proliferation at meristems, which maintain an active population of pluripotent dividing cells that differentiate at the meristem boundary to initiate new organs (Maughan, Murray & Bögre 2006; Rast & Simon 2008). Plant vegetative development is in general an indeterminate and plastic process (Rast & Simon 2008; Nieuwland, Scofield & Murray 2009). Flower development, by contrast, ends in a termination of division and produces a flower of determinate size, shape and organ number (Bortiri & Hake 2007; Sablowski 2007; Kwiatkowska 2008; Ming & Ma 2009). During both forms of growth, organ size, position and developmental timing are controlled by a number of environmental and temporal cues, mediated by hormonal control and initiated by genetic control factors (Maughan, Murray & Bögre 2006; Galinha, Bilsborough & Tsiantis 2009; Chandler 2010; Ito 2011). A large proportion of this genetic control is enacted by a class of proteins called transcription factors, which act to modify gene expression.

1.2.1 TRANSCRIPTION FACTORS CONTROL DEVELOPMENT

Transcription factors are proteins present in all forms of life that are responsible for control of gene expression at the level of transcription (Pabo & Sauer 1992). By binding to regulatory elements of DNA, the transcription factor can either block or initiate gene transcription. The thousands of different transcription factors so far discovered are classified into families according to sequence and structural homology of their DNA binding domain (Riechmann 2000), which in turn specifies their binding targets.

Developmental transcription factors bind to the regulatory regions of genes and direct their expression in specific tissues with precise developmental timing (Latchman 1997). They interact with general transcription factors (such as TFII-A, TFII_B, TFII-D and others) which form the transcription activation complex (Orphanides, Lagrange & Reinberg 1996; Dillon 2006; Kaplan 2013). RNA polymerase II can then bind to this complex and begin to transcribe an mRNA copy from the DNA template.

Genes encoding transcription factors make up a large proportion of eukaryotic genomes and are particularly important in plants, representing over 5% of the genome of *Arabidopsis thaliana* (Riechmann 2000). In animals, transcription factors regulate important developmental processes such as homeotic and cell cycle transitions (Orphanides, Lagrange & Reinberg 1996; Dillon 2006; Pavlopoulos *et al.* 2009; Kaplan 2013), for example, the HOX genes are a well-studied and important family of transcription factors that confer segmental identity during embryo development in metazoans (Pearson, Lemons & McGinnis 2005). In plants, transcription factors have been much duplicated and have diversified into new plant-specific roles such as control of organ position, patterning and developmental timing, regulation of the synthesis of pigment and other secondary metabolites, and response to environmental changes (Singh, Foley & Oñate-Sánchez 2002; Hake *et al.* 2004; Dubos *et al.* 2010; Hay & Tsiantis 2010; Shang *et al.* 2010; Bowman, Smyth & Meyerowitz 2012).

1.2.2 Transcription factors in plant development

Plant development proceeds under hormonal control and via regulation by transcription factors (Maughan, Murray & Bögre 2006; Rast & Simon 2008; Galinha, Bilsborough & Tsiantis 2009), which together ensure that organs are produced with appropriate spatial patterning and developmental timing. Plant growth originates from the population of pluripotent cells maintained at the meristem. Indeterminate vegetative growth originates at the two major meristems of the plant, the root apical meristem and shoot apical meristem. The shoot apical meristem is maintained in an undifferentiated state by the action of KNOX-class genes which are expressed throughout the meristem (Braybrook & Kuhlemeier 2010; Hay & Tsiantis 2010). The central population of true stem cells is maintained by the action of *WUSCHEL*, and immediately surrounding these cells is a region of expression of the components of the *CLAVATA* receptor-ligand complex, which represses *WUSCHEL* and allows differentiation (Maughan, Murray & Bögre 2006; Sablowski 2007; Braybrook & Kuhlemeier 2010). This ensures precise control over the number and placement of undifferentiated stem cells is maintained, while allowing the development of organs immediately adjacent to the stem cell population.

Localised accumulation of the phytohormone auxin induces the development of organ primordia, mediated by auxin transport proteins called PINs (Rast & Simon 2008; Galinha, Bilsborough & Tsiantis 2009; Hay & Tsiantis 2010). As organ primordia develop, KNOX expression is repressed by auxin in the cells that will form the developing organ (Braybrook & Kuhlemeier 2010). At this stage, organ-specific genes take over, converting each organ primordium into a site of determinate growth that will terminate at the completion of the organ. Determination of organ polarity in leaves is mediated in *Arabidopsis* by YABBY on the abaxial side of the leaf, and KANADI on the adaxial side (Kumaran, Bowman & Sundaresan 2002; Braybrook & Kuhlemeier 2010; Ha, Jun & Fletcher 2010). Tissue patterning is then determined by cell fate identity genes such as MYB transcription factors, complexes of MYB, bHLH and WD-40 proteins, and other transcription factors (Jin & Martin 1999; Ramsay & Glover 2005).

When appropriate developmental and/or environmental conditions are met, flowering will initiate by the conversion of the shoot meristem into an inflorescence meristem, also a site of indeterminate growth. The inflorescence meristem produces floral meristems, specified by the transcription factor *LEAFY*, which induces floral identity and determinate growth terminating in the completion of a flower. The floral meristem initiates floral organs in sequential whorls, ending in the reproductive whorls which terminate the meristem. The floral meristem differentiates cells into these whorls of different floral organs under the control of MADS box transcription factors. All flowers follow the same general developmental pattern. MADS box transcription factors act in a spatial arrangement described by the 'ABCE' model of flower development (Coen & Meyerowitz 1991; Bowman, Smyth & Meyerowitz 2012). In this model, A class genes alone result in sepal formation (although note that this element of the model may be specific to the Brassicaceae), A and B class together form petals, B and C class together form anthers, and C class alone form carpels. E class genes are required throughout the meristem to initiate the flower developmental program. The petal identity genes direct the expression of genes required for petal development, including, in *Antirrhinum majus*, regulating the activity of transcription factors directing cell fate such as *MIXTA* (C.Martin, unpublished).

1.2.3 Selection on transcription factors drives evolution

Since a single transcription factor can bind to multiple target genes, developmental processes involving the orchestrated action of a number of different genes can therefore be controlled by a transcription factor that can cease or initiate transcription of collections of genes at the appropriate developmental stage. Transcription factors then become common targets on which evolution can act, when an entire genetic pathway can be altered in place or timing of expression by changes in a single master regulator gene. Many well-known innovations in evolution, such as repeating body segments in arthropods, have arisen through duplication, alteration and sub-functionalisation of transcription factors (Jacob, Series & Jun 1977; Akam 1995). For example, a major event in the domestication of maize occurred through a change in the gene encoding a single transcription factor, TEOSINTE BRANCHED1 (TB1). Changes in this gene, and consequently in the downstream targets of the TB1 transcription factor, are responsible for the conversion of the highly branched wild form of teosinte into the single-stalked apical dominance seen in the crop plant maize (Doebley 2004; Studer *et al.* 2011).

1.2.4 R2R3 MYB transcription factors

The transcription factor of interest to this project is an R2R3 MYB transcription factor called *MIXTA*. MYB transcription factors are an important family of genes that are found in all eukaryotes, characterised by the presence of one or more repeats of the MYB DNA binding domain (Jin & Martin 1999). First identified as the oncogene *C-MYB* in Avian Myeloblastosis Virus (Oh & Reddy 1999), each repeat produces a helix–turn–helix motif which binds to DNA in a sequence–specific manner (Jiang, Gu & Peterson 2004). MYB transcription factors are classified by the number of these repeats and R1, R1R2R3, and R2R3 MYB genes are found in plants (Jin & Martin 1999). In animals MYB genes generally control cell cycle transitions, while in plants their roles have greatly diversified to control a number of plant-specific processes (Stracke, Werber & Weisshaar 2001). The R2R3 MYB genes have lost the R1 MYB repeat and form the largest family of plant MYB genes (Stracke, Werber & Weisshaar 2001; Dubos *et al.* 2010). They control various processes including secondary metabolite biosynthesis and cell fate determination. *Arabidopsis thaliana* has over a hundred R2R3 MYB genes which can be

separated into subgroups based on conserved motifs (Stracke, Werber & Weisshaar 2001; Dubos *et al.* 2010).

1.2.5 R2R3 MYB Subgroup 9 genes

MIXTA-like genes belong to the Subgroup 9 family of R2R3 MYB transcription factors, and contain the R2 and R3 repeats of the MYB DNA binding domain, followed by a sequence of amino acids designated the Subgroup 9 domain (Stracke, Werber & Weisshaar 2001). Recent phylogenetic analysis has shown that an ancient duplication of the R2R3 MYB Subgroup 9 genes produced two major lineages, Subgroup 9A and Subgroup 9B, both found in all seed plants (Brockington *et al.* 2013). The *MIXTA* and *MIXTA-Like* genes of *Antirrhinum* all belong to the R2R3 MYB Subgroup 9A lineage, as do other genes known to produce conical petal cells such as *PhMyb1* from *Petunia hybrida*.

1.2.6 *MIXTA* genes and their actions

MIXTA-like genes have now been identified in many diverse species of plants and in many cases, a small family of *MIXTA*-like genes control slightly different aspects of this same cell fate. In *Antirrhinum majus*, four different R2R3 MYB Subgroup 9A genes have been identified: *AmMybMIXTA*, *AmMybMl1*, *AmMybMl2* and *AmMybMl3* (Noda *et al.* 1994; Perez-Rodriguez *et al.* 2005; Jaffé, Tattersall & Glover 2007; Baumann *et al.* 2007). *MIXTA* is expressed in the petal epidermis, and causes outgrowth of the epidermal cells by regulating the expression of genes involved in directional cell outgrowth, such as cytoskeletal signalling elements as well as cell wall modifying proteins such as expansins (C. Martin, unpublished) which result in the epidermal cells forming into conical cells. The MIXTA protein can also induce the formation of trichomes, and a simple change in the timing of its expression in a transgenic plant is enough to switch developmental pathways: if *MIXTA* is expressed after cells have completed their divisions, conical cells will develop; if it is expressed while cells still show competence to divide, trichomes grow instead (Glover, Perez-Rodriguez & Martin 1998).

AmMybMl1 is expressed early in development of the ventral petal of *Antirrhinum*, and produces trichomes, conical cells and reinforced tissue around the hinge (Perez-

Rodriguez *et al.* 2005). *AmMybMl2* by contrast is expressed in petals late in flower development, as well as in expanding and mature leaves and in roots (Baumann *et al.* 2007), and *AmMybMl3* is expressed in outgrowing cells in all aerial tissues (Jaffé, Tattersall & Glover 2007). Both *AmMybMl2* and *AmMybMl3* are predicted to have a role in cellular expansion because their expression correlates with tissues containing outgrowing cells such as trichomes or conical cells, and because both genes are capable of producing ectopic conical cells when overexpressed in tobacco (Jaffé, Tattersall & Glover 2007; Baumann *et al.* 2007).

Other positive regulators of cellular outgrowth include *GdMyb25*: fibre development in cotton (*Gossypium hirsutum*) requires early expression of this gene (Machado *et al.* 2009). Tomato fruit epidermal cells show conical outgrowths, and the *MIXTA*-Like gene *TC189627* is expressed in this same tissue, suggesting that it may have a role in producing these outgrowths (Mintz-Oron *et al.* 2008). In *Lotus*, *LjMyb1* is expressed in the dorsal and lateral petals and *LjMyb2* is expressed in dorsal petals, and the timing of their expression correlates with the differentiation timing and position of conical petal cells (Weng *et al.* 2011). In *Thalictrum*, *TtMYBML2* controls development of conical cells in petaloid organs as well as possibly controlling the formation of papillate outgrowths of the stigma (Di Stilio *et al.* 2009).

Negative regulatory roles of R2R3 MYB Subgroup 9A genes have also been identified. For example, the observed epigenetic regulation of *MgMybMl8* in *Mimulus* changes leaf trichome density in response to predation. Lower expression of *MgMybMl8* is associated with a higher trichome density, suggesting a negative regulatory role of this gene (Scoville *et al.* 2011). One ambiguous case involves *NOECK* in *Arabidopsis*, which negatively regulates trichome branching, and can both positively and negatively regulate trichome expansion (Jakoby *et al.* 2008; Gilding & Marks 2010).

1.3 Pollinator behaviour

Plants elicit pollinator foraging behaviour using methods of either attraction and reward, or attraction and deception. Most flowers offer a food reward to their

pollinators, either in a protein-rich pollen or a sugary nectar solution. Many diverse animals may perform a role as pollinators, including vertebrates and invertebrates such as bees, birds, bats and beetles. This project focused on bee-pollinated species through a study of the role of conical petal cells in the pollination of flowers that offer a primarily nectar reward (*Petunia hybrida*) and flowers that offer only a pollen reward (*Solanum* species).

1.3.1 Bee vision and flower attraction

Pollinators often have innate behavioural responses to flower-like stimuli, for example bees will attempt to forage from any disc of colour that has a strong green contrast, an innate behaviour that allows flower-naive bees to find flowers (Dyer, Spaethe & Prack 2008). Once a bee has learned to associate a reward with a type of flower, they will then continue to visit flowers of that species through a behavioural trait called flower constancy, where bees preferentially visit flowers of one species or morph in runs of multiple visits, bypassing other rewarding flowers in favour of the known flower type (Free 1970; Hill, Wells & Wells 1997; Chittka, Thomson & Waser 1999).

1.3.2 Bee vision

Bees have trichromatic vision, their three colour receptors covering the green, blue and UV parts of the electromagnetic spectrum (Skorupski & Chittka 2010). These can be converted into a representation of bee perceptual colour space in order to understand the way different colours will appear to a bee, and allow us to predict how well a bee will be able to distinguish between these different colours (Chittka 1992). The resolution of bee vision requires that an angle of 15° must be subtended by a flower onto a bee's eye before a bee can identify the flower using colour vision (Chittka & Raine 2006). Recognition of targets 'smaller' than this is accomplished purely by green contrast, a monochromatic form of vision that distinguishes the relative difference between the excitation of the bee's green receptor by the background compared to the target (Chittka & Raine 2006), and bees use this mode of vision to identify flower-like objects in their environment at greater distances than those required for colour vision, allowing greater foraging efficiency. Bee vision can recognise visual effects of nano-

scale structural patterning, such as iridescence, and additionally can use this to increase the speed with which they identify a flower (Whitney *et al.* 2009b).

1.3.3 Conical cells and pollinator attraction

Conical petal cells benefit plant fecundity through their interactions with pollinators. Field trials of *Antirrhinum majus* showed that when pollinator number limits seed set, plants with conical petal cells set more seed than flat-celled *mixta* mutant plants (Glover & Martin 1998). There are many possible reasons for this, as conical petal cells are a multifunctional trait producing diverse effects on a flower. These include enhancing colour (Noda *et al.* 1994; Gorton & Vogelmann 1996), slightly increasing floral temperature (Comba *et al.* 2000; Whitney *et al.* 2011a), reducing petal wettability (Whitney *et al.* 2011b) and altering overall petal shape by changing the direction of cell expansion in the epidermis (Baumann *et al.* 2007).

The most conspicuous effect of the loss of conical cells is in the colour of the flower, as *mixta* mutant flowers have (to the human eye) a much duller colour than wild type flowers (Noda *et al.* 1994). This is because light incident on a conical-celled petal epidermis is focused into the central pigment-containing vacuole and more light is absorbed by the pigment, whereas on a flat-celled epidermis light passes through the epidermal cells and into the unpigmented mesophyll underneath (Gorton & Vogelmann 1996). More white light is also scattered back towards the observer from flat cells, which dilutes the colour signal (Noda *et al.* 1994; Gorton & Vogelmann 1996). The increased absorption of light by the conical cells also causes the increased warmth of the flower (Whitney *et al.* 2011a). Wettability is affected by the surface structure itself preventing water from spreading across the surface, and a conical-celled surface causes water to bead up and roll off the petal rather than spreading and wetting the petal (Whitney *et al.* 2011b).

Bees are able to use many of these traits as learned indicators of rewards, and some (such as temperature) are traits that a bee will seek out as a reward in itself (Dyer *et al.* 2006; Rands & Whitney 2008). While scent is an important cue in pollination by bumblebees, the loss of conical cells as a result of mutation of *MIXTA*-like genes does

not alter the type, proportion or total amount of volatiles produced, although it may affect the direction and behaviour of emitted volatiles (Whitney *et al.* 2009a).

1.3.4 Conical cells in *Antirrhinum majus*

With so many diverse effects on a flower that *may* influence bee behaviour, it is important to experimentally identify which of these traits actually *do* cause the observed preference towards conical cells. Each of the traits were isolated and tested under controlled experimental conditions. Dyer *et al* (2007) found that although bumblebees can easily distinguish the different colours of the conical- and flat-celled *Antirrhinum* flowers, they have no innate preference towards either colour. Additionally, there is no difference in salience as measured by the distance at which a bee can distinguish the flower from a neutral background (Dyer *et al.* 2007). Instead for *Antirrhinum*, tactile benefit is the reason for the attractiveness of conical-celled flowers to their pollinators. These difficult flowers can be made easier to handle by having a rough surface for the bee to grip (Whitney *et al.* 2009a).

1.3.5 Conical cells improve grip for bees handling difficult flowers

Antirrhinum flowers elicit a specific and complex set of behaviours from their pollinators, and are particularly difficult for a pollinator to handle. A pollinator must navigate a small landing platform and operate a hinge mechanism before it can reach the nectar inside each flower, requiring both dexterity and strength, as has been demonstrated in flowers of several legume species with a similar opening mechanism to *Antirrhinum* (Córdoba & Cocucci 2011). The textured surface of a conical-celled flower is easy for bees to grip and allows bees to come to rest while they drink, whereas flat-celled flowers are slippery and bees must expend energy to maintain their grip on the flower, as demonstrated using artificial flowers made from biomimetic petal surface replicas (Whitney, Federle, & Glover 2009b; Whitney *et al.* 2009a). The metabolic costs of flight are large (Kammer & Heinrich 1974), so a decreased handling difficulty that allows a bee to bring its wings to rest while feeding can increase the energy efficiency of foraging. Being able to rest while drinking may therefore provide a metabolic advantage and cause bees to favour the conical-celled flowers, and the clearly

distinguishable difference in colour enables bees to use colour as a learned cue to discriminate between flowers before landing.

1.3.6 Flower texture in pollination

Mechanosensory input of flower texture is important for the foraging of many pollinators. Hawk moths (*Manduca sexta*) are hovering pollinators and so cannot benefit from any increased grip, but can decrease their foraging time by learning tactile cues, sensed through the proboscis, specific to the flowers they forage from (Goyret & Raguso 2006). Foraging time is also decreased in hawk moths by innate responses to flower texture, such as grooves that surround the nectar. Tactile cues are often specific to one kind of pollinator, for example it has been suggested that losses of epidermal conical cells may be associated with a shift from bee pollination to bird pollination, as has been demonstrated in *Lotus* (Ojeda *et al.* 2012). Honeybees (*Apis mellifera*) are able to discriminate between different surface textures, including conical petal cells, from antennae mechanosensory input alone. They can also be trained to elicit the proboscis extension reaction in response to a specific texture and it has been proposed that this might be used by bees as a form of nectar guide (Kevan & Lane 1985; Erber *et al.* 1998). Changes in grip through textural changes can also be important for very different types of flowers: the beetle imprison-and-release pollination method of the parasitic *Hydnora africana* includes a dehiscent stage which creates a rough texture on the interior of the perianth, allowing insects to escape with their pollen load (Bolin, Maass & Musselman 2009).

1.3.7 Generalising to all flowers

Despite the obvious tactile advantage to pollinator handling of conical cells on the petals of complicated flowers, there is no single flower form that correlates with the presence of conical cells in the petal epidermis, nor is there evidence across the angiosperms of a correlation between presence of conical cells and flower presentation angle (Rands, Glover & Whitney 2011). In trying to determine why conical petal cells are so prevalent, it may not be possible to usefully generalise from studies using *Antirrhinum*. The very specific method of flower handling in *Antirrhinum* may create equally specific pollinator preferences, so the selective pressures affecting *Antirrhinum*

are very likely to differ from those of plants with simpler flowers. However, flowers that initially appear relatively easy for a pollinator to handle may still benefit from producing petal surfaces that enhance pollinator grip under certain conditions, such as when flowers are moving. This project aims to test this hypothesis using simple flowers under different conditions of motion.

1.3.8 *Petunia*

Petunia hybrida is an ideal species in which to test pollinator preference for a simple flower. Its funnel-shaped petals form a flat and easy surface on which the pollinator can land, it is naturally conical-celled, and a mutant line of plants with flat cells arising from a well characterised genetic mutation is available (Van Houwelingen *et al.* 1998; Baumann *et al.* 2007). These, alongside flowers from a line arising from reversion to the wild type, allow us to test bee preferences using isogenic lines differing only in the single trait of conical cells.

1.4 Evolutionary loss of conical cells in *Solanum*.

Five of the data chapters presented in this thesis concern the evolutionary loss of conical cells in the genus *Solanum*. Greater detail is given in each specific chapter, but this section of the Introduction provides the necessary background to set this work in context.

1.4.1 *Solanum*

While around 20% of angiosperms do not have conical petal epidermal cells, in the genus *Solanum* flat-celled species are found in much higher proportions (Glover, Nicholls and Martin, in preparation). *Solanum* is a giant genus with between 1500 and 2000 member species of diverse growth habit and life history, and its members are found worldwide. All species share a typical flower form, with five petals in an essentially actinomorphic corolla and five tubular anthers in an 'anther cone', each

anther releasing pollen from a pore at the top of the anther. This flower form requires a specialised form of pollination that can only be performed by certain bee species (Buchmann & Hurley 1978; Buchmann 1983; Harder & Barclay 1994; King & Buchmann 1996; Endress 1997; De Luca *et al.* 2012), including bumblebees (*Bombus* species), and some solitary bee species such as blue-banded bees (*Amegilla cingulata*). Honeybees (*Apis* species) do not buzz pollinate. To effect buzz pollination the bee will use its legs to hold the anther cone and then vibrate its flight muscles to resonate the anther tissue and cause the pollen to be forcefully ejected from the tube and onto the bee's body. The flowers do not contain any nectar so the protein-rich pollen, which bees require for larval nutrition, is the only reward offered. Buzz pollination also occurs in species only distantly related to *Solanum* as the product of convergent evolution, including species of *Dodecatheon*, *Vaccinium*, *Senna* and *Dianella* (Buchmann & Hurley 1978).

1.4.2 *Solanum* phylogeny

Despite recent large-scale efforts to integrate and expand the phylogenetic treatment of *Solanum* (Knapp *et al.* 2005), the scale of the genus makes it unsurprising that at the outset of this project, of the species for which petal cell shape was known only a few could be found in the latest molecular phylogenies. Additionally, of the species included in the molecular phylogenies only a few had recorded petal epidermal morphologies (Levin, Watson & Bohs 2005; Levin, Myers & Bohs 2006; Weese & Bohs 2007). Tomato was known to have conical petal cells, and *S. dulcamara* to have flat cells lost through a change in gene expression (Glover, Nicholls and Martin, in prep., Glover, Bunnewell & Martin 2004). Data from a preliminary morphological survey suggested that there may be more losses of conical cells in *Solanum*, and this project aimed to expand our understanding of the number of losses of conical cells in *Solanum* by gathering morphological data for species already present in the published molecular phylogeny, as well as by adding species for which morphological data could be determined into the existing phylogenetic framework.

1.4.3 Loss of conical cells

For *S. dulcamara* (Dulcamaroid clade of *Solanum*) the loss of petal conical cells has been shown to have occurred through a change in expression patterns of its *MIXTA*-like

genes, with highest expression now seen early in the development of leaves where they function to direct the formation of trichomes (Glover, Nicholls and Martin, in prep.). It is unknown, however, how conical cells have been lost in other flat-celled lineages, and whether a similar molecular mechanism is responsible in any of these cases. To explore the repeatability of evolution and determine whether other instances of conical cell loss have occurred through similar means, we identified two pairs of closely-related species with which to study conical petal cell loss: *S. capsicoides* and *S. sisymbriifolium* from the Leptostemonum clade, and *S. aviculare* and *S. laciniatum* from the Archaesolanum clade.

For each species, R2R3 MYB Subgroup 9A gene sequences as well as their expression and function were compared to determine the molecular mechanism by which conical cells have been lost in each case.

1.4.4 Adaptive explanation for conical cell loss

This project also investigated the adaptive significance of loss of conical cells in *Solanum.* If bees are seeking not nectar but pollen in *Solanum* flowers it is likely that the main attractant is not the petals but the anther cone, and it may no longer make a difference to pollination success whether a flower has conical petal cells or not. Conical cells could then be lost through random stochastic change, or genetic drift (Fay 2011), as drift has been identified as potentially important even in traits as strongly affected by selection as those of flowers (Schueller 2006; Tremblay & Ackerman 2007). On the other hand, it may be that the attracting anther cone is easier for a bee to see with a flat-celled background, and in this case conical cells could be actively selected against. Decreased grip on petals might even be of benefit to buzz pollinated flowers, since the vibrations causing the resonance that releases pollen are transferred through the bee's legs into the anthers and any contact between the bee's legs and the petals may lessen the effectiveness of pollen release. To distinguish between these possibilities and attempt to further understand the reasons behind conical cell loss in this genus, bumblebee preferences were tested using flat- and conical-celled artificial flowers in combination with real anthers to provide a pollen reward and realistic buzz pollination conditions.

1.5 PROJECT AIMS

To study the benefit of conical petal cells in a simple flower, we undertook a study of pollinator grip under motion using the simple, funnel-shaped flowers of *Petunia*. Using a platform shaker to mimic natural wind conditions, we presented pollinators with *Petunia* flowers of different tactile and visual properties to explore the interaction of visibility and grip in forming pollinator preferences. Then, using a molecular and morphological investigation of different species in the buzz-pollinated genus *Solanum*, we explored how conical cells have been lost multiple times across this genus. To place the petal cell changes in *Solanum* into a robust phylogenetic context, we performed a phylogenetic analysis and morphological survey followed by ancestral character reconstruction. By studying R2R3 MYB Subgroup 9A MYB transcription factors in sister species in two separate clades of *Solanum*, we investigated the genetic changes responsible for the loss of conical cells, and tested pollinator preferences to investigate whether pollinator-mediated selective pressure might have been acting during the loss of conical petal cells.

Taken together, this thesis provides an understanding of the function of micromorphological features of petals contributing to pollination success within an ecological and evolutionary framework, while maintaining a focus on the genetic changes through which evolution acts.

Chapter 2. Methods

2.1 Laboratory reagents and supplies

Standard laboratory reagents and chemicals were supplied by Fisher Scientific (Loughborough, UK), VWR (Leicestershire, UK), BDH Laboratory Supplies (Poole, UK) and Sigma–Aldrich (Dorset, UK). Cloning kits and vectors were obtained from Invitrogen Life Technologies (Paisley, UK) and Promega Corp. (Madison, WI, USA). DNA and PCR purification kits were obtained from Qiagen (Crawley, UK). Restriction endonuclease enzymes were purchased from New England Biolabs (NEB; Hertfordshire, UK). First strand cDNA synthesis kits were supplied by Amersham Biosciences (Buckinghamshire, UK). Taq DNA polymerase and dNTP mix were supplied by Bioline (London, UK), KAPA 2G polymerase was supplied by KAPA Biosystems (Boston, US). Phusion High-Fidelity DNA Polymerase was supplied by ThermoScientific (via NEB, Hertfordshire, UK). Oligonucleotide primers were obtained from Invitrogen Life Technologies (Paisley, UK) and VHBio Limited (Gateshead, UK). Bacterial culture reagents and antibiotics were obtained from Becton, Dickinson, and Co. (Sparks, MD, USA), Oxoid, Ltd. (Basingstoke, UK), and Melford Laboratories (Ipswich, UK). SEM images were taken using the FEI Philips XL30 FEGSEM. Photographic images were taken using an Olympus µ720SW camera, Nikon D80 camera, Google Nexus One smartphone, or HTC One X smartphone. Colonies of bumblebees (*Bombus terrestris*) were supplied by Syngenta Bioline Ltd. (Weert, The Netherlands). All other suppliers of kits and reagents are detailed in the text. Recipes for media and solutions are listed in Appendix 1.

2.2 PLANT SOURCES

Solanum flower tissue for DNA phylogenetic analyses was collected from the living collection at Radboud University, Nijmegen, by Professor Cathie Martin (John Innes Centre, Norwich, UK). Wild type and *phmyb1 Petunia* seed were also kindly supplied by Cathie Martin.

Seed for *Solanum* species and phylogeny outgroups were obtained from the following suppliers:

Flowers of *S. lumholtzianum, S. houstoni, S. lanceifolium* and *S. rostratum* as well as seed of *S. furfuraceum, S. prinophyllum, S. aethiopicum, S. candidum, S. argentinum, S. pseudocapsicum, S. abutiloides, S. adscendens, S. physalifolium* and *S. aviculare* were kindly supplied by Dr. Mario Vallejo-Marin (School of Biological and Environmental Sciences, University of Stirling, UK).

S. glaucophyllum and *S. seaforthianum* seed was kindly supplied by the Botanic Garden and Botanical Museum Berlin-Dahlem (Freie Universität, Berlin).

S. nitidum was supplied by Chileflora (Hijuela #2, Lihueno, Pelarco, Talca, Chile).

S. lidii, *S. vespertilio* ssp. *doramae*, *S. vespertilio* ssp. *vespertilio*, were kindly supplied by www.rareplants.de (Am Parkfeld 14 E, D-65203 Wiesbaden, Germany).

S. aethiopicum, S. wallaceii, S. appendiculatum, S. riojense, S. fiebrigii, S. physalifolium and *S. caesium* kindly supplied by Dr. Sandy Knapp (Natural History Museum, London, UK).

Flowers of *S. hindsianum* were kindly supplied by the Rancho Santa Ana Botanic Garden (1500 N College Ave, Claremont, California CA 91711, USA).

Seed for *Jaltomata procumbens* was kindly provided by Ulrike Bertram of Ökologisch-Botanischer Garten, Bayreuth, Germany from stock derived from

seed supplied by Botanical Gardens of the Rheinische Friedrich-Wilhelms-Universität Bonn, Germany.

Species detailed in Table 2.1 were kindly supplied by Gerard van der Weerden (Solanaceae Collection, Botanical and Experimental Garden and Genebank, Radboud University Nijmegen, The Netherlands):

Accession	Species name	Accession	Species name	Accession	Species name
804750136	*S. aethiopicum*	904750200	*S. fiebrigii*	814750041	*S. pubigerum*
904750241	*S. allophyllum*	904750201	*S. fraxinifolium*	804750195	*S. pyracanthos*
884750016	*S. betaceum*	924750136	*S. glaucophyllum*	944750197	*S. rugosum*
974750082	*S. capsicoides*	904750122	*S. havanense*	914750023	*S. seaforthianum*
894750095	*S. carolinense*	904750159	*S. jamaicense*	814750073	*S. torvum*
894750197	*S. citrullifolium*	834750003	*S. laciniatum*	924750074	*S. triflorum*
??????????	*S. coriaceum*	804750172	*S. mauritianum*	884750218	*S. tripartitum*
894750342	*S. crispum*	904750205	*S. montanum*		
??????????	*S. elaeagnifolium*	904750206	*S. palitans*		

Table 2.1 Accession numbers and species names of Solanum species obtained from Nijmegen Experimental and Botanic Gardens

2.3 General methods

2.3.1 Preparation of plant tissue prior to DNA/RNA extraction

Plant tissue was collected and immediately immersed in liquid nitrogen, then ground to powder in a liquid nitrogen–cooled sterile mortar and pestle and transferred using a cooled spatula to a cooled 1.5 ml tube. The tissue was either used immediately or kept at -80°C until use.

2.3.2 Nucleic acid extraction

2.3.2.1 Phenol:chloroform DNA extraction using SDS buffer

500 µl DNA extraction buffer (see Appendix 1 for recipe) was added to powdered plant tissue and mixed by vortex then incubated at 65°C for 2 minutes. 500 µl phenol:chloroform:isoamyl alcohol (28:24:1) was added and mixed by vortex then separated by centrifugation for 5 minutes at 13 000 rpm in a benchtop microcentrifuge. The supernatant was transferred to a new tube, 500µl chloroform added, the solution mixed by vortex and separated by centrifugation at 13 000 rpm for 5 minutes. The supernatant was transferred to a clean tube, and 50 µl 3M NaAc and 350 µl 100% isopropanol was added. The DNA was precipitated for a minimum of 30 minutes at 4°C then separated by centrifugation at 13 000 rpm for 5 minutes. The supernatant was discarded and the DNA pellet washed with 500 µl 70% ethanol then separated by centrifugation at 13 000 rpm for 5 minutes. The ethanol was removed and the pellet allowed to air–dry, then resuspended in 20 µl TE (see Appendix 1 for recipe) or dH2O.

2.3.2.2 Phenol:chloroform RNA extraction using SDS buffer

500 µl RNA extraction buffer (see Appendix 1 for recipe) and 150µl Tris saturated phenol were added to powdered plant tissue and mixed by vortex. 250µl chloroform was added and the solution mixed by vortex then separated by centrifugation at 14 000 rpm for 5 minutes. 450 µl 4M LiCl at 4°C was added and the RNA left to precipitate overnight at 4°C. The solution was separated by centrifugation at 14 000 rpm, then the supernatant discarded. The RNA pellet was resuspended in DNAse buffer (see Appendix 1 for recipe) then 1 µl of DNAse (RNAse free) was added and the solution incubated at 37°C for 20 minutes. 500 µl of phenol:chloroform:isoamyl alcohol (28:24:1) was added and the solution mixed by vortex then separated by centrifugation at 14 000 rpm for 5 minutes. The upper phase was removed to a clean tube and 750µl 95% ethanol with 5% 3 M NaAc (pH 5.5) added, then left at –20°C to for 1 hour to precipitate. The RNA was separated by centrifugation at 14 000 rpm for 5 minutes, the supernatant removed and the RNA pellet was washed with 500 µl 70% ethanol then separated by centrifugation at 13 000 rpm for 5 minutes. The ethanol

was removed and the pellet allowed to air–dry, then resuspended in 20 µl TE (see Appendix 1 for recipe) or dH2O.

2.3.2.3 CTAB BUFFER DNA/RNA EXTRACTION

500 µl CTAB buffer (see Appendix 1 for recipe) and 10 µl β-mercaptoethanol was added to powdered plant tissue and mixed by vortex. 500 µl chloroform:isoamyl alcohol (24:1) was added, the solution mixed by vortex, incubated at 65°C for 15 minutes, then separated by centrifugation for 5 minutes at 13 000 rpm. The supernatant was then removed to a clean 1.5 ml tube and 500 µl chloroform:isoamyl alcohol (24:1) was added then the solution mixed by vortex and separated by centrifugation for 5 minutes at 13 000 rpm. The supernatant was removed to a clean tube and 1 volume 4M LiCl added. The solution was then left overnight at 4°C to precipitate RNA. The solution was separated by centrifugation for 15 minutes at 13 000 rpm and the supernatant containing the DNA was removed to a clean tube, retaining the RNA pellet in the original tube. The RNA pellet was washed with 500 µl 70% ethanol then separated by centrifugation at 13 000 rpm for 5 minutes. The ethanol was removed and the pellet allowed to air–dry, then resuspended in 20 µl TE or dH2O. The supernatant containing the DNA was then mixed with 1 volume isopropanol, mixed by inversion and separated by centrifugation for 5 minutes at 13 000 rpm. The supernatant was removed and discarded and the DNA pellet washed with 500 µl 70% ethanol then separated by centrifugation at 13 000 rpm for 5 minutes. The ethanol was removed and the pellet allowed to air–dry, then resuspended in 20 µl TE or dH2O.

2.3.3 VISUALISATION OF NUCLEIC ACIDS BY AGAROSE GEL ELECTROPHORESIS

2.3.3.1 STANDARD GEL ELECTROPHORESIS USING TBE BUFFER

0.8% electrophoresis grade agarose was dissolved in 0.5 x TBE (see Appendix 1 for recipe) by heating for 3 minutes in a microwave. The molten gel was cooled and ethidium bromide added to a final concentration of 0.1 µg ml^{-1}. The molten gel was then poured into a 50ml, 100ml or 200ml gel tray fitted with a plastic comb to create the appropriate number and size of wells. The gel was left for 10–20 minutes to set

then placed in an electrophoresis tank and covered with 0.5 x TBE. The samples (5 µl for PCR product; 2µl plus 2µl dH2O for DNA/RNA) were then added to 1 µl loading buffer (see Appendix 1 for recipe) and transferred into the wells in the gel, alongside a 100 bp or 1 kb ladder (Bioline). An electric current was applied at 90 to 160 V using a Consort E835 powerpack (Sigma–Aldrich) until the dye neared the end of the gel. The gel was then removed and photographed under UV light.

2.3.3.2 TAE GEL ELECTROPHORESIS AND CRYSTAL VIOLET STAINING

To prevent damage to DNA from UV light that may impair ligation success, restriction enzyme-treated DNA intended for gel extraction prior to ligation was stained with the visible light stain crystal violet. Gels for crystal violet staining were made by dissolving 0.8% electrophoresis grade agarose in 1% TAE (see Appendix 1 for recipe) by heating for three minutes in a microwave. After cooling, the gel was poured into a gel mould fitted with a gel comb. The gel was left for 10-20 minutes to set then placed in an electrophoresis tank containing 1% TAE buffer to cover the gel. 50-100 µl of the digested DNA was mixed with 20 µl loading buffer then transferred to the gel. An electric current at 160 V was applied until the dye neared the end of the gel. The gel was then removed and placed in a glass dish, covered with 0.001% crystal violet solution in dH2O and rocked on a Stuart Scientific STR6 platform shaker (Bibby Scientific Limited, Staffordshire, UK) until DNA bands were visible. Bands of DNA were then cut with a scalpel and kept for gel extraction.

2.3.4 GEL EXTRACTION

Isolated gel slices containing desired DNA were cleaned using either QIAGEN MinElute Gel Extraction Kit (Crawley, UK) or Fermentas GeneJet Gel Extraction Kit (Thermo Scientific, Loughborough, UK) according to manufacturer's instructions.

2.3.5 Nucleic acid quantification

2.3.5.1 Estimation by agarose gel electrophoresis

1 µl of nucleic acid solution was added to 4 µl dH2O and 1 µl loading buffer and the yield estimated using gel electrophoresis by comparison to previous extractions of known concentration.

2.3.5.2 Spectrophotometer analysis

1 µl of nucleic acid solution was diluted with 1 ml of dH2O or TE. A blank measure of absorbance at a wavelength of 260 nm was taken using 1 ml of dH2O or TE in a glass cuvette, then the absorbance of the diluted nucleic acid solution at 260 nm was measured. The concentration of RNA in the diluted nucleic acid solution was calculated by the following formula: concentration of RNA (µg μl^{-1}) = 40 x absorbance at 260 nm.

2.3.5.3 NanoDrop spectrophotometer analysis

Later nucleic acid preparations were quantified using a NanoDrop ND-1000 spectrophotometer (Thermo Scientific, Wilmington, USA). The spectrophotometer was initialised using dH2O and a blank reading taken using 1 µl dH2O or TE. 1 µl of undiluted nucleic acid solution was then measured using either the DNA or RNA setting of the NanoDrop spectrophotometer.

2.3.6 cDNA synthesis

In order to perform PCR reactions on transcribed RNA, complementary DNA (cDNA) was synthesised using Bioline BioScript RNAse H Low, as per manufacturer's instructions, using B26 as the primer (Frohman et al., 1988). The B26 primer is composed of a poly-T region flanked by an adapter priming site. When used to prime first-strand cDNA synthesis, this produces cDNA with a known primer site (B25) following the poly-A tail of every transcript. This enables the cDNA to be

used in later production of full-length cDNA transcripts using 3'RACE (Frohman, Dush & Martin 1988).

2.3.7 Polymerase chain reaction (PCR)

PCR is a technique to amplify fragments from either genomic DNA, plasmid DNA or cDNA, and was widely used throughout this project to different experimental ends including candidate gene isolation, modification of DNA sequences, testing of ligation success, and quantification of gene expression. Here a standard basic PCR protocol is described, and any modifications specific to particular experiments are detailed as appropriate in later text. All primers are listed in Appendix 2.

Standard PCR conditions and thermocycling profile can be seen in Table 2.2. Thermocycling was carried out with TC-412, Techgene, Flexgene and TC-3000 thermocyclers (Techne, Bibby Scientific Limited, Staffordshire, UK).

Reaction conditions		Thermocycling profile		
Reagent concentration	Final [c]	Reaction phase	Temp. (°C)	Time (m)
10X reaction buffer	1X	Initial denat.	94	5
50mM MgCl2	1.5 mM	Denaturation	94	0.5
20mM dNTPs	200 µM	Primer anneal	45-60[d]	0.5
100µM forward primer	200 nM-5µM[a]	Extension	72	1
100µM reverse primer	200 nM-5µMa	Final extension	72	5
5U/µl Taq polymerase	0.75-2U[b]	Final hold	4	∞
gDNA or cDNA template	1-5µl added[c]			

Table 2.2. Reaction conditions and thermocycling sequence for a standard polymerase chain reaction (PCR). The amplification cycle, represented by shaded phase in the thermocycling sequence, was repeated 28–45 times depending on the amplification target and template type. Variation in volumes was dependent on: (a) protocol, (b) reaction volume, (c) original template concentration, (d) primer used.

Gene sequences amplified by PCR that were to be used for structural analysis or functional characterisation by heterologous transformation (see section 2.4) were amplified using Phusion High-Fidelity DNA Polymerase, a proofreading polymerase which can recognise incorrect base pairs and excise them using 3'-5' exonuclease

before continuing polymerisation activity. Use of proofreading polymerase to amplify these sequences ensured maximum accuracy in nucleotide sequences, and gave higher confidence that observed sequence differences between genes of difference species were not simply the artefacts of polymerisation errors.

2.3.8 Preparation of chemically competent *E. coli* strain DH5α

To produce large quantities of plasmid DNA, the *E. coli* strain DH5α was used. DH5α is ideal for plasmid cloning because it contains the recA gene to prevent homologous recombination, the endA1 mutation to inactivate an endogenous endonuclease that can degrade plasmid DNA, and the lacZ ΔM15 allele as an α acceptor to complete the β-galactosidase protein tetramer during blue-white screening using the lacZ gene. To maximise transformation efficiency, cells first need to be made competent to passive uptake of extracellular DNA. Chemical competence was induced using the following procedure:

50 µl from a previous batch of competent *E. coli* cells was added to 10 ml liquid LB (see Appendix 1 for recipe) and incubated at 37°C overnight in a shaking incubator. 1 ml of the culture was then diluted with 4 x 30 ml LB and incubated at 37°C for 3 hours in a shaking incubator. The cells were then isolated by centrifugation at 4°C at 4000 rpm. The supernatant was discarded and the cells resuspended in 10 ml 4°C 100 mM $MgCl_2$ then incubated on ice for 5 minutes. The cells were then isolated by centrifugation at 4°C at 4000 rpm and the supernatant discarded. The cells were resuspended in 2ml of *E.coli* freezing solution containing 60 mM $CaCl_2$ (see Appendix 1 for recipe) then frozen using liquid nitrogen and stored in aliquots of 50 µl at -80°C until use.

2.3.9 Transfer of PCR products to a plasmid vector

2.3.9.1 TA cloning using commercially supplied pGEM-T Easy kit

TA ligations were performed using the pGEM–T Easy kit (Promega, USA) which promotes specific binding of the overhanging 3' adenosine nucleotides left by Taq

polymerase to overhanging thymidine nucleotides on the pGEM–T easy plasmid vector. The pGEM-T Easy plasmid contains the β–lactamase gene, conferring resistance to ampicillin, and the lacZ gene encoding a subunit of the β–galactosidase enzyme for which the coding region is split either side of the multiple cloning site. When bacteria containing the pGEM-T Easy plasmid are grown with IPTG and X-gal, if the plasmid has ligated to itself with no insert the IPTG induces expression of the uninterrupted lacZ gene, producing β–galactosidase enzyme which then metabolises colourless X-gal to a bright blue product. When a DNA insert is present within the multiple cloning site it keeps separate the two interrupted halves of the lacZ gene and prevents production of a whole enzyme, preventing blue colonies from being produced. In this way blue-white screening allows selection of plasmids containing a DNA insert. Ligations were performed according to the manufacturer's instructions.

2.3.9.2 Blunt cloning using commercially supplied pCR-blunt kit

Blunt ligations were performed using the Zero Blunt Cloning Kit (Invitrogen Life Technologies, Paisley, UK). The plasmid confers resistance to kanamycin and Zeocin, as well as utilising a lethal screening system with the ccdB gene which, situated across the multiple cloning site, creates a toxic product to kill any bacterial cells with plasmids not containing a DNA insert. Any cells with a plasmid containing an insert do not produce functional ccdB protein so are able to grow and multiply normally. This allows screening of cells containing a plasmid with an insert present. Ligations were performed according to the manufacturer's instructions.

2.3.9.3 Blunt cloning using homemade blunt pBluescript SK- vector

Blunt ligations later in this project were performed using a homemade blunt pBluescript SK- vector. This plasmid utilises the same blue-white screening as detailed earlier for the pGEM-T Easy plasmid. It also confers resistance to ampicillin.

The pBluescript vector contains one Eco RV recognition site within the multiple cloning site. Eco RV enzyme leaves blunt ends at its recognition site, so cutting the

DNA at this site results in a linearised vector that can be used for later blunt cloning reactions.

A restriction digest of total volume 50 µl was assembled as follows: 1 µl Eco RV enzyme, 5 µl BSA (10x), 5 µl NEB Buffer 3 (10x), 5 µl plasmid (4.9 µg μl^{-1}), 34 µl dH2O. The reaction was incubated at 37°C overnight, then purified as follows: 500 µl phenol:chloroform:isoamyl alcohol (28:24:1) was added and the solution mixed by vortex then separated by centrifugation for 5 minutes at 13 000 rpm in a benchtop microcentrifuge. The supernatant was transferred to a new tube, 500µl chloroform:isoamyl alcohol (24:1) added, the solution mixed by vortex and separated by centrifugation at 13 000 rpm for 5 minutes and the supernatant transferred to a clean tube. The DNA was then precipitated by adding 500 µl isopropanol, separated by centrifugation at 14 000 rpm for 5 minutes, the supernatant discarded and the DNA pellet resuspended in 50 µl dH2O. The DNA was quantified by nanodrop spectrophotometer, then diluted to a working concentration of 25 ng μl^{-1} and stored at -20°C.

Ligations were then assembled as follows: 0.5 µl plasmid vector (25 ng μl^{-1}), 3.5 µl PCR product or gel-extract, 0.5 ul T4 ligase buffer (10x), 0.5 µl T4 ligase. Reagents were combined and left at room temperature for 1 hour.

2.3.9.4 Ligation to pGreenII for expression of genes *in planta*

The pGreenII plasmid was specifically developed for use in plant transformation via *Agrobacterium* (Hellens *et al.* 2000). It contains a multiple cloning site between the left border and right border regions that are required for recognition, transfer and insertion into the plant genome of the T-DNA region by vir genes present in *Agrobacterium*. The pGreenII plasmid also contains the pSa replication origin, recognised by the RepA replicase which is provided on a separate helper plasmid. This enables replication of pGreenII in *Agrobacterium*. It also contains the ColEI replication origin for easy replication of the plasmid in *E. coli*.

Previous work in this lab has modified the pGreenII plasmid to contain a double copy of the CaMV 35S promoter and terminator between the left and right border

regions. The 35S promoter from cauliflower mosaic virus is a strong constitutive promoter in plants, so enables constitutive expression of the gene of interest *in planta*.

Ligations to pGreenII35S were either performed using directional cloning, utilising two different restriction sites, or non-directional cloning after which plasmids must be screened for orientation. Both methods used vector and insert with overhanging 'sticky' ends due to the higher efficiency of ligation that can be achieved with sticky ends as compared to that with blunt ligation.

2.3.9.4.1 BamHI/HindIII cloning insert and vector preparation

Genes to be ligated using the restriction sites BamHI and HindIII (*S. sisymbriifolium* and *S. capsicoides Mixta-Like*) were prepared by primer modification. Primers used to amplify by PCR the entire gene were modified to add a HindIII recognition site to the forward primer and a BamHI recognition site to the reverse primer. Using plasmid template containing a proofread copy of the gene of interest, the gene was amplified by PCR using the modified primers. The resulting amplicon was then cloned and sequenced to confirm the presence of the recognition sites. The plasmid stock was then digested with BamHI and HindIII in a double digest, with reaction conditions as follows: 36 µl plasmid (approx. 200 ng μl^{-1}), 5 µl Tango buffer (10x, Thermo Scientific, Loughborough, UK), 1 µl BamHI enzyme (10U), 1 µl HindIII enzyme (10U), 9 µl dH2O.

The pGreenII plasmid contains BamHI and HindIII recognition sites and does not need to be modified prior to digestion. pGREEN was digested with reaction conditions as follows:

5 µl plasmid (approx. 5000 ng μl^{-1}), 5 µl Tango buffer (10x), 1.5 µl BamHI enzyme (15U), 1.5 µl HindIII enzyme (15U), 37 µl dH2O.

Digest reactions were left overnight at 37°C. The digested DNA fragments were then separated by gel electrophoresis to isolate the desired section of cut DNA, then gel extracted using a commercially supplied kit.

2.3.9.4.2 Non-directional cloning insert and vector preparation

The pGREEN vector contains one Eco RI recognition site within the multiple cloning site. Digesting DNA with Eco RI enzyme leaves identical sticky ends at its recognition site, so cutting the pGREEN at this site results in a linearised vector that can be used for later sticky cloning reactions. A restriction digest of total volume 50 µl was assembled as follows: 6 µl EcoRI enzyme (60U), 10 µl EcoRI Buffer (10x), 3 µl plasmid (1.5 µg μl^{-1}), 81 µl dH2O. The reaction was incubated at 37°C overnight, then cleaned with phenol:chloroform as described above.

In order to prevent the plasmid ligating its identical ends together, the plasmid was dephosphorylated. Ligation will only occur if one of the DNA ends contains a 5' phosphate group, so removing these from the vector ensures ligation only occurs between the desired insert and the vector plasmid. The dephosphorylation reaction was set up as follows: 10 µl NEB buffer 3 (10x), 3 µl calf intestinal phosphatase (CIP), 25 µl linearised pGREEN vector (100 ng μl^{-1}), 62 µl dH2O. The reaction was left for 1 hour at 37°C and then cleaned by phenol:chloroform: isoamyl alcohol as above. The yield was measured by nanodrop spectrophotometer.

Genes to be ligated using non-directional cloning (*S. laciniatum* and *S. aviculare Mixta-Like* and *S. sisymbriifolium* and *S. capsicoides Mixta*) in pGEM, pCR-blunt or pBLUESCRIPT was then digested with Eco RI with reaction conditions as for Eco RI plasmid digest above. Digest reactions were left overnight at 37°C. The digested DNA fragments were then separated by gel electrophoresis to isolate the desired section of cut DNA, then gel extracted using a commercially supplied kit.

2.3.9.4.3 Ligation of insert to pGREEN vector

To maximise ligation success, a range of insert:vector ratios were used. Molar ratios of 1:1, 2:1 and 4:1 insert:vector were the most successful, each using approximately 50 ng vector. The ligation reactions were set up for each gene as follows:

	Ligation 1	Ligation 2	Ligation 3
Vector	2 µl	2 µl	2 µl
Insert	2 µl	4 µl	6 µl
T4 DNA ligase	1 µl	1 µl	1 µl
T4 ligase buffer (10x)	1.5 µl	1.5 µl	1.5 µl
dH2O	9.5 µl	7.5 µl	5.5 µl

Table 2.3. pGREEN ligation conditions. Ligations 1, 2 and 3 used molar ratios of 1:1, 2:1 and 4:1 insert:vector respectively.

The ligation reactions were left at room temperature overnight, then transferred into *E.coli* cells prior to screening and sequencing. All resulting plasmid constructs are shown in Appendix 4.

2.3.10 Transformation of DH5α *E. coli*

For each ligation to be transferred to cells, 100 µl of chemically competent *E. coli* cells was allowed to thaw on ice. The total volume of ligation was then added to the cells and the tube gently tapped to mix. The cells were heat shocked at 42°C for 90 seconds, then immediately placed back on ice for 5 minutes to recover. 500 µl SOC medium (see Appendix 1 for recipe) was added, and the cells incubated in a shaker at 37°C for 90 minutes. Cells were spread on sterile plates of LB agar containing an antibiotic appropriate for the plasmid (pGEM-T Easy and pBluescript: 100 µg ml^{-1} ampicillin supplemented with 80 µg ml^{-1} IPTG and 80 µg ml^{-1} X–gal for blue/white screening; pGREEN and pCR blunt: 50 µg ml^{-1} kanamycin) and left at 37°C overnight to grow. Successful transformations produced a number of bacterial colonies which were then screened for the presence of the desired DNA insert using colony PCR.

2.3.11 Transformation of *Agrobacterium tumefaciens* strain GV3101

Heterologous transformation of tobacco with pGREEN II constructs was accomplished using *Agrobacterium tumefaciens* strain GV3101 as a vector for transfer of the tDNA region (DNA between the left and right border sequences, including an antibiotic resistance gene, the inserted gene of interest, promoters and terminators)

from the pGREENII plasmid to the tobacco genome. This strain of *Agrobacterium* produces nopaline as its opine, and can be selected for using rifampicin. It also contains pSOUP, the helper plasmid for pGREEN, which contains a gene for resistance to gentamycin.

For each pGREEN ligation to be transferred to cells, 80 µl of electrocompetent *Agrobacterium tumefaciens* cells was allowed to thaw on ice. 1 µl of plasmid was then transferred to an aliquot of cells and the mix transferred to a BioRad electroporation cuvette (Hertfordshire, UK). An electric field was applied using a BioRad Micropulser electroporator at 2.5 kV. 500 µl of SOC medium was added to the cells, and the mix transferred to a clean tube then left to recover for 30 minutes at 30°C in a shaking incubator. The cells were then spread on sterile plates of LB agar containing 50 µg ml^{-1} kanamycin and 25 µg ml^{-1} gentamycin and left at 30°C for 48 hours for colonies of bacteria to grow. Bacteria were then screened for the presence of the desired plasmid using colony PCR.

2.3.12 Colony screening by colony PCR (cPCR)

Bacterial colonies were screened for the presence of the desired insert and plasmid using PCR. For each colony to be screened, a small amount of the bacterial colony was transferred with a toothpick to separate PCR tubes containing 5 µl of water. A PCR reaction was then set up using conditions as detailed in section 2.3.7, with primers designed to anneal either to the plasmid or to the inserted DNA fragment within the plasmid. The PCR was run for 28 cycles, and the products separated by gel electrophoresis. Successful transformation of the correct plasmid was indicated by a DNA band of a size equal to the number of base pairs in the gene plus the section of DNA in the backbone plasmid between the plasmid primers. Appropriate colonies were then selected to purify plasmid. When screening for orientation of a gene prior to plant transformation, a combination of a plasmid primer and a gene primer was used in the PCR reaction. In this case, a band would only be present if the plasmid contained the gene in the desired orientation. An appropriate *Agrobacterium* colony could then be selected for plant transformation.

2.3.13 Growth of cells for plasmid purification

Cells were grown in liquid LB media containing antibiotic appropriate for the plasmid (detailed in section 2.3.9). *E. coli* were grown for 18 hours at 37°C and *Agrobacterium* for 36 hours at 30°C prior to plasmid purification, in 5 ml of growth media for miniprep or 100 ml of growth media for midiprep.

2.3.14 Plasmid purification by commercial plasmid purification kit

Minipreps and midipreps were performed according to EZ-10 or QIAGEN manufacturer's instructions. Yield was measured using a Nanodrop ND-1000 spectrophotometer as described in section 2.3.5.3. Plasmid was then sent to be sequenced at the Cambridge Department of Biochemistry sequencing facility (Sanger sequencing).

2.4 Transformation of tobacco leaf discs by *Agrobacterium*

Nicotiana tabacum var. Samsun (tobacco) was transformed using a modified version of Horsch et al. (1985). Young tobacco leaves were sterilised in 10% domestic bleach for 20 minutes then rinsed five times by immersion in sterile distilled water. Leaves were cut into 1 cm^2 discs in sterile water and placed on MS9 media (see Appendix 1 for recipe). The cut leaf discs were then precultured in the dark for 24 hours to ensure production of the wound response phenolic compound acetosyringone, which induces transcription of *Agrobacterium tumefaciens* virulence genes to produce higher transformation efficiency.

Agrobacterium cells transformed with one of the *Solanum* R2R3 MYB Subgroup 9A overexpression constructs were cultured overnight in LB media with 25 μg ml^{-1} gentamycin and 50 μg ml^{-1} kanamycin in a shaking incubator at 30°C, then pelleted

by centrifugation at 5000 g. The supernatant was removed and the pelleted cells resuspended in sterile dH_2O. Following preculture, tobacco leaf discs were immersed in this *Agrobacterium* suspension then transferred to MS9 media and leaf discs were cocultured with the *Agrobacterium* cells for 48 hours. Coculture was maintained at constant temperature in the dark to ensure stomatal closure and minimise plant stress.

Tobacco leaf disc explants were then transferred to MS9 media containing three antibiotics, 500 μg ml^{-1} cefotaxime and 200 μg ml^{-1} ampicillin to control the growth of *Agrobacterium* and 100 μg ml^{-1} kanamycin to select for transformed plant tissue. Explants were maintained at 23°C with 16 h light/8 h dark and transferred to new media every two weeks while callus and shoot regeneration occurred. When shoots had produced five or more leaves, they were cut at the base and transferred to MS0 rooting media with 100 μg ml^{-1} kanamycin. Rooted shoots were tested for presence and expression of the transgene using PCR, and successfully transformed plants were then transferred to soil and grown to maturity according to plant growth conditions outlined in section 2.5.3.

2.4.1 Phenotypic characterisation of tobacco overexpression lines

Transgenic tobacco plants overexpressing *Solanum* R2R3 MYB Subgroup 9A genes were monitored throughout development for any phenotypic abnormality compared to the wild type tobacco grown concurrently under the same conditions. A minimum of five independent tobacco lines expressing each transgene were grown to maturity and assessed for phenotypic abnormalities. This minimised the probability that any observed abnormal phenotype could be the result of a transformation artefact or insertion of the transgene in a position to disrupt an important endogenous gene, and allowed a high degree of confidence that the phenotypes observed resulted from action of the transgene.

2.5 Plant growth conditions

2.5.1 *Petunia* growth conditions

Petunia hybrida seeds were sown in soil and perlite (80:20) in 3-inch pots and grown in a controlled greenhouse environment at 26°C with a 16 hour light regime and watered daily. For bee behavioural experiments, flowers of similar size and maturity were collected on the morning immediately prior to experiments. When flowering slowed, plants were cut back to encourage a second flowering.

2.5.2 *Solanum* growth conditions

Solanum seeds were sown in soil and perlite (80:20) in 1-inch pots and grown in a controlled greenhouse environment at 26°C with a 16 hour light regime and watered daily. At two inches in height plants were transferred to individual 3-inch pots and maintained at the same light and water conditions until flowering.

2.5.3 Tobacco growth conditions

For tobacco transgenic experiments, tobacco seed of the variety Samsun was surface sown in Intercept®-treated soil in 6-inch pots. Seedlings were thinned out after germination so that one plant per pot remained. Stock plants were grown in a controlled greenhouse environment at 26°C with a 16 hour light regime and watered daily. After transformation, regenerated tobacco seedlings were potted in compost and medium-grain vermiculite (2:1) in 5-inch pots and watered initially with distilled water and Intercept® (0.02g per litre of soil). The plants were grown in a controlled growth room under the following conditions: temperature 20°C; humidity 60%; light 200µM; day length 16h light. Pots were in trays on an automatic water system that filled and then drained the trays four times a day.

2.6 Analysis of petal cell morphology

Petal cell morphology was analysed using scanning electron microscopy (SEM) to visualise artificial petal replicas created using the methods of Green & Linstead (1990). For *Solanum* petal cell analysis mature flowers were taken from plants and imprinted in Elite HD vinylpolysiloxane impression material (dental wax, supplied by Zhermack, Harrogate, UK). The wax was left to set, then the flowers removed and the impressions used as moulds to make epoxy petal casts. Devcon high-strength epoxy was mixed according to manufacturer's instructions and poured into the mould. Casts were removed after 12 hours and used for SEM petal cell analysis. For morphological analysis of transgenic tobacco, the following tissues were taken from plants: carpel, style, stigma, petal, stamen, filament, leaf adaxial, leaf abaxial and stem. The same imprint, set and casting procedure as for *Solanum* flowers was then followed.

2.6.1 Collection of dried herbarium specimens for analysis of *Solanum* petal cell morphology

Flowers from herbarium specimens were used for petal cell morphological analysis when no fresh material could be obtained. Specimens were kindly given by Kew Herbarium (K), Cambridge University Herbarium (CGE), the Natural History Museum Herbarium (BM) and Melbourne University Herbarium (MELU). Specimens were selected from herbarium sheets of each species and either an entire flower (if flowers were plentiful) or a single petal was taken for each species. The specimens were then transferred to labelled SEM stubs and used for SEM analysis.

2.6.2 Scanning Electron Microscopy (SEM) analysis

Epoxy casts produced from petal surfaces following the methods of (Green & Linstead 1990) or dried herbarium specimens were coated with conductive metal (gold or chromium) by the Multi-Imaging Centre service using a Quorum K756X sputter coater. Samples were then imaged using a FEI Philips XL30 FEGSEM

Scanning electron microscope 0.5 - 30 KeV with Oxford Instruments INCA EDX system running a 30 mm^2 SiLi thin window pentafet EDX detector.

2.6.3 Cryo SEM analysis

Live plants were dissected and placed on a cryo-transfer stage. Samples were then cooled using a Quorum/Emitech PP7480 cryo-transfer system and imaged using the SEM system described above.

2.7 PCR primer design

2.7.1 CODEHOP primer design

To amplify MIXTA–like genes from *S. sisymbriifolium*, *S. capsicoides* and *S. elaeagnifolium*, degenerate primers were created based on sequences of MIXTA–like genes from *S. lycopersicum*, *S. dulcamara* and *Antirrhinum majus*. The protein sequences were aligned using Clustal W and the alignment imported into Blockmaker (Henikoff et. al. 2007) from which the CODEHOP algorithm (Rose *et al.* 1998) created degenerate primers with a non–degenerate clamp region, in which the DNA sequences of the three genes were most similar, as well as a core region that was more variable. Primers were tested for specificity by BLAST search (Altschul *et al.* 1990).

2.7.2 PrimaClade primer design

A second round of primers were designed from only the known *Solanum* MIXTA–like genes, leaving only two genes to compare from *S. lycopersicum* and *S. dulcamara*. PrimaClade (Gadberry *et al.* 2005) allows degenerate or non-degenerate primers to be created from two or more sequences. Through this method specific primers were designed to directly target the Subgroup 9 domain (Stracke, Werber &

Weisshaar 2001) as well as a strongly conserved part of the MYB domain. Primers were tested for specificity by BLAST search (Altschul *et al.* 1990).

2.7.3 Specific primer design using Primer3 Plus

To design specific primers for each gene isolated, Primer3 Plus (Untergasser *et al.* 2007) was used. The gene sequence was imported to the program and appropriate conditions for use of primers, length of amplicon and target region of the gene were specified. Primers were then produced that were specific to only that gene. Primers were tested for specificity by BLAST search (Altschul *et al.* 1990).

All primer sequences can be found in Appendix 2.

2.7.4 Bioinformatics methods

To identify sequence similarity between genes isolated in this project, BLAST searches were used through the NCBI website (Altschul *et al.* 1990). Alignment of DNA and protein sequences to identify similarity as well as changes between species was performed with ClustalW (Larkin *et al.* 2007), MUSCLE (Edgar 2004) and alignments available through MEGA 5 (Tamura *et al.* 2011) and Geneious Basic 5.6.4 (Biomatters Ltd.)

2.8 Rapid amplification of cDNA ends (RACE)

To amplify the 3' end of the genes identified through degenerate or specific PCR, two forward primers (F1 and F2) were designed within each identified sequence. The F1 primer was used in conjunction with the B25 primer which acts as a reverse primer for every 3' end of cDNA present, priming at the B26 adapter sequence left after cDNA synthesis. For each sequence, a 10 to 1, 1 to 1 and 1 to 10 ratio of F1 to B25 primer was used, alongside a control of only B25. After gel electrophoresis, any bands

present in the B25-only reaction were disregarded when they appeared in other reactions. The reactions nevertheless invariably produced a range of bands, as B25 is a highly non–specific primer. Thus, the F1/B25 PCR reaction was then taken as the template for a nested PCR using the F2 primer, along with B25 for the reverse. This also often produced a range of bands, and so the amplified fragment that was closest in size to that expected from the length of other MIXTA–like genes was gel–extracted to clone and sequence.

2.9 Quantification of gene expression using quantitative RT-PCR (qPCR)

2.9.1 RNA extraction and cDNA synthesis for qPCR

RNA for quantitative analysis of gene expression was extracted using the Invitrogen Plant RNA Reagent according to manufacturer's instructions. 0.1 g of powdered plant tissue was used for each extraction. RNA was diluted to 200 ng μl^{-1} and treated with Ambion TURBO DNA-free DNase Treatment and Removal Reagents, following manufacturer's instructions for a 50 µl reaction. 3 µl (600 ng) of the treated RNA was then used for cDNA synthesis, using either Invitrogen SuperScript® III First-Strand Synthesis SuperMix for qPCR, or identical reaction conditions using Invitrogen Superscript III with both oligo(dT)20 (1.25 µM) and random hexamers (1.25 ng μl^{-1}) to prime cDNA synthesis. cDNA was then diluted 1:9 with dH_2O, and 4 µl used for each 20 µl PCR reaction.

2.9.2 Reference genes used in quantification of *Solanum* qPCR

Several control genes were tested for stability of expression across tissue types as well as efficiency of amplification in each of the *Solanum* species in which R2R3 MYB Subgroup 9A genes were to be quantified. Details of reference gene primer selection

are described in Chapter 6, section 6.2.2. All primers tested were based on the analysis of reference genes in tomato by Coker & Davies (2003).

The reference gene DNAJ (accession AF124139; heat shock N-terminal domain-containing protein, Expósito-Rodríguez *et al.* 2008) was selected as the best control to use for quantification of *Solanum* R2R3 MYB Subgroup 9A genes, based on its stability of expression across different tissues and its high overall amplification efficiency. Though optimally more than one reference gene would be used, we were unable to find more than one reference gene that showed a sufficiently high stability of expression across all tissue types for each species.

2.9.3 Reaction conditions for quantitative RT-PCR

Each 20 µl reaction contained the following reagents: cDNA 4 µl, $MgCl_2$ 3.5 mM, TrisHCL pH 8.3 10 mM, KCl 50 mM, primer 100 nM each, dNTPs 0.2 mM each, KAPA 2G Fast DNA polymerase 0.5 units, SYBR Green 0.5X, DMSO 5%.

2.9.4 Thermocycling conditions for quantitative RT-PCR

40 cycles of PCR were performed using a BioRad DNA Engine Thermocycler with cycling conditions as follows: 95 °C 1 min, 45 cycles of 95 °C 10 sec, 57 °C 10 sec, 72 °C 10 sec. A plate fluorescence reading was taken once each cycle. A melt curve to analyse the number and type of amplicon products was then performed from 60 °C to 95 °C.

2.9.5 Data analysis

All quantification of gene expression was performed using Opticon Monitor 3 software (BioRad Laboratories, Inc) and expression quantified by ΔCt analysis in comparison to fluorescence of the reference gene DNAj in each species. Each data set was then compared and statistically analysed using Microsoft Excel.

2.10 *SOLANUM* PHYLOGENETIC ANALYSIS

This project began with a number of *Solanum* species for which petal cell morphology had already been analysed. Due to the size of the genus *Solanum* (around 1500 species) the largest and most recent phylogenetic analysis (Weese & Bohs 2007) covers only 102 species from selected major clades within the genus, and many of the species useful to this project were not represented in this analysis. In order to understand the patterns of evolution of petal epidermal cell morphology, the relationships of species for which we already had morphological data were analyzed using the phylogenetic methods of Weese and Bohs (2007) which used two chloroplast (*ndhF* and *trnT-F*) and one nuclear marker (GBSSI or *waxy*). Many of our species had some sequence data available to download. For sequences that were unavailable, PCR following the methods of Weese and Bohs (2007) was used to amplify the sequences from genomic DNA obtained from plant material supplied by Nijmegen Botanic Gardens. The sequences were then cloned (as previously detailed) and sequenced.

2.10.1 PREPARATION OF BACKBONE SEQUENCE ALIGNMENT

The sequence alignment used by Weese and Bohs (2007) was downloaded from TreeBASE (www.treebase.org) and imported into BioEdit (Hall 1999). Additional sequence data from our species was added to this backbone sequence alignment as it became available. The new sequences were then aligned manually.

2.10.2 DOWNLOAD OF AVAILABLE SEQUENCES

Sequences for the nuclear gene granule-bound starch synthase (GBSSI or *waxy*), the chloroplast *trnT* to *trnF* (*trnT-F*) non-coding region and the chloroplast gene encoding a subunit of the NADH dehydrogenase complex (*ndhF*) were downloaded from the National Center for Biotechnology Information (NCBI) website. The sequences were aligned using ClustalW to confirm they were correct and in the

desired orientation, and reverse-complemented if needed. Sequences were then imported into the backbone sequence alignment.

2.10.3 PCR TO AMPLIFY UNKNOWN SEQUENCES

Primers were designed to amplify sequences for *waxy*, *trnT-F* and *ndhF* each in two halves of between 1000 and 1500 bp (see Appendix 2 for primer sequences). For some sequences, multiple bands were observed, and for others, none were. The multiple band problem was solved by employing a touchdown PCR procedure, with ten cycles at each annealing temperature, starting at 70°C and dropping in 2°C intervals to 60°C. If amplification could not be achieved at this temperature, a touchdown from 60°C to 50°C was used. The second problem, that of no bands, was solved by starting the PCR with 10 cycles at a lower annealing temperature (45°C to 52°C) and finishing with 20 cycles at a higher temperature (50°C to 55°C). All PCR reactions used an extension time of 1 m 30 s, and the primers used were as described in Weese & Bohs, 2007 and are listed in Appendix 2.

The PCR products were all cloned as described in section 2.3.9 and 2.3.10 and sequenced.

2.10.4 SEQUENCE ASSEMBLY

Sequences were assembled using CAP3 (Huang and Madan, 1999) and aligned using Clustal W in both BioEdit Sequence Alignment Editor in combination with Biology Workbench online, to ensure all sequences were correct and in the same orientation.

2.10.5 PHYLOGENETIC METHODS

The final alignment was converted to PHYLIP format and imported to the web interface of PhyML (Guindon *et al.* 2010). A maximum likelihood analysis with 100 bootstraps was run using the General Time-Reversible (GTR) model of DNA evolution, with a 4-category gamma distributed correction for rate heterogeneity and an estimation of invariant sites. A separate tree was constructed for each of

ndhF, *trnT-F* and *waxy* and then a final tree produced using sequence data from all three regions, under the same model of evolution. The final tree was imported to MEGA 5 (Tamura *et al.* 2011) and known morphological data was added to the tree as data labels. Additional morphological data was then added to the tree as it became available. Ancestral character state was analysed by parsimony using Mesquite 2.75 (Maddison & Maddison 2003).

2.11 Bumblebee Behaviour Methods

2.11.1 Bee care

Colonies of bumblebees (*Bombus terrestris*) were supplied by Syngenta Bioline Ltd (Weert, The Netherlands). Colonies were attached via a 10 mm diameter plastic tube to a 300 x 750 x 1120 mm plywood flight arena with a UV-penetrable Plexiglas lid. The inside of the box was painted in a bee-neutral shade of green.

2.11.1.1 Setting up a colony

Each new colony was acclimatised to the flight arena and its connecting tube by removing the sucrose source supplied with the box, and providing instead plastic feeders filled with 30% sucrose in the flight arena, placed directly in front of the entrance tube. The bees were then left for one to three days to discover the feeders. If after that time it was still proving a difficult task, a trail of sucrose solution was placed along the connecting tube to coax the bees out. Once the bees were feeding regularly, the feeders were placed randomly around the flight arena to encourage the bees to fly further. We used clear plastic feeders so that bees were kept colour- and flower-naïve prior to experiments.

2.11.1.2 Colony maintenance

Bees were fed 30% sucrose solution daily, and pollen for larval growth fed directly into the colony every second day. Dead bees and any rejected larvae were removed

from the flight arena and put into the freezer overnight to humanely ensure they were dead before disposing of them. The flight arena was cleaned with 30% ethanol once to twice a week, as well as immediately before any experiments.

2.11.1.3 Marking bees for experiments

In order to tell individual bees apart for consistency during experiments, bees were marked using a water–based paint. All bees that showed consistent foraging were marked with one colour of paint on one day, then the next day bees which were still foraging were marked with a second colour. Each bee was marked with a different size, number, colour or orientation of spots in order to be able to quickly distinguish each bee. Bees showing consistent foraging behaviour over several days could generally be relied upon to explore new objects placed at feeder–height in the flight arena when experiments started.

2.11.2 Standard experimental conditions

All experiments were carried out during normal daylight hours with additional illumination provided by banks of six Sylvania 36W Professional Activa 172 tubes mounted 1.8 m above the floor of a foraging arena. The frequency of the tubes was controlled with special ballasts (Philips HF-B 236 TLD) and was greater than 200 Hz. This illumination closely simulates natural daylight illumination for bee vision (Dyer & Chittka 2004).

At the beginning of the day, all but two or three plastic feeders were removed from the flight arena. The remaining feeders were left to coax previously marked consistent foragers out of the colony, but once they had fed and returned to the colony a few times the connecting tube was blocked to prevent bees entering the arena. The good foragers would continue to attempt to enter the arena and so would be ready for the experiment as soon as the flowers were set up. Of the bees remaining in the flight arena, any that attempted to return to the colony were allowed to do so by controlling the gated tube connecting the flight arena and the colony nest. All remaining bees were trapped in plastic pots and moved to the sides of the flight arena to prevent any interference with experiments. Dead bees and larvae were

removed. Once the arena was free of bees it was wiped down with 30% ethanol and allowed to dry. Individual bees were then used in each experiment as described in sections 2.11.4.3 and 2.11.5.4.

2.11.3 Reflectance spectra of flowers and flower replicas

The spectral reflectance of *Petunia* flower petals and of artificial epoxy flower discs was measured with an Ocean Optics S2000 spectrophotometer (Dundedin, Florida, USA) relative to a white reflection standard. Spectrophotometer readings were averaged over three measurements at different positions on the flower or disc.

2.11.4 *Petunia* bee preference experiments

2.11.4.1 Bee experimental methods using orbital shaker

To simulate the wind movement of flowers that a bee might encounter when foraging from flowers in the wild, we used a small laboratory shaker (Stuart SSM1 Lab-Scale Orbital Shaker, Bibby Scientific Limited, Staffordshire, UK). The shaker was covered with a bee-neutral shade of green tissue paper, and bees were trained to visit the shaker by placing their usual feeders on and around it. Bees were acclimatised to its noise and movement by running the shaker at its lowest setting of 30 rpm (0.50 Hz) for several days.

Optimal shaking speeds for the experiment were determined by testing the foraging ability of several bees across different speeds. 100 rpm was chosen as an appropriate upper limit for maximum landing difficulty, since at speeds greater than 100 rpm (1.67 Hz) most bees were unable to land on the flowers. 70 rpm (1.17 Hz) tested a moderate difficulty of landing, and the easiest conditions tested the bees with flowers stationary.

2.11.4.2 flower selection

Plants were grown from seed under greenhouse conditions as described in section 2.5.1. Flowers for experiments were chosen from three lines of *Petunia*. Plants of the

flat-celled phmyb1 mutant line were used as the flat-celled comparator in each set of experiments. Plants arising from a germinal reversion to the wild type provided an isogenic conical-celled control, and for a darkly-coloured conical-celled flower the V26 line of *Petunia* was used, which has flowers with a close match in pigment colour but much darker appearance due to the lower total amount of light reflected from the flowers. Individual flowers were selected for consistent size and maturity levels across each line, in order to minimise confounding differences between flowers.

2.11.4.3 Innate preference experiments

In each experiment ten flowers, five conical-celled and five flat-celled, were presented to individual bees in a semi–randomised array in the flight arena. Each flower was fitted with a 50 µl tube in the centre to allow for refilling of the 20 µl 30% sucrose reward. During experiments all bees were excluded from the flight arena, as described above in section 2.11.2, while flowers were placed. Once the flowers were set up, one at a time marked bees were released into the flight arena and allowed to forage until satiation. We recorded each decision as to which type of flower the bee landed on, and whether the bee then drank from the flower or aborted the landing without drinking. Each bee's foraging was recorded to 100 choices. After each foraging bout all visited flowers were replaced with fresh ones to minimise any interference from scent markings, and the flowers repositioned into a new semi-randomised array to prevent positional learning.

2.11.5 *Solanum* buzz pollination experiments

Standard bee care was as above, except pollen was not fed directly into the colony and instead bees were supplied with pollen placed in the flight arena to encourage foraging behaviour away from the colony in preparation for pollen-seeking experiments. A secondary colony of bees was used for initial observations of bee behavioural response to different arrangements of discs and real flowers in order to optimise the experimental setup. This use of a secondary colony ensured that bees from the experimental colony remained naïve to both artificial and real flowers prior to initiating experiments.

2.11.5.1 Construction of biomimetic flower replicas

Since no isogenic lines of flat-celled and conical-celled *Solanum* species could be found, artificial biomimetic petal surface replicas were used to test bee preferences. To ensure consistency of visual and chemical signals eliciting buzz pollinating behaviour in bees across conical- and flat-celled artificial flowers, as well as to allow for pollen to be used as a reward in preference tests, real flowers were used in conjunction with artificial flowers.

In order to construct artificial flower discs that could provide an appropriate flat-celled comparator to the conical cells of *S. sisymbriifolium*, flower petal surfaces of several candidate species were tested. Flowers were collected in October from the Cambridge University Botanic Garden. Adaxial petal epidermal surfaces were used to make simple, flat, epoxy resin casts using methods detailed in Green & Linstead (1990). Considerable care was taken to minimise petal ridges to create an even cell surface. Petal cell surface replicas were then imaged using the methods described above in section 2.6.2.

2.11.5.2 Artificial flower construction

To minimise experimental interference from petal size differences between conical and flat celled species, artificial cell surface discs were constructed from smaller segments shaped to resemble petals of *S. sisymbriifolium* flowers. Each disc was made from 5 g 2-ton epoxy (2.5 g resin and 2.5 g catalyst) divided between 5 segments. Manganese violet and ultramarine blue cornelissen pigments were added to the epoxy to create two shades of purple for each of the conical and flat celled discs (Table 2.4). This colour difference facilitates bee learning and recognition of the contrasting surfaces (Whitney *et al.* 2009). As the epoxy was translucent, each of the segments was backed with white paper.

	2-ton epoxy	Manganese violet cornelissen pigment	Ultramarine blue cornelissen pigment
Blue-purple (conical) flower disc	5 g	18 mg	4 mg
Pink-purple (flat) flower disc	5 g	18 mg	-

Table 2.4 Quantities of pigment used to dye each type of epoxy artificial flower discs.

S. sisymbriifolium flowers were positioned between the artificial petal cell replica disc and a second epoxy disc so petal surfaces were not visible during experiments. The anthers protruded from a small hole in the centre of each artificial flower. The flowers were kept intact to preserve any floral scent signals to the pollinator.

During experiments, artificial flowers were positioned forward facing, vertically, to imitate the natural position of flowers on the *Solanum* plants. Previous experiments have also found that grip is more important in bee choice when flowers are presented vertically, making them more difficult for bees to land on (Whitney *et al.* 2009).

2.11.5.3 FLOWER SELECTION

Whole flowers for experiments as well as individual petals used in construction of biomimetic epoxy conical-celled petal surfaces were taken from *S. sisymbriifolium* plants grown in standard greenhouse conditions as described in section 2.5.2. Only flowers reaching the stage of maturity indicated by transition from white to lilac petals were used in experiments, because in preliminary trials bees did not visit flowers at any earlier stage of development. All flowers were carefully selected to avoid those with petal or anther damage.

2.11.5.4 INNATE PREFERENCE EXPERIMENTAL CONDITIONS

Ten discs were used in each experiment, 5 conical celled and 5 flat celled in a semi-randomised array within the flight arena. *S. sisymbriifolium* flowers were assigned to discs randomly for each experiment and used for no more than 3 experiments because of the potential impact of petal damage, wilting and anther exhaustion. Flowers were collected from the plants on the day of experiments.

During experiments only a single bee was released from the colony into the arena to forage at any one time. The disc that the bee approached was recorded (position, cell type and disc ID) and whether the bee investigated (hovered in front of the flower without landing) or landed on the disc. Also noted was whether the bee landed directly on the anthers or the disc petals. After each foraging bout the flowers

and discs were repositioned in a new semi-randomised array to prevent spatial learning. Data for each bee was collected until it had completed 100 disc choices.

2.11.6 DATA ANALYSIS

Error in the experiments was calculated as the standard error from the variation between individual bees, expressed as the proportion of maximum response per bee, and calculated using Microsoft Excel.

2.11.6.1 *PETUNIA* STATISTICAL METHODS

Paired *t*-tests of bee choices were performed using Microsoft Excel to compare overall preference for conical- or flat-celled flowers, and to compare the first ten choices with the last ten choices in each test.

2.11.6.2 *SOLANUM* STATISTICAL METHODS

All statistical tests were conducted in R 2.15.2. A single sample t-test was used to test for an overall difference from random choice across all bees (n=10). X^2 tests were used to test for each individual bee preference within 100 choices (null hypothesis ratio of 50:50). A paired t-test was used to compare the mean differences in preference across all bees (n=10) between the first 20 choices and last 20 choices. Differences between individual bees were then investigated using X^2 tests. The relationship between preference for conical celled discs and experience visits summarised into 10 categories with experience level 1 (visits 1-10 being the least experienced) was investigated using ANOVA. All tests were considered at a 0.05 significance level.

Chapter 3. *Solanum* phylogenetics and character mapping

3.1 Introduction

In this project a major aim was to understand how conical petal cells evolve, not only why they have remained so prevalent throughout the angiosperms, but also to understand conversely why it is that some species have lost conical cells on their petals. *Solanum* provides an ideal system in which to explore this question because it is pollinated by bumblebees, on which previous behavioural experiments with conical cells have been conducted (Glover & Martin 1998; Whitney *et al.* 2009, 2011; Alcorn, Whitney & Glover 2012); it is an economically important genus containing potato, tomato and aubergine amongst many species of horticultural importance (Peralta & Spooner 2001; Bohs 2005; Bohs & Olmstead 2008; Zuriaga, Blanca & Nuez 2008; The Potato Genome Sequencing Consortium 2011; The Tomato Genome Consortium 2012); and finally because flat petal cells are present across this genus at a relatively high rate.

Conical cells are thought to be an ancestral feature to the angiosperms due to their prevalence and widespread occurrence across the entire angiosperm lineage (Kay, Daoud & Stirton 1981; Christensen & Hansen 1998; Whitney *et al.* 2011), including in some of the earliest diverging angiosperm groups (Alison Reed, unpublished). For *Solanum*, preliminary analysis suggests that conical cells might be an ancestral feature to this genus, for two reasons. First, preliminary studies suggest that despite

flat petal cells occurring more frequently in this genus than across the angiosperms generally, conical cells are the most common petal epidermal form in *Solanum*. Secondly, conical cells are common in species of other genera within the Solanaceae, including *Petunia* and *Nicotiana*, and in *Petunia* conical petal cell development is regulated by the same genetic pathways as in *Antirrhinum majus* (Baumann *et al.* 2007), in the sister order Lamiales. This suggests that *Solanum* species lacking conical cells may represent instances of evolutionary loss of conical cells. To gain an understanding of how conical petal cells have evolved through *Solanum*, it was necessary to determine how many species have conical petal cells and how many do not. It was particularly important to place this information within a phylogenetic context to be able to infer firstly whether conical cells are ancestral to *Solanum*, and secondly how many separate evolutionary instances of loss of conical cells have occurred. If, after a comprehensive analysis of petal cell morphology across the genus, *Solanum* was found to be predominantly conical-celled with all the occurrences of flat cells clustered phylogenetically, then it may be inferred that the loss of conical cells was an event that happened only once in *Solanum*. Conversely, there may have been multiple independent losses, and each independent loss may have arisen through a different molecular mechanism, or each may follow a common route.

This chapter aims to estimate the number and position of conical cell losses in *Solanum* using a representative sampling of species across the genus. To this end, it details a phylogenetic analysis of species with known petal cell morphology, placing these within an established phylogenetic context (Levin, Watson & Bohs 2005; Levin, Myers & Bohs 2006; Weese & Bohs 2007). It then adds to this an analysis of petal cell morphology using scanning electron microscopy (SEM) of species with previously unknown petal cell shape, which are then integrated into the phylogenetic analysis. Finally, these are combined in an ancestral character state reconstruction to predict the number and position of losses of conical cells across *Solanum*.

3.1.1 Existing phylogenetic framework

One drawback to using *Solanum* as a test genus is its vast number of member species. *Solanum* is one of the largest flowering plant genera, and current estimates of species number range from 1250 to 1700 (Weese & Bohs 2007). Historically, computational restrictions have limited the number of species that can be analysed within one single phylogenetic analysis, and constraints of funding have limited both taxon sampling and number of marker sequences. While recently the computational limitations have been overcome, the size of the genus means that, of the many phylogenetic treatments of *Solanum* completed to date, no single treatment has covered more than 10% of the total number of species. Many species have not yet been subject to a molecular phylogenetic analysis and instead remain tentatively placed phylogenetically based on comparison of morphological characters.

At the outset of this project there had been three major molecular phylogenetic treatments of *Solanum* which, when combined, give a good sampling of species across the entire genus. A phylogeny covering multiple representatives of every major clade in the genus was published by Weese & Bohs in 2007, sampling in total 102 *Solanum* species. Another phylogeny covered the Leptostemonum clade (Levin, Myers & Bohs 2006) and the final phylogeny focused in on one clade within Leptostemonum, section Acanthophora (Levin, Watson & Bohs 2005). All of these were utilised in this project: Weese & Bohs 2007 was used as a basis for the phylogeny built for this project, while the two more detailed analyses (Levin, Watson & Bohs 2005; Levin, Myers & Bohs 2006) were used for comparison to estimate the accuracy of placement of additional species added to the base tree.

3.1.2 Structure of *Solanum*

The genus *Solanum* contains twelve accepted clades, as defined in Weese & Bohs 2007 and represented by the cladogram in Figure 3.1. These further group into Clade II (Leptostemonum, Brevantherum, Geminata and Cyphomandra) and Clade I (Dulcamaroid, Morelloid, Normania, Archaesolanum, African Non-Spiny, Potato and Regmandra) as well as one early brancing clade sister to the rest of *Solanum* (Thelopodium).

The largest of the twelve clades in *Solanum* is Leptostemonum (Clade II), sometimes called *Solanum* subgenus *Leptostemonum* Bitter[1]. Also called the spiny *Solanum*s, Leptostemonum contains around 450 species with a worldwide distribution. According to the phylogenetic treatments of this group by Levin et. al. (2005, 2006) and Stern, et. al. (2011), Leptostemonum itself is made up of ten separate clades, as shown in Figure 3.2. Also within Clade II are two sister clades, Brevantherum and Geminata, and at the base of this Clade II are the tree tomatoes, Cyphomandra. Clade I contains clades Dulcamaroid, Morelloid, Normania, Archaesolanum and African Non-Spiny all in a monophyletic group, as a polytomy with Potato and Regmandra. Sister to the rest of *Solanum* is one further clade that does not fall into either Clade I or Clade II, the Thelopodium.

Due to the number of species in this genus, no single phylogenetic treatment has yet been able to analyse all species in *Solanum*. However, much of the genus has been recently analysed with either morphological or molecular phylogenetic approaches

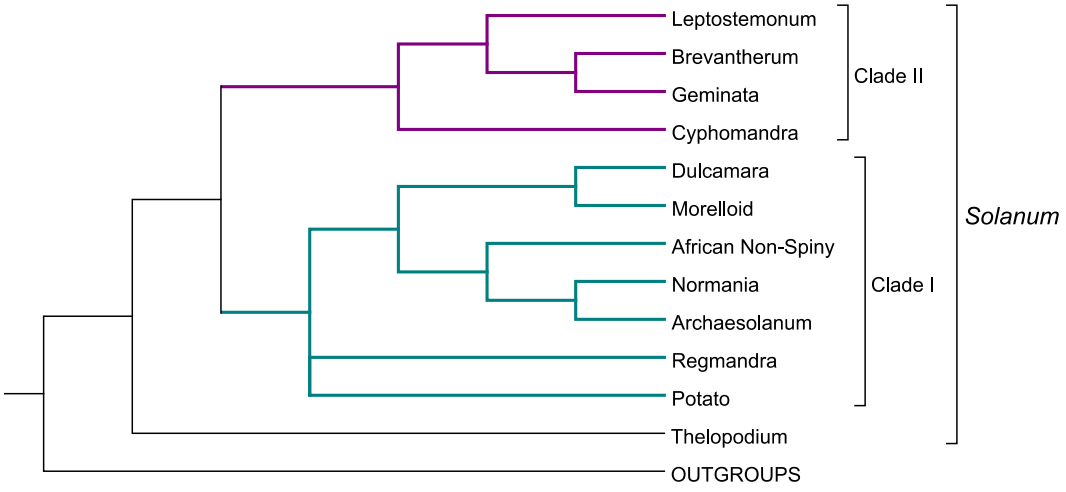

Figure 3.1 The twelve accepted clades of Solanum. The two major clades of Solanum are further divided into four and seven clades each, plus one basal clade (Thelopodium), as defined by Weese & Bohs (2007).

[1] For consistency, throughout this thesis this section of *Solanum* will be referred to simply as the clade Leptostemonum.

and as such the positions of most species are known to at least the clade level. Of the full list of the approximately 1400 species in *Solanum*, the species that fall into each of the twelve clades can be found listed online at Solanaceae Source (Natural History Museum, London, UK[2]).

3.1.3 Experimental approaches

The nucleotide alignment of Weese and Bohs (2007) was used as a base from which to build a phylogenetic analysis. This analysis used 102 *Solanum* species and 7 outgroup species. Of these, only around 20% were of known petal cell morphology.

We began this project with reliable petal cell morphology from SEM micrographs for 49 species across *Solanum*. In order to expedite identification of the positions of conical cell losses across *Solanum*, two different experimental approaches were taken. Firstly, species with known petal cell morphology were integrated into the existing phylogenetic framework. Secondly, taking species of known phylogenetic

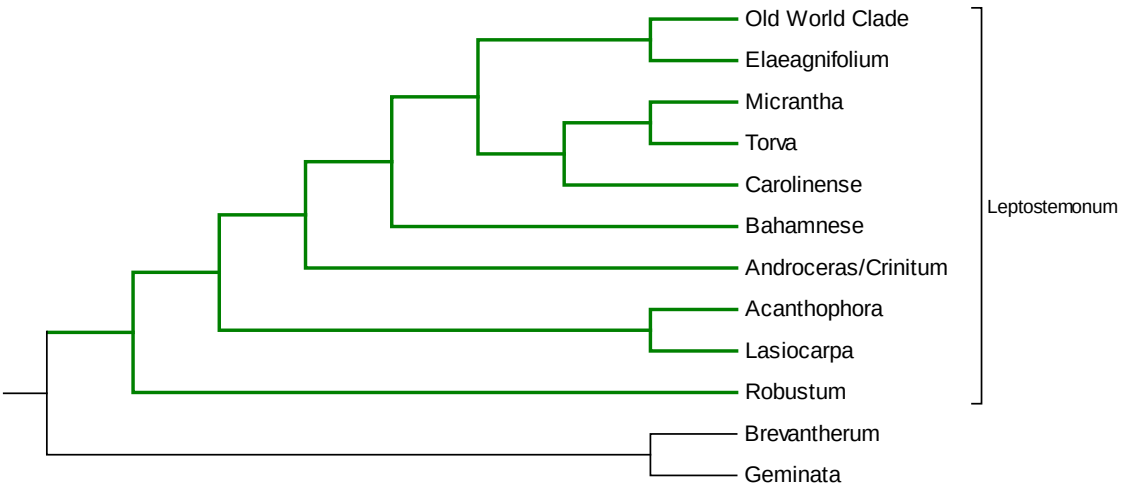

Figure 3.2 Clades within *Solanum* subgenus Leptostemonum. Clades are based on Levin, Myers, & Bohs (2006)

[2] http://www.nhm.ac.uk/research-curation/research/projects/solanaceaesource/

position but unknown petal cell morphology, petal cell morphology was analysed from fresh, fixed or dried petal material using scanning electron microscopy (SEM) analysis.

3.2 RESULTS AND DISCUSSION

3.2.1 INTEGRATION OF PHYLOGENETIC AND MORPHOLOGICAL ANALYSES

In order to integrate species of known petal cell morphology into the existing phylogenetic analyses, we assessed the availability of sequence data for the phylogenetic markers used in the Weese and Bohs (2007) analysis for species with known petal cell morphology. 23 *Solanum* species and 5 outgroup species had sufficient sequence data available to integrate these into the tree.

In addition, marker sequences were generated for eight species known to have flat cells but without molecular phylogenetic placement. PCR was used to isolate the same phylogenetic marker sequences used by Weese and Bohs (2007).

For all species, nucleotide sequences were integrated into the Weese and Bohs sequence alignment and a maximum likelihood analysis of this sequence alignment was performed to determine the phylogenetic positions of species.

To gain greater morphological coverage of the species in the original tree of Weese and Bohs (2007) petal material was obtained for species of unknown petal cell morphology, and then analysed using SEM. Some species were grown from seed, for others fixed flower material was obtained from botanic garden collections, and, finally, for species from which no fresh material could be obtained, petals were analysed from herbarium specimens. This information was then integrated with the phylogeny, and ancestral character reconstruction was used to determine the likely number and position of each loss of conical cells across *Solanum*. In total, 36 new species were added to the phylogenetic analysis of Weese and Bohs (31 *Solanum*

and 5 outgroup species), for eight of which the three phylogenetic markers were isolated and sequenced during this project. The petal cell morphology of a total of 112 species was analysed, including some duplicates for verification of cell form within and between species. 67 of these were from fresh or fixed petal material, and 64 from herbarium specimens. Our final tree therefore contained 145 species (133 *Solanum*), of which 112 (102 *Solanum*) had known petal cell morphology.

All voucher information for phylogenetic and morphological analysis is given in Appendix 5.

3.2.2 Amplification and sequencing of markers for phylogenetic analysis

The three markers used for phylogenetic analysis by Weese and Bohs (2007) included two chloroplast (*ndhF* and *trnT-F*) and one nuclear sequence region (*waxy*). In order to integrate species with known petal cell morphology into this tree, these three markers were amplified from each species. PCR was used to amplify these sequence regions from genomic DNA extracted from plant tissue obtained from the Experimental Garden and Genebank at Radboud University, Nijmegen, The Netherlands. Each region was amplified in two halves using primers listed in Weese and Bohs (2007). Alignments of the eight sequences for each gene are in Appendix 2.

3.2.3 Assembly of alignment for phylogenetic analysis

Having chosen to base our analysis on the Weese and Bohs (2007) three-gene alignment, when adding new species *ndhF*, *trnT-F* and *waxy* sequences were included where possible. Weese and Bohs (2007) showed that of the three genes and 6556 total sites used in their study, *waxy* was the most parsimony informative, containing 54% of the total parsimony informative sites of the alignment. *ndhF* and *trnT-F* each contributed 23% of the total informative sites.

Of the species not included in the tree of Weese and Bohs (2007) for which we had morphological data, many had some sequence data available from Genbank. Other sequences were kindly supplied by Gregory Wahlert (currently working with Lynn Bohs, University of Utah). Some species for which data was obtained in this way had all three markers, or at least partial sequences thereof, available for analysis. These species were added to the alignment. For species with only one or two markers available for analysis, the decision to add or not to the alignment was determined by the percentage of total informative sites each species had available. To ensure enough phylogenetic signal would be present for each species, species were only added to the alignment if near or above 50% of the total informative sites were included. Since *waxy* contributed 54% of the total informative sites in the Weese and Bohs (2007) analysis, species for which *waxy* sequence data was available were automatically included. Of the other species, only species for which both *ndhF* and *trnT-F* sequences were available were included, since these would have 46% of the total informative sites available for analysis. All other species were discarded as contributing insufficient phylogenetic signal.

Finally, since the assembled alignment contained a different number of final total characters, the number of informative sites for each marker was analysed across our alignment (summarised in Table 1). Our alignment contained 5264 total sites, of which 1302 were parsimony informative. Of these informative sites, the three markers were found to contribute in almost identical proportions to that of the Bohs

Data partition	Aligned sequence length	# parsimony informative characters	% of total inf. characters
ndhF	1992	280	22
trnT-F	1518	305	23
waxy	1754	717	55
combined	5264	1302	100

Table 1 Descriptive statistics for each data set analysed. All sequences contributed a similar sequence length, but the number of informative characters differed greatly. The largest proportion of informative characters came from *waxy*, with 55% of the total (717/1302), while *trnT-F* and *ndhF* contributed 23% and 22% respectively (305/1302 and 280/1302).

alignment (*waxy* 55%, *trnT-F* 23%, *ndhF* 22%). This confirms that the species with incomplete sequence data that we chose to include did indeed have at or near 50% informative sites, and should have sufficient phylogenetic signal to justify inclusion in this analysis.

3.2.4 Comparison of final tree with published analyses

The tree we produced took a previous alignment of 102 *Solanum* species with 7 outgroup taxa, and added a further 31 *Solanum* species and 5 outgroup species (Figure 3.3). The alignment structure and choice of genes in this study were based on those of Weese & Bohs (2007) and deviated only slightly from their final alignments as downloaded from TreeBase. Weese & Bohs (2007) analysed their alignment using parsimony and Bayesian analyses. To judge the validity of the choice of maximum likelihood as the method of phylogenetic analysis for our alignment, we compared the positions of the 109 species in common to both analyses. We also compared the positions of species not in Weese & Bohs (2007) but which appear in other phylogenetic treatments of recent years, such as a large-scale study of subgenus Leptostemonum (Levin, Myers & Bohs 2006), a more detailed treatment within the Leptostemonum, clade Acanthophora (Levin, Watson & Bohs 2005) and others covering sections within the Potato clade and the Archaesolanum clade (Zuriaga, Blanca, & Nuez 2008; Poczai, Hyvönen, & Symon 2011).

All of the 102 *Solanum* species from the original Weese & Bohs (2007) phylogenetic analysis, when analysed by Maximum Likelihood analysis, fell into phylogenetic positions in agreement with the trees of Weese & Bohs. Of the 31 new species of *Solanum* added to the tree based on that of Weese & Bohs (2007), many had been previously analysed in other recent molecular phylogenies (Levin, Watson & Bohs 2005; Levin, Myers & Bohs 2006; Ames & Spooner 2010; Stern, Weese & Bohs 2010; Stern, Agra & Bohs 2011; Poczai, Hyvönen & Symon 2011; Stern *et al.* 2013) but never all together, making direct comparison of phylogenetic position difficult in some cases. Imposing on our tree a cutoff bootstrap value of 50% and collapsing any branches below this into polytomies, all of these species also appear in

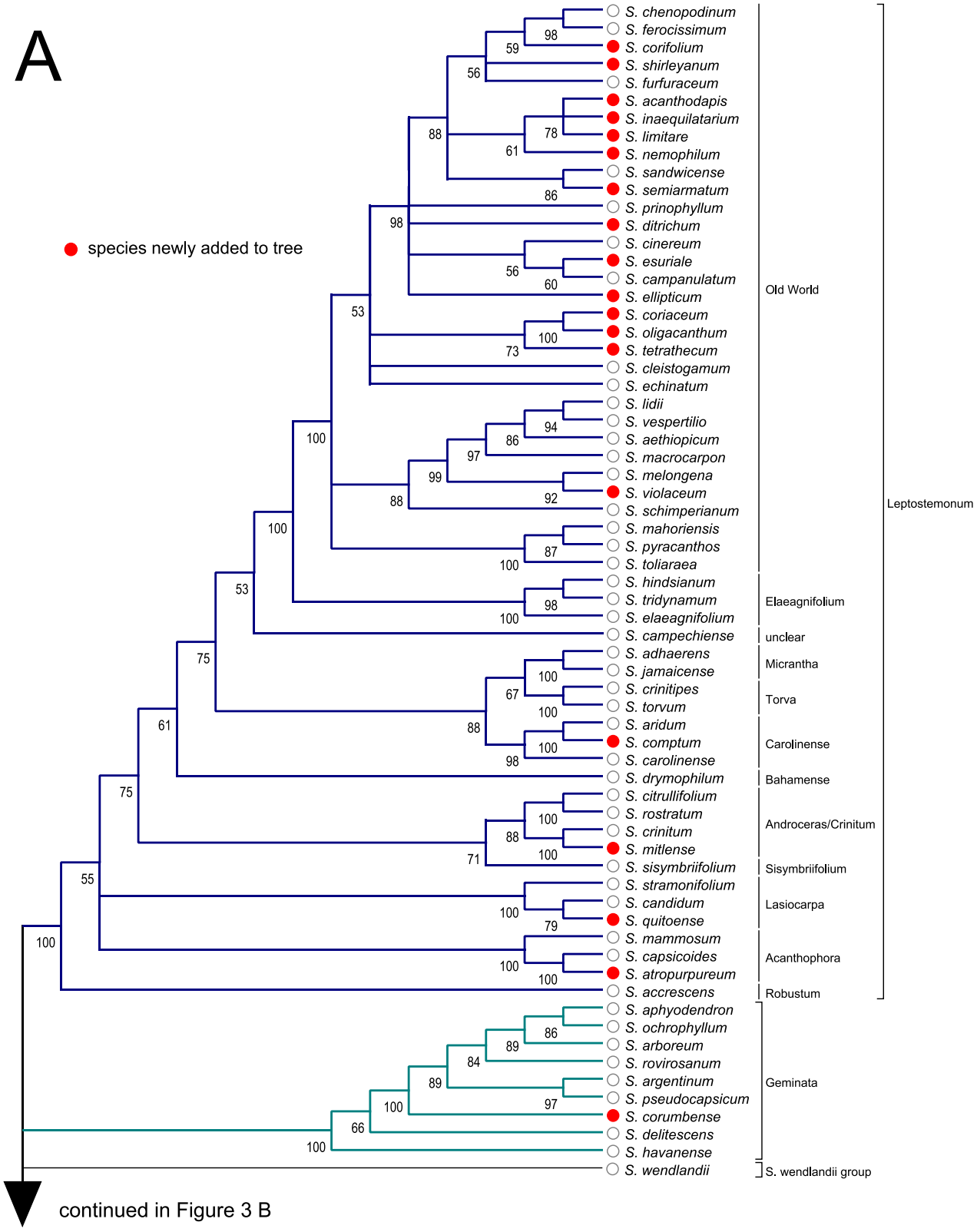
A
species newly added to tree
S. chenopodinum
S. ferocissimum
S. corifolium
S. shirleyanum
S. furfuraceum
S. acanthodapis
S. inaequilatarium
S. limitare
S. nemophilum
S. sandwicense
S. semiarmatum
S. prinophyllum
S. ditrichum
S. cinereum
S. esuriale
S. campanulatum
S. ellipticum
S. coriaceum
S. oligacanthum
S. tetrathecum
S. cleistogamum
S. echinatum
S. lidii
S. vespertilio
S. aethiopicum
S. macrocarpon
S. melongena
S. violaceum
S. schimperianum
S. mahoriensis
S. pyracanthos
S. toliaraea
S. hindsianum
S. tridynamum
S. elaeagnifolium
S. campechiense
S. adhaerens
S. jamaicense
S. crinitipes
S. torvum
S. aridum
S. comptum
S. carolinense
S. drymophilum
S. citrullifolium
S. rostratum
S. crinitum
S. mitlense
S. sisymbriifolium
S. stramonifolium
S. candidum
S. quitoense
S. mammosum
S. capsicoides
S. atropurpureum
S. accrescens
S. aphyodendron
S. ochrophyllum
S. arboreum
S. rovirosanum
S. argentinum
S. pseudocapsicum
S. corumbense
S. delitescens
S. havanense
S. wendlandii
Old World
Elaeagnifolium
unclear
Micrantha
Torva
Carolinense
Bahamense
Androceras/Crinitum
Sisymbriifolium
Lasiocarpa
Acanthophora
Robustum
Leptostemonum
Geminata
S. wendlandii group
continued in Figure 3 B

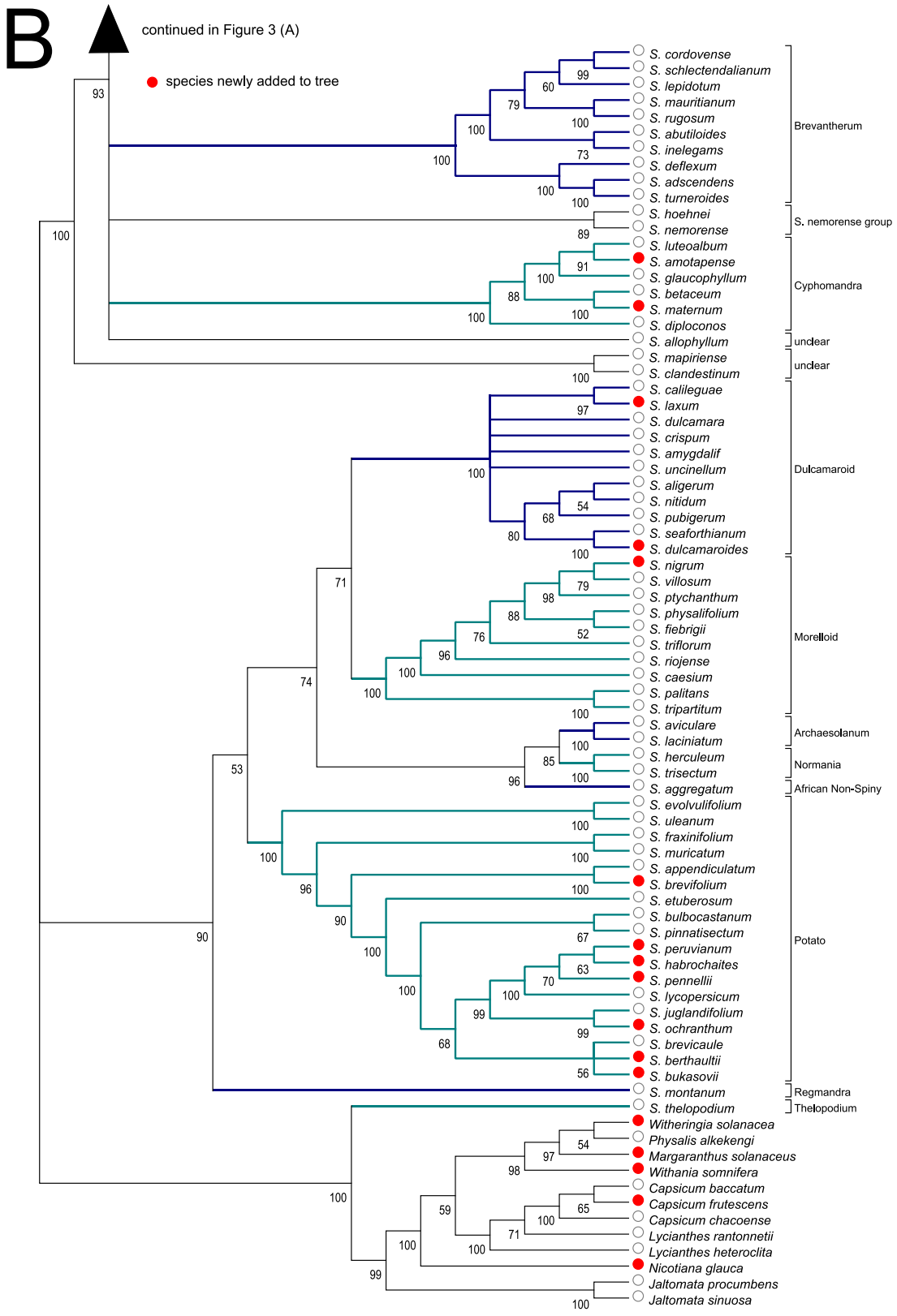

Figure 3.3 Final phylogenetic tree produced by Maximum Likelihood analysis using all three gene data sets, showing new species added to the tree. This tree uses the nucleotide alignment of 102 *Solanum* species and 7 outgroup taxa of Weese & Bohs 2007 and adds 36 new species (31 *Solanum* species and 5 outgroup species). All species in common between the two analyses appear in the same phylogenetic positions. Numbers at each node represent bootstrap values.

approximately the same phylogenetic positions as previous analyses. All appear in the same clades, and all group with the same sets of species within these clades. Some of these groupings in this analysis appear with minor differences in relatedness, or as unresolved polytomies. These differences do not affect the ancestral character state reconstruction, and additionally do not have reliable bootstrap support and so can be regarded as insignificant to this analysis. The similarity in position of common species in our final tree suggests that the choice of analysis here (maximum likelihood) is appropriate for this data, and produces similar conclusions. More importantly, the similarity in position between previous analyses and our final tree gives confidence in the positions of additional species, not previously analysed, which are incorporated in this tree.

3.2.5 Phylogenetic positions of new species added to tree

There were 25 new species added to the tree that had not received any recent molecular phylogenetic treatment. 12 species, *S. corifolium*, *S. shirleyanum*, *S. limitare*, *S. acanthodapis*, *S. inaequalitarium*, *S. semiarmatum*, *S. esuriale*, *S. ditrichum*, *S. ellipticum*, *S. oligacanthum*, *S. coriaceum* and *S. tetrathecum* (Figure 3.3) placed within the Old World Clade of Leptostemonum. *S. corifolium* places as sister to *S. chenopodinum* and *S. ferocissimum* with bootstrap support of 59%. *S. shirleyanum* then places in a polytomy with this group and *S. furfuraceum* with support of 56%. This group is then in a polytomy with *S. semiarmatum* sister to *S. sandwicense* (support 86%), and a group containing *S. acanthodapis*, *S. inaequalitarium* and *S. limitare* in a polytomy with *S. nemophilum* (support 61%). This group is then in a polytomy with one group of three species and three singleton species. *S. ditrichum* and *S. ellipticum* both place singly within this polytomy (98% support), and *S. esuriale* places as sister to *S. campanulatum* (60% support) in the group of three with *S. cinereum* (56% support). *S. coriaceum* and *S. oligacanthum* place as sister species in a group with *S. tetrathecum* (100% and 73% support respectively) in a polytomy at the base of the previously described section of the Old World Clade of Leptostemonum alongside *S. cleistogamum* and *S. echinatum* (53% support).

Outside of the Leptostemonum, *S. corumbense* fell into the Geminata clade, sister to a group containing *S. ochrophyllum* and *S. argentinum* amongst others, with 100% bootstrap support. Two species placed within the Cyphomandra, *S. amotapense* placing as sister to *S. luteoalbum* (91% support) and *S. maternum* sister to *S. betaceum* (100% support). *S. laxum* and *S. dulcamaroides* both placed in the Dulcamaroid clade, *S. laxum* sister to *S. calileguae* (97% support) and *S. dulcamaroides* sister with *S. seaforthianum* (100% bootstrap support). *S. nigrum* places within the Morelloid clade as sister to *S. villosum* with 79% support.

Seven species placed within the Potato clade. *S. brevifolium* places as sister to *S. appendiculatum* (100% bootstrap support), *S. ochranthum* is sister to *S. juglandifolium* (99% support) and *S. berthaultii* and *S. bukasovii* in a polytomy with *S. brevicaule*. Three species place in a group as sister to *S. lycopersicum* (100% support), *S. pennellii* sister to *S. habrochaites* and *S. peruvianum* (70% and 63% support respectively).

Each of these placements agrees with a preliminary placement of each of these species into clades within *Solanum* based on their morphology, by an experienced *Solanum* taxonomist, Sandy Knapp of the Natural History Museum, London, UK.

3.2.6 Reliability of epidermal petal morphological analysis

Of the data collected, petal cell morphology was scored as being highly reliable if the data was collected from fresh or fixed material (Figure 3.4).

From herbarium specimens, however, petal cell morphology could be difficult to discern. To minimise the risk of errors in judging petal cell morphology from herbarium specimens, fourteen species for which petal cell SEM images were available from fresh material were also analysed from herbarium specimens. The petal cells of the herbarium specimens were examined and imaged using SEM, and the sets of images compared. Herbarium specimens that showed tell-tale 'deflated balloon' pockets on each cell were easy to determine as conical celled and always agreed with cell shape determined from petal casts. Examples of this easily

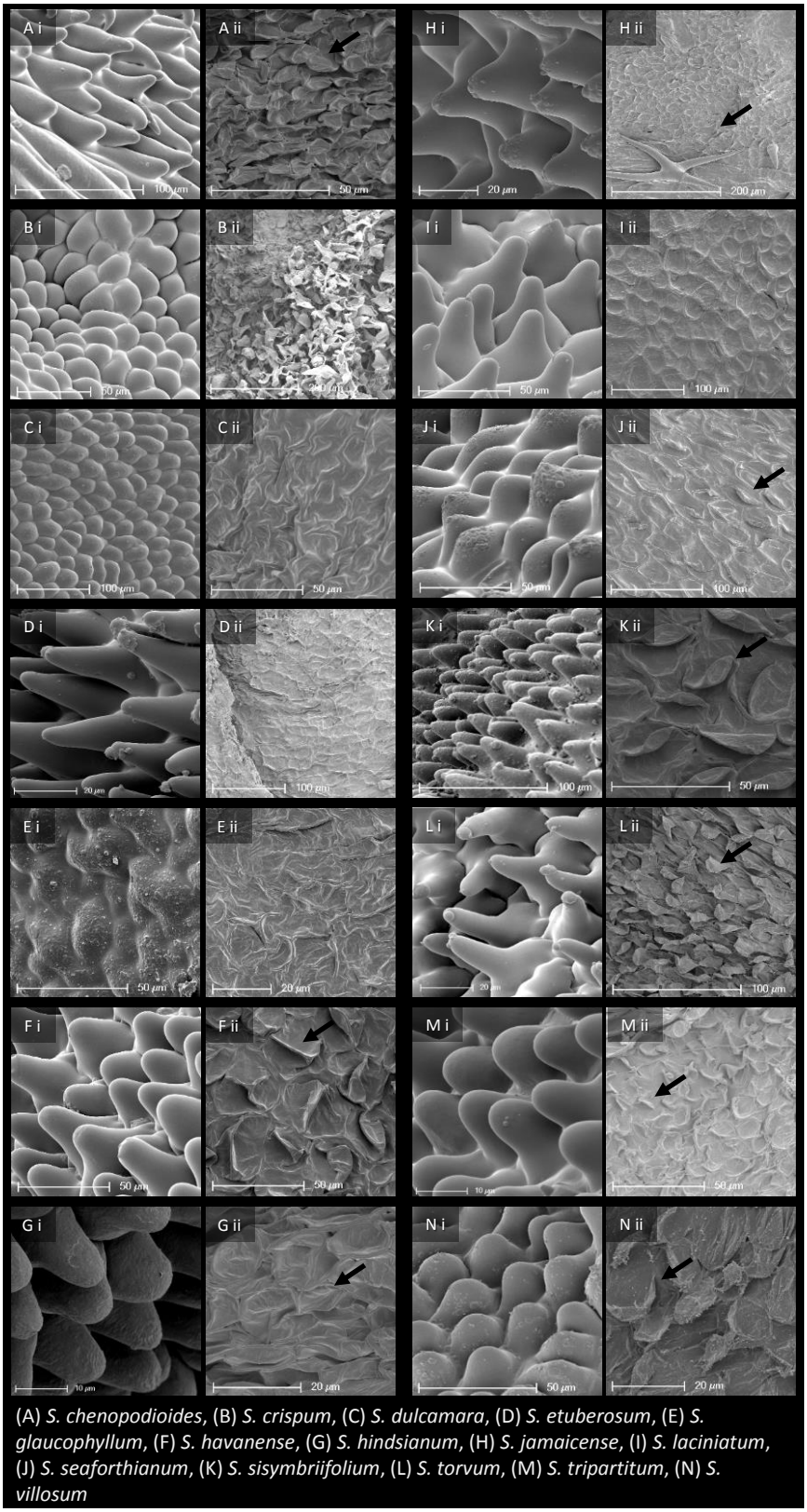

(A) *S. chenopodioides*, (B) *S. crispum*, (C) *S. dulcamara*, (D) *S. etuberosum*, (E) *S. glaucophyllum*, (F) *S. havanense*, (G) *S. hindsianum*, (H) *S. jamaicense*, (I) *S. laciniatum*, (J) *S. seaforthianum*, (K) *S. sisymbriifolium*, (L) *S. torvum*, (M) *S. tripartitum*, (N) *S. villosum*

Figure 3.4 Scanning electron micrographs of *Solanum* petal cell surfaces. Of each pair of images, (i) is an image of a cast from fresh material, or fixed material; (ii) is an image from a herbarium specimen from the same species. Arrows indicate telltale 'deflated balloon' pockets which are indicators of conical epidermal cells in herbarium specimens.

determinable petal cell form can be seen in Figure 3.4 A, F, G, I, J, K, L, M and N. Herbarium specimens lacking this distinctive feature were much harder to determine petal cell morphology from, and introduced a greater uncertainty into this analysis. If any evidence of conical cell form could be seen anywhere on the petals, these were scored as conical-celled. Examples of this can be seen in Figure 3.4 B, E and H. The final category of herbarium specimens included all specimens showing no evidence of conical cell form. The cell morphology of these specimens was more difficult to determine because of the lack of evidence. For this project we chose to take a conservative approach in order not to overestimate the number of times conical cells have been lost, and so every case that was ambiguous was scored as conical. This means that every time a herbarium specimen was scored as flat-celled, we have a high degree of certainty that this species does actually have flat petal cells.

More difficult cases included specimens with folded, wrinkled or densely trichome-covered petals. For example, with *S. crispum* the herbarium specimen showed dense trichomes across all visible surfaces, but the petals were folded and curled inwards towards the anthers and this made identification of the pollinator-facing (adaxial) side of the petals difficult. The image included here (Figure 3.4 B ii) shows a twisted petal, with trichomes on what appears to be the abaxial (back) of the petal obscuring a region where cells appear smoother, but with trichomes scattered across. The petal cast image shown (Figure 3.4 B i) shows a region of adaxial petal most representative of the majority of cells across the adaxial petal surface, though trichomes were also scattered across each petal in other sections of the cast (not shown).

The character states of all species surveyed, along with the reliability of each data point as from fresh/fixed or herbarium material, are shown in Figure 3.5.

3.2.7 Distribution of conical cell losses throughout *Solanum*

On a molecular level, losses of a trait are intuitively more likely than gains due to the high probability of any random mutation in either regulatory or coding sequences being deleterious (Charlesworth 2012). Additionally, re-evolution of a

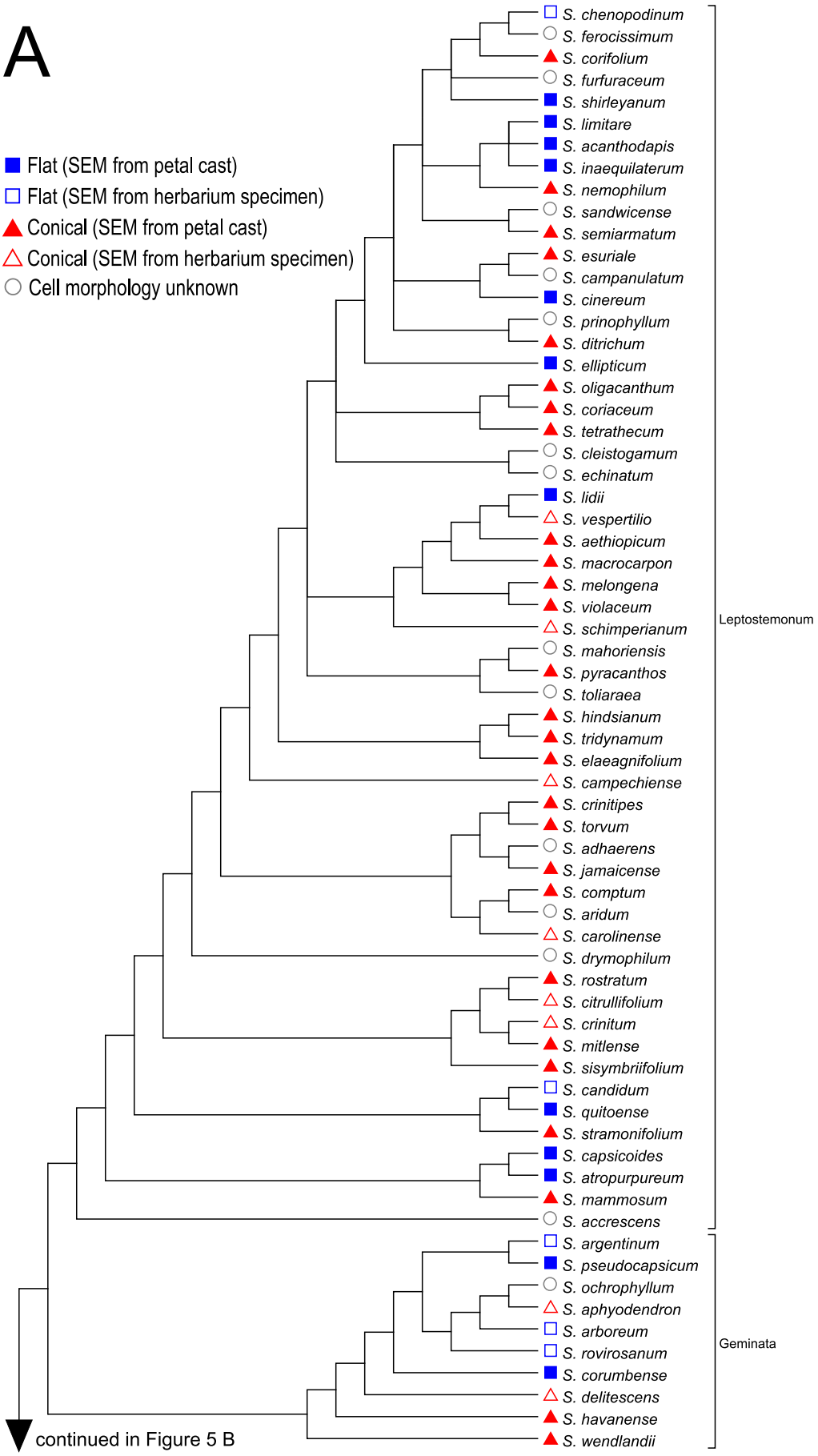
A
Flat (SEM from petal cast)
Flat (SEM from herbarium specimen)
Conical (SEM from petal cast)
Conical (SEM from herbarium specimen)
Cell morphology unknown
S. chenopodinum
S. ferocissimum
S. corifolium
S. furfuraceum
S. shirleyanum
S. limitare
S. acanthodapis
S. inaequilaterum
S. nemophilum
S. sandwicense
S. semiarmatum
S. esuriale
S. campanulatum
S. cinereum
S. prinophyllum
S. ditrichum
S. ellipticum
S. oligacanthum
S. coriaceum
S. tetrathecum
S. cleistogamum
S. echinatum
S. lidii
S. vespertilio
S. aethiopicum
S. macrocarpon
S. melongena
S. violaceum
S. schimperianum
S. mahoriensis
S. pyracanthos
S. toliaraea
S. hindsianum
S. tridynamum
S. elaeagnifolium
S. campechiense
S. crinitipes
S. torvum
S. adhaerens
S. jamaicense
S. comptum
S. aridum
S. carolinense
S. drymophilum
S. rostratum
S. citrullifolium
S. crinitum
S. mitlense
S. sisymbriifolium
S. candidum
S. quitoense
S. stramonifolium
S. capsicoides
S. atropurpureum
S. mammosum
S. accrescens
S. argentinum
S. pseudocapsicum
S. ochrophyllum
S. aphyodendron
S. arboreum
S. rovirosanum
S. corumbense
S. delitescens
S. havanense
S. wendlandii
Leptostemonum
Geminata
continued in Figure 5 B

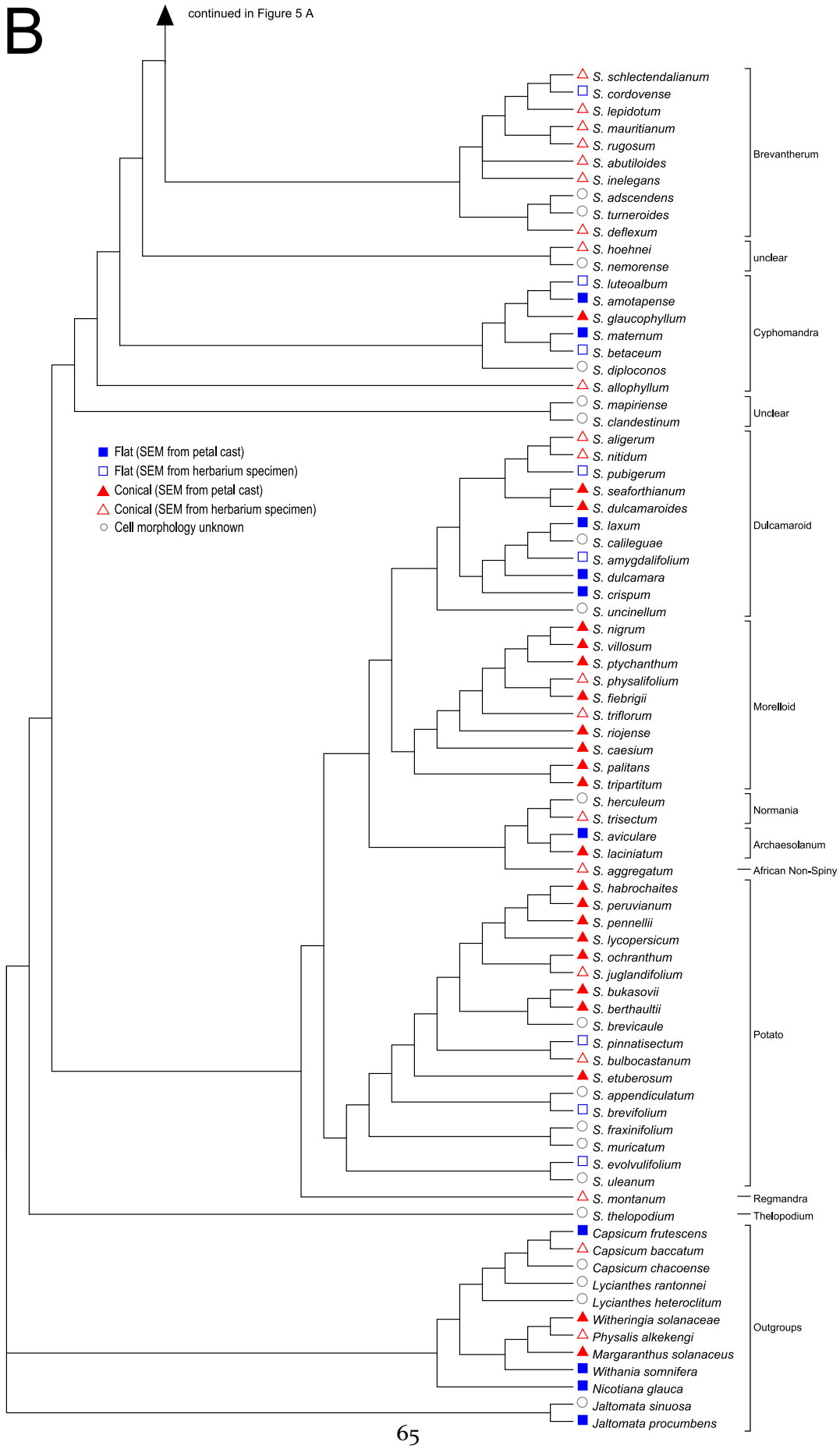
B
continued in Figure 5 A
Flat (SEM from petal cast)
Flat (SEM from herbarium specimen)
Conical (SEM from petal cast)
Conical (SEM from herbarium specimen)
Cell morphology unknown
S. schlechtendalianum
S. cordovense
S. lepidotum
S. mauritianum
S. rugosum
S. abutiloides
S. inelegans
S. adscendens
S. turneroides
S. deflexum
S. hoehnei
S. nemorense
S. luteoalbum
S. amotapense
S. glaucophyllum
S. maternum
S. betaceum
S. diploconos
S. allophyllum
S. mapiriense
S. clandestinum
S. aligerum
S. nitidum
S. pubigerum
S. seaforthianum
S. dulcamaroides
S. laxum
S. calileguae
S. amygdalifolium
S. dulcamara
S. crispum
S. uncinellum
S. nigrum
S. villosum
S. ptychanthum
S. physalifolium
S. fiebrigii
S. triflorum
S. riojense
S. caesium
S. palitans
S. tripartitum
S. herculeum
S. trisectum
S. aviculare
S. laciniatum
S. aggregatum
S. habrochaites
S. peruvianum
S. pennellii
S. lycopersicum
S. ochranthum
S. juglandifolium
S. bukasovii
S. berthaultii
S. brevicaule
S. pinnatisectum
S. bulbocastanum
S. etuberosum
S. appendiculatum
S. brevifolium
S. fraxinifolium
S. muricatum
S. evolvulifolium
S. uleanum
S. montanum
S. thelopodium
Capsicum frutescens
Capsicum baccatum
Capsicum chacoense
Lycianthes rantonnei
Lycianthes heteroclitum
Witheringia solanaceae
Physalis alkekengi
Margaranthus solanaceus
Withania somnifera
Nicotiana glauca
Jaltomata sinuosa
Jaltomata procumbens
Brevantherum
unclear
Cyphomandra
Unclear
Dulcamaroid
Morelloid
Normania
Archaesolanum
African Non-Spiny
Potato
Regmandra
Thelopodium
Outgroups

Figure 3.5 (A), (B) Final phylogenetic tree produced by Maximum Likelihood analysis using all three markers, showing known petal cell morphology states. This tree uses the nucleotide alignment of 102 *Solanum* species and 7 outgroup taxa of Weese & Bohs 2007 and adds 36 new species (31 Solanum species and 5 outgroup species). All species in common between the two analyses appear in the same phylogenetic positions. Flat-celled species appear in the Leptostemonum, Geminata, Brevantherum, Cyphomandra, Dulcamaroid, Archaesolanum and Potato clades.

trait requires either repair or re-evolution of its genetic determinants and may be difficult due to constraints imposed by previous specialisation (Tripp & Manos 2008). However, since the selective pressures acting on the trait of conical petal cells in *Solanum* are unknown, the likelihood of any mutation becoming fixed in the population, whether this mutation leads to trait loss or gain, is unknown (Hughes 2007; Fay 2011; Charlesworth 2012; Wessinger & Rausher 2012). We therefore used parsimony ancestral character reconstruction, an analysis unbiased towards either losses or gains of a trait, to predict the most likely position of each character state change. This method has been used in many recent studies to predict the ancestral state of floral morphology changes (Jaramillo, Manos & Zimmer 2004; Pérez & Arroyo 2006; Endress & Doyle 2009; Cohen 2012; Riviere *et al.* 2013).

In total, of the 104 *Solanum* species for which petal cell shape was analysed, 29% were flat-celled. Since on average only 20% of angiosperms have flat petal cells, this indicates that conical cells have been lost in *Solanum* at a higher rate than that of flowering plants in general.

Ancestral character reconstruction using parsimony to predict the most likely position of each character state change predicts that conical cells are ancestral to *Solanum*, and shows 14 potential losses of conical cells spread throughout the genus (Figure 3.6). Of the twelve *Solanum* clades for which petal cell data was obtained, seven clades contain one or more losses. Seven of the losses occur within the Leptostemonum alone, two occur in Dulcamaroides and two in Potato, and a single loss was identified in each of Geminata, Brevantherum, Archaesolanum, and at the base of Cyphomandra. This analysis also indicates four potential cases of a re-acquisition of conical petal morphology, in Leptostemonum (Old World Clade), Geminata and Potato.

The Old World Clade contains five of the losses within Leptostemonum. One is predicted to have occurred in the last common ancestor of the flat-celled species *S. chenopidinum*, *S. ferocissimum* and *S. shirleyanum*, where *S. corifolium* (conical-celled) in the same group is then predicted to have re-evolved conical petal cells. If, on the other hand, the losses of conical cells occurred prior to the divergence of *S. shirleyanum* from the section containing *S. chenopodinum*, *S. ferocissimum* and *S. corifolium*, then two independent losses of conical petal cells are predicted to have occurred in this lineage and the conical cells of *S. corifolium* would then represent the ancestral character state. Sister to this group is a section containing three flat-celled species (*S. inaequilatarium*, *S. acanthodapis* and *S. limitare*) and one species with conical petal cells (*S. nemophilum*). This group contains the second loss in this clade. The third loss is predicted from a single species, *S. cinereum*, and other single losses are predicted in *S. ellipticum* and then *S. lidii*. The final two losses are predicted from two separate instances of two flat-celled species sister to one conical-celled species, *S. candidum* and *S. quitoense* (flat-celled) sister to *S. stramonifolium* (conical-celled) and *S. capsicoides* and *S. atropurpureum* (flat-celled) sister to *S. mammosum* (conical-celled).

In Geminata, the single loss is predicted to have occurred in the last common ancestor of the group with *S. corumbense* at its base and including *S. argentinum* and *S. arboreum*. Also in this group occurs the second case of a predicted re-acquisition of conical cells, in *S. aphyodendron*. The Brevantherum clade contains only one flat-celled species, *S. cordovense*, determined by this analysis to represent another independent loss. The loss in Cyphomandra occurs at the base of this group, and indicates a re-acquisition of conical cells in *S. glaucophyllum*. The Dulcamaroid clade contains two possible predicted losses, one represented by the single species *S. pubigerum* and one by a group of species including *S. laxum* and *S. dulcamara*. One loss occurs in Archaesolanum in *S. aviculare*. The final two losses occur in Potato, one predicted to place at the base of this clade. A re-acquisition of conical cells is then predicted to occur at *S. etuberosum*, and all species in the section sister to *S. etuberosum* are conical celled except for *S. pinnatisectum*, which represents the final independent loss of conical cells identified by this study.

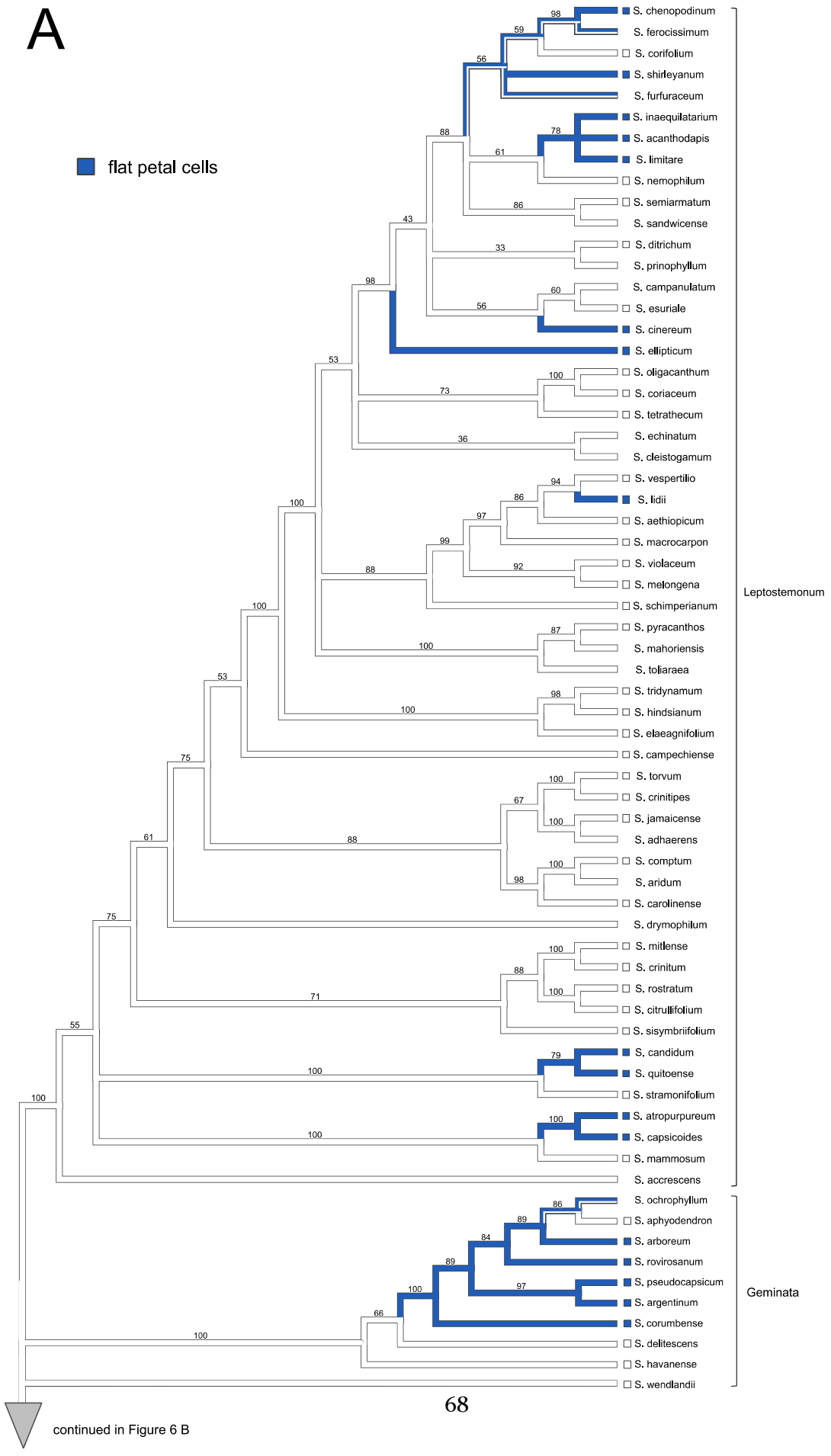
A
flat petal cells
S. chenopodinum
S. ferocissimum
S. corifolium
S. shirleyanum
S. furfuraceum
S. inaequilatarium
S. acanthodapis
S. limitare
S. nemophilum
S. semiarmatum
S. sandwicense
S. ditrichum
S. prinophyllum
S. campanulatum
S. esuriale
S. cinereum
S. ellipticum
S. oligacanthum
S. coriaceum
S. tetrathecum
S. echinatum
S. cleistogamum
S. vespertilio
S. lidii
S. aethiopicum
S. macrocarpon
S. violaceum
S. melongena
S. schimperianum
S. pyracanthos
S. mahoriensis
S. toliaraea
S. tridynamum
S. hindsianum
S. elaeagnifolium
S. campechiense
S. torvum
S. crinitipes
S. jamaicense
S. adhaerens
S. comptum
S. aridum
S. carolinense
S. drymophilum
S. mitlense
S. crinitum
S. rostratum
S. citrullifolium
S. sisymbriifolium
S. candidum
S. quitoense
S. stramonifolium
S. atropurpureum
S. capsicoides
S. mammosum
S. accrescens
S. ochrophyllum
S. aphyodendron
S. arboreum
S. rovirosanum
S. pseudocapsicum
S. argentinum
S. corumbense
S. delitescens
S. havanense
S. wendlandii
Leptostemonum
Geminata
continued in Figure 6 B

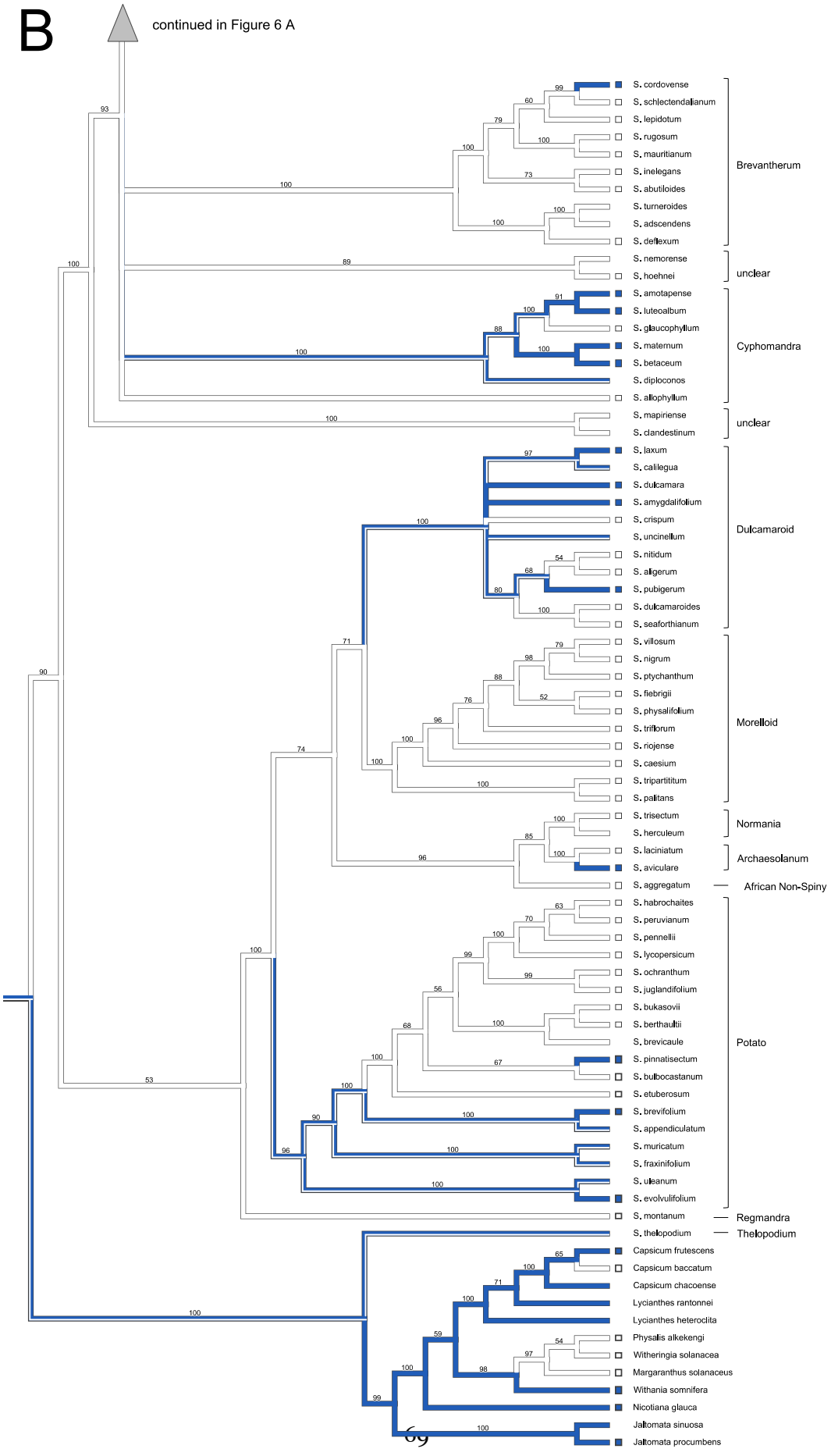
B
continued in Figure 6 A
S. cordovense
S. schlechtendalianum
S. lepidotum
S. rugosum
S. mauritianum
S. inelegans
S. abutiloides
S. turneroides
S. adscendens
S. deflexum
Brevantherum
S. nemorense
S. hoehnei
unclear
S. amotapense
S. luteoalbum
S. glaucophyllum
S. maternum
S. betaceum
S. diploconos
S. allophyllum
Cyphomandra
S. mapiriense
S. clandestinum
unclear
S. laxum
S. callilegua
S. dulcamara
S. amygdalifolium
S. crispum
S. uncinellum
S. nitidum
S. aligerum
S. pubigerum
S. dulcamaroides
S. seaforthianum
Dulcamaroid
S. villosum
S. nigrum
S. ptychanthum
S. fiebrigii
S. physalifolium
S. triflorum
S. riojense
S. caesium
S. tripartititum
S. palitans
Morelloid
S. trisectum
S. herculeum
Normania
S. laciniatum
S. aviculare
Archaesolanum
S. aggregatum
African Non-Spiny
S. habrochaites
S. peruvianum
S. pennellii
S. lycopersicum
S. ochranthum
S. juglandifolium
S. bukasovii
S. berthaultii
S. brevicaule
S. pinnatisectum
S. bulbocastanum
S. etuberosum
S. brevifolium
S. appendiculatum
S. muricatum
S. fraxinifolium
S. uleanum
S. evolvulifolium
Potato
S. montanum
Regmandra
S. thelopodium
Thelopodium
Capsicum frutescens
Capsicum baccatum
Capsicum chacoense
Lycianthes rantonnei
Lycianthes heteroclita
Physalis alkekengi
Witheringia solanacea
Margaranthus solanaceus
Withania somnifera
Nicotiana glauca
Jaltomata sinuosa
Jaltomata procumbens

Figure 3.6 (A), (B) Parsimony ancestral character reconstruction of petal cell shape ancestral state. Character states of included species are represented by a blue square for flat-celled species and a white square for conical-celled species. Predicted flat-celled ancestral state is represented by blue filled branches, conical cells by white; branches half blue, half white indicate uncertainty as to ancestral state. Parsimony analysis predicts conical cells are ancestral to Solanum and shows fourteen independent losses of conical cells. Seven of these losses occur within the Leptostemonum, and at least one loss occurs in every clade of Solanum except Normania, in which we have data for only one species. Numbers on branches represent bootstrap values.

Due to the number of outgroup species for which petal cell morphology is unknown (two-thirds of all outgroup species), the prediction of conical cell gains and losses in the outgroups is likely to be highly unreliable and should not be taken as a representation of ancestral petal cell state in the Solanaceae.

3.2.8 Comparison of ancestral character reconstruction with previous published analyses

Previous studies using ancestral character reconstruction have shown that floral traits can differ greatly in their degree of evolutionary lability. In a study of *Ruellia*, Tripp & Manos (2008) found that floral specialisations associated with bat or hawkmoth pollination, once evolved, then act to constrain plants from re-evolving traits to exploit ancestral pollinators such as bees. The opposite is true for traits associated with bee and hummingbird pollination, which they found to be highly labile and to allow pollinator shifts to occur easily (Tripp & Manos 2008). Other floral traits shown to be highly labile include corolla length in *Lithospermum* (Cohen 2012) and floral organ number in the basal angiosperms (Craene, Soltis & Soltis 2003). The analyses presented in this chapter show that conical petal cells have a similarly high degree of evolutionary lability. This suggests that as pollinator shifts occur, conical cells can be easily lost or re-evolved depending on the selective advantage to the plant.

Finally, floral evolution that appears to favour a particular pollinator specialisation may occur in the absence of any evidence of that pollinator. For example, in *Schizanthus*, Pérez & Arroyo (2006) found some correlation between pollinator shifts and floral features for bee and bird pollination, but also found that many flowers with characteristics of moth pollination had no evidence of moth pollinators actually visiting the flowers.

3.3 Conclusions

The many instances of petal cell morphology changes in *Solanum*, from conical to flat as well as from flat to conical, suggests that within this genus possession of conical cells is a highly labile trait that can change with relative ease. The major limitation of this study, like any involving a genus of this size, is that of taxon sampling. Of the total number of species in the genus *Solanum*, this analysis covers at most 11% of these species. The analysis we have completed here gives a solid preliminary estimate of the number of losses of conical petal cells that have occurred across *Solanum*. The actual number of losses across the extant species of this genus is, therefore, in all probability much greater than that predicted by this project.

While an analysis of this kind allows for broad predictions to be made regarding evolutionary patterns, the limitation of taxon sampling does restrict the precision with which we can place the ancestral losses of conical cells across the *Solanum* genus in detail. However, the major strength of this kind of analysis is that it allows us to look across the genus as a whole, identify areas of interest, and then focus study down closer into regions for more detailed analysis.

The analysis detailed in this chapter has allowed us to predict the frequency of conical cell loss across the genus *Solanum*. We predict that there are a minimum of fourteen losses of conical cells across *Solanum*, and that these are spread across seven of the twelve clades of *Solanum*. These predictions have allowed the identification of sections of *Solanum* in which to focus further study. From this information, species pairs were chosen on which to complete more detailed studies. These species, their petal morphologies and the reasons for their selection are detailed in chapter 4.

Chapter 4. *Solanum* sister species comparisons

4.1 Introduction

The previous Chapter reported evidence of multiple independent losses of conical petal cells across the genus *Solanum*. The fourteen losses identified in the previous Chapter are spread throughout *Solanum*, occurring in seven of the twelve major clades (Levin, Watson, & Bohs 2005) of which eleven clades were tested. In some clades there is evidence that more than one independent loss has occurred, such as in the Leptostemonum. As each loss represents an independent evolutionary event, the molecular means by which a loss has occurred has the potential to be different in each case.

One instance of conical petal cell loss in *Solanum* has previously been studied using *S. dulcamara* (Dulcamaroid clade). This project chose to investigate two further independent losses of conical cells in *Solanum* to in order to study the repeatability of evolution. To better understand the molecular mechanism of each loss, we selected closely related species pairs from clades other than Dulcamaroid. Each species pair comparison included one conical-celled and one flat-celled species.

Over the next three Chapters of this thesis, the sequence, expression and function of R2R3 MYB Subgroup 9A genes (Stracke, Werbfer & Weisshaar 2001; Brockington *et al.* 2013) isolated from each species will be analysed. This Chapter will describe

how each species pair was chosen and compare the amino acid sequences of proteins encoded by genes isolated from each species.

4.1.1 Expected number of R2R3 MYB Subgroup 9A genes in *Solanum* species

Conical petal cells are known to be produced by *MITXA*-Like genes, as described in Chapter 1, section 1.2.6. These genes have recently been shown to fall into the Subgroup 9A clade of the Subgroup 9 R2R3 MYB genes (Brockington *et al.* 2013). R2R3 MYB Subgroup 9A genes occur in differing numbers in different plant lineages. *Antirrhinum majus* has at least four separate Subgroup 9A genes (Noda *et al.* 1994; Martin *et al.* 2002; Jaffé, Tattersall, & Glover 2007; Baumann *et al.* 2007), while in *Petunia hybrida* to date only one Subgroup 9A gene has been identified (van Houwelingen *et al.* 1998; Baumann *et al.* 2007). The sequenced genome of *Arabidopsis thaliana* contains 2 Subgroup 9A genes (The Arabidopsis Genome Initiative 2000; Stracke *et al.* 2001). Prior to this project, *MIXTA*-like genes had been identified and studied in two *Solanum* species, *S. dulcamara* (flat-celled; Glover & Martin 1998, Glover *et al* in prep) and *S. lycopersicum* (conical-celled, work performed within this research group). Two Subgroup 9A genes each have been found in *S. lycopersicum* (*SlMIXTA*, DB707584.1, Aoki *et al.* 2010; PUT-161a, Goodstein *et al.* 2012) and in *S. dulcamara* (*SdMybML1* and *SdMybML2*, Glover et al in prep.). The screen for Subgroup 9A genes in *S. dulcamara* was of high stringency, leaving a low probability of any further Subgroup 9A genes being present and undiscovered in this species. This implies that for closely-related species within the genus *Solanum*, it would be unlikely for more than two *MIXTA*-like genes to be present in any given species. During the final years of this project the sequenced genomes of tomato (*S. lycopersicum*) and potato (*S. tuberosum*) were published (The Potato Genome Sequencing Consortium 2011; The Tomato Genome Consortium 2012), each of which was confirmed to contain two Subgroup 9A genes.

We focused our initial search on genes that were most closely related to *SdMybML2* from *S. dulcamara*. Of the two Subgroup 9A genes in *S. dulcamara*, *SdMybML2* had the strongest effect on cell outgrowth when ectopically expressed. *SdMybML2* is also

most similar in sequence to the *PhMyb1* gene, which is responsible for conical petal cell formation in *Petunia hybrida* (van Houwelingen *et al.* 1998; Baumann *et al.* 2007).

Late in this project, work by another member of the research group (Dr Samuel Brockington) produced a phylogenetic reconstruction of the Subgroup 9A R2R3 MYB genes across the plant kingdom (Brockington *et al.* 2013). This phylogeny showed that seed plant Subgroup 9 genes fall into two major lineages, the Subgroup 9A clade and Subgroup 9B clade, reflecting an ancient gene duplication event prior to the divergence of seed plants (Figure 4.1). Key representatives of the genes found during this project were included in this phylogenetic analysis, and all were found to fall within the Subgroup 9A clade.

The Subgroup 9A clade is divided into two lineages, *MIXTA* and *MIXTA*-like, which originated from a duplication at the base of the core eudicots (Brockington *et al.* 2013). The *MybMx* genes found in this project were all found to group within the *MIXTA* lineage, and the *MybML* genes within the *MIXTA*-like lineage. Representatives of both these lineages have been previously shown to be capable of producing a conical-celled phenotype. The Subgroup 9A genes previously characterised in *S. dulcamara* also follow this pattern, with *SdMybML2* being orthologous to the *MybML* genes characterised in this project (i.e. a member of the *MIXTA*-LIKE clade) and *SdMybML1* orthologous to the *MybMx* genes characterised here (i.e. a member of the *MIXTA* clade).

Functions of Subgroup 9B genes are largely unexplored and no genes in this clade have been associated with a conical cell phenotype, except for one from *Lotus japonicus*, a Rosid, which is only distantly related to *Solanum* (an Asterid). Subgroup 9B consists of two major subclades, *Myb 17* (from *Arabidopsis thaliana AtMyb17*) and *Myb 17*-like. The *Lotus japonicus* gene in this subgroup that produces a conical cell phenotype when expressed in tobacco is in the *Myb 17*-like clade, while the only genes from the genus *Solanum* that appear in the Subgroup 9B clade have never been functionally characterised, have not been shown to be associated with a conical cell phenotype, and are more closely related to *AtMyb17,* which has been associated

with flowering commitment (Jakoby *et al.* 2008; Zhang *et al.* 2009; Winter *et al.* 2011).

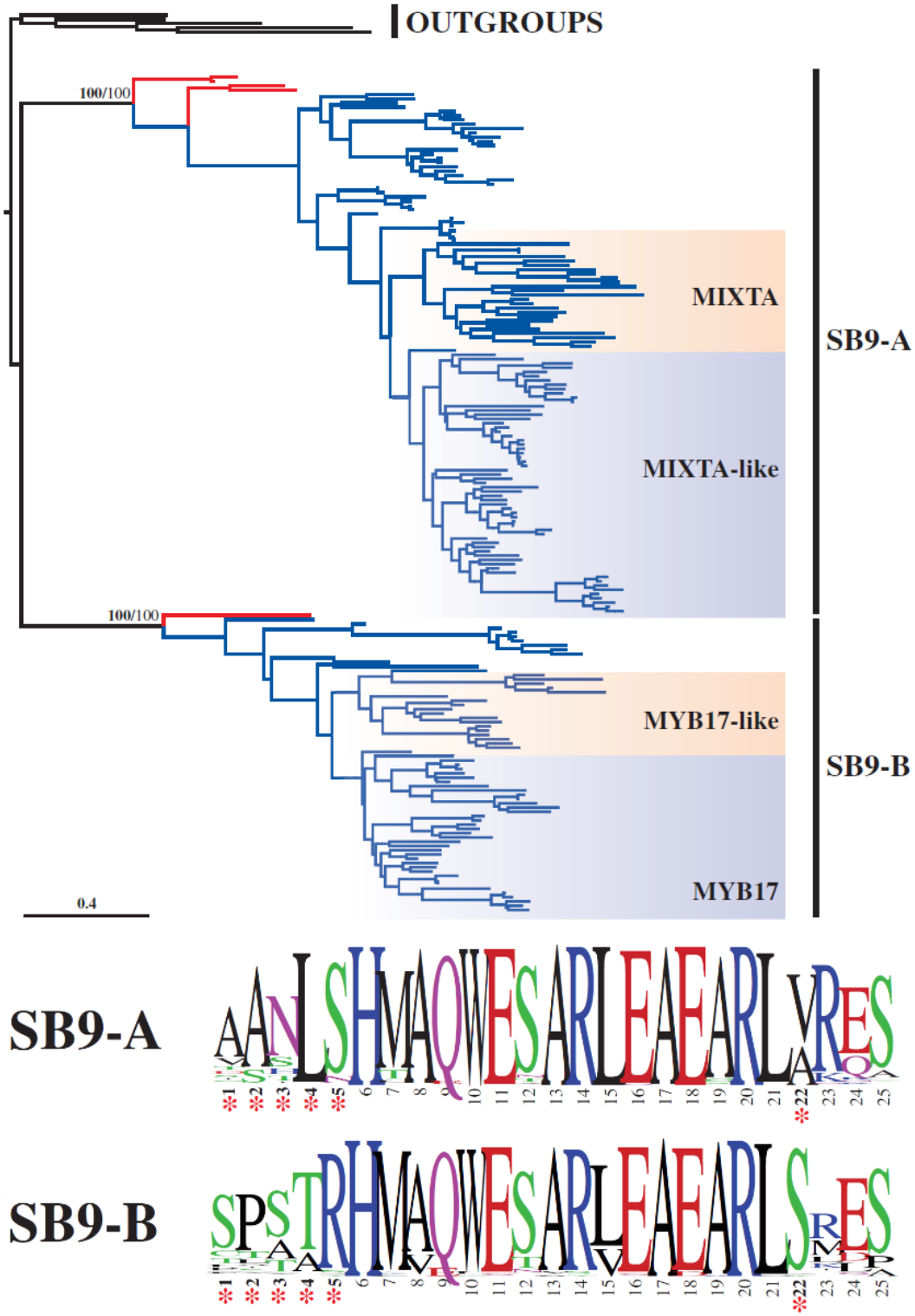

Figure 4.1 Overview of the R2R3 MYB Subgroup 9A gene phylogeny. Red lines correspond to gymnosperm species, blue lines to angiosperm species and black lines to outgroup species. All Solanum genes discovered and characterised by this project fall into the SB9-A clade. Figure taken from Brockington et al. (2013).

4.1.2 R2R3 MYB Subgroup 9A genes in *Solanum dulcamara*

Prior to this project, one loss of conical cells that occurred in the Dulcamaroid clade of *Solanum* had been studied in *S. dulcamara*. This species was shown to have lost conical cells through a change in expression of its *MIXTA* genes, which now produce trichomes on the leaf surface (B. Glover *et. al.* in prep).

Two genes that contain the MYB Subgroup 9 domain (as described by Stracke, Werber & Weisshaar 2001) were isolated from *S. dulcamara*, *SdMybML1* and *SdMybML2*. Heterologous expression of *SdMybML1* and *SdMybML2* in tobacco produced ectopic conical cells on carpel tissue, showing that the proteins encoded by the two genes were able to recognise and bind to the promoters of target genes required for conical cell formation in a closely-related species. This shows that the proteins are still able to function as an initiator of conical cell outgrowth, and suggests that it is not a change to the proteins that has caused the loss of conical petal cells in this species. Transcript reduction of *SdMybML1* by RNAi resulted in lower trichome density on leaves, and overexpression increased trichome density on leaves as well as producing outgrowths of petal epidermal cells. Transcript reduction of *SdMybML2* by RNAi reduced average trichome length, and overexpression produced increased trichome number and length on the leaves as well as producing petal epidermal outgrowths. These data show that these two proteins are capable of inducing conical cell differentiation in the petals of *S. dulcamara* and additionally that they are also capable of affecting trichome number and length in the leaves.

Overexpression of *AmMIXTA* in *S. dulcamara* produced outgrowths of the petal epidermal cells, mostly domed cells, but occasional trichomes also developed. Conical cells also formed on the leaves, along with an increase in leaf trichome density. That *AmMIXTA* can produce these cellular outgrowths in *S. dulcamara* suggests that *AmMIXTA* is similar enough to *SdMybML1* and *SdMybML2* that it is able to recognise and bind to the target genes required for conical cell formation in *S. dulcamara*. More importantly, this result indicates that the pathway required for conical cell formation is still present and able to be recruited to cellular outgrowth.

This strongly suggests that it is the regulation of the pathway that has changed, rather than any downstream targets, to cause the loss of conical cells in the petals.

Quantitative RT-PCR showed *SdMybML1* to have high expression in leaves at all stages of development, and low expression in flowers and all other organs tested. *SdMybML2* was highly expressed in developing leaves at 10mm in length, but showed low expression at other leaf developmental stages, in flowers, and in all other tissue types measured. This shows that the level of expression of the Subgroup 9 genes is highest where cellular outgrowths are produced, and low in petals where cells are flat. Taken together, the data collected in this related study on *S. dulcamara* indicate that a change in expression pattern of the R2R3 MYB Subgroup 9A genes has caused the loss of conical petal epidermal cells.

4.1.3 Choice of species

At the beginning of this project only a few closely-related species that were reliably placed in recent molecular phylogenies had recorded petal epidermal cell shape. Additionally, many of the species with recorded petal epidermal cell shape were known to have a growth habit that would preclude greenhouse cultivation, such as the tree species of the Cyphomandra clade. These constraints significantly limited the options for our choice of sister species pairs for comparison.

The Leptostemonum clade contained the largest number of possible test candidates, and it also brought the additional benefit of being relatively distant from the Dulcamaroid clade where one instance of conical cell loss had already been investigated. We were able to infer at the outset of this project, from preliminary data available in the lab, that the loss of conical petal cells in the Dulcamaroid clade most likely occurred in a separate event from the loss of conical cells in Leptostemonum. This was later confirmed by the phylogenetic and character mapping work described in Chapter 3.

From Leptostemonum *S. capsicoides* was selected as a flat-celled test species, and *S. sisymbriifolium* as the conical-celled comparator (Figure 4.3 A-D). Both these species

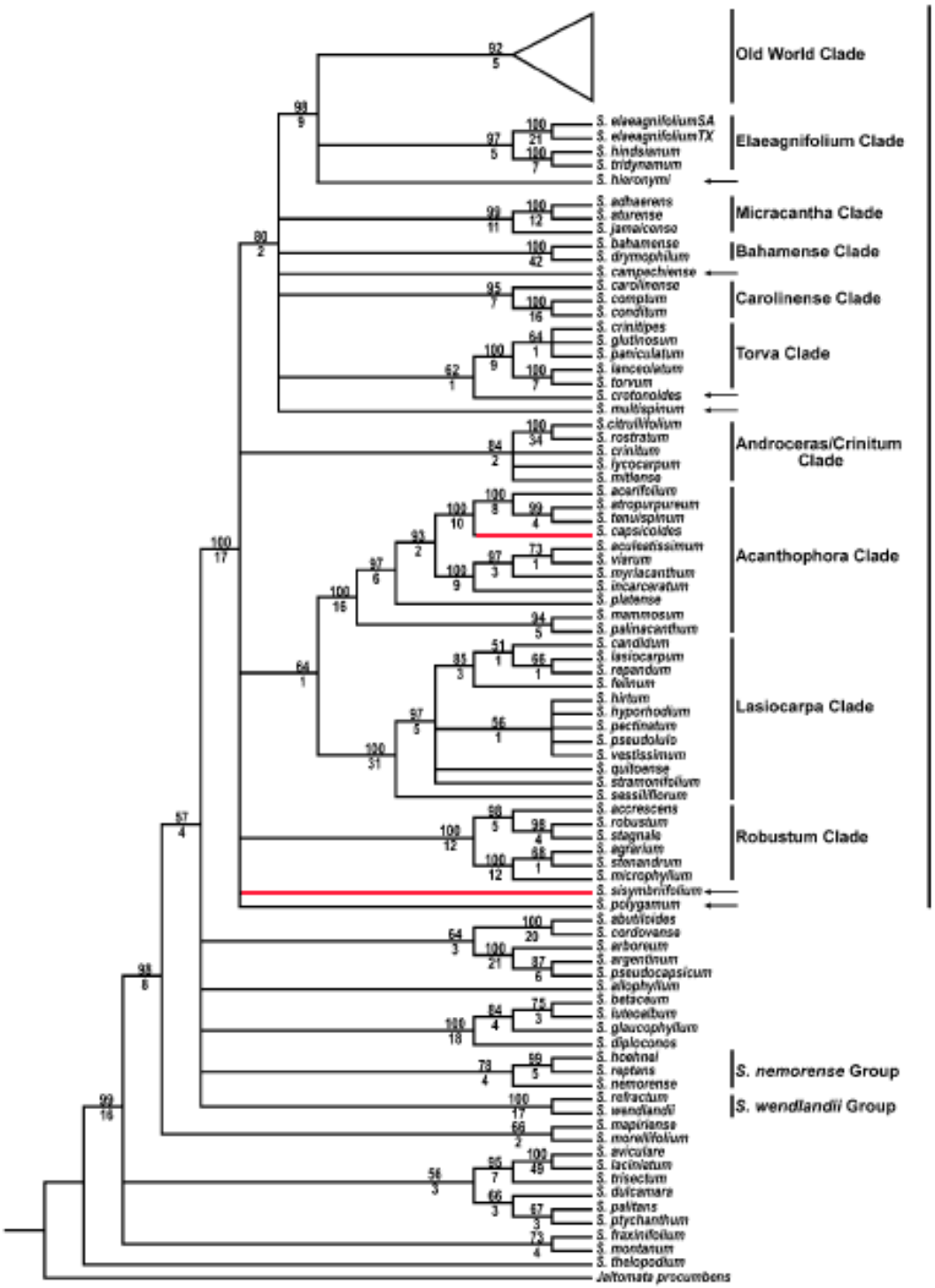

Figure 4.2 Tree showing phylogenetic placement of *S. capsicoides* and *S. sisymbriifolium* (highlighted in red) within *Solanum* subgenus Leptostemonum. Parsimony bootstrap consensus tree taken from (Levin, Myers, & Bohs 2006). Within the Leptostemonum, *S. capsicoides* is in the clade Acanthophora and *S. sisymbriifolium* was unable to be placed within the named ten clades of Leptostemonum.

are small and easy to grow, with seed available from the Botanic Gardens at Nijmegen. They are not true sister species, but of the experimentally amenable conical-celled species available to use as a comparator for *S. capsicoides*, *S. sisymbriifolium* was the most closely related that could be identified at the start of the project (Figure 4.2).

The Leptostemonum is divided into ten distinct clades (Levin *et al.* 2005, 2006; Stern, Agra, & Bohs 2011). *S. capsicoides* is in one of these clades, Acanthophora. According to Bohs 2005 and Levin *et al.* 2006, *S. sisymbriifolium* was not yet placed within any of these clades but remained unresolved at the level of this polytomy. By this placement, *S. sisymbriifolium* therefore could not be determined to be more or less closely related to any of the clades at this polytomy. As the placement of *S. capsicoides* suggested this loss of conical cells occurred independently in this species or a narrow lineage around it, any conical-celled member of the Leptostemonum would be a reasonable representative of the ancestral conical-celled form. *S. sisymbriifolium* was the most closely related species known to have conical petal cells at the time, and as such this species was chosen as the comparator to *S. capsicoides*. Once the phylogenetic analysis in Chapter 3 was complete, it was found that *S. sisymbriifolium* placed at the base of the Androceras/Crinitum clade of

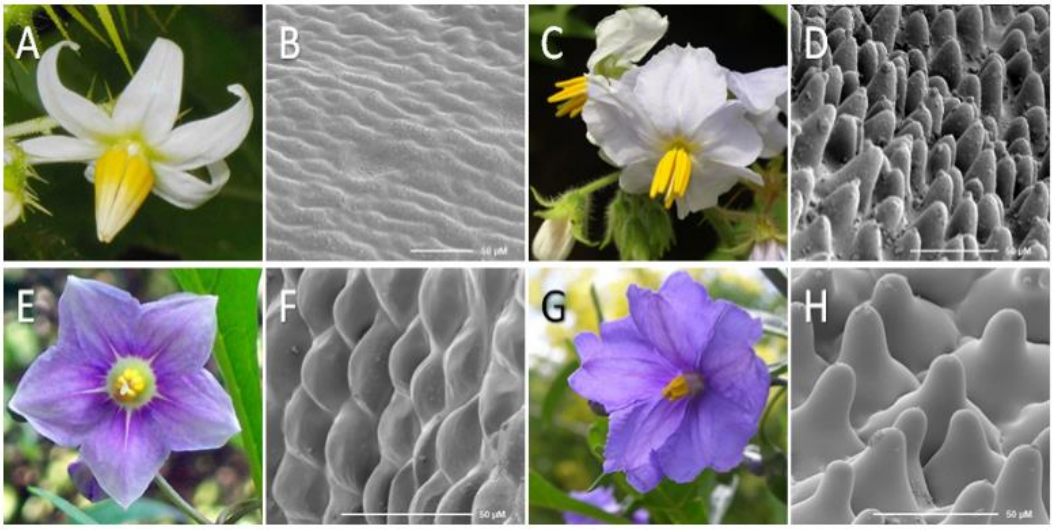

Figure 4.3. Photos and scanning electron micrographs of the petals of *Solanum* species used in this project. (A, B) *S. capsicoides*, (C, D) *S. sisymbriifolium*, (E, F) *S. aviculare*, (G, H) *S. laciniatum*. Electron micrographs show epidermal petal cells of each species

Leptostemonum, sister to a polytomy of Acanthophora (containing *S. capsicoides*) and Lasiocarpa. Additionally, according to our character mapping, the loss of conical cells in *S. capsicoides* remains as initially indicated as an independent loss in the Acanthophora. This therefore leaves *S. sisymbriifolium* as a good representative of ancestral conical cell form and a legitimate comparator for *S capsicoides*.

The second set of sister-species was chosen after the analysis described in Chapter 3 was completed. This allowed us to choose species in a different clade again, with greater confidence that the evolutionary loss of conical cells in this new chosen clade was indeed separate to losses studied in the Leptostemonum and Dulcamaroid clades. Of the possible candidates identified, we chose Solanum aviculare (flat) and Solanum laciniatum (conical) from the Archaesolanum clade (Figure 4.4). According to the most recent phylogenetic treatment of this section (Poczai, Hyvönen, & Symon 2011), these are true sister species. They are also easily cultivated garden plants for which seed is available commercially as well as from the Botanic Gardens at Nijmegen.

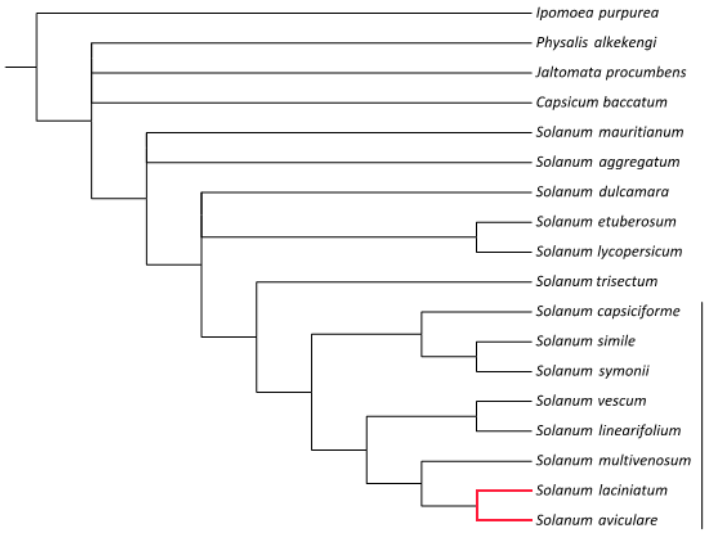

Figure 4.4 Kangaroo apple (*Solanum* section Archaesolanum) phylogeny showing position of *S. laciniatum* and *S. aviculare* (highlighted in red). Figure adapted from Poczai et al. 2011. The section Archaesolanum is shown by the black line. *S. aviculare* and *S. laciniatum* are here shown to be sister species.

4.2 Results and Discussion

4.2.1 Cell shape of species pairs

S. capsicoides petal epidermal cells are elongate at the base and each cell has a very slight curvature perpendicular to the plane of the epidermal surface, but in aggregate across the petal surface the cells are effectively flat (Figure 4.3 B). Its comparator species *S. sisymbriifolium* has petal epidermal cells that are predominately circular in cross-section at the base, which incline steeply to tall cones with a rounded top. The tight spacing at the base of these cells produces a dense surface of cones (Figure 4.3 D). *S. aviculare* petal epidermal cells are circular at the base and have a lens-shaped (lenticulate) curvature perpendicular to the plane of the epidermal surface (Figure 4.3 F), while *S. laciniatum* petal epidermal cells are wide at the base and narrow sharply, forming an almost cylindrical shape with rounded top. This produces a surface with conical cells much less densely packed than that of *S. sisymbriifolium*. Each of these petal surface textures may function in very different ways with respect to insect grip, interactions with water, scent dispersal, colour, and any other trait affected by cell shape.

4.2.2 PCR amplification of SUBGROUP 9A genes from *Solanum* species

Using specific primers designed from *S. lycopersicum* and *S. dulcamara SdMybML2* homologues, full-length genes were amplified from cDNA and/or genomic DNA in all four species. These genes were named *MybML* due to their homology to the *MIXTA*-like lineage of Subgroup 9A identified by Brockington *et al.* (2013), rather than maintaining the unpublished nomenclature of *S. dulcamara SdMybML1* and *SdMybML2*.

In addition to the primary species of interest to this project, tissue samples from other *Solanum* species became available through the petal cell morphology survey

described in the previous Chapter. When time and resources were permitting, RNA and DNA were extracted from these species and PCR amplification of Subgroup 9A genes was attempted from cDNA and genomic DNA using *Solanum*-specific primers as described above. In many cases this amplification was successful and a full-length gene was amplified and sequenced. This allowed for the comparison of a greater number of *MybML* genes across *Solanum*, giving insight into the degree of conservation of this gene across *Solanum* as well as into the kinds of mutations that are common. Amino acid sequences of all *MybML* genes identified are shown in alignment in Figure 4.5.

To ensure a complete analysis of Subgroup 9A genes and their possible functions, we also searched for genes similar to *SdMybML1*. Using primers designed from *SdMybML1*, sequences were identified from *S. capsicoides* cDNA and *S. sisymbriifolium* genomic DNA respectively. These were named *MybMx* for their homology with the *MIXTA* lineage of Subgroup 9A as identified by (Brockington *et al.* 2013).

4.2.3 Other sources of *Solanum* Subgroup 9A gene sequences.

Further *Solanum* EST, cDNA and genomic DNA sequences of Subgroup 9A genes were identified in NCBI's GenBank (Benson *et al.* 2005). These sequences were downloaded and used in alignments for better identification of *MIXTA*-like genes as well as the design of primers with greater likelihood of binding to typical conserved regions of *Solanum* Subgroup 9A genes.

The genome sequences of potato and tomato, when published, were made available to search through BLAST (Altschul *et al.* 1990) and specific genome websites. The potato genome (The Potato Genome Sequencing Consortium 2011) allowed for the identification of the potato *MybMx* homologue, and the tomato genome (The Tomato Genome Consortium 2012) for the tomato *MybMx* homologue. *MybML* sequences for these species had already been identified.

4.2.4 Gene structures of *MybML* and *MybMx*

Analysis of genomic DNA sequences using NetPlantGene (Hebsgaard *et al.* 1996) predicted two introns for each gene, and further predicted these to occur in positions similar to the introns of *AmMybMl2* and *AmMybMl1* of *Antirrhinum* as well as those of other similar genes. Comparison of these genomic sequences with cDNA sequences of each gene isolated from the same species confirmed the position of these introns. Knowledge of these positions allowed for later primer design across these exon-intron boundaries to selectively amplify from cDNA to accurately test transcription levels

4.2.5 *Solanum MybML* proteins show a high degree of sequence identity and structural conservation

MybML genes isolated from each species show a high degree of sequence similarity to members of the Subgroup 9A *MIXTA*-like clade that are known to produce conical-celled phenotypes, including *AmMybMl2*, *PhMyb1* and *SdMybMl2*. As shown in Figure 4.5, the *Solanum MybML* genes identified by this project share 94% identity with the amino acid sequence of *SdMybML2*, 89% identity with *AmMybMl2*, and 93% identity with *PhMyb1*. Structural analysis of the amino acid sequences by metaPrDOS (Ishida & Kinoshita 2008) predicts each amino acid sequence to contain both of the R2R3 MYB repeats at the N-terminus, and also predicts a putative second structured domain closer to the C-terminus, which is predicted to mediate downstream effector protein recruitment. This putative second domain has not been previously described in the literature, nor is it of a structure type that has been well-studied. However, its predicted function is consistent with the activity of a transcription factor, and its prediction is well supported by the metaPrDOS analysis. For these reasons this putative domain has been included in further analysis.

Between our selected sister species pairs, all proteins are extremely similar in amino acid sequence with only a few amino acid changes difference between each pair of proteins. None of the genes contain major changes that could interrupt protein

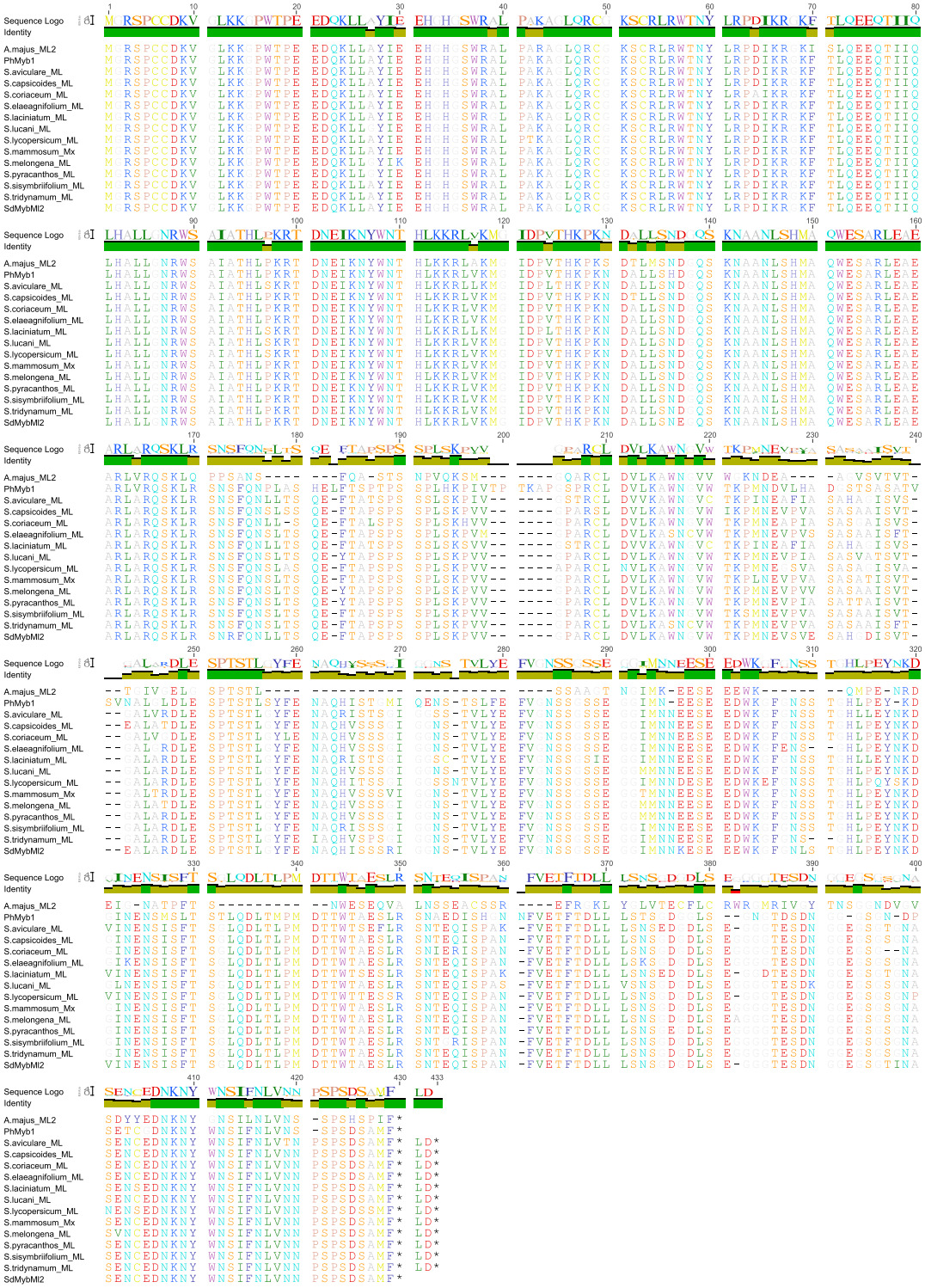

Figure 4.5 Alignment of full length *MIXTA*-like (MybML) protein sequences. The sequences identified by this project show 88% mean pairwise identity compared to known members of the *MIXTA*-like lineage of Subgroup 9A ([Brockington et al]). Each amino acid is represented by a different colour. The sequence logo shows amino acid frequency at each site. Identity shows the relative conservation at each site: red, less than 30% conservation; yellow, 30% - 99% conservation; green, 100% conservation. (Genbank numbers: PhMyb1 GI:20562, AmMybMl2 GI:56069812)

function, such as frameshifts, early stop codons, or large insertions or deletions, suggesting that at least on a superficial level all appear to remain functional proteins.

More detailed analysis of *S. sisymbriifolium* (C) and *S. capsicoides* (F) protein sequences (both 417 amino acids (aa) in length, Figure 4.7) shows that they are identical except for 11 amino acid changes. None of these changes occur in the MYB DNA binding domain. Three occur in regions with no predicted structure, and eight occur within the putative protein recruitment domain. Of these eight, two are conservative changes unlikely to produce any significant difference in the functioning of the protein, based on the BLOSUM62 substitution matrix (Henikoff & Henikoff 1992) and chemical similarity. The final six amino acid changes within this domain are non-conservative and their effect on protein function is unknown, though might indicate a divergence in binding partners and a change in protein:protein interactions.

S. aviculare (F) and *S. laciniatum* (C) protein sequences (both 416 aa, Figure 4.8) are identical except for 10 amino acid differences. One of these occurs within the R2R3 MYB DNA binding domain and is a non-conservative change. Four amino acid changes occur in the predicted protein recruitment domain, one of which is a conservative change and three are non-conservative. The effects of these changes are unknown, although the lower number of changes between these proteins in this predicted domain (four changes) than between the *S. sisymbriifolium* and *S. capsicoides* proteins (eight changes) implies a lower probability of divergence in downstream binding partners. The remaining five amino acid changes between these proteins occur in regions of no predicted structure. The non-conservative amino acid difference within the MYB DNA binding domain occurs within a predicted helix at position 39, where *S. aviculare* (F) has an alanine, an amino acid with a high helical propensity, whereas *S. laciniatum* (C) has a glycine, which has a low helical propensity. This difference in helical propensity has the potential to disrupt the secondary structure of *S. laciniatum MybML* and therefore negatively affect DNA binding. This would impair the functionality of this protein. However, *S. laciniatum* has conical petal cells and so must have at least one functional protein capable of initiating conical cell outgrowth. On the basis of relative expression levels,

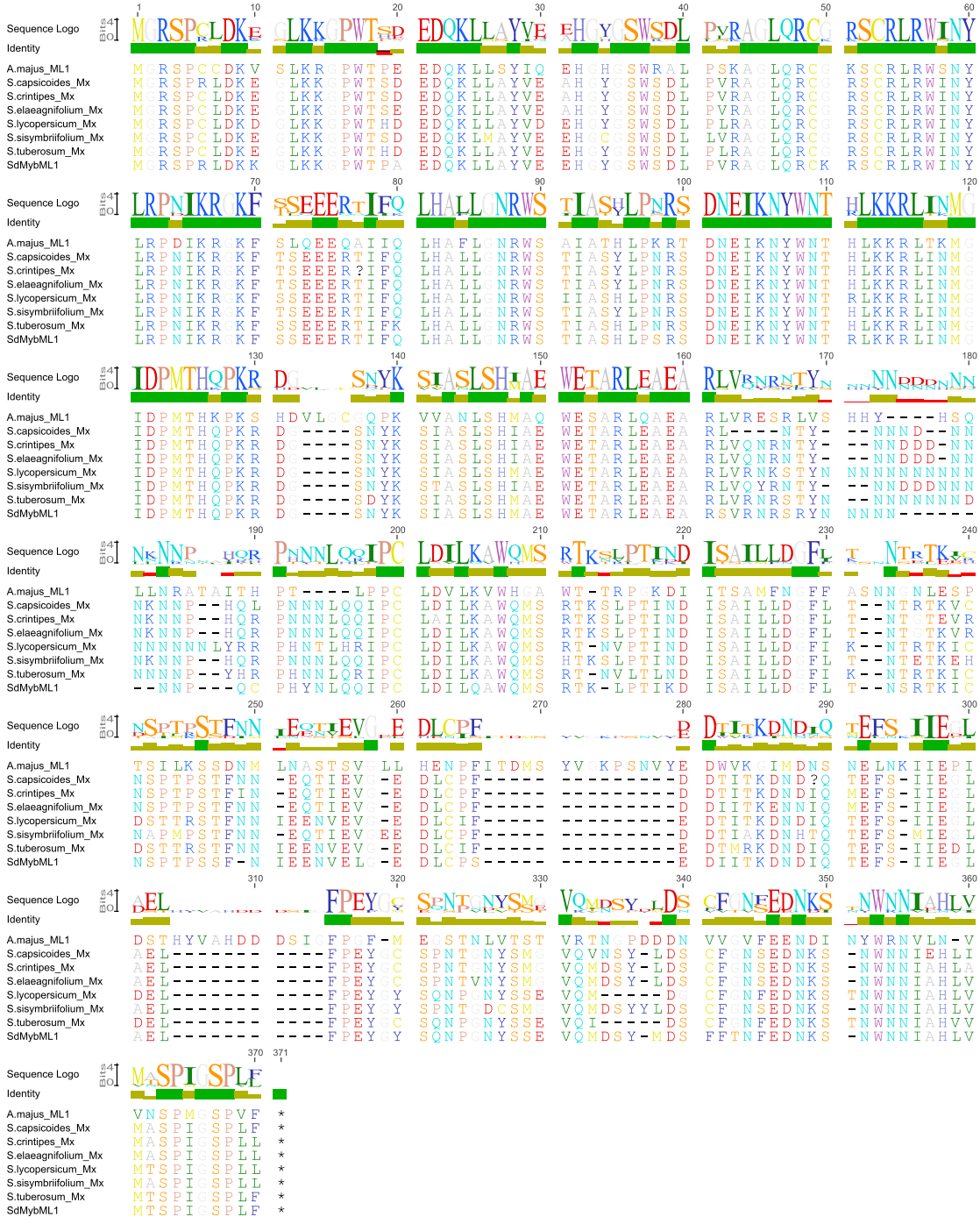

Figure 4.6. Alignment of full length *MIXTA* (*MybMx*) protein sequences. The sequences isolated in this clade show 73% mean pairwise similarity to *Antirrhinum majus AmMybML1* and 84% mean pairwise similarity to *S. dulcamara SdMybML1*. All genes in this alignment are members of the *MIXTA* lineage of Subgroup 9A. Each amino acid is represented by a different colour. The sequence logo shows amino acid frequency at each site. Identity shows the relative conservation at each site: red, less than 30% conservation; yellow, 30% - 99% conservation; green, 100% conservation. (Genbank number: AmMybMl1 GI:51895756)

we believe that *MybML* is the gene most likely to be primarily responsible for the conical cell phenotype in this species. If this prediction is correct, then it would imply that this amino acid change does not disrupt the secondary structure of this protein. To further understand whether this protein retains its ability to produce a conical cell phenotype, functional analysis by heterologous expression in tobacco was performed and is described in Chapter 6.

Even if this amino acid change has not affected the secondary structure of the DNA binding domain of *S. laciniatum* MybML, the change could still potentially affect the overall DNA binding affinity of this section of protein. To determine the likelihood of this amino acid difference having an effect on DNA binding, the amino acid sequences for the R2R3 Myb domains were mapped onto the crystal structure of the R2R3 Myb domain (Figure 4.9 A) as solved for the oncogene C-Myb (Ogata *et al.* 1994). Based on this C-Myb tertiary structure, the single amino acid difference between the MybMl proteins of *S. laciniatum* and *S. aviculare* is predicted to occur

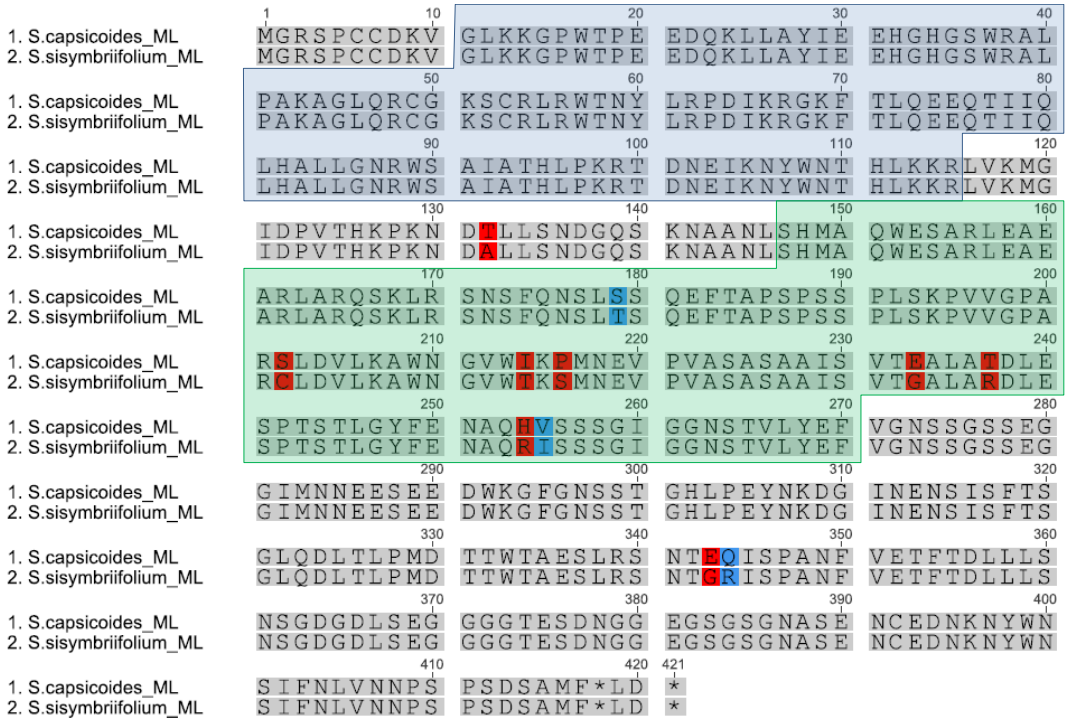

Figure 4.7 Amino acid alignment of *S. sisymbriifolium* and *S. capsicoides MybML* protein sequences showing predicted structural regions and amino acid differences. The blue shaded region shows the predicted R2R3 MYB domain, and the green shaded region shows the putative protein recruitment domain. Amino acids in red are predicted to be non-conservative changes, and in blue are conservative.

in a position facing away from the DNA binding surface of the protein. A difference in amino acid at this position in the protein is unlikely to cause any change to the strength or specificity of DNA binding.

Overall, the R2R3 MYB domains of the *MybML* proteins across all 4 species show almost perfect conservation of the DNA binding domain. The only non-conservative (based on BLOSUM62 matrix and chemical similarity) mutation in this domain is in a position predicted to point away from the DNA-binding face of the protein, and is extremely unlikely to affect the binding strength or capability of the DNA binding domain.

The putative protein recruitment domains show a greater divergence, but the type of domain predicted is less well studied than the MYB DNA binding domain. It has no solved crystal structure and no tools are available for prediction of function, and

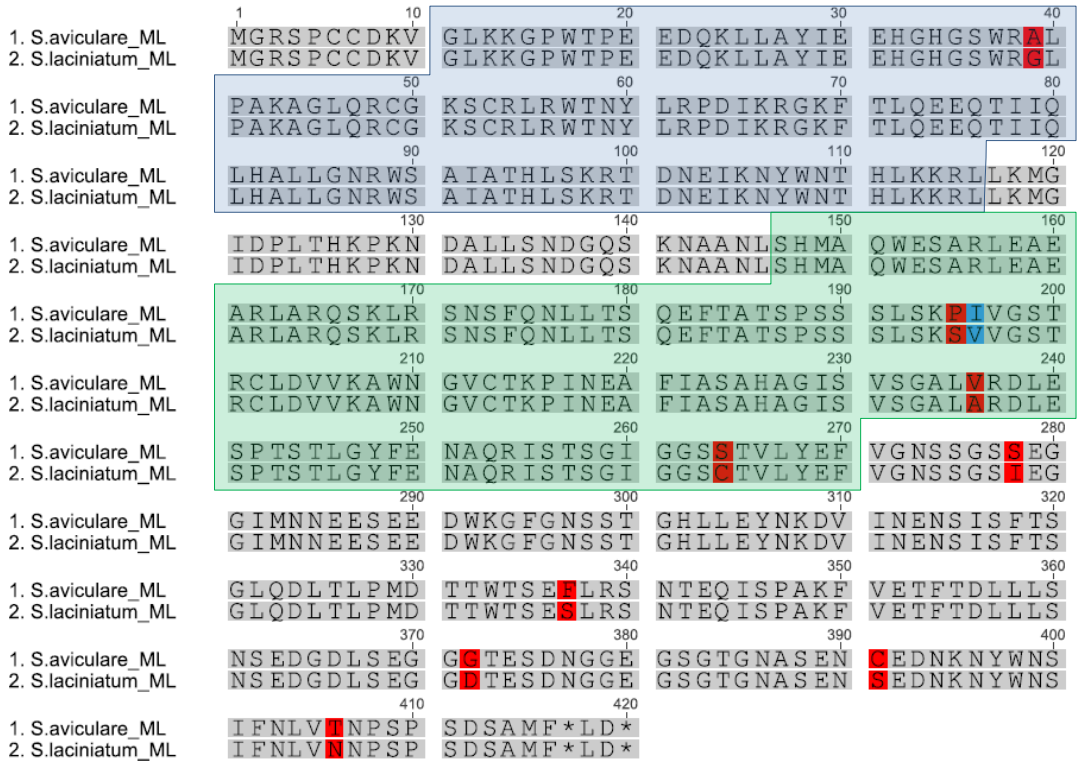

Figure 4.8 Amino acid alignment of *S. aviculare* and *S. laciniatum MybML* protein sequences showing predicted structural regions and amino acid differences. The blue shaded region shows the predicted R2R3 MYB domain, and the green shaded region shows the predicted protein recruitment domain. Amino acids in red are predicted to be non-conservative changes, and in blue are conservative.

as such the amino acid changes within this domain are of unknown effect to the functionality of each protein.

4.2.6 *MybMx* (*MybML1*) proteins show greater amino acid sequence divergence

The *MybMx* genes isolated in this project show 73% sequence similarity to *Antirrhinum majus AmMybML1* and 84% sequence similarity to *S. dulcamara*

SdMybML1. *S. sisymbriifolium* and *S. capsicoides* MybMx amino acid sequences differ to a greater degree than do their MybML proteins, with *S. capsicoides* MybMx having four separate deletions, of four, two, one and one amino acids in length, as well as 26 amino acid differences.

S. capsicoides and *S. sisymbriifolium* MybMx have four amino acid differences within the MYB DNA binding domain. Tertiary structure prediction based on C-Myb predicts these all to occur away from the DNA binding face of the protein (Figure 4.9 B) and therefore to have a low probability of affecting function.

The C-terminal regions of the *S. capsicoides* and *S. sisymbriifolium* MybMx proteins show a significant reduction in the degree of structuredness when compared to MybML proteins of the same species. Combined with the large number of non-conservative amino acid changes, this suggests that while the MybMx proteins from these species may be able to functionally complement one another, they are unlikely to interact with the same downstream effectors as the MybML proteins.

We were unable to isolate *S. aviculare* and *S. laciniatum MybMx* genes during this project, either from cDNA or genomic DNA.

4.2.7 Comparison of *MybML* and *MybMx* protein function predictions

The DNA binding region of the MybMx proteins is structurally similar to that of the MybML proteins (Figure 4.9 C). Based on comparison to the structure of C-Myb, the

seven amino acid differences between *S. capsicoides* MybMx and MybML all occur on the non-DNA binding surfaces of the protein which implies that they retain their DNA binding function. The high conservation of the DNA binding region compared to the protein interaction domain suggests that the *MybMx* genes are under positive selection to be retained for a function different to that which the *MybML* genes perform.

The degree of sequence divergence between two homologs does not necessarily correspond to the degree of functional divergence. *Gossypium GhMyb25* is able to functionally complement the *Arabidopsis gl1* mutant despite sharing only 44% sequence identity (Wang *et al.* 2004), whereas a single amino acid difference in the single repeat MYB *ETC2* (K19E) is responsible for trichome patterning variation in natural *Arabidopsis* populations (Hilscher, Schlötterer, & Hauser 2009). In this Chapter protein analysis has shown that there is a low probability that the amino acid changes between Subgroup 9A proteins in *Solanum* sister species are sufficient to cause differences in functionality. However, although computational protein function prediction based on amino acid sequence has substantially improved in recent years, limitations still remain (Radivojac *et al.* 2013). It is therefore necessary

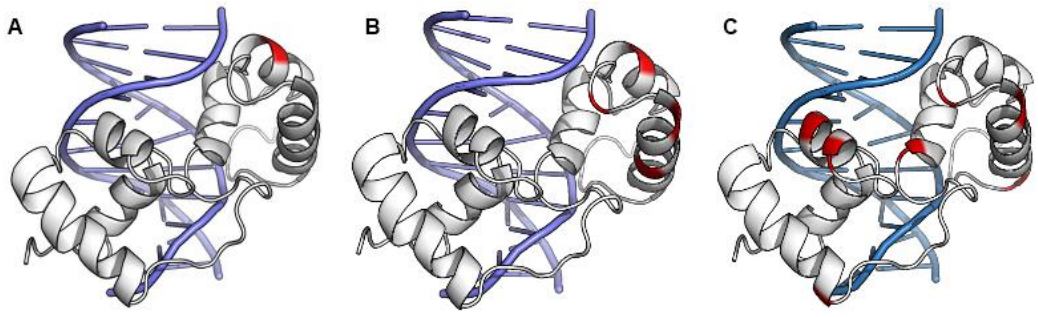

Figure 4.9 Protein structure of R2R3 MYB domain from Subgroup 9A genes, shown binding DNA. This projection uses a homology model to predict amino acid positioning of the DNA binding domain of pairs of Subgroup 9A proteins based on the tertiary structure of C-Myb (Ogata *et al.* 1994). Sections in red show amino acid differences between each protein pair. All proteins are predicted to retain a structurally intact Myb domain. (A) *S. aviculare* and *S. laciniatum* MybML proteins, showing in red the single non- conservative amino acid change. This single amino acid change is facing away from the DNA binding face of the protein and is unlikely to affect DNA binding. (B) *S. sisymbriifolium* and *S. capsicoides* MybMx proteins, showing four amino acid differences. None of the amino acid changes occur on the DNA binding face of the protein. (C) Variation in amino acid sequence between MybMx and MybML Myb domains (*S. capsicoides* genes used for comparison). The MybMx and MybML protein sequences differ by several amino acids, but as with variation within each protein type, all amino acid changes face away from the DNA binding face. This strongly suggests that both protein types retain very similar DNA binding function.

to perform functional characterisation of these proteins using living plants. To this end, experiments assessing *Solanum* Subgroup 9A protein function using heterologous overexpression in tobacco are detailed in Chapter 5.

4.3 Conclusions

To investigate the repeatability of evolution by comparison of independent losses of conical cells within the genus *Solanum*, we chose two pairs of closely related species to investigate. Within each pair we selected one species without conical petal cells, and one species with conical petal cells. From the subgenus Leptostemonum we chose *S. capsicoides* (F) and *S. sisymbriifolium* (C), both of which belong to clades that are unresolved in a polytomy at the base of the Leptostemonum, *S. capsicoides* from the Acanthophora clade and *S. sisymbriifolium* being unplaced within a clade but emerging within this basal polytomy. From the Archaesolanum clade we chose the true sister-species *S. aviculare* (F) and *S. laciniatum* (C).

Using a candidate gene approach, and starting from the premise that the most likely genes responsible for the control of conical petal cell formation in our species would be homologous and very similar in sequence to *SdMybML1* and *SdMybML2* from *S. dulcamara* and *SlMIXTA* from tomato, we were able to design primers specific to *SdMybML1*-like and specific to *SdMybML2*-like genes. Using these primers we successfully isolated *SdMybML2*-like genes from all of our selected sister species, and *SdMybML1*-like genes from *S. sisymbriifolium* and *S. capsicoides*. We named these genes following the work of Brockington et al, naming the *SdMybML2* homologues (which fell into the *MIXTA*-LIKE section of SBG9-A) *MybML* and the *SdMybML1* homologues (which form part of the *MIXTA* section of SBG9-A) *MybMx*.

Analysis of *MybML* (*S. sisymbriifolium*, *S. capsicoides*, *S. aviculare*, *S. laciniatum*) DNA sequences showed high sequence similarity and conserved intron positions when compared to other *MIXTA*-like genes. The MybML amino acid sequences showed very high conservation across all species, with only 10/417 and 11/416 amino

acid differences between sister species pairs. The Myb DNA binding domain shows the highest conservation overall, with no changes between *S. sisymbriifolium* and *S. capsicoides*, and only one change between *S. laciniatum* and *S. aviculare*, which is predicted to be situated away from the DNA-binding face of the protein and is unlikely to affect DNA binding.

Protein structure analysis predicts the MybML proteins to contain another structured domain, nearer the C-terminal, likely to function as a protein recruitment domain. This putative second domain of the MybML proteins is less highly conserved than the Myb domain, with four amino acid differences between *S. capsicoides* and *S. sisymbriifolium*, and eight amino acid differences between *S. aviculare* and *S. laciniatum*. Many of these are conservative amino acid changes unlikely to affect protein function, but some changes are non-conservative. Since this putative second domain at the C-terminal is of a protein domain type that is very little studied, it is not possible at this time to predict possible effects of these amino acid changes on protein function.

Analysis of *MybMx* DNA sequences from *S. sisymbriifolium* and *S. capsicoides* (*MybMx* genes from *S. aviculare* and *S. laciniatum* could not be isolated during this project) shows conserved intron positions and on average high sequence similarity when compared to other Subgroup 9A genes, similarly to *MybML* genes. There are a larger number of nucleotide differences, however, many of which were non-synonymous and produce concomitant amino acid differences. There are also several deletions of one or more amino acids in length in *S. capsicoides* MybMx as compared to *S. capsicoides* MybMx. Six of the amino acid changes occur within the Myb DNA binding domain, though as with the single amino acid change between *S. aviculare* and *S. laciniatum* MybML these are all predicted to be positioned away from the DNA binding face of the protein. The putative C-terminal protein recruitment domain is predicted to be less structured when compared to the *MybML* proteins, suggesting this protein may have a function differing from that of the *MybML* genes.

From these predictions based on amino acid sequence and predicted secondary structure, it is likely that the MybML proteins in all 4 species retain similar functionality. Additionally, the MybMx proteins may be performing a related but distinct role in the formation of cellular outgrowth. That all proteins appear to retain functionality suggests that in each sister species pair, a change in petal cell phenotype from conical to flat has in each case most likely occurred through means other than protein function change of the regulating Subgroup 9A MYBs.

To test the ability of each protein to initiate cellular outgrowth into conical cells or trichomes, we used heterologous expression of each gene in tobacco (*Nicotiana tabacum* var. Samsun) under the 35S promoter. The expression levels of each gene were then compared across species at differing developmental stages of leaves and flowers. These experiments, detailed in Chapters 5 and 6, allowed us to gain further insight into whether a protein function change, or a change in expression, was responsible for the loss of conical petal cells in *S. capsicoides* and *S. aviculare*.

Chapter 5. Flat-celled *Solanum* species retain protein function of R2R3 MYB Subgroup 9A genes

5.1 Introduction

It was shown in Chapter 4 that the R2R3 MYB Subgroup 9A genes isolated from *Solanum* species showed a high degree of amino acid and nucleotide sequence conservation. There were few amino acid differences between homologous proteins of flat-celled and conical-celled sister species, and the positions of these changes were observed to occur in positions within the protein that were predicted to be unlikely to disrupt the DNA binding or protein recruitment functions of these proteins. We therefore predict that each of these *Solanum* R2R3 MYB Subgroup 9A proteins should retain the ancestral ability to recruit cell wall modifying components and produce conical outgrowths of epidermal cells. In this next Chapter, we aimed to determine whether each protein does in fact have the ability to produce conical cells using heterologous expression in tobacco under a strong constitutive promoter.

Using expression in tobacco as a bioassay for the activity of R2R3 MYB Subgroup 9A genes is a well-established assay to determine whether these proteins are capable of producing cell outgrowth into a conical cell form. If the proteins prove capable of producing cellular outgrowth in tobacco, it can be inferred that they retain the DNA binding and protein recruitment ability that can drive the expression of target genes

that modify the cell wall and drive cell expansion, and are capable of directing expression of these genes in their native species.

If the R2R3 MYB Subgroup 9A genes are still capable of producing conical cells, as shown by heterologous expression in tobacco, in those species which have lost petal conical cells, then this loss must be caused by a molecular mechanism other than loss of protein function. Alternative explanations for the loss of conical petal cells include loss of expression of R2R3 MYB Subgroup 9A genes in the petal tissues, or a change in an important downstream target. A change in expression of the R2R3 MYB Subgroup 9A genes is the more likely mechanism. Any change in downstream genes may have more serious effects on general plant development because the likely targets of R2R3 MYB Subgroup 9A proteins are genes responsible for modifying the cell wall and promoting cell expansion, and are thus required for multiple aspects of plant development.

Previous studies of expression of R2R3 MYB Subgroup 9A genes in tobacco have used a double CaMV35S promoter to drive strong, constitutive expression of the transgene (Glover, Perez-Rodriguez & Martin 1998; Perez-Rodriguez *et al.* 2005; Jaffé, Tattersall & Glover 2007; Baumann *et al.* 2007; Di Stilio *et al.* 2009, M. Thomas PhD Thesis 2010). The most frequently observed phenotype in these expressing lines of tobacco was outgrowths on the epidermis of the ovary, either producing conical cells or longer outgrowths forming trichomes. Cells of this tissue are flat in the wild type. Longer trichomes, conical cells and, in some cases, ectopic stomata are also occasionally observed in the inner corolla tube, style, stigma, anther, filament and leaves. Expression of Subgroup 9A genes also often produces longer outgrowths of cells in tissues that are normally conical-celled, such as on the tips of the petals.

In this Chapter I describe the phenotypes produced by heterologous expression of *Solanum* R2R3 MYB Subgroup 9A genes in tobacco, and discuss the implications of each phenotype.

5.2 Results and Discussion

5.2.1 Transformation of R2R3 MYB Subgroup 9A genes into tobacco

Plasmids for *Agrobacterium*-mediated transformation of R2R3 MYB Subgroup 9A genes were produced using pGREEN II as the binary expression construct. A modified pGREEN II plasmid containing a double CaMV promoter and terminator flanking a multiple cloning site was used as a base in each case to build constructs containing each R2R3 MYB Subgroup 9A gene. An example of such a construct can be seen in Figure 5.1, showing the construct built to contain *S. capsicoides* Mx. Each construct used was identical to this one, but each containing a different R2R3 MYB Subgroup 9A gene. *S. laciniatum*, *S. aviculare*, *S. sisymbriifolium* and *S. capsicoides* ML genes and *S. sisymbriifolium* and *S. capsicoides* Mx genes were all transferred into pGREEN II::35S using directional or non-directional cloning as described in Chapter 2, section 2.3.9.4. An example of a plasmid construct (pGREENII::35S containing *S. capsicoides Mixta*) is shown in Figure 5.1, and all pGREENII::35S plasmid constructs used in this study are detailed in Appendix 4.

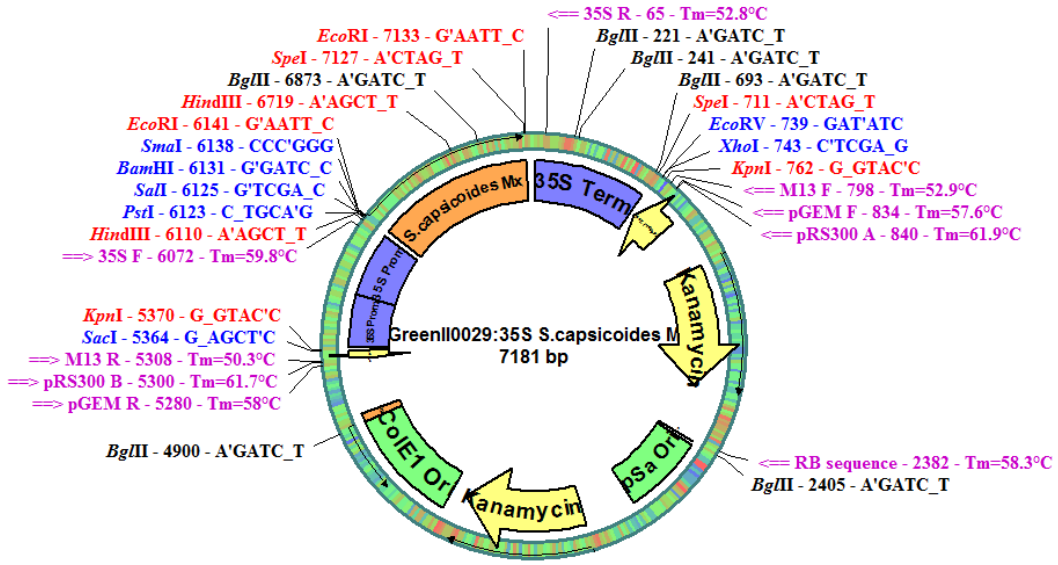

Figure 5.1 Vector map of pGreenII expression construct used to generate transgenic tobacco. *S. capsicoides Mx* has been inserted between a double CaMV 35S promoter and terminator in a pGREENII backbone plasmid to produce constitutive expression of this gene when transformed into tobacco. All other plasmids are shown in Appendix 4.

Agrobacterium-mediated transformation of each R2R3 MYB Subgroup 9A gene into tobacco using the methods of Berendzen et al. (2005) induced callus formation in over 90% of explant discs. Of these, on average approximately 50% were found to be successfully transformed with the appropriate R2R3 MYB Subgroup 9A transgene. These plants were then grown to maturity under long day conditions as specified in Methods section 2.4. Leaf tissue of mature plants was then tested for transgene expression by RT-PCR using gene-specific primers. DNA bands after gel electrophoresis for lines of tobacco expressing each construct are shown in Figure 5.2. Plants from a minimum of three independent lines for each gene were phenotypically characterised using scanning electron microscopy.

5.2.2 Phenotypes of *Solanum Mixta-Like* genes expressed in tobacco

Expression of *S. laciniatum* (C), *S. aviculare* (F), *S. sisymbriifolium* (C) and *S. capsicoides* (F) ML genes in tobacco produced conical outgrowths of the ovary abaxial epidermis (Figure 5.3 C ii-iv, Figure 5.4 C ii, Figure 5.6 C ii, Figure 5.5 C ii).

Tobacco plants expressing *S. laciniatum* (C) *ML* showed normal growth habit and normal leaf and flower morphology (Figure 5.3 A, B). Cells of the ovary abaxial epidermis showed conical outgrowths in an irregular pattern (Figure 5.3 C iii), as well as occasional ectopic stomata (Figure 5.3 C ii). No other tissues imaged by SEM showed any abnormal phenotype.

Tobacco plants expressing *S. aviculare* (F) *ML* showed normal growth habit and normal leaf and flower morphology (Figure 5.4 A, B). Cells of the ovary abaxial epidermis showed patches of conical outgrowths across the epidermal surface (Figure 5.4 C). No other tissues imaged by SEM showed any abnormal phenotype.

Tobacco plants expressing *S. sisymbriifolium* (C) *ML* showed normal growth habit and normal leaf and flower morphology (Figure 5.5 A, B). Cells of the ovary abaxial

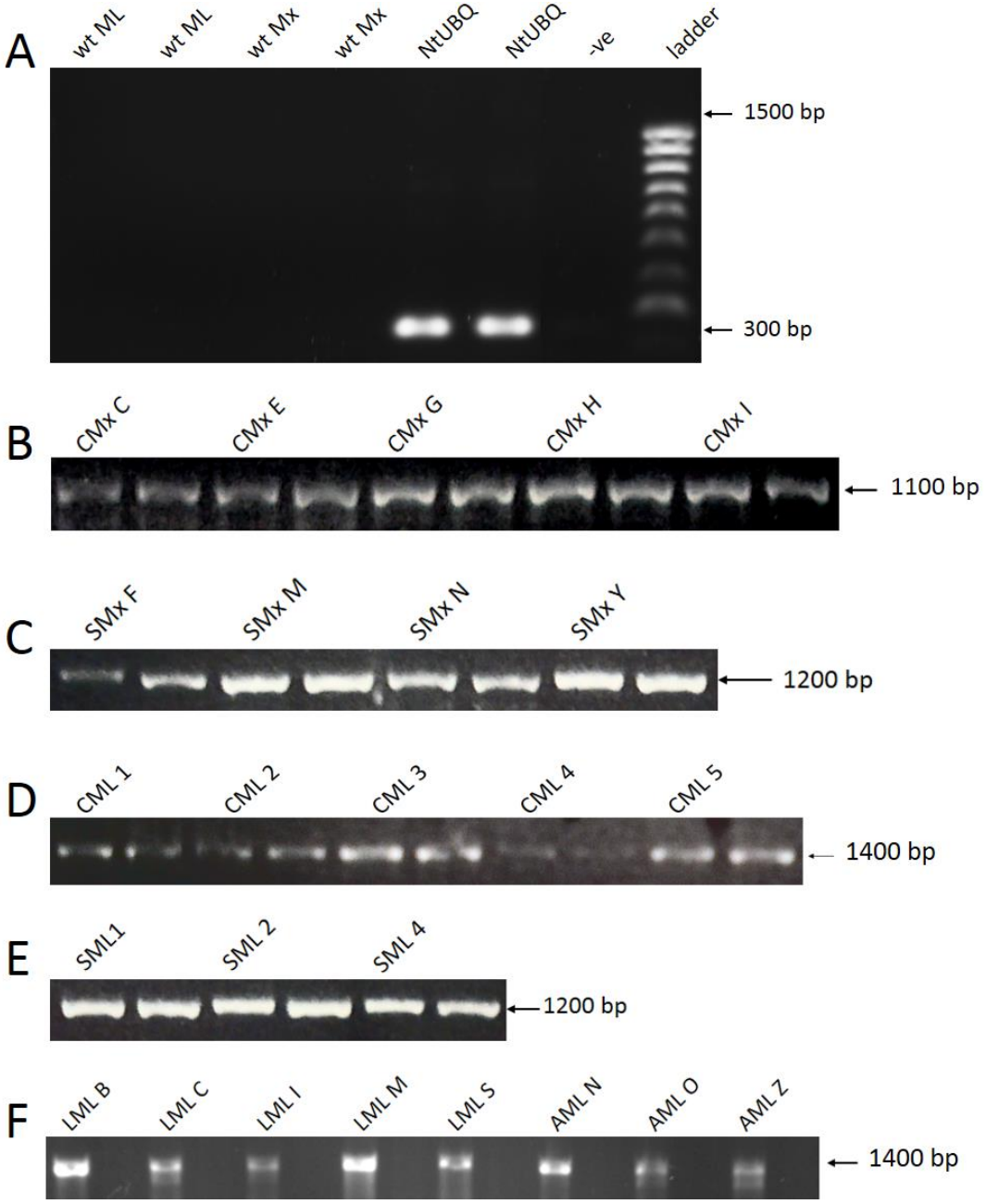

Figure 5.2 Gel electrophoresis of RT-PCR to confirm expression in lines of tobacco transformed with *Solanum* R2R3 MYB Subgroup 9A genes. All ML reactions used primers SMxEnd F/R, and all Mx reactions used primers SMl1End F/R (see Appendix 2). (A) wt ML = control reaction using *Mixta-Like* primers with wild type tobacco as template. wt Mx = control reaction using *Mixta* primers with wild type tobacco as template. NtUBQ = positive control reaction using ubiquitin primers using wild type tobacco as template. –ve = negative control reaction using ubiquitin primers with no template. (B) CMx = *S. capsicoides Mixta*. (C) SMx = *S. sisymbriifolium Mixta*. (D) CML = *S.capsicoides Mixta-Like*. (E) SML = *S. sisymbriifolium Mixta-Like*. (F) LML = *S. laciniatum Mixta-Like*, AML = *S. aviculare Mixta-Like*. Labels (letter or number) following species and gene name correspond to independent insertion lines in tobacco. All unlabelled bands are duplicate reactions of the previous lane.

epidermis showed conical outgrowth of all cells across the epidermal surface (Figure 5.5 C). No other tissues imaged by SEM showed any abnormal phenotype.

Tobacco plants expressing *S. capsicoides* (F) *ML* showed normal growth habit and normal leaf and flower morphology (Figure 5.6 A, B). Cells of the ovary abaxial epidermis showed tall conical outgrowth of all cells across the epidermal surface as well as rarely ectopic stomata (Figure 5.6 C). No other tissues imaged by SEM showed any abnormal phenotype.

5.2.3 Phenotypes of *Solanum Mixta* genes expressed in tobacco

Tobacco plants expressing *S. sisymbriifolium* (C) *Mx* showed normal growth habit and normal leaf and flower morphology (Figure 5.7 A, B). Cells of the ovary abaxial epidermis showed conical outgrowths as well as intermittent longer outgrowths into unicellular and multicellular trichomes (Figure 5.7 C). Cells of the inner corolla tube (petal adaxial) epidermis showed occasional ectopic stomata and trichomes (Figure 5.7 D). Cells of the distal portion of the style epidermis showed ectopic trichomes (Figure 5.7 E). No other tissues imaged by SEM showed any abnormal phenotype.

Tobacco plants expressing *S. capsicoides* (F) *Mx* showed normal growth habit and normal leaf and flower morphology (Figure 5.8 A, B). Cells of the ovary abaxial epidermis showed patchy conical outgrowths as well as intermittent multicellular trichomes each with a rounded, glandular apical cell (Figure 5.8 C). Occasional trichomes with a tapered apex were also observed. Cells of the inner corolla tube (petal adaxial) epidermis showed occasional ectopic stomata and multicellular trichomes (Figure 5.8 D). No other tissues imaged by SEM showed any abnormal phenotype.

5.2.4 Comparison of *Solanum* sister species ML expression phenotypes

All phenotypes discussed here for each gene were consistent across several different independent lines of tobacco, and all images shown are representative of the phenotypes observed. A minimum of three lines of tobacco originating from independent gene insertions were compared for each gene tested.

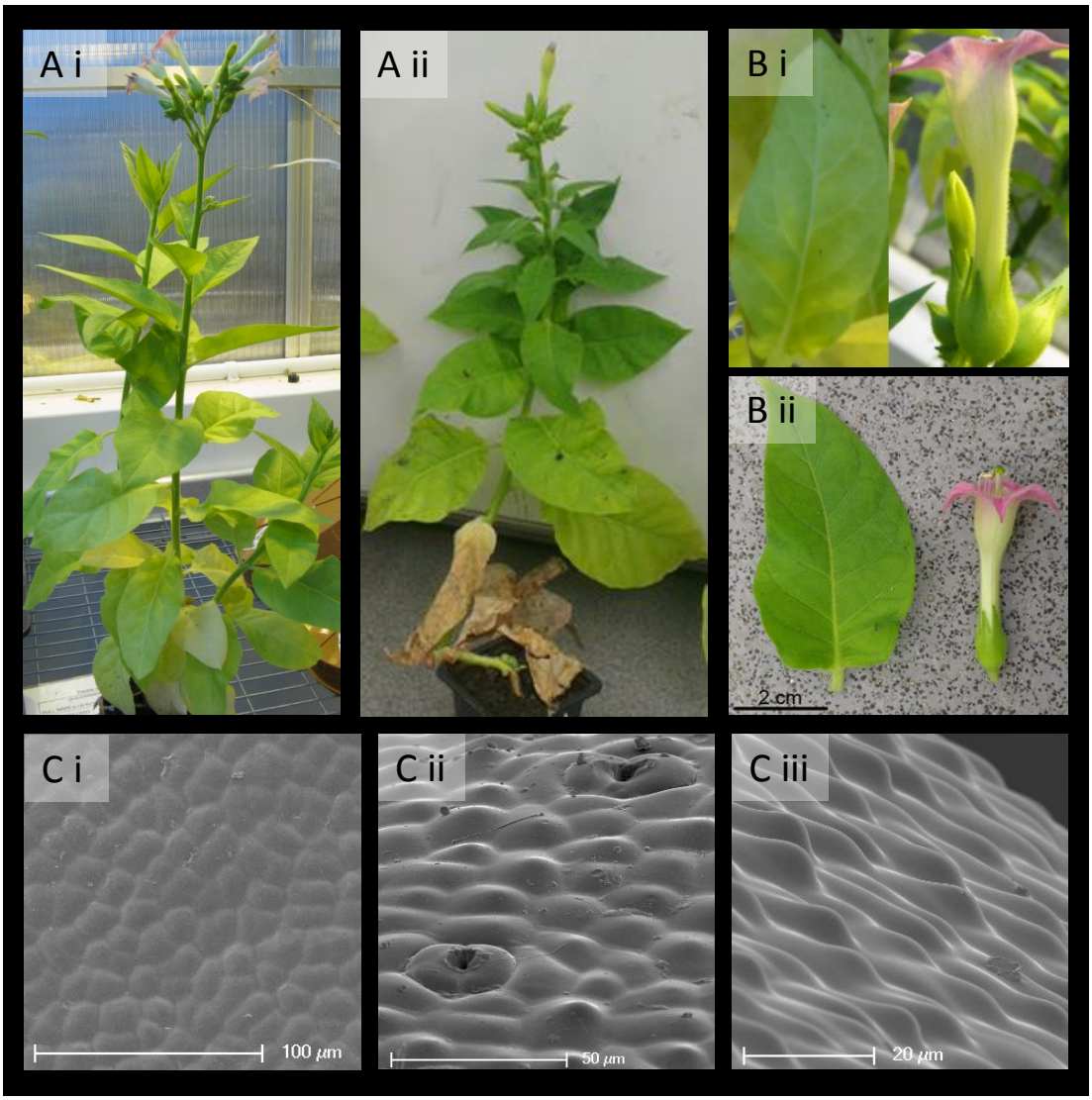

Figure 5.3 Tobacco expressing *S. laciniatum* ML. (A) Plant growth habit. i, wild type. ii, *S. laciniatum* ML transgenic. (B) Leaf and flower. i, wild type. ii, *S. laciniatum* ML transgenic. (C) SEM of ovary abaxial epidermis. i,wild type. ii,iii, *S. laciniatum* ML transgenic. Transgenic plants were of normal growth habit, leaf shape and size, and normal flower morphology. SEM of ovary abaxial epidermis shows conical outgrowths across the entire ovary abaxial epidermis, as well as rarely ectopic stomata.

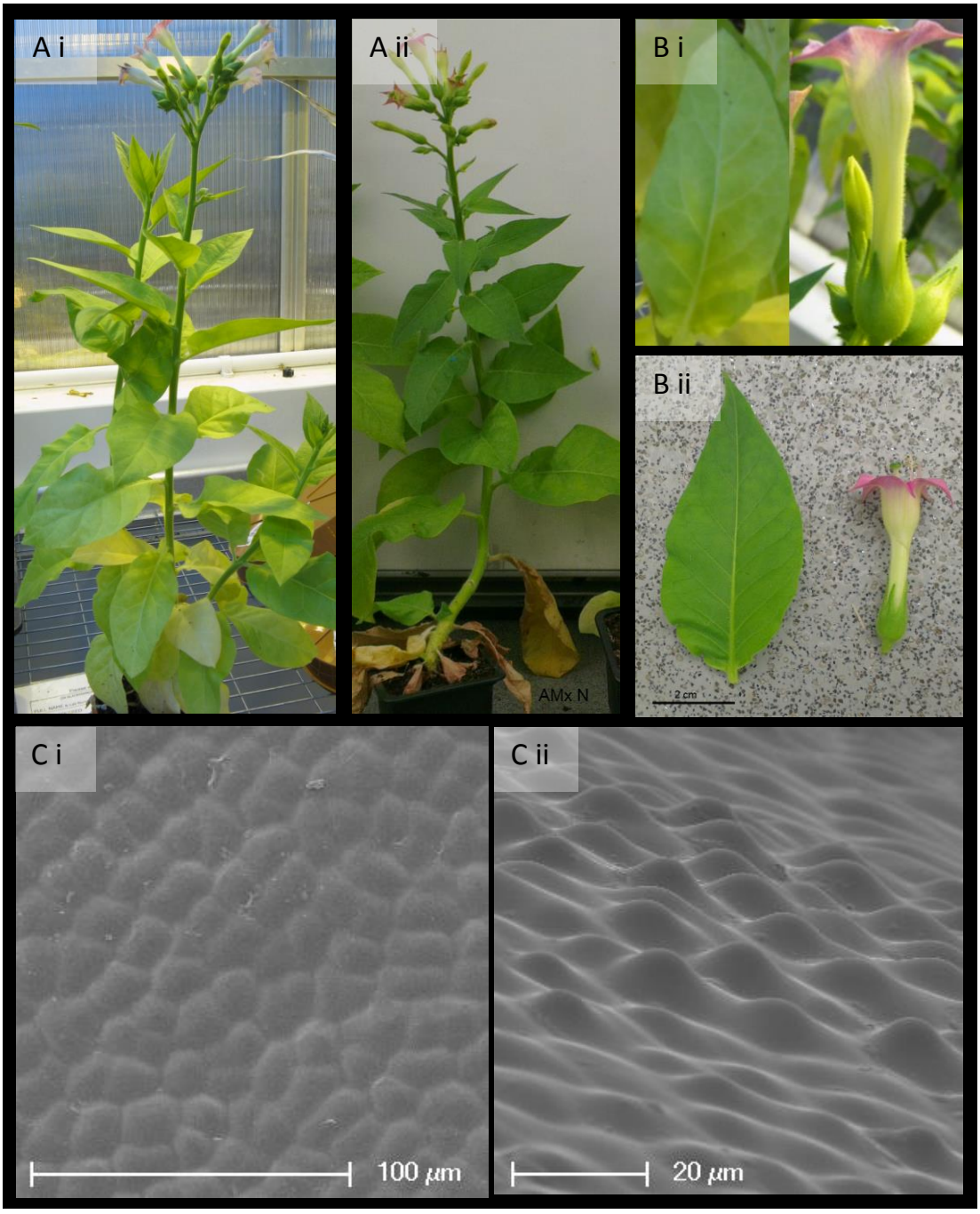

Figure 5.4 Tobacco expressing *S. aviculare* ML. (A) Plant growth habit. i, wild type. ii, *S. aviculare* ML transgenic. (B) Leaf and flower. i, wild type. ii, *S. aviculare* ML transgenic. (C) SEM of ovary abaxial epidermis. i,wild type. ii, *S. aviculare* ML transgenic. Transgenic plants were of normal growth habit, leaf shape and size, and normal flower morphology. SEM of the carpel shows conical outgrowths across the entire ovary abaxial epidermis.

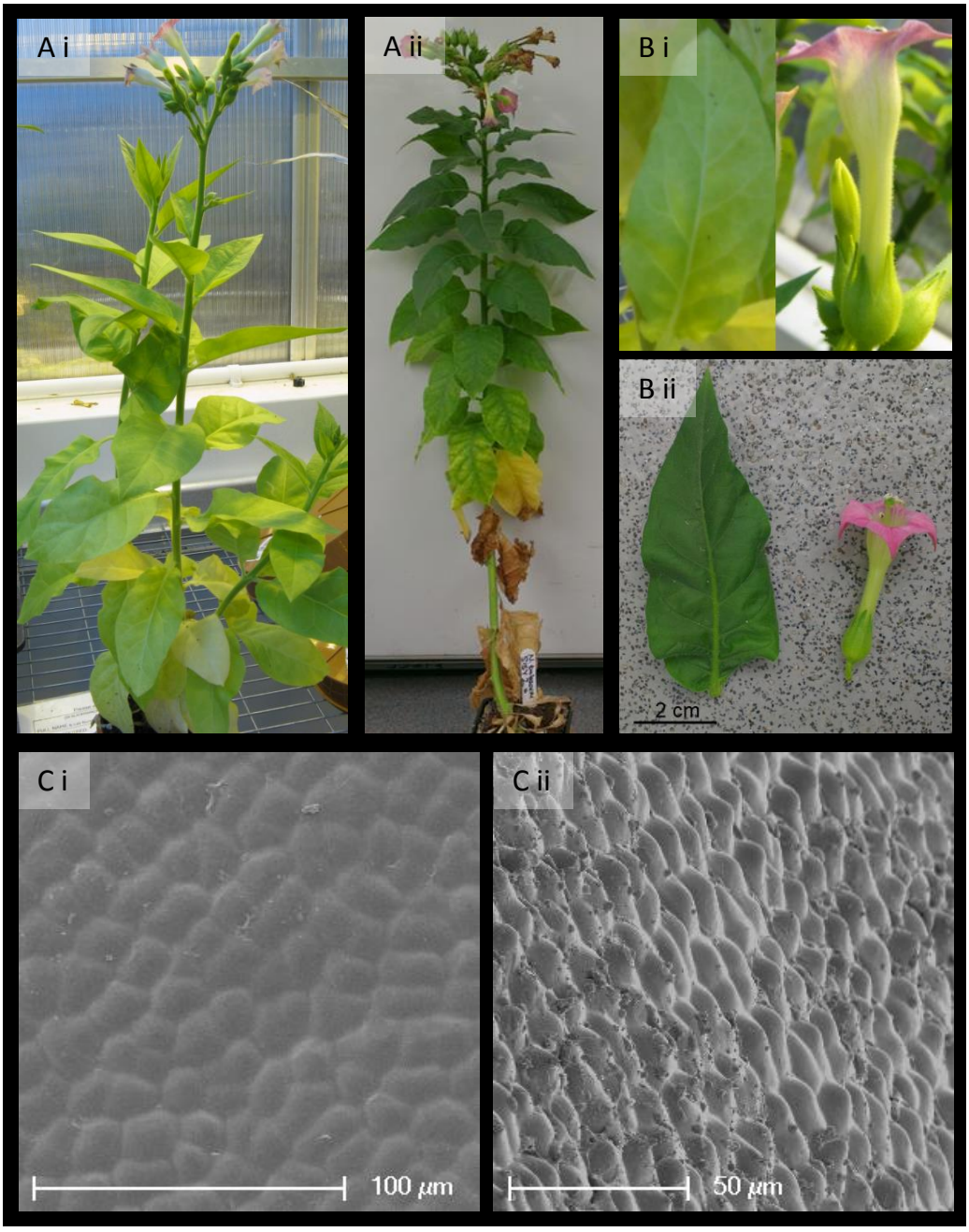

Figure 5.5 Tobacco expressing S. sisymbriifolium ML. (A) Plant growth habit. i, wild type. ii, S.sisymbriifolium ML transgenic. (B) Leaf and flower. i, wild type. ii, S. sisymbriifolium ML transgenic. (C) SEM of ovary abaxial epidermis. i,wild type. ii S. sisymbriifolium ML transgenic. Transgenic plants were of normal growth habit, leaf shape and size, and normal flower morphology. SEM of the carpel shows conical outgrowths across the entire ovary abaxial epidermis.

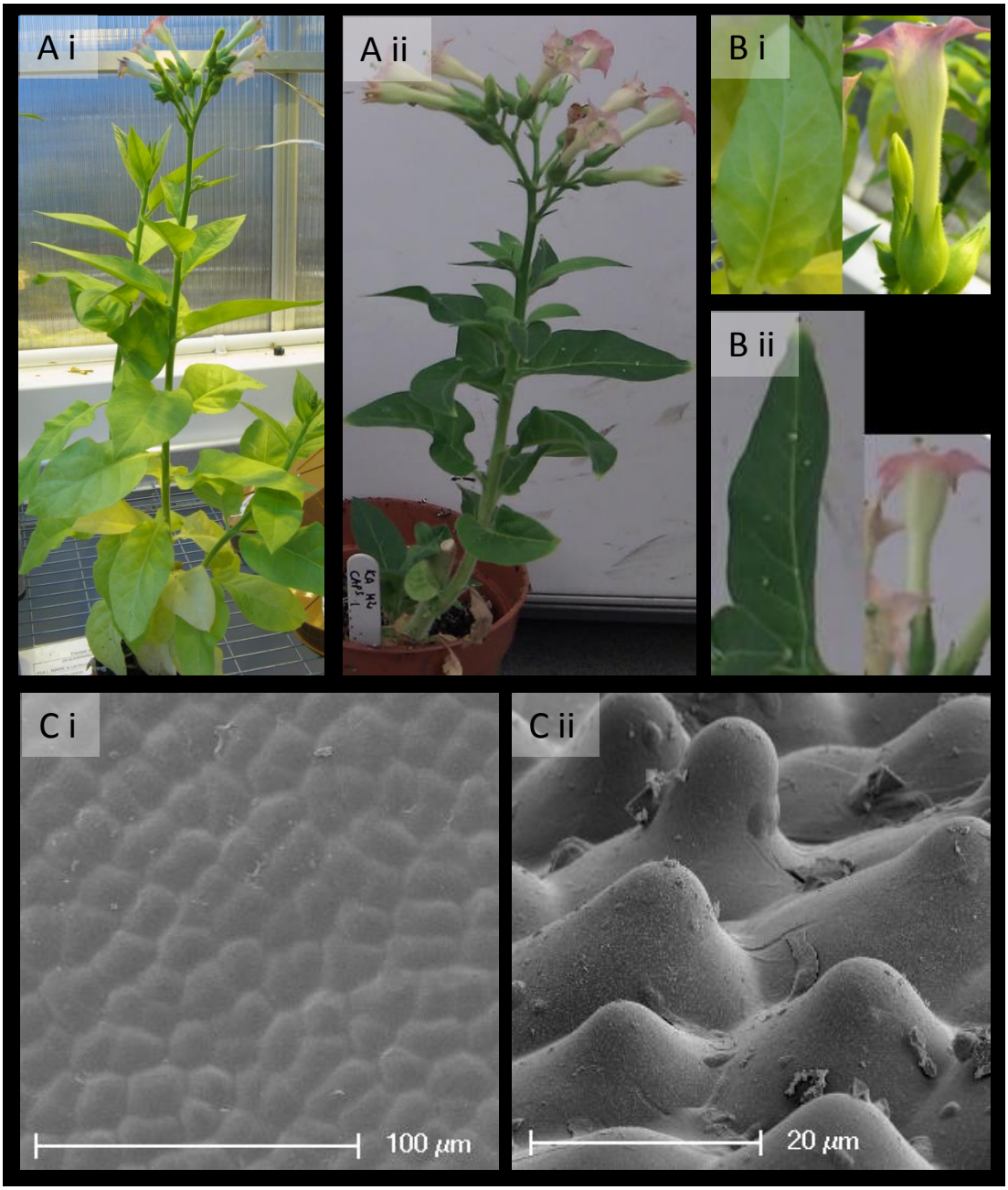

Figure 5.6 Tobacco expressing *S. capsicoides* ML. (A) Plant growth habit. i, wild type. ii, *S.capsicoides* ML transgenic. (B) Leaf and flower. i, wild type. ii, *S. capsicoides* ML transgenic. (C) SEM of ovary abaxial epidermis. i,wild type. ii *S. capsicoides* ML transgenic. Transgenic plants were of normal growth habit, leaf shape and size, and normal flower morphology. SEM of the carpel shows conical outgrowths across the entire ovary abaxial epidermis.

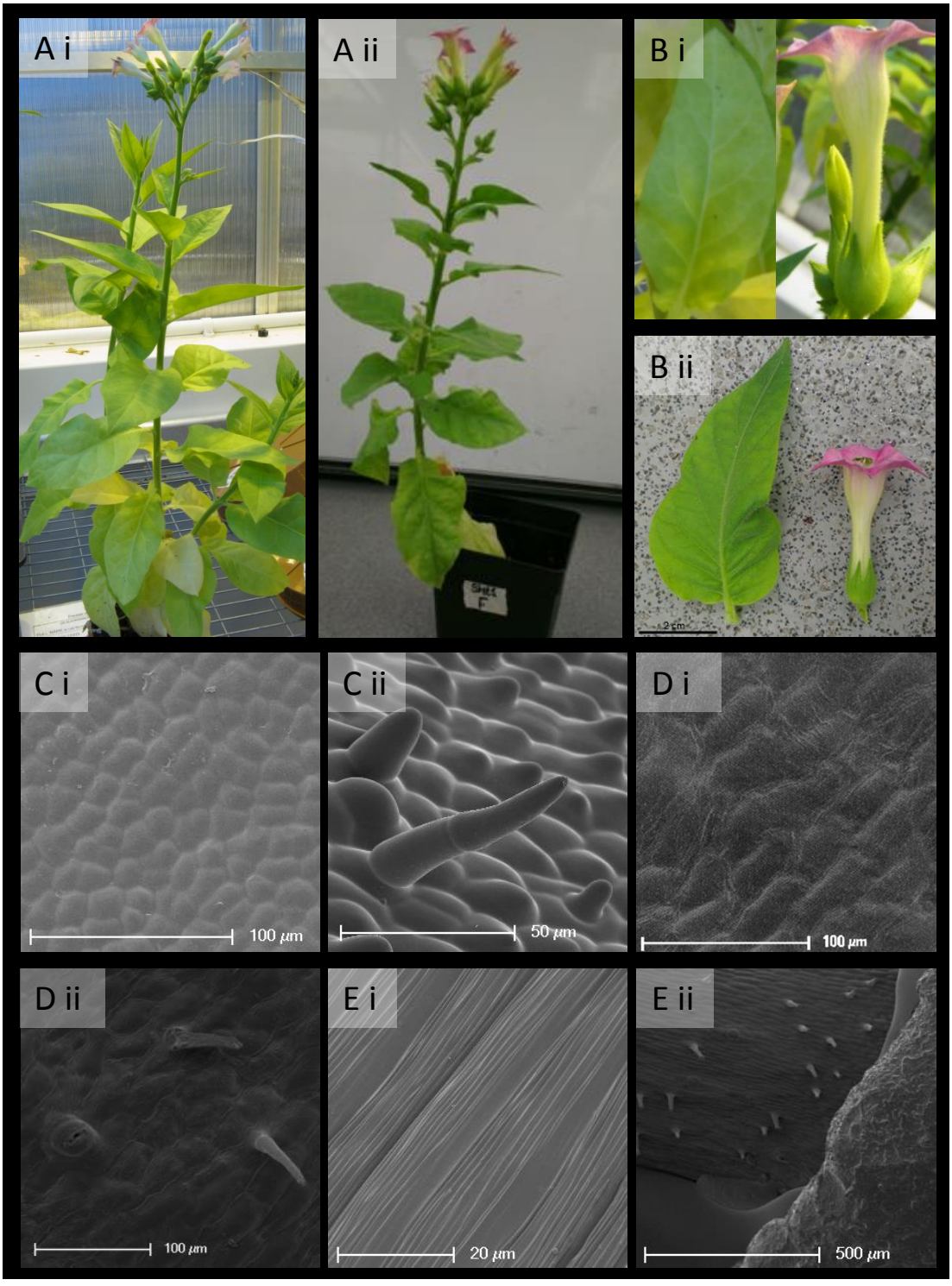

Figure 5.7 Tobacco expressing *S. sisymbriifolium* Mx. (A) Plant growth habit. i, wild type. ii, *S.sisymbriifolium* Mx transgenic. (B) Leaf and flower. i, wild type. ii, *S. sisymbriifolium* Mx transgenic. (C) SEM of ovary abaxial epidermis. i,wild type. ii *S. sisymbriifolium* Mx transgenic. (D) SEM of inner corolla tube. i,wild type. ii *S. capsicoides* Mx transgenic. (E) SEM of style epidermis. i,wild type. ii *S. capsicoides* Mx transgenic. Transgenic plants were of normal growth habit, leaf shape and size, and normal flower morphology. SEM of carpel shows conical outgrowths across the entire ovary abaxial epidermis, as well as ectopic trichomes. SEM of inner corolla (petal adaxial) epidermis shows ectopic trichomes and stomata, and the distal portion of the style shows ectopic trichomes.

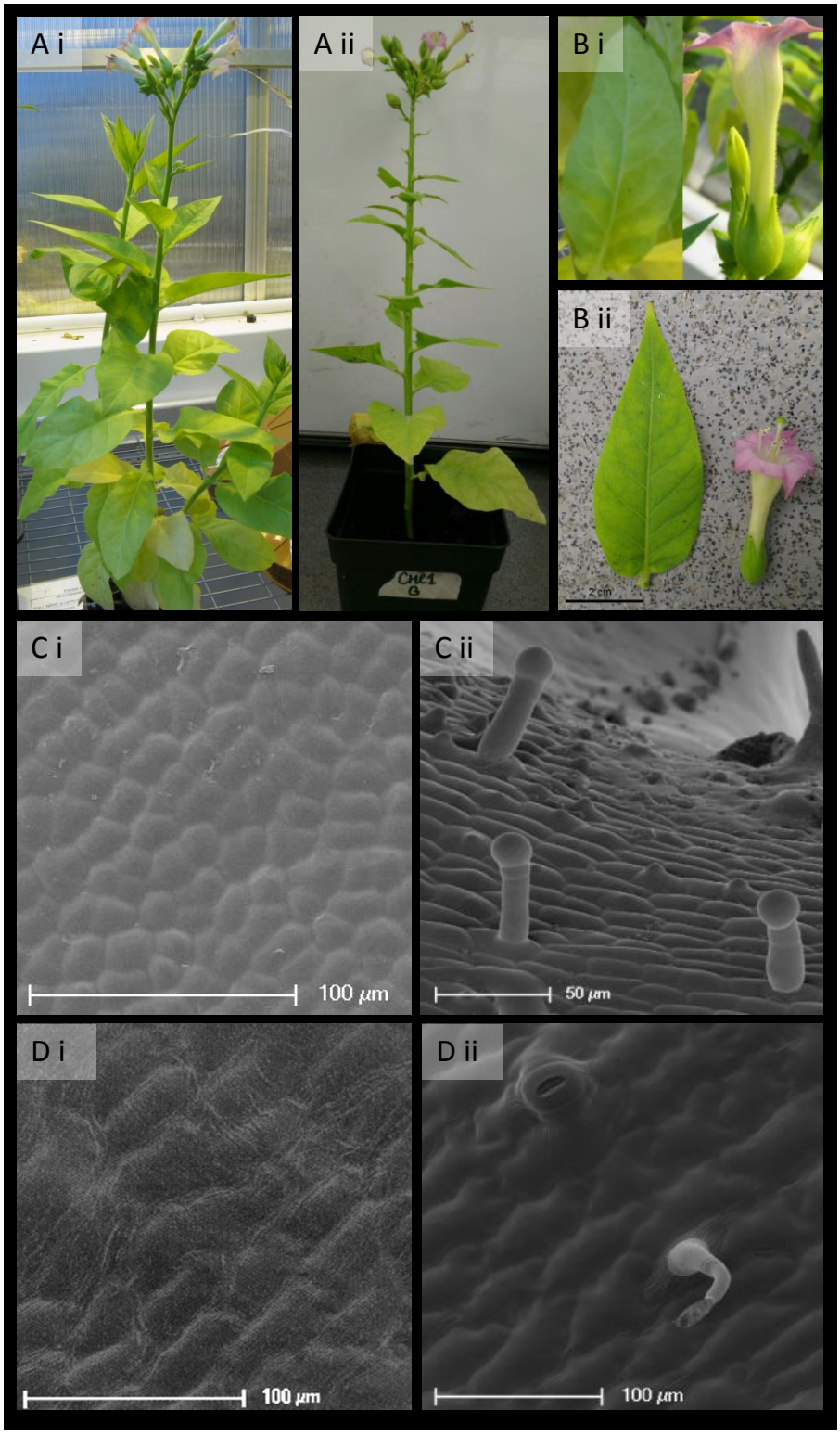

Figure 5.8 Tobacco expressing *S. capsicoides* Mx. (A) Plant growth habit. i, wild type. ii, *S. capsicoides* Mx transgenic. (B) Leaf and flower. i, wild type. ii, *S. capsicoides* Mx transgenic. (C) SEM of ovary abaxial epidermis. i,wild type. ii *S. capsicoides* Mx transgenic. (D) Corolla tube inner (petal adaxial) epidermis. i,wild type. ii *S. capsicoides* Mx transgenic. Transgenic plants were of normal growth habit, leaf shape and size, and normal flower morphology at the macro level. SEM of carpel shows conical outgrowths across the entire ovary abaxial epidermis as well as ectopic multicellular trichomes. SEM of the inner corolla tube (petal adaxial) epidermis shows ectopic trichomes and stomata.

S. laciniatum (C) and *S. aviculare* (F) *Mixta-Like* expression in tobacco produced similar phenotypes, with both genes producing plants that were phenotypically normal except for producing ectopic conical cells on the ovary abaxial epidermis. The one difference was that *S. laciniatum* (C) additionally produced ectopic stomata on the ovary abaxial epidermis. This shows that these genes both have a similar capability to produce conical cells, and there is no evidence of any impairment in the *Mixta-Like* gene in flat-celled *S. aviculare*. *S. sisymbriifolium* (C) and *S. capsicoides* (F) *Mixta-Like* expression in tobacco also resulted in similar phenotypes, with plants morphologically normal except for ectopic conical cells on the ovary abaxial epidermis. *S. capsicoides* (F) *Mixta-Like* also produced occasional ectopic stomata on the ovary abaxial epidermis, and this phenotype was not observed for *S. sisymbriifolium* (C) *Mixta-Like*.

The similarity in phenotypes of all four Mixta-Like proteins suggests that all retain a very similar capability to produce conical outgrowth in their native species. While the Mixta-Like protein from one species in each sister species pair was also capable of producing ectopic stomata, in one case it was the conical-celled species and in the other it was the flat-celled species that produced this phenotype. This phenotype in tobacco is therefore not correlated with the presence or absence of conical petal cells in the native species.

5.2.5 Comparison of *S. sisymbriifolium* and *S. capsicoides Mixta* and *Mixta-Like* expression phenotypes

S. sisymbriifolium (C) and *S. capsicoides* (F) *Mixta* genes expressed in tobacco produce phenotypes subtly different to that observed for the *Solanum Mixta-Like* genes described, though again the phenotypes are very similar within this sister species pair. Genes from both species produced conical outgrowths of the ovary abaxial epidermis, as well as intermittent trichomes in this same tissue. Both species produced tapered multicellular trichomes on the ovary abaxial epidermis as well as multicellular trichomes with a glandular apical cell, though *S. capsicoides Mixta* appeared to induce a greater proportion of this second type of trichome. Both genes also induced formation of ectopic trichomes and stomata on the inner corolla tube epidermis. *S. sisymbriifolium* (C) *Mixta* also produced trichome-like outgrowths of the distal portion

of the style in the area nearest the stigma. The differences between phenotypes are minor, and these results suggest that each gene retains a similar functionality. This suggests that there has been no loss of functionality of the *Mixta* gene in the flat-celled species *S. capsicoides* compared to the conical-celled *S. sisymbriifolium*.

5.2.6 Comparison of *Solanum* R2R3 MYB Subgroup 9A expression phenotypes with Subgroup 9A genes previously studied

None of the genes studied produced any phenotypic changes in tobacco vegetative tissues. This phenotype differs from the original *AmMIXTA* expression phenotype in tobacco, which showed outgrowths of the epidermis into conical cells and/or trichomes in all aerial tissues, both vegetative and reproductive (Glover, Perez-Rodriguez & Martin 1998).

The phenotypes of *Mixta-Like* expression in tobacco observed in this study most closely resemble those obtained from expression of *AmMYBML2, AtMYB16, PhMYB1* and *TtMybMl2* (from *Thalictrum thalictroides*). These genes, when expressed in tobacco, produced conical outgrowths of the ovary abaxial epidermis (Baumann *et al.* 2007; Di Stilio *et al.* 2009) but did not produce trichomes of the ovary abaxial epidermis as was observed for *AmMIXTA* (Glover, Perez-Rodriguez & Martin 1998). Similarly to phenotypes observed in this study, expression of *Gorteria* R2R3 MYB Subgroup 9A genes in tobacco also produced conical outgrowths of the ovary abaxial epidermis, and conical outgrowths and ectopic stomata on the inner corolla tube epidermis (M. Thomas, PhD thesis 2009). Floral tissues that normally produce cellular outgrowths in wild type tobacco plants showed increased magnitude of these outgrowths in expressing lines of each of *AmMYBML2, AtMYB16* and *PhMYB1* (Baumann *et al.* 2007), but this phenotype was not observed in expression lines of *Solanum Mixta-Like* genes in this study.

Solanum Mixta expression in tobacco produced epidermal outgrowths in reproductive tissues, producing conical cells as well as multicellular trichomes. This phenotype is most similar to the phenotype of tobacco plants expressing *AmMybMl1*, which produced no outgrowths in tobacco vegetative tissues, but produced both conical cells

and multicellular trichomes on the ovary abaxial epidermis and trichomes in the corolla (Perez-Rodriguez *et al.* 2005).

5.2.7 Implications of phenotypic differences arising from expression of R2R3 MYB Subgroup 9A *Mixta* and *Mixta-like* genes in tobacco

Phenotypes observed when *Solanum Mx* genes were expressed in tobacco included epidermal outgrowths in a greater number of aerial tissues than when *Solanum* ML genes were expressed. *Mx* genes also produced longer outgrowths in the form of unicellular and multicellular trichomes, while *ML* genes only produced conical cells, like small papillae. An explanation for this could be that *Mx* genes might drive the expression of different target genes, preferentially effecting the production of trichomes, and might suggest a divergence of function between *Mx* and *ML* genes in their native species, where *Mx* genes may function to produce trichomes or longer cellular outgrowths, whereas ML genes could be driving outgrowth into the shorter conical cell form. Alternatively, *Mx* genes may simply activate higher levels of transcription in target genes, or bind more strongly to promoters. Since all expression in these experiments was driven by the same promoter, differences in expression pattern or level should not account for these differences, although transgene insertion into highly expressed or highly repressed regions of the genome can influence observed phenotype.

SdMybMl1 and SdMybMl2 proteins from *S. dulcamara* (F) when expressed in tobacco produced conical cells in the ovary abaxial epidermis (Glover, Nicholls and Martin, in prep.), similarly to *Solanum* Mx and ML proteins in this study. In *S. dulcamara* itself, expression analysis, expression, and gene downregulation by RNAi of each gene indicate that both are involved in leaf trichome formation (Glover, Nicholls and Martin, in prep.), and that each protein is capable of producing both conical cells and trichomes in their native species. However, neither protein from *S. dulcamara* was able to produce trichomes when expressed in tobacco. This shows that while expression in tobacco is a useful bioassay to assess the capability of a gene to produce cellular outgrowth in a heterologous species in comparison to previous genes of the same family, still the specific phenotype observed in tobacco may not correlate with the specific outgrowth

role each gene has in its native species. It is clear from the phenotypes of tobacco expressing each gene that the properties of *SdMybMl1* and *SdMybMl2* are have changed in comparison to R2R3 MYB Subgroup 9A genes previously assayed using this method. However, the specific changes to the proteins themselves are unknown, and could include changes such as an increase or decrease of their DNA binding specificities, or altered interactions with protein binding partners causing the phenotypes of each protein in their native *S. dulcamara* to differ from that observed when expressed in tobacco.

5.3 Conclusions

These results show that all of the *Solanum* R2R3 MYB Subgroup 9A genes tested have the ability to produce cellular outgrowth when ectopically expressed in tobacco. It can then be inferred that the amino acid changes in these genes have not disrupted their ability to bind to DNA and recruit the proteins necessary for expression of genes producing cell wall modifying proteins and cell expansion, and thus produce conical cells in their host species. This suggests that in species without conical petal cells another molecular mechanism, such as a change in expression patterns, has been responsible for this loss of the conical cell form. This hypothesis is explored in Chapter 6.

Chapter 6. Changes in R2R3 MYB Subgroup 9A gene expression correlate with conical petal cell loss in *Solanum*

6.1 Introduction

A major aim of this project was to determine the molecular mechanism behind the losses of conical cells in *S. capsicoides* (Leptostemonum) and *S. aviculare* (Archaesolanum). This Chapter will focus on the experiments designed to determine whether expression profile differences in the *MIXTA-Like* genes of each species correlate with the appearance of conical cells in the petal epidermis.

One loss of conical cells in *Solanum* (*S. dulcamara*, Dulcamaroid clade) is already known to be correlated with a change in expression patterns of its two R2R3 MYB Subgroup 9A genes (Glover, Nicholls and Martin, in prep.). To determine whether a similar change in expression could have caused the two independent cases of conical petal cell loss in *S. capsicoides* and *S. aviculare*, preliminary semi-quantitative RT-PCR was used to broadly gauge expression across different tissues, followed by a more robust fluorescence-based quantitative RT-PCR (qRT-PCR, or qPCR) analysis.

qPCR requires careful selection of reference genes to allow for accurate and reliable quantification of the genes of interest. Quantification of levels of expression of a gene across different tissues requires a comparator of one or more reference genes that are expressed in close to equivalent levels across all tissues. This allows for the expression levels of the genes of interest to be estimated by comparison relative to these stable reference genes. Since no reference gene shows perfectly equivalent expression across all tissue types, ideally three reference genes would be used in combination to minimise the error introduced by natural gene expression variability across different tissues. Several previous studies have tested the suitability of control genes in *Solanum*, and appropriate primers were selected from two high-quality analyses using *S. lycopersicum* (Coker & Davies 2003; Expósito-Rodríguez *et al.* 2008). To determine their validity for quantification of our genes of interest, these primers were tested for their stability and expression efficiency in each species.

Using SEM analysis of petal cell surfaces (adaxial epidermis) across different developmental stages, our analysis was refined to tissues most likely to show differences in expression levels. Finally, the relative expression of the *MIXTA-Like* gene was analysed across these tissues for each species using qPCR.

6.2 Results and Discussion

6.2.1 Preliminary expression analysis using RT-PCR

To test whether expression levels of R2R3 MYB Subgroup 9A genes differ between tissue types or between species a preliminary analysis using semi-quantitative RT-PCR was performed.

Using RT-PCR, we tested whether each of the R2R3 MYB Subgroup 9A genes showed detectable expression levels in each species. Of the two R2R3 MYB Subgroup 9A genes predicted for each *Solanum* species, only the *MIXTA-Like* gene was reliably amplified from cDNA from all four species. Attempts at PCR amplification of *MIXTA* genes from

each species consistently failed when using cDNA template across multiple developmental stages of leaf and flower tissue, though consistent amplification using genomic DNA template showed that the primers, reaction conditions and cycling conditions used were able to reliably amplify this gene. We chose therefore to focus our experiments on the *MIXTA-Like* gene in each species. Using cDNA of multiple tissue types from *S. capsicoides* and *S. sisymbriifolium* RT-PCR analyses were performed with primers designed and tested for specific detection of the *MIXTA-Like* gene (see Chapter 4, section 4.2.3). Each analysis was repeated several times and across different annealing temperatures in order to maximise the likelihood that any expression would be detected, using agarose gel electrophoresis, ethidium bromide staining and UV photography to detect and quantify the amplification. We found that of all the PCR analyses, at least one showed minimally detectable *MIXTA-Like* gene expression in all tissues of both species. However, most of these tissues did not show reliable amplification in every PCR conducted. All tissue types fell into one of two categories: we scored a tissue type as showing no or low *MIXTA-Like* expression if a band was seen in less than 20% of the total number of PCR reactions conducted on that tissue type, whereas if a band was seen in more than 80% of PCR reactions conducted on a tissue type, we scored this as showing reliable and significant expression.

S. sisymbriifolium showed expression of the *ML* gene in flower buds, mature petals and young leaves, and also produced the brightest DNA bands overall (Figure 6.1). In *S. capsicoides MIXTA-Like* expression was undetectable by PCR analysis most of the time. When occasionally a DNA band of the appropriate size was amplified (for example, from petal tissue, as shown in Figure 6.1) the tissue type from which this band originated was inconsistent. All of these tissues were therefore scored as showing no or low expression. Additionally, all bands seen for this species were faint. This suggests that in *S. capsicoides*, *MIXTA-Like* expression is very low in all tissues.

This initial investigation suggested that there may indeed be differences in expression between different species and tissue types, but the unreliability in detected expression also highlighted the inherent limitations of a semi-quantitative assay judged by subjective assessment of brightness of fluorescence using ethidium bromide as a stain for DNA. These initial analyses did give an indication that a more reliable qRT-PCR

using cycle-by-cycle fluorescence quantification could yield results relevant to this project.

A full semi-quantitative analysis was not performed for *S. laciniatum* and *S. aviculare*, though preliminary PCR assays using cDNA from leaf and flower tissue showed these genes were amplifiable from all tissues. These species were therefore also included in further qPCR analyses.

6.2.2 Choice of tissues for expression analysis

If *MIXTA-Like* gene activity was indeed responsible for the formation of conical cells in these *Solanum* species, we would expect its expression to be highest in (a) species that have conical petal cells, and (b) tissues at a developmental stage immediately prior to and during conical cell formation. A developmental series of *S. sisymbriifolium* (conical-celled) inflorescences was therefore analysed to determine the stages at which conical cell formation occurred. Epidermal cell morphology (petal adaxial epidermis) was analysed from six stages of *S. sisymbriifolium* inflorescences, from 3 mm buds to mature flowers (Figure 6.2). This developmental series shows that in *S. sisymbriifolium* adaxial petal cells remain flat until after the buds reach 1 cm in length. These buds are easily identified as being small and green, with no petal tissue having yet expanded beyond the thick, protective sepal layer. By the time the buds are 2 cm long (Figure 6.2 E), conical cells are near to fully developed as compared to those of the mature petal

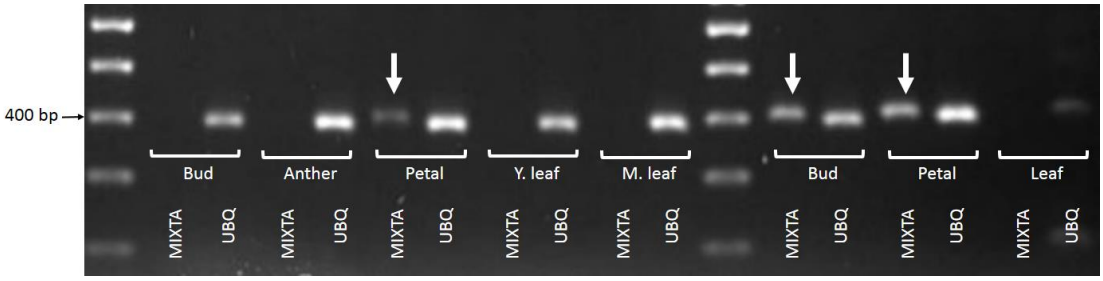

Figure 6.1 Semi-quantitative RT-PCR for *MIXTA-Like* gene expression in different tissues from *S. capsicoides* (left) and *S. sisymbriifolium* (right). Each tissue type shows a test lane (left, *MIXTA-Like*) and a control lane (right, ubiquitin). Lanes showing a band for the *MIXTA-Like* gene are indicated with an arrow. This gel shows detectable expression in mature petal tissues of both species, as well as in buds of *S. sisymbriifolium*. The strongest expression level is in the petals and buds of *S. sisymbriifolium*.

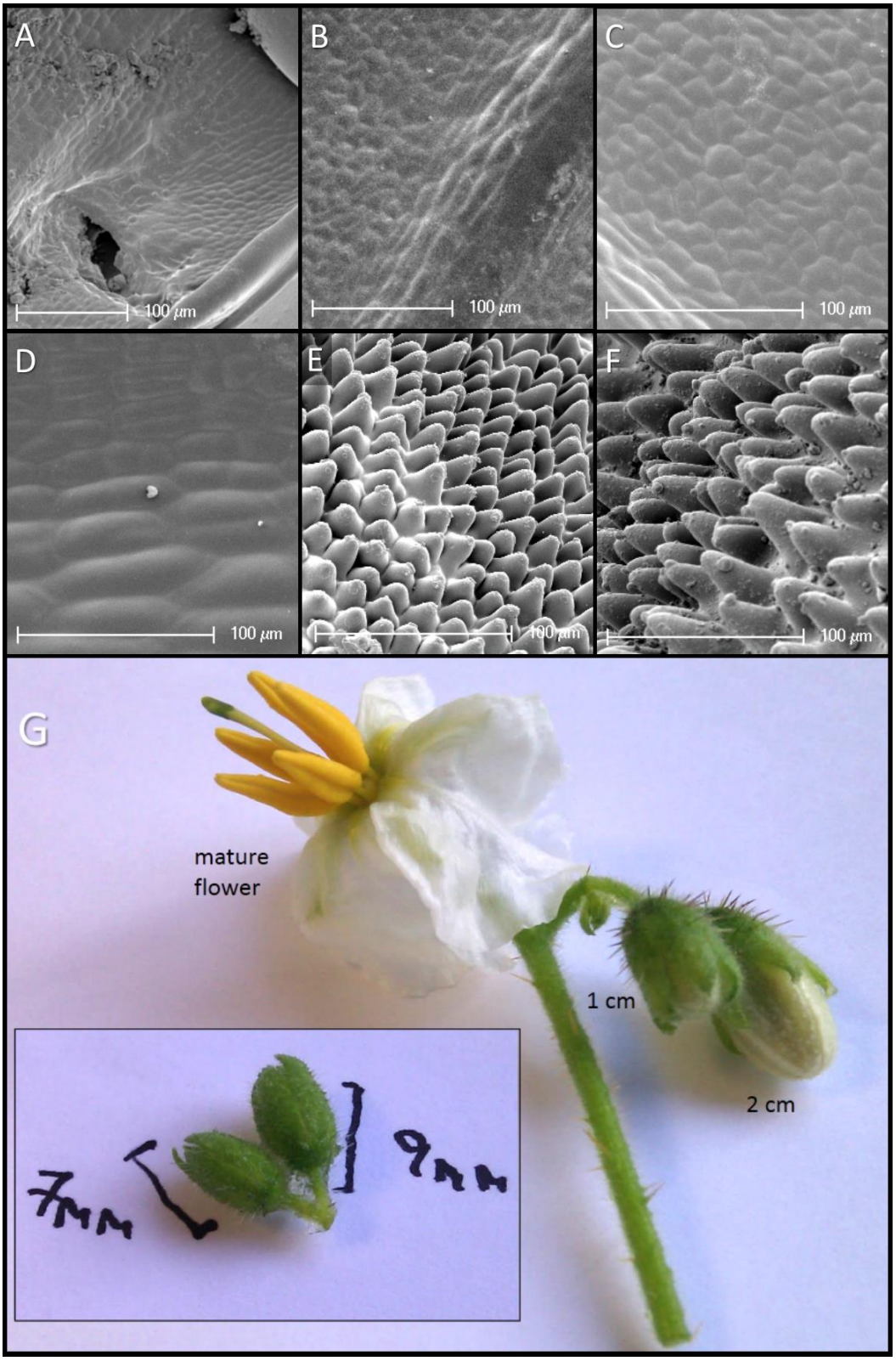

Figure 6.2 *S. sisymbriifolium* petal developmental series. Petal adaxial epidermal surfaces from (A) 3 mm bud. (B) 7 mm bud. (C) 9 mm bud. (D) 1 cm bud. (E) 2 cm bud. (F) Mature flower petal. Conical cells form between 1 cm and 2 cm buds, which also coincides with a rapid expansion of the whole flower bud. (G) Photographs of *S. sisymbriifolium* flowers at 7 mm, 9 mm, 1 cm, 2 cm and mature flower.

(Figure 6.2 F). This shows that conical cells initiate and complete development between these two stages, while buds are expanding but before the petals open. It is likely that if, as in other species, the R2R3 MYB Subgroup 9A genes are responsible for the formation of conical petal cells in *S. sisymbriifolium*, the developmental stage at which expression of these genes is highest would be between the 1 cm and 2 cm stages. For our quantitative analysis of *MIXTA-Like* expression levels, three developmental stages were therefore compared: (1) bud < 1 cm, before conical cells start to form; (2) bud 1 > 2 cm, during initiation and elongation of conical petal cells; (3) mature petal, after conical cells have fully formed. This gives the greatest probability of detecting any differences in expression between developmental stages. For *S. capsicoides* (flat celled), only two developmental stages of petal were used, for two reasons: firstly, *S. capsicoides* does not have conical cells and as such there are no significantly different stages of petal cell expansion. Secondly, because its flowers are small and not very numerous, collecting enough tissue for RNA extraction was extremely difficult, particularly in the youngest tissues. For this species we therefore tested only two developmental stages of petal tissue, one set of RNA pooled from petals of multiple bud development stages, and a second from petals of mature flowers. Expression in young and mature leaves of each species was also tested.

After *S. laciniatum* (conical celled) and *S. aviculare* (flat celled) were selected as a second sister-species pair, it was decided to compare expression in tissues of equivalent maturity. The stages for these species were determined by similarity to *S. sisymbriifolium* flower developmental stages: the earliest stage tested used petals from buds in which petals had not yet expanded beyond the calyx ("young bud"), the intermediary stage used petals from buds that had petals extended beyond the calyx but that had not yet opened ("mature bud"), and the most mature stage used petals from young but fully opened flowers ("mature petal"). It was not possible to extract RNA of sufficient quality and quantity from conical-celled *S. laciniatum* and this species was therefore not included in our analysis.

6.2.3 Reference gene suitability testing

To determine whether the chosen primers would be suitable for use in the *Solanum* species studied by this project, some preliminary testing was required. Using cDNA from the five different tissues of *S. aviculare* and *S. sisymbriifolium* and four of *S. capsicoides*, four potential reference genes were tested for stability of expression across different tissues, as well as efficiency of amplification overall.

Preliminary quantitative testing of control primers for CAC (Clathrin adaptor complexes medium subunit; Endocytic pathway), DNAj (heat shock N-terminal domain-containing protein), GAPDH (Glyceraldehyde-3-phosphate dehydrogenase; Glycolysis, Gluconeogenesis) and SAND (SAND family protein) (originally designed and tested for *S. lycopersicum*, Expósito-Rodríguez *et al.* 2008) showed CAC and DNAj to be the most stable primers overall, with amplification efficiencies in tomato of 80% and 100% respectively. An amplification efficiency of 100% indicates perfect doubling of the target sequence each cycle. Primers for the *MIXTA-Like* genes were carefully designed so that the reverse primer would bind to cDNA with half of the primer binding before the first intron and the second half of this same primer binding after the intron. This design across an intron/exon boundary ensures that the amplicon can only be amplified from processed transcripts with this intron removed, preventing contamination of the fluorescence signal from any residual genomic DNA.

CAC and DNAj both showed a high level of amplification, 89% and 88% respectively, whereas SAND was lower at 80% (Table 6.1). The primers to amplify MIXTA-Like genes showed an amplification efficiency of 94%. Amplification efficiencies over 80% are sufficient for accurate quantitative PCR analysis (Raymaekers *et al.* 2009).

For each species, DNAj showed the most stable expression across all tissues (Figure 6.3), with each species producing threshold cycle (Ct) values, or the cycle number at which the fluorescence can be reliably determined to be above background levels (Bustin *et al.* 2009, 2010; Taylor *et al.* 2010), with a standard deviation average less than one cycle per tissue type. This means that the changes in expression of the *MIXTA-Like* gene in each species can be quantified relative to this standard with confidence that they will accurately reflect differences in expression levels in these tissues.

Name	cDNA amplicon (nt)	Genomic amplicon (nt)	Primer efficiency (%)	Stability across tissue types
CAC	173	610	89	N
DNAj	158	570	88	Y
SAND	164	n/a	80	N
MIXTA-Like	97	n/a	94	n/a

Table 6.1 Amplicon size, primer amplification efficiency and stability across different tissue types for each primer set tested. Three sets of primers for three different reference genes were tested, as well as primers designed to amplify the *MIXTA-Like* gene from all species

6.2.4 Quantitative RT-PCR expression analysis of *MIXTA-Like* genes

Expression levels for each tissue type were tested using three biological replicates and three technical replicates (9 replicates in total per gene, for each tissue type). Any replicate for which the melt curve analysis or gel electrophoresis indicated that observed fluorescence was primarily due to primer dimer rather than the expected amplicon was excluded from the analysis.

Mixta-Like expression in *S. sisymbriifolium* (conical) was highest of the three species tested (Figure 6.4). Expression levels within this species are, overall, two to three times higher than that of any tissue in *S. aviculare* or *S. capsicoides* (both flat). Within this species, *MIXTA-Like* expression is highest in floral tissues, and slightly lower in both young and mature leaves. Expression of the *MIXTA-Like* gene is highest, and also of greatest variability, in petals from young flower buds < 2 cm.

Expression in leaves of *S. sisymbriifolium* was a little lower than in flowers, but still over twice as high as expression in either of the flat-celled species. Both *S. capsicoides* (F) and *S. sisymbriifolium* (C) have prominent leaf trichomes, but leaves of *S. sisymbriifolium* are covered much more densely with these hairs.

Expression of *MIXTA-Like* across all tissues of the two flat-celled species, *S. capsicoides* and *S. aviculare*, was significantly lower than that in *S. sisymbriifolium*.

In *S. aviculare* (flat celled), expression of *MIXTA-Like* was highest in young leaves and mature buds. Mature petals and young buds show expression at about half these levels, and mature leaves show the lowest expression at a third of the expression seen in young leaves.

S. capsicoides (flat celled) showed the lowest expression overall, but most importantly, shows no detectable expression in petals of developing buds. In this species expression is highest in young leaves, showing levels of expression equivalent to that in young leaves of *S. aviculare*. Expression levels around half that of young leaves were detected in mature leaves, and almost negligible expression was seen in mature petals.

These expression profiles broadly correlate with the presence of conical cells. The conical-celled species, *S. sisymbriifolium*, shows the highest expression overall and within this species the greatest levels of expression are seen in the petal tissues. The

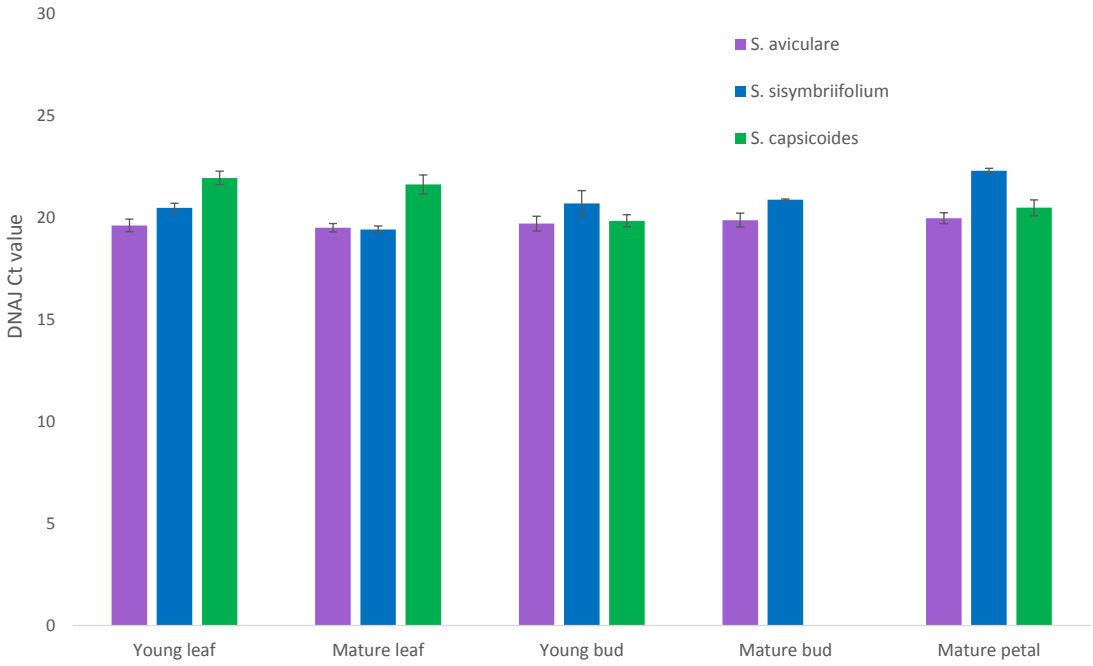

Figure 6.3 Ct values of control gene DNAj across different tissues in all species studied. This gene shows the lowest variability between tissue types and across species of all the control genes tested, varying in the threshold cycle number (Ct) by less than three cycles between species and tissue types. This then gives the best consistency for quantification of the gene of interest. Error bars are ± 1 standard deviation.

highest *MIXTA-Like* expression is found in petals from the youngest bud stage, before conical cells begin to form, and in mature petal tissue. This suggests that if *MIXTA-Like* is controlling conical cell formation in this species, its average expression is highest in buds prior to the initiation of conical cell outgrowth. However, expression at this developmental stage is also the most variable, as shown by the large size of the error bars representing the SEM for this set of data. Expression during the next developmental stage, while conical cells are forming in mature buds, is much more consistent though on average slightly lower than that seen in young buds. Expression in mature petals is similar to levels in young buds, though again this expression shows less variation as shown by the smaller SEM than in young buds.

Epidermal petal cells of *S. capsicoides* and *S. aviculare* differ in that while those of *S. capsicoides* are completely flat, *S. aviculare* has cells that are slightly domed or

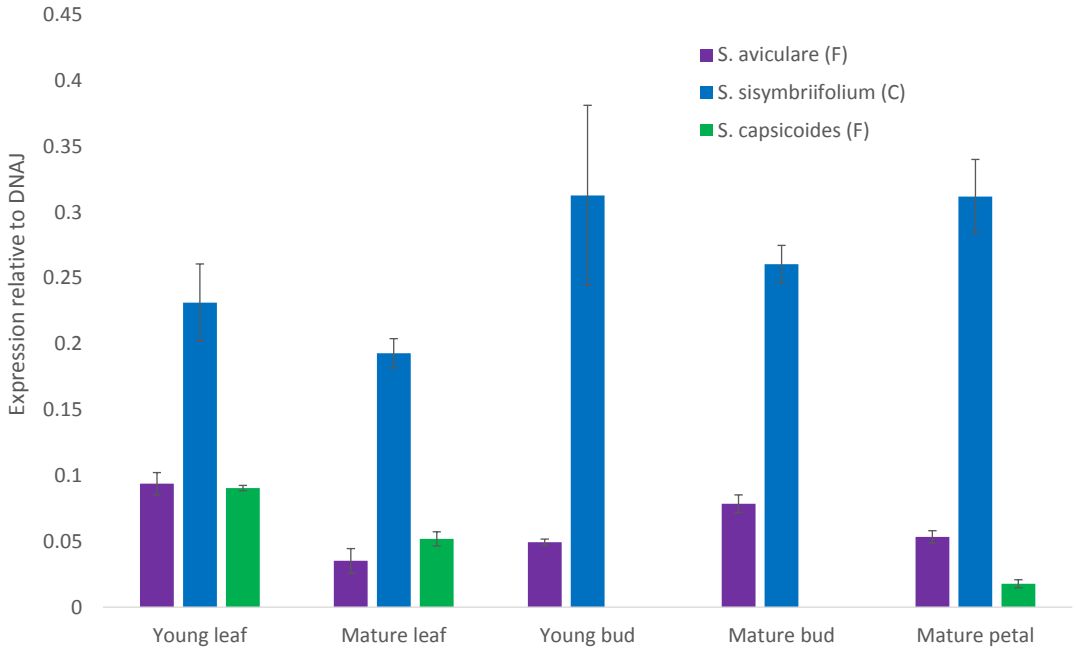

Figure 6.4 Relative expression levels of *MIXTA-like* genes across different tissues and developmental stages for *S. sisymbriifolium*, *S. capsicoides* and *S. aviculare*. All values are reported relative to the same standard reference gene, DNAj, and are the mean of 2-3 biological replicates each with 3 technical replicates. Of the test gene, *MIXTA-Like* from each species, *S. sisymbriifolium* (C) shows the highest expression overall with expression levels in *S. aviculare* (F) and *S. capsicoides* (F) showing similar and much lower expression overall. No data is shown for *S. capsicoides* bud tissue because the melt curve and gel electrophoresis indicated that all fluorescence in this tissue type was due to primer dimer, indicating that any *MIXTA-Like* expression in this tissue is undetectably low. Across the three species, the level of *MIXTA-Like* transcript correlates with the presence of conical cells, with little to no expression in *S. capsicoides* (F) flowers, highest expression in *S. sisymbriifolium* (C) flowers and low expression in *S. aviculare* (F) flowers. Since flowers of *S. aviculare* have slightly domed rather than fully flat epidermal cells, this small amount of *MIXTA-Like* expression may be responsible for this small amount of conical outgrowth. Error bars are ± SEM.

lenticulate. Comparing the expression of *MIXTA-Like* in these two species, in petals of *S. aviculare* where cells are lenticulate, some *MIXTA-Like* expression is present during the early and intermediate bud developmental stages. This could suggest that a low level of *MIXTA-Like* expression is causing the outgrowth of these cells into a short domed cell. This contrasts both with *S. sisymbriifolium*, which shows high *MIXTA-Like* expression during these two bud stages and has tall and pronounced conical petal cells, and with *S. capsicoides*, which has no detectable *MIXTA-Like* expression in its buds and has petal cells that are flat.

The observed expression patterns of *Mixta-Like* genes in the conical-celled species *S. sisymbriifolium* show that conical petal cells are correlated with high *Mixta-Like* expression. Additionally, in the flat-celled species *S. aviculare* and *S. capsicoides* a lack of *Mixta-Like* expression correlates with flat petal cells. This suggests that the evolutionary loss of conical petal cells in *S. capsicoides* and *S. aviculare* has occurred through a loss of *Mixta-Like* gene expression in the petals.

Expression of the second R2R3 MYB Subgroup 9A gene, *Mixta*, could not be detected in any species during preliminary testing so this gene was not included in the quantitative analyses detailed in this Chapter. It is still possible that *Mixta* is expressed in association with conical cell development but that this expression was missed by these preliminary tests, however this is unlikely since this testing included petal developmental stages associated with the initiation and outgrowth of conical cells. It is therefore unlikely that *Mixta* is involved in petal epidermal development or the formation of conical cells in these species.

6.3 Conclusions

The correlation between the presence of conical petal cells and higher overall *MIXTA-Like* gene expression, particularly in developing flower buds, suggests that a change in expression could indeed account for the loss of conical cells in *S. capsicoides* and *S. aviculare*. Expression level of *MIXTA-Like* in the conical-celled *S. sisymbriifolium* across

all tissues is at a minimum twice as high as that of any tissue in either of the flat-celled species, and expression is highest in petal tissues.

It was shown in Chapter 5 that there is little difference in R2R3 MYB Subgroup 9A protein function between sister species. We therefore conclude that the evolution of flat petal cells in *S. aviculare* and *S. capsicoides* has occurred through regulatory change and not through a change in protein function. This reiterates findings from *S. dulcamara*, in which conical petal cells have been lost through a change in R2R3 MYB Subgroup 9A gene expression (Glover, Nicholls and Martin, in prep.). In combination with the results of ancestral character reconstruction showing that each of these losses occurred in separate evolutionary events (Chapter 3, section 3.2.7), we conclude that the loss of conical cells in *Solanum* has occurred multiple times through similar molecular mechanisms. This provides an example of repeatability in the genetic changes associated with convergent evolution of a floral trait.

Chapter 7. Conical cells and flower movement affect pollinator preference

7.1 Publication

The work presented in this chapter has been published in the journal *Functional Ecology* as 'Flower movement increases pollinator preference for flowers with better grip' (Alcorn, Whitney & Glover 2012).

7.2 Introduction

In this chapter the mechanisms causing pollinator preference in favour of conical cells are investigated. Conical cells are common across the angiosperms and occur in diverse species with many different flower forms. In trying to understand what possible common benefit conical cells might bring to all these different species, this diversity must be taken into account.

As discussed in Chapter 1 sections 1.1.2 and 1.3, studies of *Antirrhinum majus* clearly show that conical cells provide a tactile advantage to pollinator handling for these

complicated flowers (Whitney *et al.* 2009). However, looking more widely across the angiosperms there is no shared flower form that correlates with the presence of conical cells in the petal epidermis. There is also no evidence of a correlation between presence of conical cells and flower presentation angle (Rands, Glover & Whitney 2011). In trying to determine why conical petal cells are so prevalent, it may not be possible to usefully generalise from studies using *Antirrhinum*. The very specific method of flower handling in *Antirrhinum* may create equally specific pollinator preferences, so the selective pressures affecting *Antirrhinum* are very likely to differ from those of plants with simpler flowers.

7.2.1 Motion and bee vision

Flowers that initially appear relatively easy for a pollinator to handle may still benefit from producing petal surfaces that enhance pollinator grip in different and variable environmental conditions. One such condition may be when flowers are moving.

Motion is an integral part of a bee's perception of their environment. Bees have limited use of binocular stereopsis (Brünnert, Kelber, & Zeil 1994), and their ability to perceive depth and position in three-dimensional space is strongly dependent on motion parallax, the perceived change in position of stationary objects due to movement of the observer (Lehrer et al. 1988; Srinivasan, Lehrer, & Horridge 1990). Bee target detection is significantly improved in 3D tasks when bees use motion parallax in conjunction with colour cues (Kapustjansky, Chittka, & Spaethe 2010) and bees are also innately attracted to moving objects (Lehrer & Srinivasan 1992). Recently, plants have been shown to exploit movement as a cue for pollinator attraction, with increased stalk length and increased flower 'waviness' correlating with increased attractiveness to pollinators (Warren & James 2008). Increased flower mobility also increases pollen transfer in hummingbird pollinated species of *Impatiens*, but significantly reduces the efficiency of hummingbird foraging (Hurlbert, Hosoi, & Temeles 1996).

7.2.2 *Petunia*

Flowers that move in the breeze may be able to take advantage of a bee's normal use of motion as part of their visual system to increase the attractiveness of those flowers. However, the motion of flowers under natural variable wind conditions could make even simple flowers more difficult for a pollinator to land on and handle. In order to understand the effect of motion on pollinator preference, and investigate the possible benefits of conical petal cells to a simple flower, bee preferences were tested using *Petunia hybrida* (Figure 7.1) which has conical petal cells in the wild type. The flowers of *Petunia* consist of a short tube opening in a flared trumpet-shape to a broad, flat surface that provides a landing platform on which bees easily land and grip while drinking from the central tube. Since this floral morphology contributes little inherent handling difficulty, this makes *Petunia* an ideal flower with which to investigate the benefits of conical petal cells under conditions of flower motion.

To test bee preferences for *Petunia* flowers differing only in the shape of their petal cells, we used a line of *Petunia* in which the *PhMYB1* gene, responsible for the formation of conical cells, is disrupted by insertion of the dTph1 transposon. This results in petal epidermal cells that are much flatter than the tall cones of the wild type (Van Houwelingen *et al.* 1998; Baumann *et al.* 2007). Using the *phmyb1* mutant and a revertant wild type line from which the transposon has excised germinally, bee preferences for flowers with flat or conical cells were tested.

7.2.3 Conical cells and motion in pollinator preference

To test whether bee preference for different epidermal morphologies changes under different handling conditions, an added tactile difficulty was imposed by presenting bees with moving flowers to mimic the motion of flowers under variable natural wind conditions.

To simulate the wind movement that a bee might encounter when foraging in the wild, a small laboratory orbital shaker was used (Figure 7.2). The platform of this shaker moves in a rotational motion which simulated the motion of flowers moving in the breeze. To determine the optimal speed for this motion, preliminary observations were made of single bees foraging from flowers placed on the platform while it was moving at different speeds. At 70 rpm, most bees were able to forage from the flowers, but when the speed was increased to 100 rpm only a few bees were

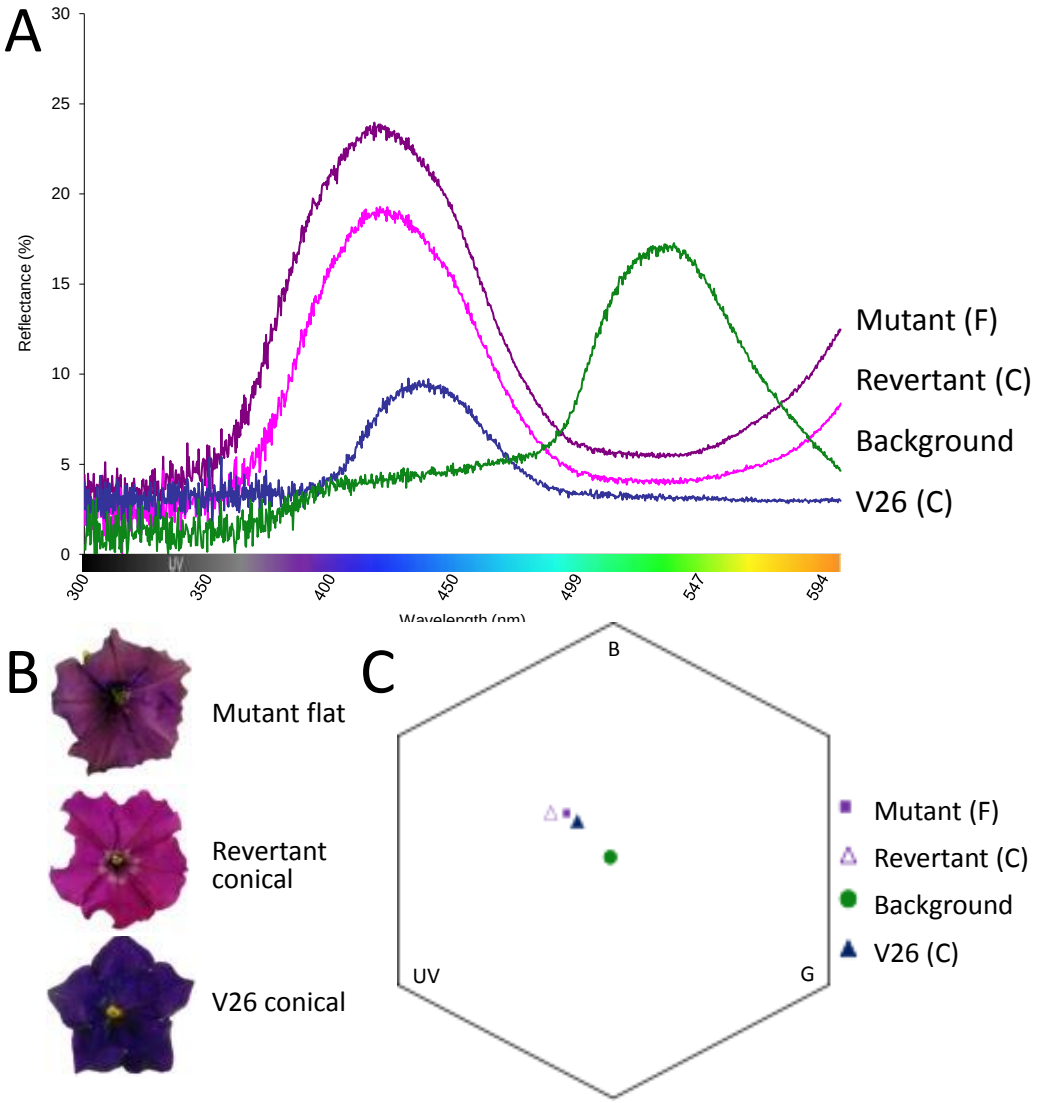

Figure 7.1 Flower colour of each of the three lines used in this study. (A) Spectrophotometer readings of light reflectance of the three flower types. C = conical-celled, F = flat-celled. (B) Flowers from the three lines of *Petunia* used in this experiment, showing similarity of colour to the human eye. (C) Colour hexagon positions of each flower, showing that all three flower types are very close in bee colour space. Axes represent the relative excitation of each bee colour receptor. UV: ultraviolet; B: blue; G: green.

able to successfully land on and drink from the flowers. 70 rpm was chosen to test a moderate handling difficulty, and 100 rpm to test a strong handling difficulty.

7.2.4 Colour and visual difficulty in pollinator preference

Efficiency in foraging time is an important factor for bees when choosing which flowers to visit. A flower that is difficult to see may cause a delay in detection, leading bees to preferentially visit flowers they detect more easily. By using flowers of the V26 line of *Petunia*, which are of similar hue but are much darker than those of the *phmyb1* line and its revertant (Figure 7.1), we were able to test the effect of visual difficulty on bee preferences for conical cells. This allowed us to study the interaction between tactile and visual advantages, and to understand the trade-offs bees make to maximise their foraging efficiency.

7.3 Results and discussion

7.3.1 Spectral analysis of *Petunia* flowers

The reflectance spectra for all three flowers across wavelengths visible to bees were measured using a spectrophotometer, with the resulting data shown in Figure 7.1 A. The reflectance spectra for flowers of the isogenic lines show a very similar relationship to those of conical– and flat–celled *Antirrhinum majus* flowers (Dyer *et al.* 2007), in that while the position of the peaks of reflectance (and hence perceived colour) were very similar, more light was reflected overall from the flat-celled mutant flowers. Of the three lines, the V26 flowers reflected the lowest amount of light, due to increased pigment content. The percentage of light reflected by both the revertant and mutant flowers at their peak wavelengths are in the normal range for flowers, but the V26 flowers reflect less than 10% of overall incident light, which is extremely low for a flower (Chittka *et al.* 1994).

The position of each flower in bee perceptual colour space was calculated using the hexagon method of (Chittka 1992). The colour hexagon is used to represent bee subjective hue based on the relative excitation of each of the three bee colour receptors on a scale from 0 (centre of the hexagon) to 1 (UV, blue and green corners). This gives a graphical representation of the colour each flower will appear to a bee, as the angle at which a colour is positioned from the centre of the hexagon represents bee subjective hue. It also shows how similar or different colours will appear in comparison to each other, as shown by the distance in hexagon units between colours. The three flowers used in this study are very close to each other in bee perceptual colour space, as shown by their relative positions on the colour hexagon in Figure 7.1 C. The colour difference from revertant to mutant flowers was 0.08 units, and from V26 to mutant 0.05 units. Bees find colours less than 0.1 units apart very difficult to distinguish (Dyer & Chittka 2004a, 2004b).

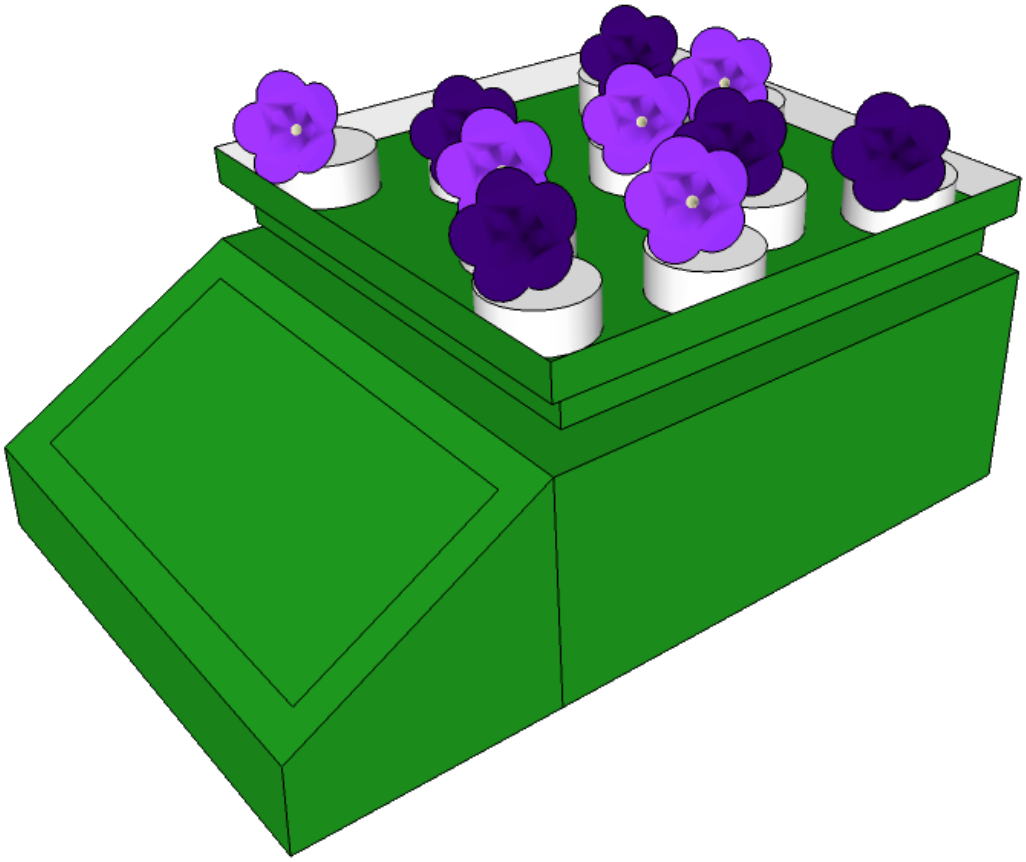

Figure 7.2 Diagram of the shaker showing its green tissue paper camouflage, and positioning of the flowers used in experiments.

The colours of the flowers used in these experiments are very similar to bees, and bees will usually only discriminate between such similar colours after differential conditioning (Dyer & Chittka 2004a). Under these conditions bees are capable of a maximum discrimination of around 70% of visits favouring the rewarding colour. We would therefore not expect to see a preference greater than 70% for any flower type when bees are presented with such similar colours, even if foraging from one flower type greatly disadvantaged the bee.

7.3.2 Bumblebees prefer conical-celled *Petunia* flowers when plants are isogenic.

Five conical-celled and five flat-celled flowers were used to test bee preferences in each experiment, during which single bees were allowed to forage freely from randomised arrays of these flowers. Each flower was fitted with a small tube into which equal amounts of 30% sucrose was pipetted, to maintain a standard reward between all flower types. Single, flower-naïve bees were released into a flight arena containing the flower array on the shaker platform. In this experiment the shaker platform was kept stationary to allow us to test bee preference for conical-celled or flat-celled *Petunia* flowers with no additional handling difficulty.

To test bumblebee preference for *Petunia* flowers differing only in the presence or absence of conical cells, we used flowers of the flat-celled *phmyb1* mutant line alongside flowers of a conical-celled isogenic revertant arising from this line. Bees presented with stationary arrays of flat-celled and conical-celled flowers in equal numbers chose conical-celled flowers 57% of the time (16 bees to 100 choices each, $p < 0.001$, Figure 7.3). This shows that bees prefer conical-celled *Petunia* flowers when conical-celled flowers present no additional visual disadvantage (Figure 7.3). This is as expected when compared to field trials of isogenic lines of *Antirrhinum* which showed bees to favour conical-celled *Antirrhinum* flowers over flat-celled mutants (Glover & Martin 1998).

The preference in favour of conical-celled *Petunia* flowers was evident within the first ten choices each bee made, and the preference did not change throughout the

experiment (learning curve for stationary flowers shown in Figure 7.4 A). Since conical- and flat-celled flowers with the same pigment colour are equally salient for bees (Dyer *et al.* 2007), and their preference is evident before any tactile benefits could have been learned, bee preference for conical-celled rather than flat-celled flowers of isogenic lines suggests an innate preference based on visual cues

.

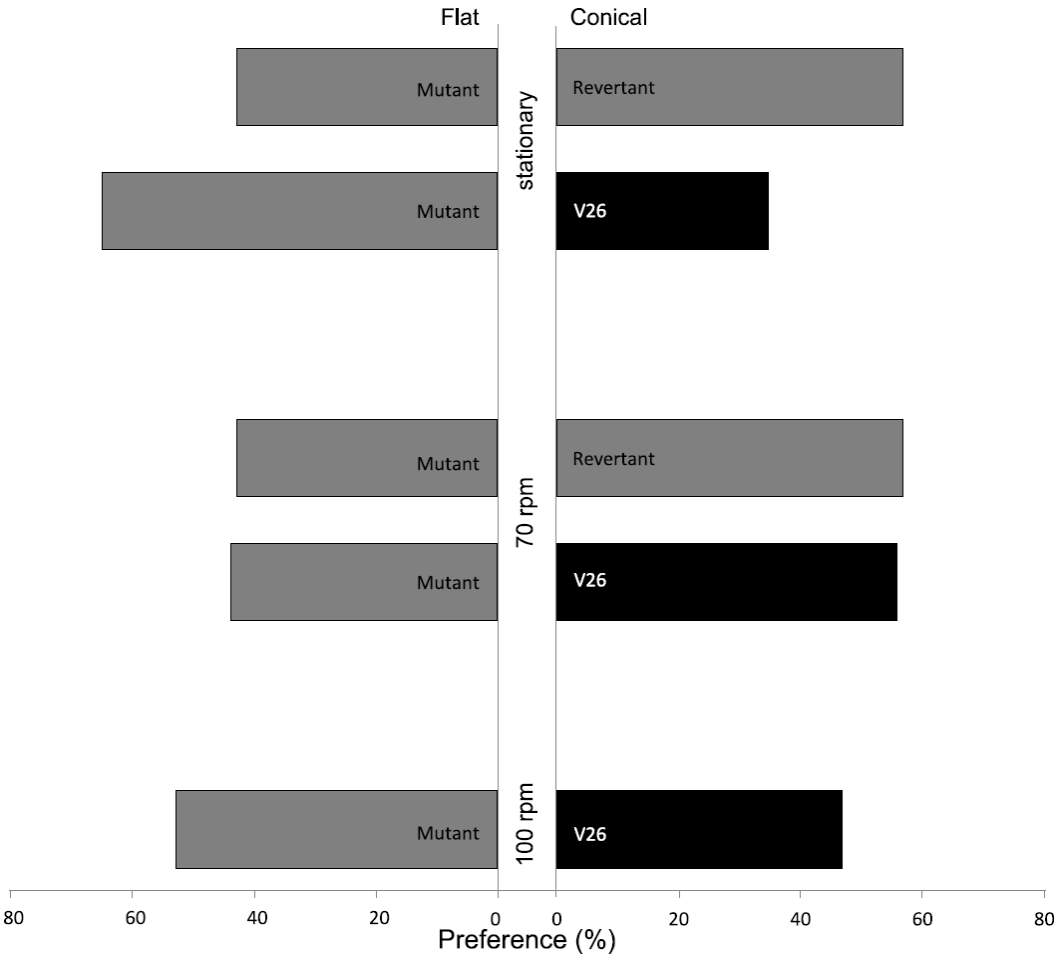

Figure 7.3 Overall bee preference for conical- and flat-celled flowers across different speeds. Preference is shown as percentage of total choices averaged across all bees tested in each experiment. Mutant and revertant flowers are of the same pigment colour, while V26 flowers are darker due to an increase in the amount of pigment. Bees prefer conical-celled revertant flowers when presented alongside mutant flat-celled flowers regardless of flower movement. However, bees prefer mutant flowers against darker, conical-celled V26 flowers when the flowers are stationary, but when flowers are moving the bees prefer the conical-celled V26 flowers.

7.3.3 Moving isogenic flowers do not elicit innate or learned changes in preference

To test whether an increased handling difficulty would change bumblebee preferences, we performed the same sets of preference experiments while moving the shaker platform (Figure 7.2) at 70 rpm to simulate the effects of wind movement on flowers. Bees presented with flowers of the isogenic lines on a moving platform did not show any significant increase or decrease in preference compared to the original stationary experiment (Figure 7.3). Bees still chose the conical-celled flowers 57% of the time, and, similarly to the stationary experiment, this preference did not change over time (Figure 7.4 A). This shows that the bees did not gain any additional advantage from the revertant flowers under conditions of increased handling difficulty (Figure 7.4 A).

7.3.4 Bumblebees prefer flat-celled *Petunia* flowers when conical-celled flowers are more darkly pigmented

To test bee preference for conical or flat cells when the conical-celled flowers were at a disadvantage visually, the same preference experiments were performed using arrays of the darker and harder to see V26 line conical-celled flowers presented alongside the mutant flat-celled flowers. This time the bees showed a very different preference, favouring the flat-celled mutant flowers 65% of the time and the V26 only 35% while the flowers were stationary ($p < 0.001$, Figure 7.3).

7.3.5 Motion increases bumblebee preference for darkly pigmented conical-celled flowers

When the V26 and mutant flowers were moving at 70 rpm, initially bees showed a similar preference to when these flowers were stationary. However, in this moving array bee preference for conical-celled V26 flowers over mutant flat-celled flowers increased markedly, bringing the overall average percentage of drinks on V26 up to 56% ($p = 0.026$, Figure 7.3). This preference emerged as a product of learning across

the hundred choices each bee made. During the first ten visits to flowers moving at 70 rpm bees visited conical-celled V26 flowers only 43% of the time, a preference level similar to that observed for stationary flowers (Figure 7.4 B). As the bees grew more experienced, however, the proportion of visits to conical-celled V26 flowers rapidly increased. At 50 visits the average preference for V26 flowers was 52%, and by the end of their hundred choices the bees visited V26 flowers 62% of the time ($p < 0.001$). This shows that the initial primarily visual preference was overcome by a learned tactile advantage that the conical-celled flowers gave under the new, moving conditions. Additionally, each flower choice was made before the bee landed on the flower, showing that a visual cue was allowing them to quickly discriminate in favour of this tactile advantage.

When the speed of the shaker was increased to 100 rpm, only a small proportion of bees were able to complete the task (n=7). The preference in favour of the conical-

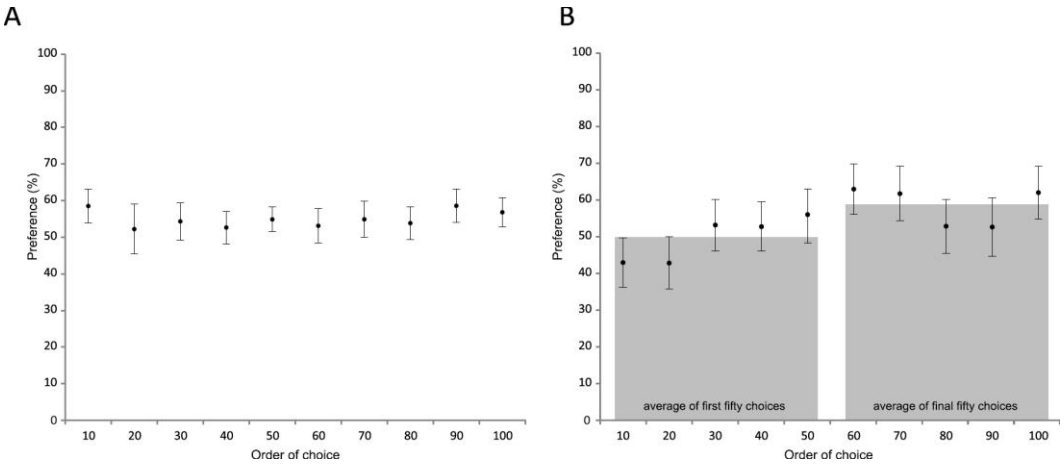

Figure 7.4 Learning curves showing percentage of bee preference for conical-celled flowers per ten choices while flowers were moving (not shown: reciprocal preference for flat-celled flowers). (A) Revertant flowers. Bees show no change in preference over their hundred choices. (B) V26 flowers. Bees show a gradual increase in preference over their hundred choices. The average of the final 50 choices is higher than for their first fifty choices because the bees are learning to favour the conical-celled flowers. Error bars represent standard error.

celled flowers dropped to around 47%, though this is not statistically significantly different from the preference at 70 rpm ($t = 0.746$, $p = 0.46$).

7.3.6 Brightness, motion as an attractant, and handling difficulty interact to create changing pollinator preferences

Bumblebee vision is not usually affected by brightness, but at extremes of high or low light bees become unable to distinguish colour. This is because when too much or too little light is incident on an ommatidium in a bee's eye, all three photoreceptors excite equally and the bee perceives the colour as closer to white or black (Kien & Menzel 1977; Backhaus 1991, 1992; Chittka 1992). V26 flowers are unusually strongly pigmented and reflect little light, so will be difficult for a bee to distinguish from the background. This is supported by the results of the stationary mutant vs. V26 preference experiment when bees preferred the mutant flowers that were easiest to see. This preference did not change as the bees grew more experienced throughout the 100 visits of the stationary trial, showing that the bees were not learning any advantage or disadvantage to change this initial visual preference.

In *Silene maritima* it has been shown that the length of a flower's stalk determines the flower's attractiveness to hoverfly pollinators by increasing the extent to which these flowers 'wave' in the wind, and an increase in stalk length increased the number of pollinator visits each flower received. However, flowers with the longest stalks experienced pollinator visits that were shorter in duration and showed a concomitant decrease in pollination success (Warren & James 2008). This may be caused by the increased difficulty in handling these flowers while moving. These experiments show that for hoverflies pollinating *Silene*, a trade-off has to be reached between the attractiveness of greater flower motion, and the inherent handling difficulty this motion creates. In our experiments, when the V26 and mutant flowers were moving, bees initially discriminated against the V26 flowers but their preference increased over the course of the trial, ending at a preference for conical-celled V26 flowers at levels similar to those observed when isogenic flowers were presented. The change in preference observed when the V26 and mutant flowers

were moving shows that the bees' preference for the conical-celled V26 flowers is a product of learning, in which the bees overcome their initial visual preference to take advantage of the tactile benefit associated with the darker flowers.

The movement of flowers may also increase their visibility. Since motion parallax (a product of the bee's own movement) is so important to bee vision and target detection (Lehrer *et al.* 1988), additional motion could further contribute to the ease with which a bee can detect the flower and contribute to the flower's attractiveness. While the *Petunia* flowers in the experimental setup described here would be stationary with respect to the shaker platform, the bees would see movement against the body of the shaker and the walls of the flight arena. The movement could contribute to the bee's normal use of motion parallax and create greater distinction between the flower and the background, helping to remove some of the visual disadvantage of the V26 flowers.

Since conical cells convey a fecundity benefit to flowers that are difficult to handle (such as *Antirrhinum*) by giving their pollinators a tactile benefit (Whitney *et al.* 2009), a similar tactile benefit under motion may explain why conical cells have persisted throughout evolution in flowers that are easy for pollinators to handle, where movement in the wind has produced additional difficulty. The metabolic costs of flight and foraging are large (Kammer & Heinrich 1974), and the less energy a bee has to expend foraging from each flower, the more sugar is left for the colony. As pollinators quickly learn the metabolic benefit in expending less energy 'hanging on' to conical–celled flowers, even a small deviation from equal preference would be enough to convey a large difference in fitness to conical-celled plants over evolutionary time.

The fitness benefits of conical cells for flowers that are difficult for pollinators to grip begin to explain the prevalence of this structure on the petal epidermal surface. Conical cells have a range of functions, each of which may be important in specific habitats or with different pollinators. The diversity of size and shape of conical cells supports the hypothesis that petal micromorphology can be optimised for both pollinator and habitat (Whitney *et al.* 2011). This chapter has shown that there are

interactions between the different properties of conical cells, in this case influencing flower-pollinator interactions through both visual and tactile effects. To establish the extent to which petal micromorphology is optimised, greater knowledge about the specific interactions between plants and their pollinators is required.

7.4 Conclusions

Conical cells have multifunctional properties, and we find that these properties interact to enhance pollination success. When flowers are stationary, we find that bees prefer conical-celled flowers unless the conical-celled flowers are harder to see. When flowers are moving, however, bees always visit conical-celled flowers more than flat-celled flowers, regardless of visual difficulty. Since bees prefer moving targets (Lehrer & Srinivasan 1992), and conical cells help bees to grip flowers as well as enhancing visually appealing floral properties such as colour, the presence of conical cells in conjunction with flowers that can move in the breeze might make a powerful attractant for pollinators. Conical cells alone are not particularly visually attractive and moving flowers alone are not easy to handle, but the combination of these two properties might act synergistically to maximise pollinator attraction and foraging efficiency, explaining the prevalence of conical cells across the angiosperms.

Chapter 8. Do bees prefer conical or flat cells on *Solanum* flower petals?

8.1 Attribution

The experiments in this chapter were performed in collaboration with a rotation student, Felicity Bedford (University of Cambridge, feb39@cam.ac.uk).

8.2 Introduction

Flowers can provide protein-rich pollen, sugar-rich nectar or a combination of the two as rewards to pollinators. Many flowers provide pollen only, without nectar, as a food source which bees use to meet the protein requirements of their larvae. Of the flowers that provide pollen only, a subset use a very specific method of pollination in which enlarged hollow anthers, often arranged in a cone, release pollen from apical pores in response to vibrations produced by a pollinating insect (Buchmann & Hurley 1978; Buchmann 1983). Called pollination by sonication or 'buzz pollination', this form of pollination has been observed in at least 20,000 species (De Luca *et al.* 2012) and is the primary mode of pollination for the genus *Solanum*.

8.2.1 MECHANICS OF BUZZ POLLINATION

Buzz pollination is performed by solitary bees and bumblebees, but is rarely observed in honeybees (Buchmann & Hurley 1978; Kearns & Inouye 1997). In buzz-pollinated flowers, the bee grasps the anthers with its legs and uses its flight muscles, disengaged from the wings, to create vibration that produces a resonance within the anther tube. This resonance causes pollen to be ejected from the apical pore of the anther. For crops such as tomatoes and aubergines (*S. lycopersicum* and *S. melongena*) that are often grown in greenhouses with no access to wild pollinators, plants are self-compatible but produce a higher crop yield when actively pollinated (Banda & Paxton 1991; Asada & Ono 1996; Hogendoorn *et al.* 2006; Katja, Steven & K 2007). Plants can be pollinated by hand, using a mechanical sonicator or a tuning fork to cause a discharge of pollen which is then brushed onto receptive stigmas. However, commercially supplied bumblebees are widely preferred as a method of inducing pollination by sonication due to their greater efficiency compared to manual pollination by humans (Banda & Paxton 1991).

During buzz pollination, bees focus primarily on the anthers. Bees land directly on the anthers, gripping with their legs and curling their bodies around to cover the apical pores as shown in Figure 8.1. Bees have been reported to rarely land on or even touch the petals of buzz-pollinated flowers (Buchmann 1983; King & Buchmann 1996; Glover, Bunnewell & Martin 2004; De Luca *et al.* 2012). Since the tactile advantage of extra grip

Figure 8.1 Examples of buzz pollination. Lasioglossum spp. collecting pollen from Solanum lycopersicum. (B) Green sweat bee (Augochloropsis metallica) collecting pollen from Solanum elaeagnifolium. (C) Bombus bimaculatus. collecting pollen from Dodecatheon meadia.

Photographs supplied courtesy of: (A) Karen Retra http://www.flickr.com/photos/karenretra/; (B) Valerie Bugh, larvalbug.com; (C) James C. Trager, taken in eastern Missouri USA http://beetlesinthebush.wordpress.com/author/jtrager/.

provided by conical petal cells has been shown to be the primary reason behind bumblebee preference for conical-celled flowers (Whitney *et al.* 2009; Alcorn, Whitney & Glover 2012), the lack of bee contact with petals in buzz-pollinated species suggests an explanation for the loss of conical epidermal cells. The role of conical cells in providing grip for pollinating bees may no longer be of any relevance or importance in buzz-pollinated species.

Genetic drift, or genetic change based on random stochastic fluctuation rather than active selection, can occur when selection pressure on a trait (either positive or negative) is absent, or of negligible effect over a relevant evolutionary timescale (Fay 2011). Since conical cells are known to increase pollinator preference in both *Antirrhinum* and *Petunia* (Dyer et al. 2007; Whitney et al. 2009; Alcorn, Whitney & Glover 2012), then if conical cells simply no longer provide any advantage for the plant and are largely unnoticed by pollinators, losses of conical cells in buzz-pollinated species may be attributed simply to genetic drift. Drift is known to affect floral features, as in the example of *Lepanthes* orchids which display no association between different colour morphs and fitness (Tremblay & Ackerman 2007).

An alternative explanation for the loss of conical cells in buzz-pollinated species, which offer only pollen and no nectar to their pollinators, may be that conical cells in some way detract from the primary attractant of the central anther cone. The anther cone is a large, showy structure that is often brightly coloured (in the case of *Solanum*, the anthers are bright yellow) and pollinating bees avoid contact with flower petals entirely, landing directly into position grasping the anthers with their legs to facilitate transmission of the high-frequency buzzes bees produce to release pollen. Efficient flower handling may be hindered if a bee is distracted by showy petals, and instead flowers may benefit from producing flowers that to a bee's eye appear plain, and the function of the petals then might be purely to act as a background or foil for the anthers to increase anther cone visibility. In each of these cases, conical cells could have been lost due to active pollinator-mediated selection against conical cells, or selection in favour of flat cells. Selection against one trait that acts in favour of a reciprocal trait is common in evolution, such as in the preference of hummingbirds in favour of red over white flowers in *Ipomoea* (Meléndez-Ackerman, Campbell & Waser 1997), and the

selection against plain flowers by both birds and bees in favour of nectar guides in *Delphinium* (Waser & Price 1983).

In this chapter, experiments designed to distinguish between these alternative hypotheses are described. Bumblebee preferences for conical- or flat-celled flowers are tested, when foraging for pollen from poricidal anthers. Biomimetic petal replicas made from epoxy cast in dental wax impressions of petal surfaces were used to construct artificial flowers, as described in section 2.11.3.2. Real flowers were integrated into the artificial petal constructs such that petals were obscured but anthers could protrude in a natural orientation from the centre of the artificial flowers. Bee preference in favour of conical-celled or flat-celled flowers while pollen-collecting could then be tested.

8.3 Results and discussion

8.3.1 Flower petal surfaces

To compare artificial conical-celled flowers with artificial flat-celled flowers, two species with comparable petal surfaces needed to be found. Ideally these species should

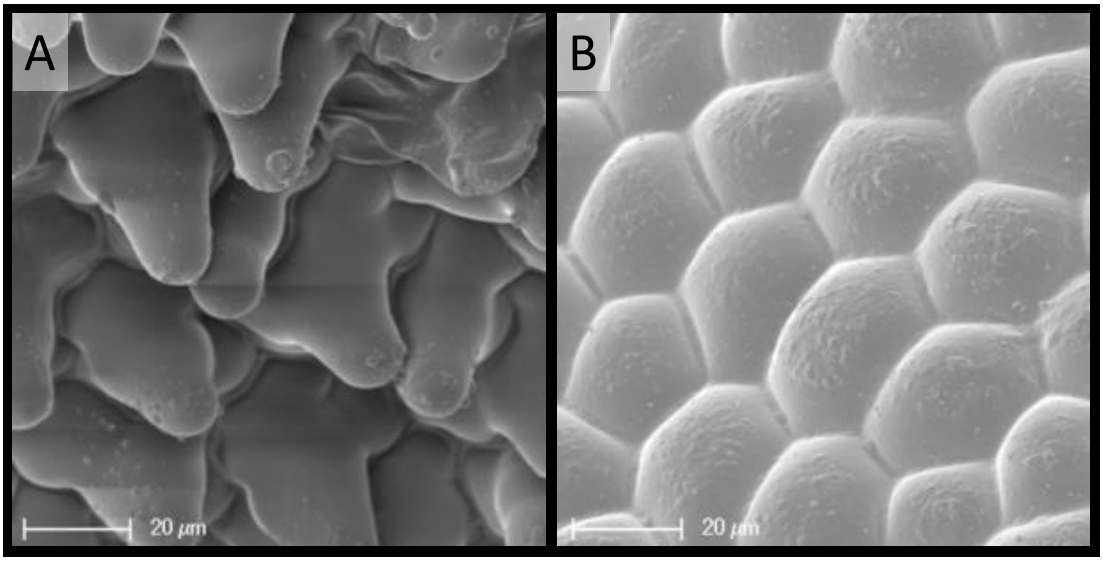

Figure 8.2 (A) Scanning Electron Microscope images (SEM) of *S. sisymbriifolium* petal (conical celled species) (B) SEM of *Impatiens tinctoria* subsp. *elegantissima* petal (flat celled species).

be similar in surface macrostructure of ridges and tissue folds as well as in cell surface (cuticular) microstructure, but differing only in whether or not they had conical cells. Artificial flowers were constructed from petal imprints of real flowers as described in section 2.11.5.2. *S. sisymbriifolium* petals were used to construct conical-celled artificial flowers (Figure 8.2 A). To find an appropriate comparator species, nine different species from local florists or flowering in Cambridge University Botanic Garden with suitable petal size and texture were imaged using scanning electron microscopy. Impatiens tinctoria subsp. elegantissima was chosen to construct flat celled artificial flowers, due to its similarity in cell surface texture and cell base width to S. sisymbriifolium (Figure 8.2 A, B). Discs were colour-coded pink-purple and blue-purple to allow bees to learn to associate any benefit with a visual cue and so facilitate our detection of any preferences bees might display (Figure 8.4, see Methods section 2.11.5.2).

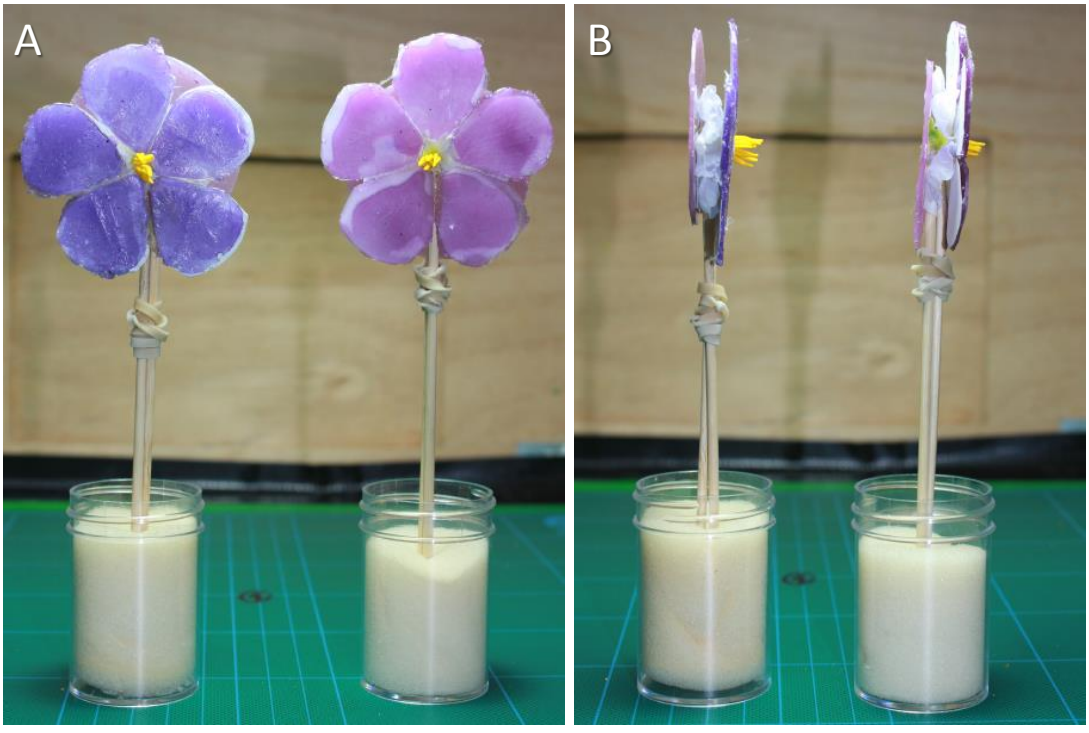

Figure 8.3 Experimental set up of blue-purple (C) and pink-purple (F) artificial flowers using real anthers as an attractant and reward source. In each case, Solanum sisymbriifolium flowers are positioned with anthers protruding through the centre of artificial flowers, and held in place using an epoxy disc pressed to the back of each flower.

8.3.1.1 Spectral Properties of artificial flowers

The reflectance spectra of the discs for wavelengths visible to bees are shown in Figure 8.4 A, showing that each colour has a peak in a similar wavelength, but the blue-purple coloured discs (C) have a higher peak towards the UV end of the spectrum whereas the pink-purple coloured discs (F) reflect more light in the blue and green parts of the bee visual range. The positions of each colour in relative bee perceptual colour space are shown in Figure 8.4 B. The difference between the disc colours is 0.121 hexagon units. Dyer and Chittka (2004) described a hexagon distance of 0.152 and above as a perceptually large colour distance, which bees can learn to discriminate to a high degree of accuracy with absolute conditioning. Colours as little as 0.045 hexagon units apart can be discriminated using differential conditioning techniques (Dyer & Chittka 2004).

Disc colour differences for this study should therefore be sufficiently different for bees to be able to distinguish easily, and if a benefit for either disc type is perceived then bees should be able to learn to associate this benefit with the colour of the appropriate disc. The colours were close enough in bee perceptual space that a confounding effect

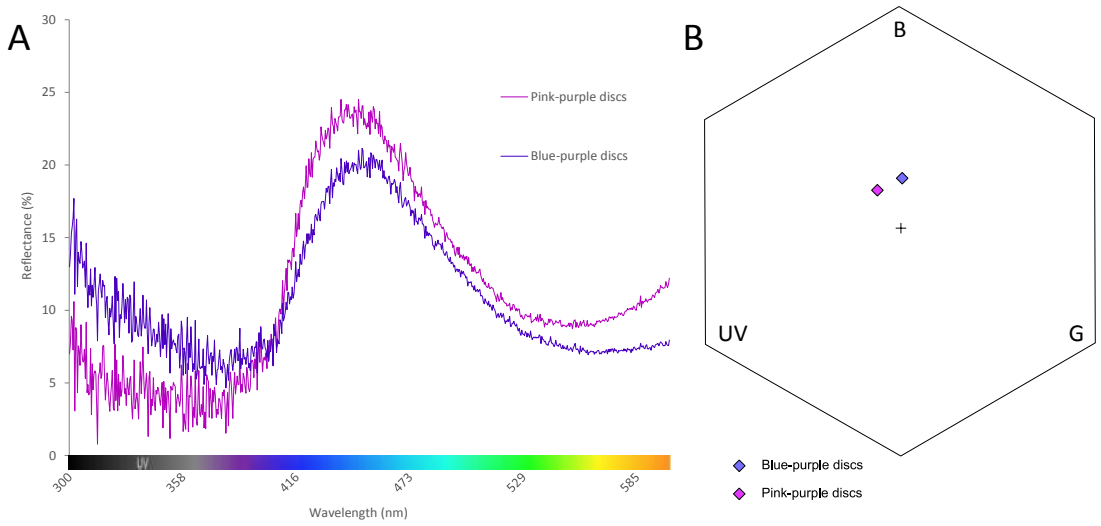

Figure 8.4 (A) Spectrophotometer readings of percentage reflectance of flower discs. (B) Colour hexagon showing the separation of disc colours in bee perceptual colour space. Blue-purple flowers (C) show a higher reflectance towards the UV end of the bee visual range, while pink-purple flowers (F) have higher reflectance in the blue and green parts of the bee visual range. The position of each of these colours in the colour hexagon shows that these colours will appear very similar to bees, though are predicted to be easily distinguishable. Axes represent the relative excitation of each bee colour receptor. UV: ultraviolet; B: blue; G: green.

caused by perception-based preference for either of the colours is unlikely, and neither colour type was overall of unusually low or high total reflectance nor were reflectance levels significantly different between the two.

8.3.2 Bee behavioural observations

Bumblebee colonies and flight arenas were set up as described in Methods section 2.11. Preliminary observations of the test colony using *S. sisymbriifolium* flowers were made in order to compare foraging behaviour from real and artificial flowers to ensure consistency of behaviour before starting experiments. Bees exhibited similar behaviours in their pollen foraging behaviour when foraging from real flowers as they did from artificial flowers, and did so in a similar time frame. Examples of bee behaviour while foraging from artificial flowers are shown in Figure 8.5. Bees visited several flowers within each foraging excursion before returning to the colony. Bees visited only fully mature *S. sisymbriifolium* flowers after development of purple pigmentation, while younger white flowers and flower buds were not visited. There was no reduction in visitation of individual flowers during the observation period, indicating that even under heavy levels of visitation by bees flowers did not develop anther exhaustion that might cause confounding effects on bee preferences through diminishing reward levels in visited flowers.

Figure 8.5 Typical bee foraging behaviour on artificial flowers with real anthers from *S. sisymbriifolium* flowers positioned behind artificial flower petal casts.

8.3.3 Observation of foraging behaviour.

Although landings on disc petals were recorded as part of the experiment, they occurred extremely rarely. Bee landings on disc petals accounted for only 2 of the total of 1000 landings recorded during the experiments. All other landings were directly onto anthers.

8.3.4 Bee cell type preference

Overall, bees landed on conical-celled flower discs 49.2% of the time and flat-celled discs 50.8% of the time (492 versus 508 lands) (Figure 8.6). This is not significantly different from a random allocation of choices between flat and conical celled discs (t=-0.499, df=9, p=0.630). While small differences can be seen between the preferences

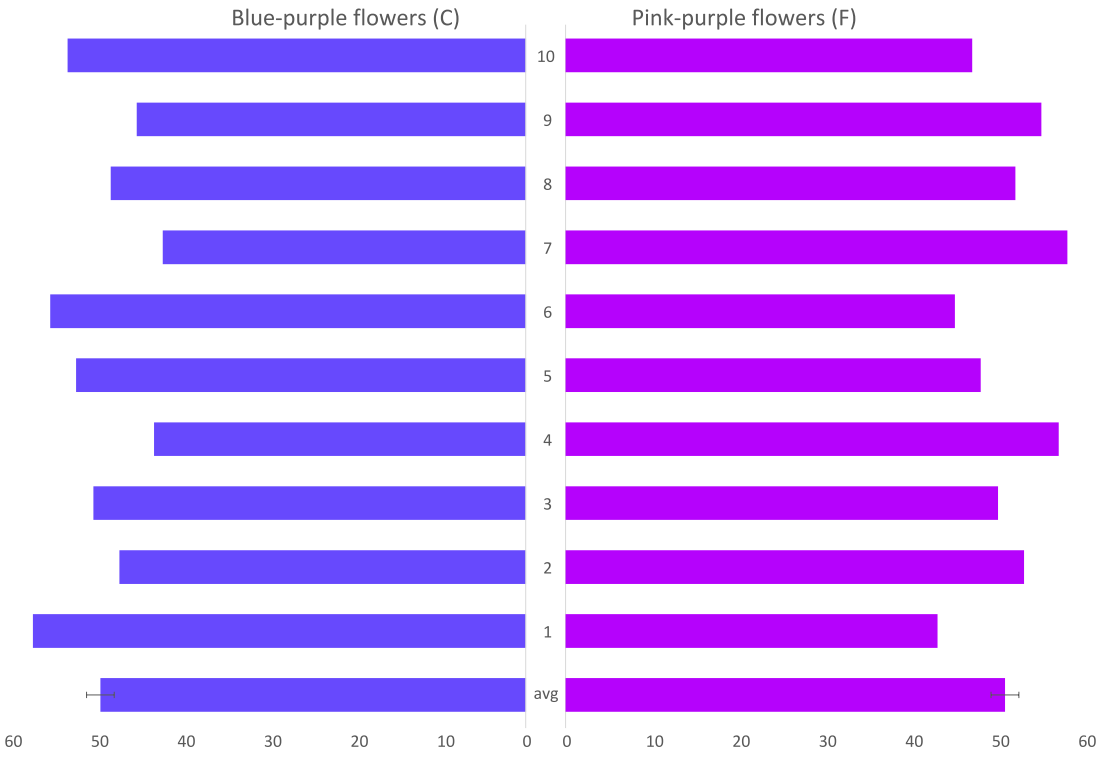

Figure 8.6 Percentage choices for each bee (1-10) and mean (n=10) for conical and flat celled artificial flowers. While many bees display a preference in favour of either conical- or flat-celled flowers, this preference averages to approximately 50:50 when averaged over ten bees, suggesting that these apparent preferences represent random stochastic variation. Error bars are SEM.

exhibited by each of the individual 10 bees tested (Figure 8.6), no bee showed a significant preference for conical or flat celled flowers (Table 8.1). If conical cells did increase pollinator attraction, perhaps by increasing the grip provided to pollinators as demonstrated in studies of nectar-rewarding flowers (Whitney *et al.* 2009; Alcorn, Whitney & Glover 2012), bees would be observed to choose conical celled flower discs more frequently. However, in this study bees showed no consistent preference in favour of either flat-celled or conical-celled petal surfaces across their 100 choices (Figure 8.6 and Figure 8.7).

8.3.5 Change in cell type preference with experience

To test whether bees exhibited a learned change in their preference for conical-celled or flat-celled flowers while foraging for pollen, we analysed change in preference between the first twenty choices and the last twenty choices each bee made, as well as the means across all bees. No significant difference was observed between the mean preference for inexperienced (first 20 choices) and experienced bees (last 20 choices) ($t=-1.325$, $df=9$, $p=0.218$, Figure 8.7). There is considerable variation in the responses of individual bees over the course of the experiments (Figure 8.7 A). Although several bees do show a learned preference in this study (bees 1,2,3,7 and 9; Table 8.2), the preference

Bee	Conical:Flat choices	X^2	p
1	57:43	1.96	0.162
2	47:53	0.36	0.549
3	50:50	0.00	1.000
4	43:57	1.96	0.162
5	52:48	0.16	0.689
6	55:45	1.00	0.317
7	42:58	2.56	0.120
8	48:52	0.16	0.689
9	45:55	1.00	0.317
10	53:47	0.36	0.549

Table 8.1 Results of chi squared analyses comparing the ratio of conical:flat discs visited, tested against the null hypothesis of a preference of 50:50. No significant differences were found at a 0.05 acceptance level.

they display is not consistent and some bees appear to favour conical cells while others appear to favour flat cells. When averaged over a statistically significant ten bees, these apparent preferences cancel out and show that overall there is no consistent preference in favour of either cell type. A learning curve showing preference levels at ten-choice intervals across all bees (Figure 8.7 B) showed no change in preference as experience increased ($F=2.793$, $df=99$, $p=0.098$), and considerable variation in preference is exhibited at all experience levels.

The lack of preference either in favour of or against conical celled flowers in this study suggests that the loss of conical cells from the petals observed in many *Solanum* species is not due to selection driven by flower visitor preference. Instead, the lack of pollinator preference exhibited by foraging bumblebees suggests that random stochastic changes (genetic drift) rather than pollinator driven selection is more likely to have caused the loss of conical petal cells across buzz pollinated *Solanum* species. This further supports previous findings by this work (chapter 7) and others (Whitney *et al.* 2009) that in species with flowers requiring petal manipulation by pollinators, the selective benefits of increased pollinator grip are responsible for maintaining conical cells. Other identified functions of conical cells such as in influencing colour and wettability

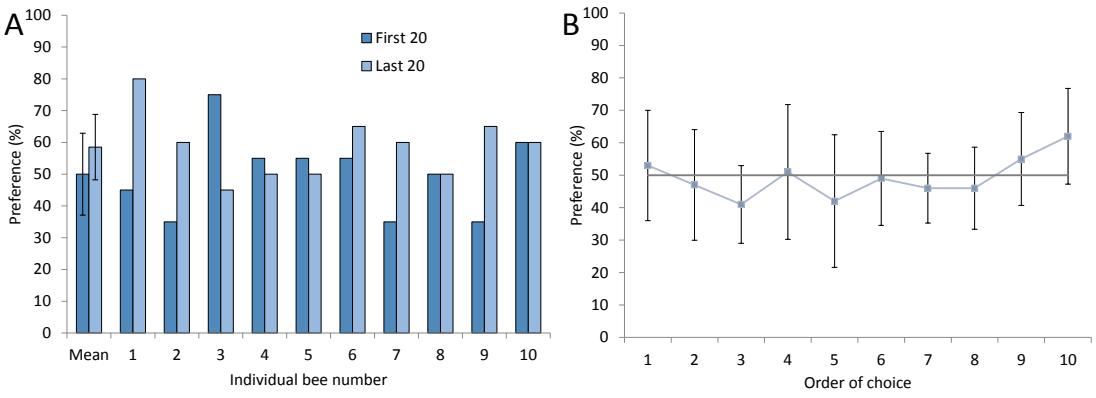

Figure 8.7 Comparison of choices made by bees across increasing experience levels. (A) Bee preference in favour of conical-celled artificial flowers for each individual bee when inexperienced (first 20 choices) and experienced (last 20 choices) and mean across all bees. (B) Percentage preference (mean across all ten bees) for conical celled discs as experience increases, with grey line showing grand mean showing no preference in favour of either cell type (50%). Error bars show ± standard deviation.

(Whitney *et al.* 2011), may contribute selective pressures that act on conical cells in buzz-pollinated species in the absence of a role for grip, but this data set provides no evidence for or against these possibilities. Indirect selection based on energetic expenditure to produce conical outgrowths of petal cells is another possible cause of conical cell loss, a process often attributed to character reduction or vestigialisation. This process occurs when a trait becomes non-functional or selectively disadvantageous and the trait then atrophies over time, as has been observed in the wings of flightless birds (Fong, Kane & Culver 1995). Costs to the plant may include cell wall components such as cellulose and pectin, cuticular waxes, cytoskeletal elements, and energy required to rearrange cell wall components into the conical shape. Further investigation into whether there is a higher cost to producing conical cells rather than flat cells would be needed to differentiate between the two hypotheses of drift or indirect selection.

Bee	First 20: Last 20 conical preference %	X^2	p
1	**45:80**	**9.80**	**0.002**
2	**35:60**	**6.58**	**0.010**
3	**75:45**	**7.50**	**0.006**
4	55:50	0.23	0.626
5	55:50	0.23	0.626
6	55:65	0.83	0.361
7	**35:60**	**6.58**	**0.010**
8	50:50	0.00	1.000
9	**35:65**	**8.00**	**0.005**
10	60:60	0.00	1.000

Table 8.2 Results of chi squared analyses comparing the preference ratio of first and last 20 choices against the null hypothesis of no change in preference. Though some bees display a change in preference across their hundred choices, these differences disappear when a statistically significant average over ten bees is considered, as shown in Figure 9.6. Significant results at a level of 0.05 are shown in bold.

8.4 Conclusions

We find that bumblebees show no preference for or against conical petal cells while buzz pollinating. This suggests that the loss of conical cells on the petals of *Solanum* species is not driven by pollinator-mediated selection, and instead may be due to genetic drift or indirect selection. Previous chapters in this study have shown that the loss of conical petal cells in *Solanum* species is not associated with any change in protein function, and instead the loss of conical cells has occurred through a change in expression of R2R3 MYB Subgroup 9A genes, similarly to a change in expression observed in *S. dulcamara* (Glover, Nicholls and Martin, in prep.). In combination with this behavioural study, we suggest that the loss of conical cells in *Solanum* has occurred multiple times through the same genetic changes, and acting under a similar evolutionary mechanism, that of genetic drift.

Chapter 9. General discussion and conclusions

This work has explored the evolution of conical petal cells using multiple experimental approaches, combining phylogenetic surveys and molecular characterisation of gene function and expression with behavioural analyses of bumblebee preference to identify possible selective pressures. A study of possible selective pressures acting on conical cells was conducted by an investigation of pollinator preference for conical- or flat-celled *Petunia* flowers under conditions of simulated flower movement using bumblebee pollinators. A phylogenetic and morphological survey of conical cell loss in the genus *Solanum* was used to understand how frequent and widespread these losses have been. A molecular characterisation of genes known in other species to be responsible for producing conical cell form was undertaken in two *Solanum* species pairs differing in petal cell morphology, in order to investigate the mechanism of conical cell loss in each instance. Finally, artificial petal replicas in combination with real anthers were used to conduct a study of bumblebee preferences for conical cells while foraging for pollen (by buzz-pollination). This work has shown that conical cells increase bumblebee preference for flowers that are moving, and that in *Solanum* there have been multiple independent losses of conical petal cells. Two of these losses have occurred through similar molecular means, that of a change in regulatory gene expression patterns. Bumblebees do not display a preference in favour of either conical- or flat-celled flowers while buzz pollinating. These results show that conical cells are a trait under more than a single simple selective pressure, as bumblebee preferences in *Petunia*, and previously shown in *Antirrhinum*, differ from those identified by this study in the buzz-pollinated genus *Solanum*. We provide evidence for convergent evolution

in the loss of conical cells in *Solanum*, as we find multiple independent instances of conical cell loss, two of which appear to have each occurred through a change in the expression patterns of R2R3 MYB Subgroup 9A genes. These results help expand our understanding of the complex pressures that can act on a single multifunctional trait, as well as providing evidence for the repeatability of evolution on a molecular level.

9.1 Conical cells are subject to different selective pressures in species with different modes of pollination

This study identified two different modes of evolution for conical cells. First, evidence of active selection in favour of conical cells was identified in *Petunia*, where flowers with conical cells are preferred by pollinators when these flowers are moving. Secondly, in *Solanum*, no evidence was found of pollinator preference for or against conical petal cells. This may imply that conical cells provide no benefit to pollinators in flowers that are buzz pollinated, and that they may be lost simply due to genetic drift or due to indirect pressures working through the cost of their development.

Evolution in floral traits is frequently assumed to be under the influence of pollinator-mediated selection, rather than a passive, stochastically-driven genetic drift or indirect effects of selection acting on non-floral traits. Often this assumption proves correct, as in the case of the classic evolutionary study by Waser & Price (1983) who found active selection in favour of multicoloured blue and white flower colour morphs over pure white morphs in *Delphinium*. In this example the colours were shown to produce a pattern that pollinating bees and hummingbirds use as nectar guides, and so decrease flower handling time and increase foraging efficiency. There are, however, many instances of floral trait changes with no evidence of active selection. For example, Tremblay & Ackerman (2007) found that floral colour traits in *Lepanthes* orchids showed no association of floral colour with fitness, suggesting that these polymorphisms are not under active selection but instead are neutral with respect to

one another under the conditions investigated. Additionally, recent island colonisation by *Nicotiana glauca* showed the evolution of increased corolla length compared to mainland populations, correlating with longer-beaked species of pollinating birds present on the island (Schueller 2006). However, no evidence of increased pollen transfer or seed set in plants with longer corollas could be detected, showing that even correlation of floral traits with pollinator morphology may exist independently of pollinator-mediated selection. Selection acting on a floral trait may also act independently of pollinator-mediated selection. Schemske & Bierzychudek (2007) found populations of blue- and white-flowered *Linanthus* showed a geographic separation into two monomorphic populations of different flower colour across two sides of a ravine. This separation of flower colour populations was previously thought to be the product of genetic drift, however Schemske and Bierzychudek did find evidence of selection. While they found no evidence that selection was acting directly on flower colour itself, instead they proposed that selection acting on a different, as yet unidentified, trait might cause indirect selection to maintain flower colour in each population. Such selection might work through genetic linkage of the floral trait under analysis to another trait under direct selection. Evolution of floral traits may also be affected by selection pressures other than those from pollinators. In South African *Protea* species, Carlson & Holsinger (2010) found that although pollinators did not display a preference in favour of any flower colour morphs, white flowers produced seeds that were larger and had a higher germination rate but also experienced higher predation from Lepidopteran larvae. Similarly, pollinators of *Claytonia virginica* showed consistent preference for increased flower pigmentation (Frey 2004), but darker-flowered plants experienced increased predation. Evolution of a floral trait may also be affected by closely related species occurring in sympatry, for example several floral traits in *Ipomoea hederacea* exhibit evidence of selection when this species co-occurs with *Ipomoea purpurea* (Smith & Rausher 2008).

Genetic drift may play a large role in evolution. The Neutral Theory of evolution postulates that the overwhelming majority of nucleotide changes observed in nature are the result of random, stochastic variation, assuming that deleterious mutations are eliminated from the population, and that the contribution of active selection is important but small in its percentage contribution to the total number of changes

present in populations (Kimura 1968; Fay 2011). In the absence of evidence of selection, drift may be proposed to explain observed evolutionary changes. However, it must always be remembered that there may remain a selective pressure acting on the trait that is merely as yet unidentified. In *Solanum* there are many other possible sources of selective pressure that might be acting on conical petal cells. Much about the adaptive value of floral traits in *Solanum* is unknown, and future work may identify direct or indirect pressures acting on conical petal cells. Conical cells focus incident light into the pigment-filled central vacuole of each epidermal cell and cause greater absorption of white light, creating a colour signal of greater spectral purity which bees can distinguish from the colour signal of a flat-celled flower epidermis (Noda *et al.* 1994; Glover & Martin 1998; Dyer *et al.* 2007). Conical cells on the petals have also been previously observed to have a visual effect that is perceivable by pollinating insects independently of colour effects, proposed to be a function of the light-scattering properties of conical cells (H. Whitney, pers. comm.). In buzz-pollinated species in which the tubular anthers are the primary focus of the pollinator's attention (Buchmann & Hurley 1978; Harder & Barclay 1994; De Luca *et al.* 2012), visual effects of the petals may be of lesser importance than they are in species which provide nectar as the reward and use the petals as the primary attractant. Conversely, it may be that the visual effects of conical cells provide a distraction from the anthers and therefore impair pollinator foraging efficiency. Petals in buzz-pollinated species may act only to provide a foil against which anthers are more visible to foraging bees, or may be the site of production of pollinator-attracting volatiles.

The cost to the plant of making conical cells on the petals is as yet unknown. Some of the targets of the R2R3 MYB Subgroup 9A gene *MIXTA* in *Antirrhinum* have been determined, and all are involved in cell wall modification and cell expansion (C. Martin, personal communication). Conical petal cells have an equivalent cell volume as compared to flat cells, but conical cells have a greater amount of cell wall material overall (Noda *et al.* 1994). Cell wall is composed of polysaccharides, waxes and proteins, and the cost to the plant in creating this additional wall will therefore involve increased photosynthesis as well as the metabolic costs of wax biosynthesis and protein production. The degree to which this will affect the plant in terms of proportional metabolic cost is unknown. In *Antirrhinum* and *Petunia*, mutants without conical cells

show a greater widthways expansion of the whole epidermal cell layer in which conical cells have been lost (Baumann *et al.* 2007), implying that the total expansion of each cell may in fact be similar whether conical cells are produced or not, and that the energetic cost of conical cell formation may be minimal. The result of this cell layer expansion is the formation of petals that are more reflexed than that of wild type. Reflexed petals are frequently found as a feature of buzz-pollinated species (Harder & Barclay 1994). If reflexed petals confer an adaptive advantage to buzz-pollinated species, perhaps through creating easier access to the anthers, and the loss of conical cells can cause a conversion to a reflexed petal form, then it may be that pollinator-mediated selection acts not on the petal cell shape directly but on the secondary effect of a loss of conical cells that changes macroscopic petal morphology. On the other hand, many *Solanum* species have reflexed petals and most also have conical petal cells. It may be then that either the loss of conical cells is only one way in which *Solanum* flowers can evolve reflexed petals, or that loss of conical cells is unrelated to the presence of reflexed petals. Since the anther cone itself in *Solanum* has been shown to be subject to convergent evolution (Glover, Bunnewell & Martin 2004), it is reasonable to postulate that other floral features, such as petal reflexion, might also have evolved through differing means, and so the loss of conical cells might be only one of several ways in which *Solanum* flowers can evolve a reflexed petal form.

During buzz pollination, bees grip the anthers and do not usually come into contact with flower petals (Buchmann 1983; De Luca *et al.* 2012). It may be that in *Solanum*, extra grip on the petals is a detriment rather than a benefit to pollinating insects. The external anther epidermis was composed of smooth, flat cells in all *Solanum* species surveyed by this project. This implies that during buzz pollination, grip of the surface of the epidermal cells may be unimportant. Bees have been shown to be able to interact with conical cells using the claws at the tips of their legs (Whitney, Federle & Glover 2009). It may then be that the grasping motion of a bee's tarsal claws into the tissue of the anthers during buzz pollination can no longer utilise conical cells for grip. Instead, static effects, friction between the smooth surface of a bee's leg and the smooth anther, or even an interaction between the hairs on a bee's leg with the anthers, might be important for grip, or for pollen release and collection. It is also feasible that conical cells in some way interfere with the resonance transmitted from the bee to the inside

of the anthers. This resonance is required for the release of pollen, and any effect that could dampen the transmitted vibration might impair the release of pollen and therefore decrease fitness either by a decrease in the amount of pollen available for transfer between flowers, or by pollinator-mediated selection as pollinating bees learn to associate these flowers with a less rewarding food source.

This work could be usefully expanded by greater investigation into possible selective pressures acting on conical petal cells and their loss in *Solanum*, as well as by investigating the apparent re-evolution of conical cells we have identified in several clades. A study of pollinator interaction with reflexed and non-reflexed petals might provide insight into whether the expansion of the cell layer through the loss of conical cells might be a driver of conical cell loss.

Isogenic comparisons of bumblebee preference for conical and flat celled flowers in *Solanum* would also provide greater certainty as to the role of pollinator preference in the evolution of conical cells in buzz pollinated species. Additionally, across *Solanum* there are many different flower forms, including heterantherous species, species with reflexed, straight or forward-reflexed petals, species with petals fused into a single disc of tissue and species with petals distinct and separate, as well as much variation in petal colour. There is also great variation in the presence and type of trichomes on the flowers. Any of these features might influence pollinator interactions with the flowers while buzz pollinating, and therefore might also affect pollinator-mediated selective pressures on conical petal cells. Further investigation into each of these flower types could provide more information into the evolution of conical cells in buzz-pollinated species.

9.2 Molecular analysis of conical cell loss provides evidence of convergent evolution through regulatory change

To understand why conical cells are sometimes lost, petal morphology was studied in the genus *Solanum*. Using character mapping and phylogenetic approaches, multiple independent losses of conical cells across *Solanum* were identified. Though we were only able to survey and analyse petal cell morphology for 104 species (around 5-10% of the total number of species in *Solanum*), at least one independent loss of conical cells was identified within all but one of the twelve major clades of *Solanum*, and in some cases more than one independent loss was found within a single clade. Additionally, evidence was found of potential re-acquisitions of conical petal cells. Together these results suggest that conical cells are a highly labile trait that is relatively easy both to lose and to regain in evolutionary time.

Two pairs of species with contrasting conical/flat petal epidermal morphology were selected. To test the protein function of the R2R3 MYB subgroup 9A genes from each species, they were transformed into tobacco plants under the control of a double CaMV 35S promoter, following the established protocol that has been used in multiple previous studies to investigate protein function of R2R3 MYB Subgroup 9A genes (Glover, Perez-Rodriguez & Martin 1998; Perez-Rodriguez *et al.* 2005; Jaffé, Tattersall & Glover 2007; Baumann *et al.* 2007). Despite the changes observed between the protein sequences of R2R3 MYB Subgroup 9A genes in *Solanum* species pairs, each gene identified was capable of directing conical cell fate following heterologous expression in tobacco. This indicates that for each case of conical cell loss, it was not a change in the R2R3 MYB Subgroup 9A protein itself that caused the change in petal cell morphology.

To test whether changes in the expression of R2R3 MYB Subgroup 9A genes could be responsible for the losses of conical cells in *Solanum*, quantitative RT-PCR (qPCR) was used to compare expression levels between conical-celled and flat-celled species. The expression levels of *ML* genes from *S. sisymbriifolium* (C), *S. capsicoides* (F) and *S. aviculare* (F) were compared across two tissue types at different developmental stages. We found that the conical-celled species *S. sisymbriifolium* showed the highest expression levels in all tissues, and that expression was highest overall in petals. *S. capsicoides* and *S. aviculare* both showed much lower levels of *ML* gene expression overall, and the lowest expression levels were seen in the petals. This suggests that the

loss of *ML* expression in these two flat-celled species may be responsible for the loss of conical cells on their petals. These analyses suggest that a change in the expression of this gene has caused the losses of conical cells, as high expression of R2R3 MYB Subgroup 9A *Mixta-Like* genes correlates with the presence of conical petal cells. R2R3 MYB Subgroup 9A proteins act as trans-regulatory elements for target genes. The changes in the expression of the *Mixta-Like* genes in these cases of conical cell loss suggest that cis-regulatory changes (changes in the promoter regions of these genes), or trans factors controlling their transcription, may be responsible for their changes in expression pattern.

Our findings of multiple losses of conical cells across *Solanum*, combined with a previous study in *S. dulcamara* (Glover, Nicholls and Martin, in prep.), show that at least three of the independent instances of convergent evolution of flat petal cells in this genus have occurred through similar means: that of a change in expression patterns of the controlling gene. The question of whether evolution more frequently occurs through changes in expression or through changes in protein function has been much debated (Doebley & Lukens 1998; Irish & Litt 2005; Martin, Ellis & Rook 2010; Wessinger & Rausher 2012). Changes in gene expression due to changes in either the expression or function of transcription factors can play a large role in evolution. Through a change in a transcription factor, entire developmental pathways may be altered, moved or duplicated, allowing existing structures to be used as the basis for creation of new morphologies to fill new roles (Jacob 1977). The diversification and subfunctionalisation of transcription factors has been responsible for a large proportion of phenotypic diversity amongst flowering plants (Doebley & Lukens 1998; Martin, Ellis & Rook 2010; Winter *et al.* 2011; Airoldi & Davies 2012; Yang & Wang 2013). For example, novel floral organ formation in the Ranunculaceae has occurred through duplication and subfunctionalisation of MADS box genes (Sharma & Kramer 2013), and the chloroplast transcription factor GLK has undergone functional specialisation between the divergence of mosses and higher plants, as indicated by the ability of *PpGLK* (from moss) to partially complement *Arabidopsis* loss of function mutants but the inability of *Arabidopsis GLK* to complement *Physcomitrella* loss of function mutants (Bravo-Garcia, Yasumura & Langdale 2009).

Reproductive barriers are often associated with specific kinds of evolution. Regulatory changes are associated most frequently with pre-pollination (pre-zygotic) reproductive isolation, whereas both regulatory sequence and protein function changes are common in the evolution of post-zygotic barriers (Rieseberg & Blackman 2010). Processes thought likely to have evolved through trans-regulatory changes may in fact turn out to have evolved through entirely different means. For example, in the metal hyperaccumulating species *Arabidopsis halleri*, metal uptake was thought to be due to trans regulation of an assortment of metal hyperaccumulation genes, but instead the hyperaccumulation ability of this species when compared to *Arabidopsis thaliana* was found to be due to an increase in copy number of these genes, as well as changes in their cis-regulatory sequences (Hanikenne *et al.* 2008). Additionally, cis and trans changes may act in opposition to minimise the effect of evolutionary changes, such as has been observed in *Arabidopsis* allopolyploids which show compensating interactions between cis and trans regulatory changes that lead to stabilising selection (Shi *et al.* 2012). Evolutionary shifts in flower colour can be associated with specific kinds of molecular evolution. For example, transitions to white or yellow flowers tend to be mediated by changes in trans-regulation by R2R3 MYB transcription factors, whereas the mode of evolution producing changes from blue to red pigmentation differs depending on whether the starting pigment is delphinidin or cyanidin (Wessinger & Rausher 2012).

This work has shown that a change in expression patterns is associated with the loss of conical cells in *Solanum* species. It is, however, unknown whether cis or trans regulatory changes of these genes was responsible for the observed differences in expression between species pairs. This work could be usefully expanded by isolation of and further investigation into promoter regions of *Solanum* R2R3 MYB Subgroup 9A genes to develop our understanding of how the expression of these genes have changed. Promoter-reporter gene fusions would greatly expand our understanding of the regulation of expression in each gene by allowing the identification of the regions of promoter sequence that are required for timing and tissue specificity in expression. Comparisons of promoter sequences and function between species would also be valuable. Additionally, to explain the observed patterns of R2R3 MYB Subgroup 9A gene expression in leaves of many species investigated by this study, it would be useful to

undertake an investigation into possible leaf phenotypes caused by R2R3 MYB Subgroup 9A gene expression via morphological survey to identify possible phenotypic effects of these genes, as well as by studying knockouts of each gene to identify phenotypic changes in plants when each protein is not present.

Further quantitative PCR should be completed in order to expand the comparison of the expression of *Mixta-Like* genes in sister species *S. aviculare* (F) and *S. laciniatum* (C). Additionally, the lack of expression of *Mixta* in each species should be investigated further in order to understand if this gene is simply expressed in an as yet uninvestigated tissue type or developmental stage, or if expression has been lost entirely and therefore whether *Mixta* genes in these species could be in the process of pseudogenisation (Hughes & Liberles 2008).

9.3 Conical cell loss, grip and surface texture in other plant-pollinator interactions

Little work has been done, outside that described and discussed in this thesis, on the effects of conical cells, grip and other petal surface interactions between pollinator and plant. However, there are many such interactions that show great potential for grip and surface texture to play an important role, such as those seen in pollination by small landing moths, or by nectar-feeding birds. Equally, there may be many interactions in which the loss of conical cells may provide the benefit. Instances of conical petal cell loss independent of the genus *Solanum* may be associated with pollinator shifts away from landing pollinators. For example, hovering pollinators such as hummingbirds, hawkmoths and hoverflies do not land on flowers and as such could not benefit from increased grip. However, other functions of conical cells may still affect these pollinators, such as the use of conical cells as textural cues to facilitate beak or proboscis positioning. Each of these unexplored possibilities merits further study, and this section will describe in greater detail some examples of plant-pollinator interactions for which grip and conical petal cells may be important, and where conical cells may be lost.

Moth pollination is common and occurs in species as diverse as *Gladiolus* (Iridaceae; Alexandersson & Johnson 2002), *Qualea grandiflora* (Myrtales), *Roupala montana* (Proteaceae; Oliveira, Gibbs & Barbosa 2004) and *Petunia axillaris* (Solanaceae; Hoballah *et al.* 2005). Large hawkmoths hover and require large amounts of nectar to fuel their flight, while small settling moths often have lower metabolic rates and may spend large amounts of time crawling across and between flowers (Oliveira, Gibbs & Barbosa 2004). Moth pollinators have been shown to benefit from tactile cues sensed through the proboscis in two ways. Tactile cues can increase the efficiency of moth foraging by facilitating orientation on a flower, and their presence can be learned as a cue associated with rewarding flowers. Conversely, abnormal textural patterning, such as unnaturally-oriented epidermal grooves, can decrease the foraging speed of hawk moths (Goyret & Raguso 2006). Whether epidermal patterning involving conical cells has similar effects on moth behaviour is unknown.

A less common form of moth pollination occurs in species such as *Pachycereus schottii* (Cactaceae), in which adult moths (*Upiga virescens*, Pyralidae) pollinate flowers while laying a single egg in each flower, which then hatch into seed-eating larvae (Horn & Holland 2010). Little is known of how changes to floral features affect either pollinator attraction or pollination efficiency in this sort of moth-pollination system. Textural cues and increased grip may conceivably affect moth grip or behaviour while laying eggs, and adhesion of eggs to floral tissues may be affected positively or negatively by the presence of conical cells.

While hummingbirds generally hover while drinking from flowers, other bird pollinators such as honeyeaters and sunbirds do land while drinking. They do not, however, land on petals but instead perch on a reinforced stem or branch (Anderson, Cole & Barrett 2005; Cronk & Ojeda 2008) and therefore could not benefit from the grip provided by conical cells on flower petals. Bird pollination can be associated with adaptions to discourage invertebrate interest, such as changes in flower colour away from the optimal bee visual spectrum (Shrestha *et al.* 2013). Plants may even evolve features that prevent invertebrate access to floral rewards, such as in *Eucalyptus stoatei* (Myrtaceae) which is pollinated by honeyeaters and produces pendular flowers with stamens arranged in an insect-excluding dome (Hopper & Moran 1981). Ojeda *et al.*

(2012) identified a correlation between loss of conical cells in *Lotus* and transition to bird pollination, and postulated that the loss of conical cells in this species acts as an anti-bee feature in concert with pro-bird traits such as the reflexion and reduction of the dorsal petal. They do, however, suggest that the small remaining patch of conical cells at the opening of the flower may function to guide birds during beak insertion. This suggests that, while the loss of conical cells can be associated with shifts away from insect pollination, it may still provide benefits in other pollination syndromes.

Future work into pollination shifts associated with petal epidermal cell changes would benefit from exploring different kinds of pollinator shift across the angiosperms, particularly those involving a shift to or away from bee pollination. Additionally, many diverse pollinators may potentially be affected by conical petal cells since any pollinator that interacts with flower petals may benefit from increased grip or mechanosensory learning associated with texture, including pollinating beetles, flies, other invertebrates, and mammals. It would therefore be useful to survey the frequency of occurrence of conical petal cells in association with many different pollination syndromes, as well as exploring possible interactions of these pollinators with conical cells.

9.4 Conclusions

From this study, we conclude:

1. Phylogenetic analyses and ancestral character reconstruction show that conical cells have been independently lost multiple times in the genus *Solanum*. Evidence also suggests conical cells have repeatedly re-evolved in flat-celled lineages.

2. Two *Solanum* species pairs were selected for study:

    S. sisymbriifolium (C) and *S. capsicoides* (F), Leptostemonum

S. laciniatum (C) and *S. aviculare* (F), Archaesolanum

R2R3 MYB Subgroup 9A genes were identified from each species and comparison of protein sequences between species pairs predicts similar functionality and any differences observed are unlikely to account for petal cell shape differences.

3. Heterologous transformation of each R2R3 MYB Subgroup 9A gene into tobacco shows all proteins are capable of producing conical epidermal outgrowths, consistent with that observed for other R2R3 MYB Subgroup 9A genes known to be responsible for conical petal cell outgrowth in other species. Protein function cannot therefore account for the differences in petal cell shape between species

4. qRT-PCR shows higher expression of R2R3 Subgroup 9A genes in correlation with a conical cell phenotype. Low to no expression is observed for species with flat petal cells. This suggests that the loss of conical cells can be associated with a change in the expression pattern of these genes, and provides evidence of convergent evolution in the loss of conical petal cells in *Solanum*.

5. In *Petunia*, conical petal cells provide grip for foraging bees. When flowers are moving, bees increase their preference for flowers with conical cells, even when the conical-celled flowers are associated with a visual disadvantage.

6. In *Solanum*, bees show no preference for or against conical petal cells. This suggests that the loss of conical petal cells in *Solanum* are not due to pollinator-mediated selection, and that these losses are due either to genetic drift, or selection unrelated to pollinator choice.

This study combines phylogenetic, molecular genetic and behavioural analyses in the study of a floral trait, and allows for a powerful analysis of evolutionary changes. By seeking to understand both the molecular changes through which evolution acts as well as the selective pressures that drive evolution, using a multidisciplinary and integrative approach, we can gain a greater insight into the mechanisms and causes of evolutionary change.

References

Airoldi, C. A & Davies, B. (2012) Gene duplication and the evolution of plant MADS-box transcription factors. *Journal of Genetics and Genomics = Yi Chuan Xue Bao*, **39**, 157–65.

Akam, M. (1995) Hox genes and the evolution of diverse body plans. *Philosophical Transactions of the Royal Society of London. Series B, Biological sciences*, **349**, 313–9.

Alcorn, K., Whitney, H. & Glover, B. (2012) Flower movement increases pollinator preference for flowers with better grip (ed G Kudo). *Functional Ecology*, **26**, 941–947.

Alexandersson, R. & Johnson, S.D. (2002) Pollinator-mediated selection on flower-tube length in a hawkmoth-pollinated Gladiolus (Iridaceae). *Proceedings of the Royal Society B: Biological Sciences*, **269**, 631–6.

Altschul, S.F., Gish, W., Miller, W., Myers, E.W.W. & Lipman, D.J. (1990) Basic local alignment search tool. *Journal of Molecular Biology*, **215**, 403–10.

Ames, M. & Spooner, D. (2010) Phylogeny of Solanum series Piurana and related species in Solanum section Petota based on five conserved ortholog sequences. *Taxon*, **59**, 1091–1101.

Anderson, B., Cole, W.W. & Barrett, S.C.H. (2005) Botany: specialized bird perch aids cross-pollination. *Nature*, **435**, 41–2.

Aoki, K., Yano, K., Suzuki, A., Kawamura, S., Sakurai, N., Suda, K., Kurabayashi, A., Suzuki, T., Tsugane, T., Watanabe, M., Ooga, K., Torii, M., Narita, T., Shin-I, T., Kohara, Y., Yamamoto, N., Takahashi, H., Watanabe, Y., Egusa, M., Kodama, M., Ichinose, Y., Kikuchi, M., Fukushima, S., Okabe, A., Arie, T., Sato, Y., Yazawa, K., Satoh, S., Omura, T., Ezura, H. & Shibata, D. (2010) Large-scale analysis of full-length cDNAs from the tomato (Solanum lycopersicum) cultivar Micro-Tom, a reference system for the Solanaceae genomics. *BMC Genomics*, **11**, 210.

Asada, S. & Ono, M. (1996) Crop Pollination by Japanese Bumblebees, Bombus spp.(Hyrnenoptera: Apidae): Tomato Foraging Behavior and Pollination Efficiency1. *Applied Entomology and Zoology*, **31**, 581–586.

Backhaus, W. (1991) Color opponent coding in the visual system of the honeybee. *Vision Research*, **31**, 1381–97.

Backhaus, W. (1992) The Bezold-Brücke Effect in the Color Vision System of the Honeybee. *Vision Research*, **32**, 1425–1431.

Banda, H.J. & Paxton, R.J. (1991) Pollination of greenhouse tomatoes by bees. *Acta Horticulturae*, **288**, 194–198.

Baumann, K., Perez-Rodriguez, M., Bradley, D., Venail, J., Bailey, P., Jin, H., Koes, R., Roberts, K. & Martin, C.R. (2007) Control of cell and petal morphogenesis by R2R3 MYB transcription factors. *Development*, **134**, 1691–701.

Benson, D. A, Karsch-Mizrachi, I., Lipman, D.J., Ostell, J. & Wheeler, D.L. (2005) GenBank. *Nucleic Acids Research*, **33**, D34–8.

Berendzen, K., Searle, I., Ravenscroft, D., Koncz, C., Batschauer, A., Coupland, G., Somssich, I.E. & Ulker, B. (2005) A rapid and versatile combined DNA/RNA extraction protocol and its application to the analysis of a novel DNA marker set polymorphic between Arabidopsis thaliana ecotypes Col-0 and Landsberg erecta. *Plant Methods*, **1**, 4.

Bohs, L. (2005) Major clades in Solanum based on ndhF sequence data. *Monographs in Systematic Botany*.

Bohs, L. & Olmstead, R.G. (2008) Phylogenetic Relationships in Solanum (Solanaceae) Based on ndhF Sequences. *Systematic Botany*, **22**, 5–17.

Bolin, J.F., Maass, E. & Musselman, L.J. (2009) Pollination Biology of Hydnora africana Thunb. (Hydnoraceae) in

Namibia: Brood-Site Mimicry with Insect Imprisonment. *International Journal of Plant Sciences*, **170**, 157–163.

Bortiri, E. & Hake, S. (2007) Flowering and determinacy in maize. *Journal of Experimental Botany*, **58**, 909–16.

Bowman, J.L., Smyth, D.R. & Meyerowitz, E.M. (2012) The ABC model of flower development: then and now. *Development*, **139**, 4095–8.

Bravo-Garcia, A., Yasumura, Y. & Langdale, J. A. (2009) Specialization of the Golden2-like regulatory pathway during land plant evolution. *The New Phytologist*, **183**, 133–41.

Braybrook, S. A & Kuhlemeier, C. (2010) How a plant builds leaves. *The Plant Cell*, **22**, 1006–18.

Brockington, S.F., Alvarez-Fernandez, R., Landis, J.B., Alcorn, K., Walker, R.H., Thomas, M.M., Hileman, L.C. & Glover, B.J. (2013) Evolutionary Analysis of the MIXTA Gene Family Highlights Potential Targets for the Study of Cellular Differentiation. *Molecular Biology and Evolution*, **30**, 526–40.

Buchmann, S.L. (1983) Buzz Pollination in Angiosperms. *Handbook of Experimental Pollination Biology* (eds C.E. Jones & R.J. Little), pp. 73–113. Scientific and Academic Editions, NY.

Buchmann, S.L. & Hurley, J.P. (1978) A biophysical model for buzz pollination in angiosperms. *Journal of theoretical biology*, **72**, 639–57.

Bustin, S. A, Beaulieu, J.-F., Huggett, J., Jaggi, R., Kibenge, F.S.B., Olsvik, P. a, Penning, L.C. & Toegel, S. (2010) MIQE précis: Practical implementation of minimum standard guidelines for fluorescence-based quantitative real-time PCR experiments. *BMC Molecular Biology*, **11**, 74.

Bustin, S. a, Benes, V., Garson, J. a, Hellemans, J., Huggett, J., Kubista, M., Mueller, R., Nolan, T., Pfaffl, M.W., Shipley, G.L., Vandesompele, J. & Wittwer, C.T. (2009) The MIQE guidelines: minimum information for publication of quantitative real-time PCR experiments. *Clinical Chemistry*, **55**, 611–22.

Carlson, J.E. & Holsinger, K.E. (2010) Natural selection on inflorescence color polymorphisms in wild Protea populations: The role of pollinators, seed predators, and intertrait correlations. *American Journal of Botany*, **97**, 934–44.

Chandler, J.W. (2010) The Hormonal Regulation of Flower Development. *Journal of Plant Growth Regulation*, **30**, 242–254.

Charlesworth, B. (2012) The effects of deleterious mutations on evolution at linked sites. *Genetics*, **190**, 5–22.

Chittka, L. (1992) The colour hexagon: a chromaticity diagram based on photoreceptor excitations as a generalized representation of colour opponency. *Journal of Comparative Physiology A*, **170**, 533–543.

Chittka, L. & Raine, N.E. (2006) Recognition of flowers by pollinators. *Current Opinion in Plant Biology*, **9**, 428–35.

Chittka, L., Shmida, A., Troje, N. & Menzel, R. (1994) Ultraviolet as a component of flower reflections, and the colour perception of Hymenoptera. *Vision Research*, **34**, 1489–508.

Chittka, L., Thomson, J.D. & Waser, N.M. (1999) Flower Constancy, Insect Psychology, and Plant Evolution. *Naturwissenschaften*, **86**, 361–377.

Christensen, K.I. & Hansen, H.V. (1998) SEM-studies of epidermal patterns of petals in the angiosperms. *Opera Botanica*, 1–91.

Coen, E.S. & Meyerowitz, E.M. (1991) The war of the whorls: genetic interactions controlling flower development. *Nature*, **353**, 31–7.

Cohen, J. (2012) Continuous characters in phylogenetic analyses: patterns of corolla tube length evolution in Lithospermum L.(Boraginaceae). *Biological Journal of the Linnean Society*, **107**, 442–457.

Coker, J.S. & Davies, E. (2003) Selection of candidate housekeeping controls in tomato plants using EST data. *BioTechniques*, **35**, 740–2, 744, 746 passim.

Comba, L., Corbet, S. A., Hunt, H., Outram, S., Parker, J.S. & Glover, B.J. (2000) The role of genes influencing the corolla in pollination of Antirrhinum majus. *Plant, Cell and Environment*, **23**, 639–647.

Córdoba, S. a & Cocucci, A. a. (2011) Flower power: its association with bee power and floral functional morphology in papilionate legumes. *Annals of Botany*, 919 –931.

Craene, L. De, Soltis, P. & Soltis, D. (2003) Evolution of floral structures in basal angiosperms. *International Journal of Plant …*, **164**, S329–S363.

Crepet, W.L. & Niklas, K.J. (2009) Darwin's second "abominable mystery": Why are there so many angiosperm species? *American Journal of Botany*, **96**, 366–81.

Cronk, Q. & Ojeda, I. (2008) Bird-pollinated flowers in an evolutionary and molecular context. *Journal of Experimental Botany*, **59**, 715–27.

Dillon, N. (2006) Gene regulation and large-scale chromatin organization in the nucleus. *Chromosome Research*, **14**, 117–26.

Doebley, J. (2004) The genetics of maize evolution. *Annual Review of Genetics*, **38**, 37–59.

Doebley, J. & Lukens, L. (1998) Transcriptional regulators and the evolution of plant form. *The Plant Cell*, **10**, 1075–82.

Dubos, C., Stracke, R., Grotewold, E., Weisshaar, B., Martin, C. & Lepiniec, L. (2010) MYB transcription factors in Arabidopsis. *Trends in Plant Science*, **15**, 573–81.

Dyer, A.G. & Chittka, L. (2004a) Biological significance of distinguishing between similar colours in spectrally variable illumination: bumblebees (Bombus terrestris) as a case study. *Journal of Comparative Physiology A*, **190**, 105–14.

Dyer, A.G. & Chittka, L. (2004b) Fine colour discrimination requires differential conditioning in bumblebees. *Naturwissenschaften*, **91**, 224–7.

Dyer, A.G. & Chittka, L. (2004c) Bumblebees (Bombus terrestris) sacrifice foraging speed to solve difficult colour discrimination tasks. *Journal of Comparative Physiology A*, **190**, 759–63.

Dyer, A.G., Spaethe, J. & Prack, S. (2008) Comparative psychophysics of bumblebee and honeybee colour discrimination and object detection. *Journal of Comparative Physiology A*, **194**, 617–27.

Dyer, A.G., Whitney, H.M., Arnold, S.E.J., Glover, B.J. & Chittka, L. (2006) Behavioural ecology: bees associate warmth with floral colour. *Nature*, **442**, 525.

Dyer, A.G., Whitney, H.M., Arnold, S.E.J., Glover, B.J. & Chittka, L. (2007) Mutations perturbing petal cell shape and anthocyanin synthesis influence bumblebee perception of Antirrhinum majus flower colour. *Arthropod-Plant Interactions*, **1**, 45–55.

Edgar, R.C. (2004) MUSCLE: multiple sequence alignment with high accuracy and high throughput. *Nucleic Acids Research*, **32**, 1792–7.

Endress, P.K. (1997) Relationships between floral organization, architecture, and pollination mode inDillenia (Dilleniaceae). *Plant Systematics and Evolution*, **206**, 99–118.

Endress, P.K. & Doyle, J. a. (2009) Reconstructing the ancestral angiosperm flower and its initial specializations. *American Journal of Botany*, **96**, 22–66.

Erber, J., Kierzek, S., Sander, E. & Grandy, K. (1998) Tactile learning in the honeybee. *Journal of Comparative Physiology A*, **183**, 737–744.

Expósito-Rodríguez, M., Borges, A. a, Borges-Pérez, A. & Pérez, J. a. (2008) Selection of internal control genes for quantitative real-time RT-PCR studies during tomato development process. *BMC Plant Biology*, **8**, 131.

Fay, J.C. (2011) Weighing the evidence for adaptation at the molecular level. *Trends in Genetics*, **27**, 343–9.

Fiz-Palacios, O., Schneider, H., Heinrichs, J. & Savolainen, V. (2011) Diversification of land plants: insights from a family-level phylogenetic analysis. *BMC Evolutionary Biology*, **11**, 341.

Fong, D., Kane, T. & Culver, D. (1995) Vestigialization and loss of nonfunctional characters. *Annual Review of Ecology and Systematics*, **26**, 249–268.

Free, J. (1970) The flower constancy of bumblebees. *The Journal of Animal Ecology*, **39**, 395–402.

Frey, F.M. (2004) Opposing natural selection from herbivores and pathogens may maintain floral-color variation in Claytonia virginica (Portulacaceae). *Evolution*, **58**, 2426–37.

Frohman, M.A., Dush, M.K. & Martin, G.R. (1988) Rapid production of full-length cDNAs from rare transcripts: amplification using a single gene-specific oligonucleotide primer. *Proceedings of the National Academy of Science of the United States of America*, **85**, 8998–9002.

Gadberry, M.D., Malcomber, S.T., Doust, A.N., Kellogg, E. a & Elizabeth, A. (2005) Primaclade--a flexible tool to find conserved PCR primers across multiple species. *Bioinformatics*, **21**, 1263–4.

Galinha, C., Bilsborough, G. & Tsiantis, M. (2009) Hormonal input in plant meristems: A balancing act. *Seminars in Cell & Developmental Biology*, **20**, 1149–56.

Gilding, E.K. & Marks, M.D. (2010) Analysis of purified glabra3-shapeshifter trichomes reveals a role for NOECK in regulating early trichome morphogenic events. *The Plant Journal*, **64**, 304–17.

Glover, B.J., Bunnewell, S. & Martin, C.R. (2004) Convergent evolution within the genus Solanum: the specialised anther cone develops through alternative pathways. *Gene*, **331**, 1–7.

Glover, B.J. & Martin, C.R. (1998) The role of petal cell shape and pigmentation in pollination success in Antirrhinum majus. *Heredity*, **80**, 778–784.

Glover, B.J., Perez-Rodriguez, M. & Martin, C. (1998) Development of several epidermal cell types can be specified by the same MYB-related plant transcription factor. *Development*, **125**, 3497–508.

Goodstein, D.M., Shu, S., Howson, R., Neupane, R., Hayes, R.D., Fazo, J., Mitros, T., Dirks, W., Hellsten, U., Putnam, N. & Rokhsar, D.S. (2012) Phytozome: a comparative platform

for green plant genomics. *Nucleic Acids Research*, **40**, D1178–86.

Gorton, H.L. & Vogelmann, T.C. (1996) Effects of Epidermal Cell Shape and Pigmentation on Optical Properties of Antirrhinum Petals at Visible and Ultraviolet Wavelengths. *Plant Physiology*, **112**, 879–888.

Goyret, J. & Raguso, R. a. (2006) The role of mechanosensory input in flower handling efficiency and learning by Manduca sexta. *The Journal of Experimental Biology*, **209**, 1585–93.

Green, P.B. & Linstead, P. (1990) A procedure for SEM of complex shoot structures applied to the inflorescence of snapdragon (Antirrhinum). *Protoplasma*, **158**, 33–38.

Guindon, S., Dufayard, J.-F., Lefort, V., Anisimova, M., Hordijk, W. & Gascuel, O. (2010) New algorithms and methods to estimate maximum-likelihood phylogenies: assessing the performance of PhyML 3.0. *Systematic Biology*, **59**, 307–21.

Ha, C.M., Jun, J.H. & Fletcher, J.C. (2010) Control of Arabidopsis leaf morphogenesis through regulation of the YABBY and KNOX families of transcription factors. *Genetics*, **186**, 197–206.

Hake, S., Smith, H.M.S., Holtan, H., Magnani, E., Mele, G. & Ramirez, J. (2004) The role of knox genes in plant development. *Annual Review of Cell and Developmental Biology*, **20**, 125–51.

Hall, T.A. (1999) BioEdit: a user-friendly biological sequence alignment editor and analysis program for Windows 95/98/NT. *Nucleic acids symposium series* pp. 95–98.

Hanikenne, M., Talke, I.N., Haydon, M.J., Lanz, C., Nolte, A., Motte, P., Kroymann, J., Weigel, D. & Krämer, U. (2008) Evolution of metal hyperaccumulation required cis-regulatory changes and triplication of HMA4. *Nature*, **453**, 391–5.

Harder, L. & Barclay, R. (1994) The functional significance of poricidal anthers and buzz pollination: controlled pollen removal from Dodecatheon. *Functional Ecology*, **8**, 509–517.

Hay, A. & Tsiantis, M. (2010) KNOX genes: versatile regulators of plant development and diversity. *Development*, **137**, 3153–65.

Hebsgaard, S.M., Korning, P.G., Tolstrup, N., Engelbrecht, J., Rouzé, P. & Brunak, S. (1996) Splice site prediction in Arabidopsis thaliana pre-mRNA by combining local and global sequence information. *Nucleic Acids Research*, **24**, 3439–52.

Hellens, R.P., Edwards, E. a, Leyland, N.R., Bean, S. & Mullineaux, P.M. (2000) pGreen: a versatile and flexible binary Ti vector for Agrobacterium-mediated plant transformation. *Plant Molecular Biology*, **42**, 819–32.

Henikoff, S. & Henikoff, J.G. (1992) Amino acid substitution matrices from protein blocks. *Proceedings of the National Academy of Sciences of the United States of America*, **89**, 10915–9.

Hill, P., Wells, P. & Wells, H. (1997) Spontaneous flower constancy and learning in honey bees as a function of colour. *Animal Behaviour*, **54**, 615–27.

Hilscher, J., Schlötterer, C. & Hauser, M.-T. (2009) A single amino acid replacement in ETC2 shapes trichome patterning in natural Arabidopsis populations. *Current Biology*, **19**, 1747–51.

Hoballah, M.E., Stuurman, J., Turlings, T.C.J., Guerin, P.M., Connétable, S. & Kuhlemeier, C. (2005) The composition and timing of flower odour emission by wild Petunia axillaris coincide with the antennal perception and nocturnal activity of the pollinator Manduca sexta. *Planta*, **222**, 141–50.

Hogendoorn, K., Gross, C.L., Sedgley, M. & Keller, M.A. (2006) Increased Tomato Yield Through Pollination by Native Australian Amegilla chlorocyanea (Hymenoptera: Anthophoridae). *Journal of Economic Entomology*, **99**, 828–833.

Hopper, S. & Moran, G. (1981) Bird pollination and the mating system of Eucalyptus stoatei. *Australian Journal of Botany*, 625–638.

Horn, K.C. & Holland, J.N. (2010) Discrimination among floral resources by an obligately pollinating seed-eating moth : host-marking signals and pollination and florivory cues. , 119–129.

Horsch, R. B.; Fry, J. E.; Hoffmann, N. L.; Eichholtz, D.; Rogers, S. G.; Fraley, R.T. (1985) A simple and general method for transferring genes into plants. *Science*, **227**, 1229–31.

Van Houwelingen, A., Souer, E., Spelt, K., Kloos, D., Mol, J. & Koes, R. (1998) Analysis of flower pigmentation mutants generated by random transposon mutagenesis in Petunia hybrida. *The Plant Journal*, **13**, 39–50.

Hughes, A L. (2007) Looking for Darwin in all the wrong places: the misguided quest for positive selection at the nucleotide sequence level. *Heredity*, **99**, 364–73.

Hughes, T. & Liberles, D. A. (2008) The power-law distribution of gene family size is driven by the pseudogenisation rate's heterogeneity between gene families. *Gene*, **414**, 85–94.

Irish, V.F. & Litt, A. (2005) Flower development and evolution: gene duplication, diversification and redeployment. *Current Opinion in Genetics & Development*, **15**, 454–60.

Ishida, T. & Kinoshita, K. (2008) Prediction of disordered regions in proteins based on the meta approach. *Bioinformatics*, **24**, 1344–8.

Ito, T. (2011) Coordination of flower development by homeotic master regulators. *Current Opinion in Plant Biology*, **14**, 53–9.

Jacob, F. (1977) Evolution and tinkering. *Science*, **196**, 1161–1166.

Jaffé, F.W., Tattersall, A. & Glover, B.J. (2007) A truncated MYB transcription factor from Antirrhinum majus regulates epidermal cell outgrowth. *Journal of Experimental Botany*, **58**, 1515–24.

Jakoby, M.J., Falkenhan, D., Mader, M.T., Brininstool, G., Wischnitzki, E., Platz, N., Hudson, A., Hülskamp, M., Larkin, J. & Schnittger, A. (2008) Transcriptional profiling of mature Arabidopsis trichomes reveals that NOECK encodes the MIXTA-like transcriptional regulator MYB106. *Plant Physiology*, **148**, 1583–602.

Jaramillo, M., Manos, P. & Zimmer, E. (2004) Phylogenetic relationships of the perianthless Piperales: reconstructing the evolution of floral development. *International Journal of Plant …*, **165**, 403–416.

Jiang, C., Gu, X. & Peterson, T. (2004) Identification of conserved gene structures and carboxy-terminal motifs in the Myb gene family of Arabidopsis and Oryza sativa L. ssp. indica. *Genome biology*, **5**, R46.

Jin, H. & Martin, C.R. (1999) Multifunctionality and diversity within the plant MYB-gene family. *Plant Molecular Biology*, **41**, 577–85.

Kammer, a E. & Heinrich, B. (1974) Metabolic rates related to muscle activity in bumblebees. *The Journal of Experimental Biology*, **61**, 219–27.

Kaplan, C.D. (2013) Basic mechanisms of RNA polymerase II activity and alteration of gene expression in Saccharomyces cerevisiae. *Biochimica et biophysica acta*, **1829**, 39–54.

Katja, H., Steven, C. & K, M.A. (2007) Original article Foraging behaviour of a blue banded bee , Amegilla chlorocyanea in greenhouses : implications for use as tomato pollinators *. , **38**, 86–92.

Kay, Q., Daoud, H. & Stirton, C. (1981) Pigment distribution, light reflection and cell structure in petals. *Botanical Journal of the Linnean Society*, **83**, 57–84.

Kearns, C.A. & Inouye, D.W. (1997) Pollinators, Flowering Plants, and Conservation Biology. *BioScience*, **47**, 297–307.

Kevan, P.G. & Lane, M.A. (1985) Flower petal microtexture is a tactile cue for bees. *Proceedings of the National Academy of Sciences of the United States of America*, **82**, 4750–2.

Kien, J. & Menzel, R. (1977) Chromatic properties of interneurons in the optic lobes of the bee. *Journal of Comparative Physiology A*, **34**, 17–34.

Kimura, M. (1968) Evolutionary Rate at the Molecular Level. *Nature*, **217**, 624–626.

King, M.J. & Buchmann, S.L. (1996) Sonication dispensing of pollen from Solanum laciniatum flowers. *Functional Ecology*, **10**, 449–456.

Knapp, S., Bohs, L., Spooner, D., Nee, M., Bennett, J., Walley, L. & Clark, J. (2005) Taxonomy as a team sport: PBI Solanum or how to monograph a monster. *International Botanical Congress*

Kumaran, M.K., Bowman, J.L. & Sundaresan, V. (2002) YABBY Polarity Genes Mediate the Repression of KNOX Homeobox Genes in Arabidopsis. *The Plant Cell*, **14**, 2761–2770.

Kwiatkowska, D. (2008) Flowering and apical meristem growth dynamics. *Journal of Experimental Botany*, **59**, 187–201.

Larkin, M. a, Blackshields, G., Brown, N.P., Chenna, R., Mcgettigan, P. a, McWilliam, H., Valentin, F., Wallace, I.M., Wilm, A., Lopez, R., Thompson, J.D., Gibson, T.J. & Higgins, D.G. (2007) Clustal W and Clustal X version 2.0. *Bioinformatics*, **23**, 2947–8.

Latchman, D.S. (1997) Transcription factors: An overview. *The International Journal of Biochemistry & Cell Biology*, **29**, 1305–1312.

Lehrer, M. & Srinivasan, M. V. (1992) Freely flying bees discriminate between stationary and moving objects: performance and possible mechanisms. *Journal of Comparative Physiology A*, **171**, 457–467.

Lehrer, M., Srinivasan, M. V., Zhang, S.W. & Horridge, G. a. (1988) Motion cues provide the bee's visual world with a third dimension. *Nature*, **332**, 356–357.

Levin, R., Myers, N. & Bohs, L. (2006) Phylogenetic relationships among the" spiny Solanums"(Solanum subgenus Leptostemonum, Solanaceae). *American Journal of Botany*, **93**, 157–169.

Levin, R., Watson, K. & Bohs, L. (2005) A four-gene study of evolutionary relationships in Solanum section Acanthophora. *American Journal of Botany*, **92**, 603–612.

De Luca, P. a, Bussière, L.F., Souto-Vilaros, D., Goulson, D., Mason, A.C. & Vallejo-Marín, M. (2012) Variability in

bumblebee pollination buzzes affects the quantity of pollen released from flowers. *Oecologia*.

Machado, A., Wu, Y., Yang, Y., Llewellyn, D.J. & Dennis, E.S. (2009) The MYB transcription factor GhMYB25 regulates early fibre and trichome development. *The Plant Journal*, **59**, 52–62.

Maddison, W.P. & Maddison, D.R. (2003) Mesquite : A modular system for evolutionary Mesquite installation for evolutionary analysis.

Martin, C.R., Bhatt, K., Baumann, K., Jin, H., Zachgo, S., Roberts, K., Schwarz-Sommer, Z., Glover, B.J. & Perez-Rodriguez, M. (2002) The mechanics of cell fate determination in petals. *Philosophical Transactions of the Royal Society of London. Series B, Biological sciences*, **357**, 809–13.

Martin, C., Ellis, N. & Rook, F. (2010) Do transcription factors play special roles in adaptive variation? *Plant Physiology*, **154**, 506–11.

Maughan, S.C., Murray, J. a H. & Bögre, L. (2006) A greenprint for growth: signalling the pattern of proliferation. *Current Opinion in Plant Biology*, **9**, 490–5.

Meléndez-Ackerman, E., Campbell, D. & Waser, N. (1997) Hummingbird behavior and mechanisms of selection on flower color in Ipomopsis. *Ecology*, **78**, 2532–2541.

Ming, F. & Ma, H. (2009) A terminator of floral stem cells. *Genes & development*, **23**, 1705–8.

Mintz-Oron, S., Mandel, T., Rogachev, I., Feldberg, L., Lotan, O., Yativ, M., Wang, Z., Jetter, R., Venger, I., Adato, A. & Aharoni, A. (2008) Gene expression and metabolism in tomato fruit surface tissues. *Plant Physiology*, **147**, 823–51.

Van der Niet, T. & Johnson, S.D. (2012) Phylogenetic evidence for pollinator-driven diversification of angiosperms. *Trends in Ecology & Evolution*, **27**, 353–61.

Nieuwland, J., Scofield, S. & Murray, J. a H. (2009) Control of division and differentiation of plant stem cells and their derivatives. *Seminars in Cell & Developmental Biology*, **20**, 1134–42.

Noda, K., Glover, B.J., Linstead, P. & Martin, C.R. (1994) Flower colour intensity depends on specialized cell shape controlled by a Myb-related transcription factor. *Nature*, **369**, 661–4.

Ogata, K., Morikawa, S., Nakamura, H., Sekikawa, a, Inoue, T., Kanai, H., Sarai, a, Ishii, S. & Nishimura, Y. (1994) Solution structure of a specific DNA complex of the Myb DNA-binding domain with cooperative recognition helices. *Cell*, **79**, 639–48.

Oh, I.H. & Reddy, E.P. (1999) The myb gene family in cell growth, differentiation and apoptosis. *Oncogene*, **18**, 3017–33.

Ojeda, I., Santos-Guerra, A., Caujapé-Castells, J., Jaén-Molina, R., Marrero, Á. & C. B. Cronk, Q. (2012) Comparative Micromorphology of Petals in Macaronesian Lotus (Leguminosae) Reveals a Loss of Papillose Conical Cells during the Evolution of Bird Pollination. *International Journal of Plant Sciences*, **173**, 365–374.

Oliveira, P.E., Gibbs, P.E. & Barbosa, A.A. (2004) Moth pollination of woody species in the Cerrados of Central Brazil: a case of so much owed to so few? *Plant Systematics and Evolution*, **245**, 41–54.

Orphanides, G., Lagrange, T. & Reinberg, D. (1996) The general transcription factors of RNA polymerase II. *Genes & Development*, **10**, 2657–2683.

Pabo, C.O. & Sauer, R.T. (1992) Transcription factors: structural families and principles of DNA recognition. *Annual Review of Biochemistry*, **61**, 1053–95.

Pavlopoulos, A., Kontarakis, Z., Liubicich, D.M., Serano, J.M., Akam, M., Patel, N.H. & Averof, M. (2009) Probing the evolution of appendage specialization by Hox gene misexpression in an emerging model crustacean. *Proceedings of the National Academy of Sciences of the United States of America*, **106**, 13897–902.

Pearson, J.C., Lemons, D. & McGinnis, W. (2005) Modulating Hox gene functions during animal body patterning. *Nature reviews. Genetics*, **6**, 893–904.

Peralta, I. & Spooner, D. (2001) Granule-bound starch synthase (GBSSI) gene phylogeny of wild tomatoes (Solanum L. section Lycopersicon Wettst. subsection Lycopersicon). *American Journal of Botany*, **88**, 1888–1902.

Pérez, F. & Arroyo, M. (2006) Ancestral reconstruction of flower morphology and pollination systems in Schizanthus (Solanaceae). *American Journal of Botany*, **93**, 1029–1038.

Perez-Rodriguez, M., Jaffé, F.W., Glover, B.J. & Martin, C.R. (2005) Development of three different cell types is associated with the activity of a specific MYB transcription factor in the ventral petal of Antirrhinum majus flowers. *Development*, **132**, 359–70.

Poczai, P., Hyvönen, J. & Symon, D.E. (2011) Phylogeny of kangaroo apples (Solanum subg. Archaesolanum, Solanaceae). *Molecular Biology Reports*, **38**, 5243–59.

Radivojac, P., Clark, W.T., Oron, T.R., Schnoes, A.M., Wittkop, T., Sokolov, A., *et al.* (2013) A large-scale evaluation of computational protein function prediction. *Nature Methods*, **10**, 221–229.

Ramsay, N. a & Glover, B.J. (2005) MYB-bHLH-WD40 protein complex and the evolution of cellular diversity. *Trends in Plant Science*, **10**, 63–70.

Rands, S.A., Glover, B.J. & Whitney, H.M. (2011) Floral epidermal structure and flower orientation: getting to grips with awkward flowers. *Arthropod-Plant Interactions*, **5**, 279–285.

Rands, S.A. & Whitney, H.M. (2008) Floral temperature and optimal foraging: is heat a feasible floral reward for pollinators? *PloS ONE*, **3**, e2007.

Rast, M.I. & Simon, R. (2008) The meristem-to-organ boundary: more than an extremity of anything. *Current Opinion in Genetics & Development*, **18**, 287–94.

Raymaekers, M., Smets, R., Maes, B. & Cartuyvels, R. (2009) Checklist for optimization and validation of real-time PCR assays. *Journal of Clinical Laboratory Analysis*, **23**, 145–51.

Riechmann, J.L. (2000) Arabidopsis Transcription Factors: Genome-Wide Comparative Analysis Among Eukaryotes. *Science*, **290**, 2105–2110.

Rieseberg, L.H. & Blackman, B.K. (2010) Speciation genes in plants. *Annals of Botany*, **106**, 439–55.

Riviere, S., Clayson, C., Dockstader, K., Wright, M. a. R. & Costea, M. (2013) To attract or to repel? Diversity, evolution and role of the "most peculiar organ" in the Cuscuta flower (dodder, Convolvulaceae)—the infrastaminal scales. *Plant Systematics and Evolution*, **299**, 529–552.

Rose, T.M., Schultz, E.R., Henikoff, J.G., Pietrokovski, S., McCallum, C.M. & Henikoff, S. (1998) Consensus-degenerate hybrid oligonucleotide primers for amplification of distantly related sequences. *Nucleic Acids Research*, **26**, 1628–35.

Sablowski, R. (2007) Flowering and determinacy in Arabidopsis. *Journal of Experimental Botany*, **58**, 899–907.

Schemske, D.W. & Bierzychudek, P. (2007) Spatial differentiation for flower color in the desert annual Linanthus parryae: was Wright right? *Evolution*, **61**, 2528–43.

Schueller, S.K. (2006) Island–mainland difference in Nicotiana glauca (Solanaceae) corolla length: a product of pollinator-mediated selection? *Evolutionary Ecology*, **21**, 81–98.

Scoville, A.G., Barnett, L.L., Bodbyl-Roels, S., Kelly, J.K. & Hileman, L.C. (2011) Differential regulation of a MYB transcription factor is correlated with transgenerational epigenetic inheritance of trichome density in Mimulus guttatus. *The New Phytologist*.

Shang, Y., Venail, J., Mackay, S., Bailey, P., Schwinn, K.E., Jameson, P.E., Martin, C.R. & Davies, K.M. (2010) The molecular basis for venation patterning of pigmentation and its effect on pollinator attraction in flowers of Antirrhinum. *New Phytologist*, no–no.

Sharma, B. & Kramer, E. (2013) Sub- and neo-functionalization of APETALA3 paralogs have contributed to the evolution of novel floral organ identity in Aquilegia (columbine, Ranunculaceae). *The New Phytologist*, **197**, 949–57.

Shi, X., Ng, D.W.-K., Zhang, C., Comai, L., Ye, W. & Chen, Z.J. (2012) Cis- and trans-regulatory divergence between progenitor species determines gene-expression novelty in Arabidopsis allopolyploids. *Nature Communications*, **3**, 950.

Shrestha, M., Dyer, A.G., Boyd-Gerny, S., Wong, B.B.M. & Burd, M. (2013) Shades of red: bird-pollinated flowers target the specific colour discrimination abilities of avian vision. *The New Phytologist*, **198**, 301–10.

Singh, K., Foley, R. & Oñate-Sánchez, L. (2002) Transcription factors in plant defense and stress responses. *Current Opinion in Plant Biology*, **5**, 430–436.

Skorupski, P. & Chittka, L. (2010) Photoreceptor spectral sensitivity in the bumblebee, Bombus impatiens (Hymenoptera: Apidae). *PloS ONE*, **5**, e12049.

Smith, R. & Rausher, M. (2008) Selection for character displacement is constrained by the genetic architecture of floral traits in the ivyleaf morning glory. *Evolution*, **62**, 2829–2841.

Soltis, P.S. & Soltis, D.E. (2004) The origin and diversification of angiosperms. *American Journal of Botany*, **91**, 1614–1626.

Stern, S., Agra, M. & Bohs, L. (2011) Molecular delimitation of clades within New World species of the "spiny solanums" (Solanum subg. Leptostemonum). *Taxon*, **60**, 1429–1441.

Stern, S., Bohs, L., Giacomin, L., Stehmann, J. & Knapp, S. (2013) A Revision of <I>Solanum</I> Section <I>Gonatotrichum</I>. *Systematic Botany*, **38**, 471–496.

Stern, S., Weese, T. & Bohs, L. (2010) Phylogenetic relationships in Solanum section Androceras (Solanaceae). *Systematic Botany*, **35**, 885–893.

Di Stilio, V.S., Martin, C.R., Schulfer, A.F. & Connelly, C.F. (2009) An ortholog of MIXTA-like2 controls epidermal cell shape in flowers of Thalictrum. *The New Phytologist*, **183**, 718–28.

Stracke, R., Werber, M. & Weisshaar, B. (2001) The R2R3-MYB gene family in Arabidopsis thaliana. *Current Opinion in Plant Biology*, **4**, 447–456.

Studer, A., Zhao, Q., Ross-Ibarra, J. & Doebley, J. (2011) Identification of a functional transposon insertion in the maize domestication gene tb1. *Nature Genetics*, **43**, 1160–3.

Sun, G. (1998) In Search of the First Flower: A Jurassic Angiosperm, Archaefructus, from Northeast China. *Science*, **282**, 1692–1695.

Sun, G., Ji, Q., Dilcher, D.L., Zheng, S., Nixon, K.C. & Wang, X. (2002) Archaefructaceae, a new basal angiosperm family. *Science*, **296**, 899–904.

Tamura, K., Peterson, D., Peterson, N., Stecher, G., Nei, M. & Kumar, S. (2011) MEGA5: Molecular Evolutionary Genetics Analysis using Maximum Likelihood, Evolutionary Distance, and Maximum Parsimony Methods. *Molecular Biology and Evolution*, **28**, 2731–2739.

Taylor, S., Wakem, M., Dijkman, G. & Alsarraj, M. (2010) *A Practical Approach to RT-qPCR--Publishing Data That Conform to the MIQE Guidelines*.

The Arabidopsis Genome Initiative. (2000) Analysis of the genome sequence of the flowering plant Arabidopsis thaliana. *Nature*, **408**, 796–815.

The Potato Genome Sequencing Consortium. (2011) Genome sequence and analysis of the tuber crop potato. *Nature*, **475**, 189–95.

The Tomato Genome Consortium. (2012) The tomato genome sequence provides insights into fleshy fruit evolution. *Nature*, **485**, 635–41.

Tremblay, R.L. & Ackerman, J.D. (2007) Floral color patterns in a tropical orchid: Are they associated with reproductive success? *Plant Species Biology*, **22**, 95–105.

Tripp, E.A. & Manos, P.S. (2008) Is floral specialization an evolutionary dead-end? Pollination system transitions in Ruellia (Acanthaceae). *Evolution*, **62**, 1712–37.

Untergasser, A., Nijveen, H., Rao, X., Bisseling, T., Geurts, R. & Leunissen, J. a M. (2007) Primer3Plus, an enhanced web interface to Primer3. *Nucleic Acids Research*, **35**, W71–4.

Wang, S., Wang, J.-W., Yu, N., Li, C.-H., Luo, B., Gou, J.-Y., Wang, L.-J. & Chen, X.-Y. (2004) Control of plant trichome development by a cotton fiber MYB gene. *The Plant Cell*, **16**, 2323–34.

Warren, J. & James, P. (2008) Do flowers wave to attract pollinators? A case study with Silene maritima. *Journal of Evolutionary Biology*, **21**, 1024–9.

Waser, N.M. & Price, M. V. (1983) Pollinator behaviour and natural selection for flower colour in Delphinium nelsonii. *Nature*, **302**, 422–424.

Weese, T.L. & Bohs, L. (2007) A Three-Gene Phylogeny of the Genus <I>Solanum</I> (Solanaceae). *Systematic Botany*, **32**, 445–463.

Weng, L., Tian, Z., Feng, X., Li, X., Xu, S., Hu, X., Luo, D. & Yang, J. (2011) Petal Development in Lotus japonicus. *Journal of iltegrative Plant Biology*, **53**, 770–782.

Wessinger, C.A. & Rausher, M.D. (2012) Lessons from flower colour evolution on targets of selection. *Journal of Experimental Botany*, **63**, 5741–9.

Whitney, H.M., Bennett, K.M.V., Dorling, M., Sandbach, L., Prince, D., Chittka, L. & Glover, B.J. (2011a) Why do so many petals have conical epidermal cells? *Annals of Botany*, **108**, 609–16.

Whitney, H.M., Chittka, L., Bruce, T.J. a & Glover, B.J. (2009a) Conical epidermal cells allow bees to grip flowers and increase foraging efficiency. *Current Biology*, **19**, 948–53.

Whitney, H., Federle, W. & Glover, B.J. (2009) Grip and slip: Mechanical interactions between insects and the epidermis of flowers and flower stalks. *Communicative & Integrative Biology*, **2**, 505.

Whitney, H.M., Kolle, M., Andrew, P., Chittka, L., Steiner, U. & Glover, B.J. (2009b) Floral iridescence, produced by diffractive optics, acts as a cue for animal pollinators. *Science*, **323**, 130.

Whitney, H.M., Poetes, R., Steiner, U., Chittka, L. & Glover, B.J. (2011b) Determining the contribution of epidermal cell shape to petal wettability using isogenic Antirrhinum lines. *PloS ONE*, **6**, e17576.

Winter, C.M., Austin, R.S., Blanvillain-Baufumé, S., Reback, M. a, Monniaux, M., Wu, M.-F., Sang, Y., Yamaguchi, A., Yamaguchi, N., Parker, J.E., Parcy, F., Jensen, S.T., Li, H. & Wagner, D. (2011) LEAFY target genes reveal floral regulatory logic, cis motifs, and a link to biotic stimulus response. *Developmental Cell*, **20**, 430–43.

Yang, R. & Wang, X. (2013) Organ Evolution in Angiosperms Driven by Correlated Divergences of Gene Sequences and Expression Patterns. *The Plant Cell*, 1–13.

Zhang, Y., Cao, G., Qu, L.-J. & Gu, H. (2009) Characterization of Arabidopsis MYB transcription factor gene AtMYB17 and its possible regulation by LEAFY and AGL15. *Journal of Genetics and Genomics = Yi Chuan Xue Bao*, **36**, 99–107.

Zuriaga, E., Blanca, J. & Nuez, F. (2008) Classification and phylogenetic relationships in Solanum section Lycopersicon based on AFLP and two nuclear gene sequences. *Genetic Resources and Crop Evolution*, **56**, 663–678.

Appendix 1. Solutions and Media (in alphabetical order)

CTAB buffer
100 mM Tris HCl
20 mM EDTA pH 8
1.4 M NaCl
1% PVP 40
4% CTAB

DNA extraction buffer
50 mM EDTA
0.1 M NaCl
0.1 M Tris HCl pH 8.0
1% SDS
(autoclaved)

E. coli freezing solution
60 mM $CaCl_2$
15% glycerol
10 mM PIPES
(autoclaved)

Gel loading buffer
30% glycerol
0.25% bromophenol blue
0.25% xylene cyanol
10mM Tris HCl pH 7.6

*LB bacterial growth media**
10 g L^{-1} tryptone
5 g L^{-1} yeast extract
5 g L^{-1} NaCl
1 L dH_2O
(autoclaved)

*MS9 Media***
4.4 g L^{-1} MS salts
3% w/v sucrose
0.8% w/v Bacto Agar
1 µg ml^{-1} 6-benzylamino-purine
0.5 µg ml^{-1} indole-3-acetic acid
(adjusted to pH 5.9 with NaOH)

RNA extraction buffer
1 mM EDTA
0.1 M NaCl
10 mM Tris HCl pH 7.0
1% SDS
(autoclaved)

SOC bacterial growth media
2% tryptone
0.5% yeast extract
20 mM glucose
20 mM NaCl
10 mM $MgCl_2$
10 mM $MgSO_4$
2.5 mM KCl
(autoclaved)

10 x TAE buffer
0.4 M Tris base
0.2 M acetic acid
10mM EDTA pH 8.0

10 x TBE buffer
880 mM Tris base
880 mM boric acid
40 mM EDTA pH 8.0

* For solid LB media, 10 g L^{-1} agar added before autoclaving.

** For MS0 rooting media, both hormones were omitted.

Appendix 2. PCR primer sequences

Primer purpose and name	Primer sequence
Degenerate PCR for *Solanum Mixta*	
Myb F1	GGACCTTGGACTCCTGAAGAAGAYCARAARYT
Myb R5	AAGTTGAAWGATGGTTYGTTCTTC
3'RACE for *Solanum*	
S.sisy-3'RACE FWD1	AGCTTATATCGAAGAACACGGC
S.sisy-3'RACE FWD2	TACCTGCCAAAGCTGGACTT
Specific PCR for *Solanum MIXTA* and *Mixta-Like*	
Solanum Mixta F1	ATCGAAGAACATGGTCATGGTAG
Solanum Mixta R1	GCGAGTCTAGCTTCGGCTT
Solanum Mixta-Like End F	ATGGGTCGATCTCCATGTTGTG
Solanum Mixta-Like End R	CCTAGTCTAATTAGAACATTGCTGAATC
Solanum Ml1 End F	AGCTAGGTAATTACCATGGGAAGA
Solanum Ml1 End R	CTTAGAATAATGGAGATCCAATTGGTGAAG
Positive controls	
Solanum lycopersicum ubiquitin F	CCAAGATCCAGGACAAGGAA
Solanum lycopersicum ubiquitin R	TAAAATCAATCGCCTCCAGC
Nicotiana ubiquitin F	GAGCTCTGACACCATCGACA
Nicotiana ubiquitin R	ACATCACGACCACAACCAGA

Solanum phylogenetics*	
ndhF F1 (1F)	ATGGAACAKACATATSAATATGC
ndhF R1 (1318R)	CGAAACATATAAAATGCRGTTAATCC
ndhF F2 (972F)	GTCTCAATTGGGTTATATGATG
ndhF R2 (2110R)	CCCCCTAYATATTTGATACCTTCTCC
trnT-F F1 (a)	CATTACAAATGCGATGCTCT
trnT-F R1 (d)	GGGGATAGAGGGACTTGAAC
trnT-F F2 (c)	CGAAATCGGTAGACGCTACG
trnT-F R2 (f)	ATTTGAACTGGTGACACGAG
Waxy FWD2 (WaxyF) F1	CGGGTAATGACAATATCCCC
Waxy Rev2 (1171R) R1	TCATACCCATCAATGAAATC
Waxy Fwd3 (1058F) F2	ATTCCCTGCTACTTGAAGTC
Waxy R1b (2R, 20nt) R2	GTTCCATATCGCATAGCATG
Quantitative PCR	
SlDNAj F	GAGCACACATTGAGCCTTGAC
SlDNAj R	CTTTGGTACATCGGCATTCC
(a/l) MLqPCR F	ATGGGTCGATCTCCATGTTG
(a/l) MLqPCR R	GTCCAGCTTTGGCAGGTAAT

*names in brackets refer to names as given in Weese & Bohs, 2007.

Appendix 3. Petal epidermal SEM images for all specimens collected in this project.

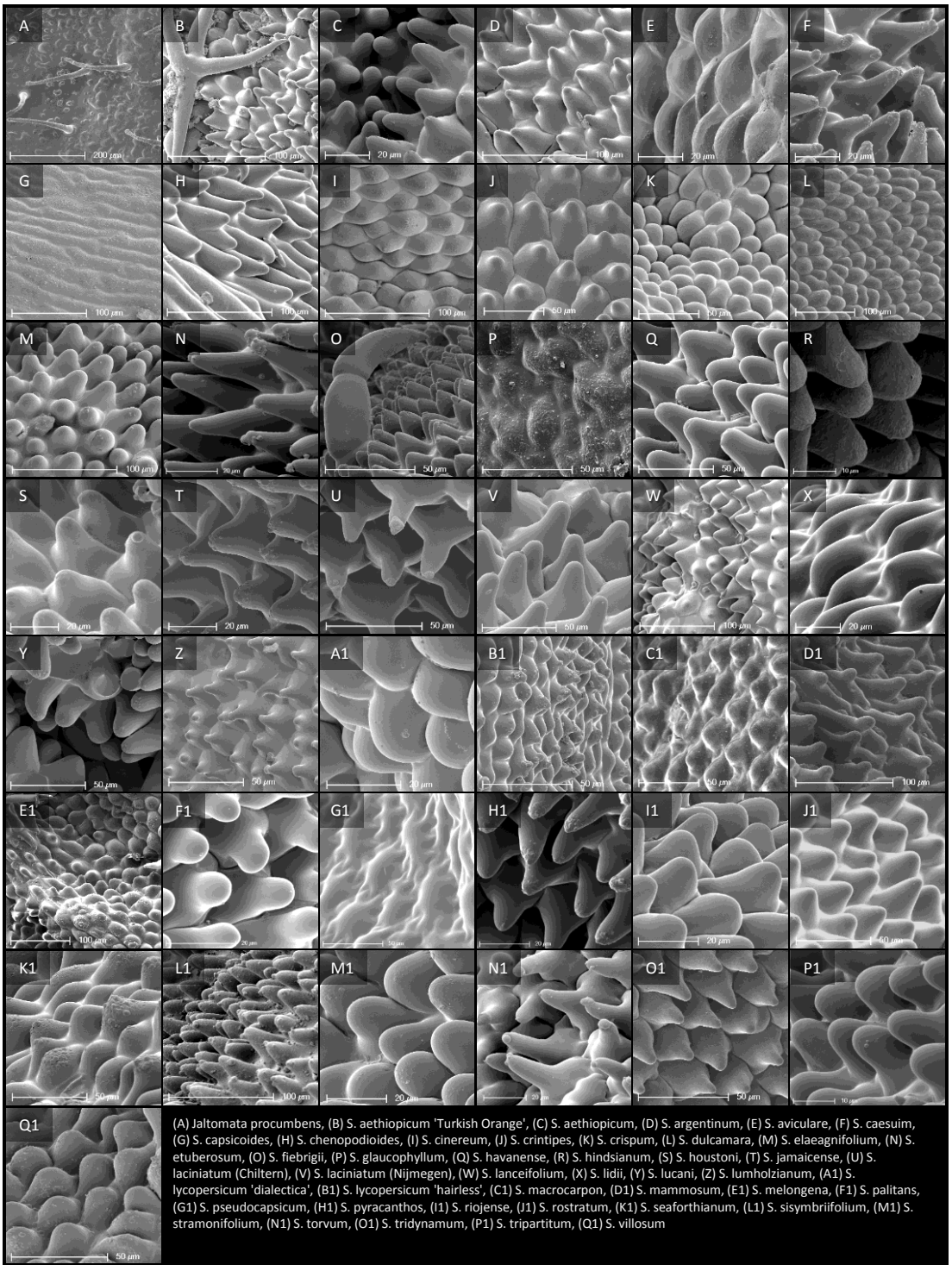

(A) Jaltomata procumbens, (B) S. aethiopicum 'Turkish Orange', (C) S. aethiopicum, (D) S. argentinum, (E) S. aviculare, (F) S. caesuim, (G) S. capsicoides, (H) S. chenopodioides, (I) S. cinereum, (J) S. crintipes, (K) S. crispum, (L) S. dulcamara, (M) S. elaeagnifolium, (N) S. etuberosum, (O) S. fiebrigii, (P) S. glaucophyllum, (Q) S. havanense, (R) S. hindsianum, (S) S. houstoni, (T) S. jamaicense, (U) S. laciniatum (Chiltern), (V) S. laciniatum (Nijmegen), (W) S. lanceifolium, (X) S. lidii, (Y) S. lucani, (Z) S. lumholzianum, (A1) S. lycopersicum 'dialectica', (B1) S. lycopersicum 'hairless', (C1) S. macrocarpon, (D1) S. mammosum, (E1) S. melongena, (F1) S. palitans, (G1) S. pseudocapsicum, (H1) S. pyracanthos, (I1) S. riojense, (J1) S. rostratum, (K1) S. seaforthianum, (L1) S. sisymbriifolium, (M1) S. stramonifolium, (N1) S. torvum, (O1) S. tridynamum, (P1) S. tripartitum, (Q1) S. villosum

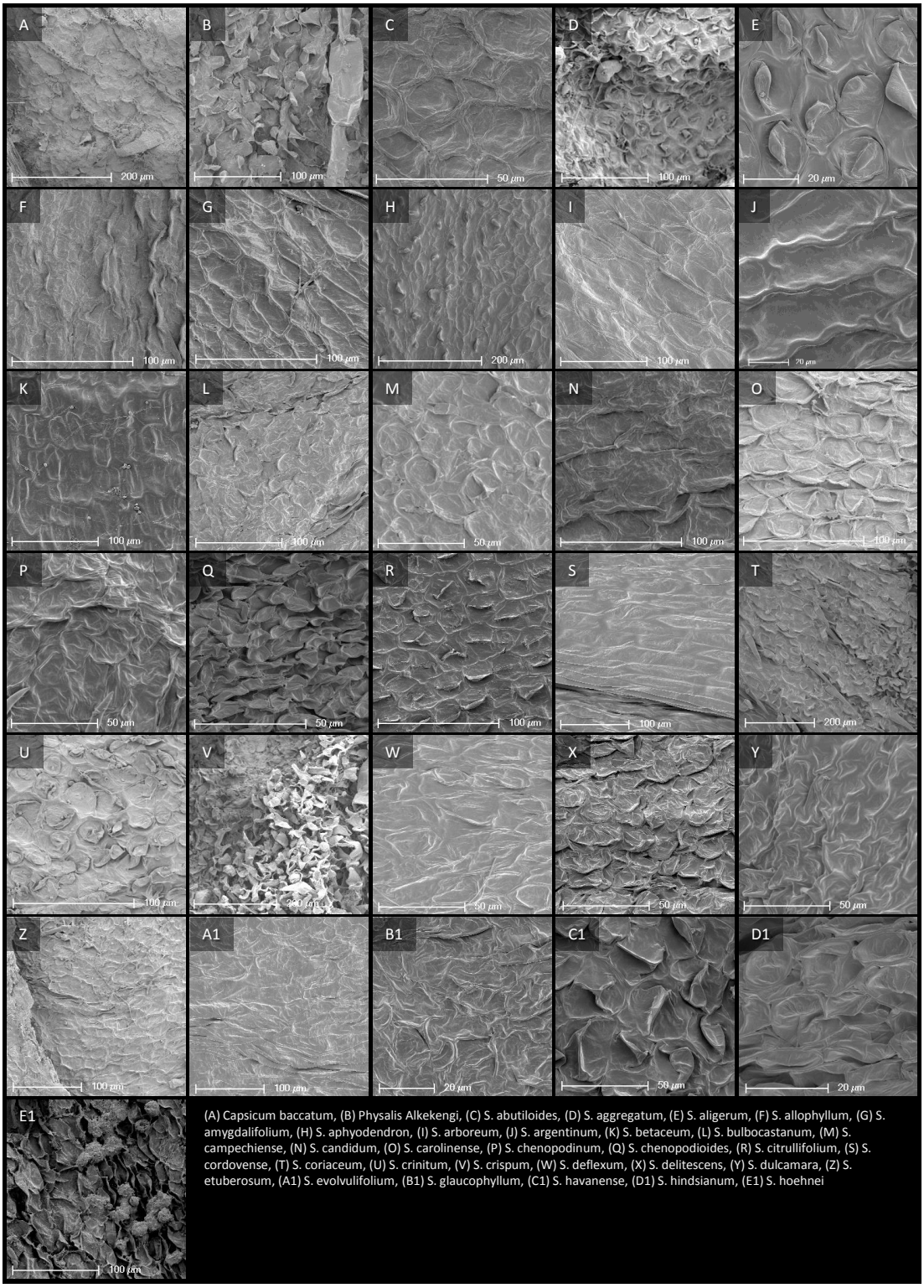

(A) Capsicum baccatum, (B) Physalis Alkekengi, (C) S. abutiloides, (D) S. aggregatum, (E) S. aligerum, (F) S. allophyllum, (G) S. amygdalifolium, (H) S. aphyodendron, (I) S. arboreum, (J) S. argentinum, (K) S. betaceum, (L) S. bulbocastanum, (M) S. campechiense, (N) S. candidum, (O) S. carolinense, (P) S. chenopodinum, (Q) S. chenopodioides, (R) S. citrullifolium, (S) S. cordovense, (T) S. coriaceum, (U) S. crinitum, (V) S. crispum, (W) S. deflexum, (X) S. delitescens, (Y) S. dulcamara, (Z) S. etuberosum, (A1) S. evolvulifolium, (B1) S. glaucophyllum, (C1) S. havanense, (D1) S. hindsianum, (E1) S. hoehnei

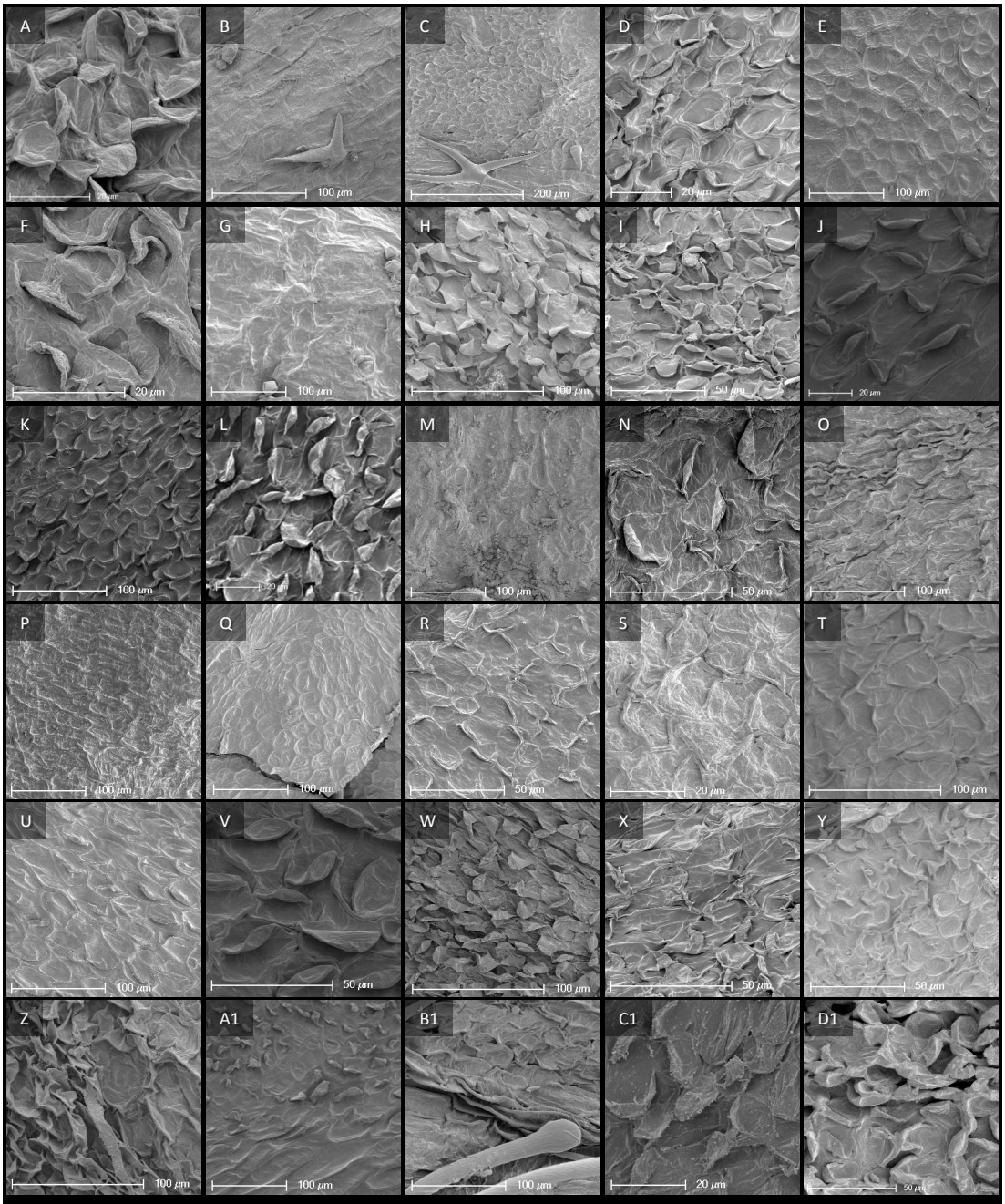

(A) S. inelegans, (B) S. jamaicense 2, (C) S. jamaicense, (D) S. juglandifolium, (E) S. laciniatum, (F) S. lepidotum, (G) S. luteoalbum, (H) S. mauritianum, (I) S. montanum, (J) S. nigrum, (K) S. nitidum, (L) S. physalifolium, (M) S. pinnatisectum, (N) S. prinophyllum, (O) S. pubigerum, (P) S. rovirosanum, (Q) S. rugosum, (R) S. wendlandii, (S) S. schimperianum, (T) S. schlechtendalianum, (U) S. seaforthianum 2, (V) S. seaforthianum, (W) S. sisymbriifolium, (X) S. torvum, (Y) S. triflorum, (Z) S. tripartitum, (A1) S. trisectum, (B1) S. tuberosum, (C1) S. vespertilio, (D1) S. villosum

Appendix 4. pGREENII::35S expression vectors containing *Solanum* Subgroup 9A genes

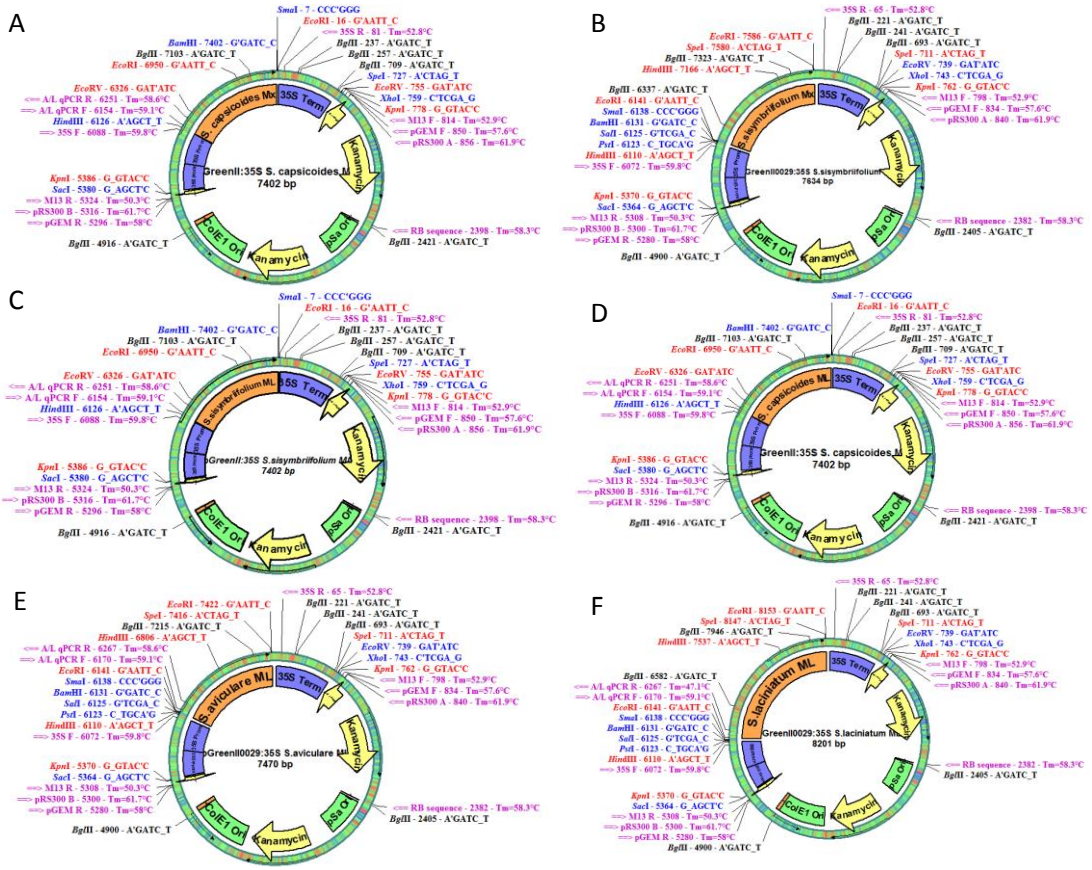

(A) S. capsicoides Mixta (B) *S. sisymbriifolium Mixta* (C) *S. sisymbriifolium Mixta-Like* (D) *S. capsicoides Mixta-Like* (E) *S. aviculare Mixta-Like* (F) *S. laciniatum Mixta-Like*

All ligation conditions are detailed in Methods section 2.3.9.4.

Appendix 5. Phylogeny voucher list

Species	Phylogeny voucher	Morphology voucher	
		Material type	Source/voucher
Capsicum baccatum	ndhF: Bolivia, Eshbaugh 1584 (MU), trnT-F, waxy: USA (cultivated), Bohs 2564 (UT); U08916, DQ180415, DQ169007.	Herbarium	CGE [collector unknown]
Capsicum chacoense	Bolivia, Eshbaugh 1586A (MU); AF500809, DQ180416, DQ169008.	-	-
Capsicum frutescens	ndhF: LB10911-99, trnT-F: LB1018, waxy: B. Walsh 15, UWM AF397125	Seed	924750057
Jaltomata procumbens	Mexico, Davis 1189A; U47429, DQ180419, AY996374.	Seed	Botanical Gardens of the Rheinische Friedrich-Wilhelms-Universität Bonn
Jaltomata sinuosa	Bolivia, Nee et al. 51830 (NY); AF500835, DQ180418, DQ169009.	-	-
Lycianthes heteroclita	Costa Rica, Bohs 2376 (UT); U72756, DQ180414, DQ169010.	-	-
Lycianthes rantonnei	BIRM S.0928, Olmstead S-96 (WTU); AF500840, DQ180417, DQ169011.	-	-
Margaranthus solanaceus	Mexico, Olmstead S-37 (WTU); EU580912, EU581025, AY665939.1	Seed	NIJ904750101
Nicotiana glauca	ndhF, trnT-F: Argentina, Nee & al. 51725 (BM); AJ585910 AJ577414; waxy: BM Nee et al. 51725 FN562129.1	Seed	NIJ914750031
Physalis alkekengi	D'Arcy collection, D'Arcy 17707 (MO); U08927, DQ180420, DQ169012.	Herbarium	CGE [collector unknown]
S. abutiloides	BIRM S.0655, Olmstead S-73 (WTU); U47415, AY266236, AY562948.	Flower	Dr. Mario Vallejo-Marin (School of Biological and Environmental Sciences, University of Stirling, UK).
		Herbarium	BM 000849450
S. acanthodapis	Australia, Bohs 3575, NIJ A74750019*	Flower	NIJA74750019
S. accrescens	Costa Rica, Bohs 2556 (UT); AF500795, DQ180473, AY996375.	-	-
S. adhaerens	Costa Rica, Bohs 2473 (UT); AF224061, DQ180474, AY996377.	-	-
S. adscendens	Bolivia, Bohs & Nee 2738 (UT); AF500796, DQ180421, DQ169013.	Flower	Dr. Mario Vallejo-Marin (School of Biological and Environmental Sciences, University of Stirling, UK).
S. aethiopicum	BIRM S.0344, Olmstead S-74 (WTU); AF500797, DQ180394, AY996378.	Seed	NIJ804750136
		Flower	Dr. Mario Vallejo-Marin (School of Biological and Environmental Sciences, University of Stirling, UK).
		Seed	Sandy Knapp (Natural History Museum, London, UK)
S. aggregatum	South Africa, Olmstead 99-25 (WTU); AF500798, DQ180460, DQ169014.	Herbarium	CGE J Lindley
S. aligerum	Bolivia, Nee et al. 51822 (NY); AF500799, DQ180441, DQ169015.	Herbarium	BM 00578971

S. allophyllum	Panama, Bohs 2339 (UT); U47416, DQ180422, AY996379.	Herbarium	BM 000600995
		Seed	NIJ904750241
S. amotapense	Peru, J.G Hawkes 2422, NIJ 904750175*	Flower	NIJ904750175
S. amygdalifolium	Argentina, Nee & Bohs 50840 (NY); AF500800, DQ180442, DQ169016.	Herbarium	CGE Buenos Aires, Fox.
S. aphyodendron	Colombia, Olmstead S-92 (WTU); AF500801, DQ180423, DQ169017.	Herbarium	BM 000579035
S. appendiculatum	Mexico, Anderson 1401 (CONN); AF224062, DQ180461, DQ169018.	Seed	Sandy Knapp (Natural History Museum, London, UK)
S. arboreum	Costa Rica, Bohs 2521 (UT); U47417, DQ180424, AY996381.	Herbarium	BM 000579086
S. argentinum	Argentina, Bohs 2539 (UT); U72752, DQ180425, AY996382.	Herbarium	BM 000849194
		Flower	Dr. Mario Vallejo-Marin (School of Biological and Environmental Sciences, University of Stirling, UK).
S. atropurpureum	Nijmegen 80475010; trnT-F: AY559237, waxy: AY562951	Flower	NIJ924750039
S. aviculare	BIRM S.0809, no voucher; U47418, AY562952, AY559238.	Flower	Dr. Mario Vallejo-Marin (School of Biological and Environmental Sciences, University of Stirling, UK).
S. berthaultii	waxy** Bolivia, J.G. Hawkes 6451, PI498096, Bolivia, J.G. Hawkes 6552, PI498105, Bolivia, HAO 76, PI545851, Bolivia, HAO 58, PI545922, Argentina, HOF 1714 PI566799; HM561735.1, HM561734.1, M561731.1, AY875437.1, AY875438.1, HM561733.1, AY875436.1, HM561732.1	Flower	John Innes, Norwich
S. betaceum	Bolivia, Bohs 2468 (UT); U47428, DQ180426, AY996387.	Herbarium	CGE Caudler
		Herbarium	CGE J Lindley
		Seed	NIJ884750016
S. brevicaule	Bolivia, Hawkes et al. 6701 (PTIS); AF500803, DQ180443, DQ169019.	-	-
S. brevifolium	Ecuador, Bohs 3117, NIJ A44750268; (ndhF: trnT-F, waxy)*	Flower	NIJA44750268
S. bukasovii	waxy: Peru, HJT 1337 PI210042, HM561736.1	-	-
S. bulbocastanum	Mexico, Tarn 153 (PTIS); AF500804, DQ180444, DQ169020.	Herbarium	BM 000579124
S. caesium	Bolivia, Bohs et al. 2815 (UT); AF500805, DQ180445, DQ169021.	Seed	Sandy Knapp (Natural History Museum, London, UK)
S. calilegua	Argentina, Nee & Bohs 50809 (NY); AF500806, EF068252, DQ169022.	-	-
S. campanulatum	BIRM S.0387, Olmstead S-78 (WTU); AF500807, DQ180395, AY996388.	-	-
S. campechiense	Costa Rica, Bohs 2536 (UT); AF224071, DQ180475, AY996389.	Herbarium	BM 000579138
S. candidum	ndhF: BIRM S.0975, Olmstead S-100 (WTU), trnT-F, waxy: Costa Rica, Bohs 2898 (UT); AF224072, AY266237, AY562953.	Herbarium	BM 000848481
		Flower	Dr. Mario Vallejo-Marin (School of Biological and Environmental Sciences, University of Stirling, UK).
S. capsicoides	Peru, Bohs 2451 (UT); AF500808, AY266251, AY562954.	Seed	NIJ974750082
S. carolinense	BIRM S.1816, Olmstead S-77 (WTU); AF500811, DQ180476, AY996392.	Herbarium	CGE Engelmann
		Seed	NIJ894750095
S. chenopodinum	BIRM S.0813, no voucher; AF500812, DQ180396, AY996393.	Herbarium	BM 000900482
S. cinereum	NIJ 904750120, Bohs 2852 (UT); AF500813, DQ180397, AY996394.		

S. citrullifolium	BIRM S.0127, Olmstead S-79 (WTU); AF500814, DQ180477, AY996395.	Herbarium	BM 000942787
		Seed	NIJ894750197
S. clandestinum	Bolivia, Nee et al. 51781 (NY); DQ392957, DQ180462, DQ169023.	-	-
S. cleistogamum	BIRM S.0844, Olmstead S-80 (WTU); AF500815, DQ180478, AY996397.	-	-
S. comptum	Paraguay, C.V. Morton, Bohs 3193 (UT); trnT-F: GU591009, waxy: AY996399	Flower	NIJA44750263
S. conditum	Bolivia, Bohs & Nee 2733 (NY); AF500816, DQ180479, AY996400.	-	-
S. cordovense	Costa Rica, Bohs 2693 (UT); U72751, DQ180480, AY996401.	Herbarium	BM 000596710
S. coriaceum	French Guiana, RE 1724, NIJ A44750296*	Flower	NIJA44750296
S. corifolium	Bohs 3520 UT; trnT-F: GQ163496; waxy: GQ163644	Flower	NIJA74750008
S. corumbense	Bolivia, Bohs 2739, NIJ994750103*	Flower	NIJ994750103
S. crinitipes	Colombia, Olmstead S-81 (WTU); AF500817, DQ180481, AY996402.	-	-
S. crinitum	NIJ 924750049, Bohs 2850 (UT); AF500818, DQ180482, AY996403.	Herbarium	CGE Brazil, Gardner 2267
S. crispum	BIRM S.0486, no voucher; AF500819, DQ180446, DQ169024.	Herbarium	CGE Lechler
		Seed	NIJ894750342
S. deflexum	Costa Rica, Bohs 2715 (UT); AF500820, DQ180427, DQ169025.	Herbarium	BM 000579556
S. delitescens	Argentina, Nee & Bohs 50810 (NY); AF500821, DQ180428, DQ169026.	Herbarium	BM 000935849
S. diploconos	Brazil, Bohs 2335 (UT); AY049014, DQ180429, AY996407.	-	-
S. ditrichum	Bohs 3568 UT; trnT-F: GQ163504.1; waxy: GQ163652.1	-	-
S. drymophilum	Puerto Rico, Bohs 2461 (UT); AF500823, DQ180483, AY996409.	-	-
		Seed	B & T World Seeds, France. 5036
S. dulcamara	USA, no voucher; U47419, AY266231, AY996410.	Herbarium	CGE [collector unknown]
S. dulcamaroides	trnT-F, waxy; LB712, LB2548	Flower	NIJA44750177
S. echinatum	ndhF, trnT-F: NIJ 954750052, Bohs 2727 (UT), waxy: Australia, Symon 17102 (AD); AF500824, DQ180398, AY996411.	-	-
S. elaeagnifolium	ndhF: USA, Olmstead S-82 (WTU), trnT-F: Paraguay, Bohs 3204 (UT), waxy: Paraguay, Bohs 3199 (UT); AF224067, DQ180399, AY996412.	Seed	NIJA24750020
S. ellipticum	Australia, Bohs & Bean 3540, Nijmegen A74750004*	Flower	NIJA74750004
S. esuriale	Bohs 3259 UT; trnT-F: GQ163508.1, waxy: GQ163655.1	Flower	NIJA24750038
S. etuberosum	Chile, PI 498311, Contreras 1322 (UAC); AF500825, DQ180463, DQ169027.	Herbarium	CGE J. G Hawkes
S. evolvulifolium	Panama, Knapp & Mallet 9178 (BM); AF500826, DQ180464, DQ169028.	Herbarium	BM 000579337
S. ferocissimum	BIRM S.0819, Olmstead S-83 (WTU); AF500827, DQ180400, AY996415.	Herbarium	BRI AQ618425
S. fiebrigii	Bolivia, Bohs et al. 2784 (UT); AF500828, DQ180447, DQ169029.	Seed	NIJ904750200
		Seed	Sandy Knapp (Natural History Museum, London, UK)
S. fraxinifolium	Costa Rica, Bohs 2558 (UT); AF500810, DQ180465, AY996416.	Seed	NIJ904750201
S. furfuraceum	BIRM S.1442, Olmstead S-84 (WTU); AF500829, DQ180401, AY996417.	Flower	Dr. Mario Vallejo-Marin (School of Biological and Environmental Sciences, University of Stirling, UK).
S. glaucophyllum	D'Arcy collection, no voucher; U72753, DQ180430, AY996418.	Herbarium	BM 000846520
		Seed	NIJ924750136

		Seed	Botanic Garden and Botanical Museum Berlin-Dahlem (Freie Universität, Berlin), 2406.
S. habrochaites	waxy: Peru, LA 1353, LA 1928, LA 1223; AY875632.1, AY875633.1, AY875631.1	Flower	NIJ894750234
S. havanense	NIJ 904750122, Bohs 3076 (UT); AF500830, DQ180431, DQ169030.	Herbarium	BM 000849137
		Seed	NIJ904750122
S. herculeum	Morocco, Jury 13742 (RNG); AF224065, DQ180466, DQ169031.	-	-
S. hindsianum	Mexico, Bohs 2975 (UT); AF500831, DQ180402, AY996424.	Herbarium	BM 000579380
		Flower	Rancho Santa Ana Botanic Garden (1500 N College Ave, Claremont, California CA 91711, USA).
S. hoehnei	Brazil, Folli 1668 (MO); AF500832, DQ180484, AY996426.	Herbarium	BM 000929921
S. inaequilaterum	Bohs 3576 UT; trnT-F: GQ163521.1, waxy: GQ163666.1	Flower	NIJA74750020
S. inelegans	Bolivia, Nee et al. 51813 (NY); AF500833, DQ180432, DQ169032.	Herbarium	BM 000846221
S. ipomoeoides	Bolivia, Bohs & Nee 2766 (UT); AF500834, DQ180448, DQ169033.	-	-
S. jamaicense	BIRM S.1209, Olmstead S-85 (WTU); AF224073, DQ180485, AY562956.	Herbarium	BM 000579430
		Herbarium	CGE [collector unknown]
		Seed	NIJ904750159
S. juglandifolium	Colombia, Rick et al. 7546 (PTIS); AF500837, DQ180449, DQ169034.	Herbarium	BM 000778149
S. laciniatum	New Zealand, Bohs 2528 (UT); U47420, DQ180467, AY996431.	Herbarium	CGE C. M. Lemann
		Seed	NIJ834750003
S. laxum	trnT-F, waxy: Bohs LB1152, LB1182	-	-
S. lepidotum	Costa Rica, Bohs 2621 (UT); AF500838, DQ180486, DQ169035.	Herbarium	BM 000072713
S. lidii	NIJ 934750022, Bohs 2903 (UT); AF500839, DQ180403, AY996434.	Seed	www.rareplants.de (Am Parkfeld 14 E, D-65203 Wiesbaden, Germany).
S. limitare	Australia, Bohs & Bean 3526, NIJA74750002*	Flower	NIJA74750002
S. luteoalbum	BIRM S.0042, Bohs 2337 (UT); U72749, DQ180433, AY562957.	Herbarium	BM 000887708
S. lycopersicum	USA (cultivated), no voucher; U08921, DQ180450, DQ169036.	Seed	Cambridge Botanic Gardens
S. macrocarpon	BIRM S.0133, Olmstead S-88 (WTU); AF224068, DQ180404, AY996436.	-	-
S. mahoriensis	Madagascar, Bohs 2576 (UT); AF500841, DQ180405, AY996437.	-	-
S. mammosum	BIRM S.0983, Olmstead S-89 (WTU); AF224074, AY266232, AY562958.	Flower	Nijmegen, number unknown
S. mapiriense	Bolivia, Nee & Solomon 30305 (UT); AF500842, DQ180434, AY996439.	-	-
S. maternum	waxy: Bohs LB45	Flower	NIJ974750136
S. mauritianum	BIRM S.0860, Olmstead S-90 (WTU); AF500843, DQ180487, DQ169037.	Seed	NIJ804750172
S. melongena	BIRM S.0657, Olmstead S-91 (WTU); AF224069, DQ180406, AY562959.	Seed	Nicky's Mail Order Seeds, UK. Aubergine 'Baby Belle', NIC/ML13104V
S. mitlense	trnT-F, waxy: Bohs LB929	-	-
S. montanum	NIJ 904750205, Bohs 2870 (UT); AF500844,DQ180468, AY996443.	Herbarium	CGE Peru, Mathews, 846
		Seed	NIJ904750205
S. muricatum	Colombia, Olmstead S-93 (WTU); AF500846, DQ180469, DQ169038.		

S. nemophilum	Bohs 3535 UT; ndhF: GQ163540.1, waxy: GQ163681.1	Flower	NIJA74750017
S. nemorense	Bolivia, Bohs & Nee 2757 (UT); AF500847, DQ180488, AY996447.		
S. nigrum	ndhF, waxy: Bohs LB141	Herbarium	CGE [collector unknown]
S. nitidum	Bolivia, Nee 31944 (NY); AF224075, DQ180451, DQ169039.	Herbarium	BM 000887805
		Seed	Chileflora (Hijuela #2, Lihueno, Pelarco, Talca, Chile).
S. ochranthum	waxy: Peru, LA2682,LA 3650; AY875566.1,AY875567.1	Flower	NIJA74750054
S. ochrophyllum	Bolivia, Bohs & Nee 2805 (UT); AF500848, DQ180435, DQ169040.		
S. oligacanthum	Bohs 3256 UT; trnT-F: GQ163546.1, waxy: GQ163686.1	Flower	NIJA24750041
S. palitans	BIRM S.0837, 70, Bohs 2449 (UT); AF224064, DQ180452, AY996449.	Seed	NIJ904750206
S. pennellii	nhdf: M.Dillon 8779A, FJ914030.1; trnT-F: Chile, 0045Chi, AB515389.1, AB515391.1, AB515409.1, AB515411.1, AB515388.1, AB515390.1, AB515408.1, AB515410.1; waxy: LA716 AY875411.1, AY875634.1, LA1376 AY875635.1, LA1926 AY875636.1	Flower	NIJ894750192
S. peruvianum	waxy: LA2964, LA3156, LA1331, LA1379, LA1973, LA1305, LA107, LA1283, LA444, LA2328, LA378, LA2548, LA1609, LA1351, LA2157, LA2172, LA1910, LA1305p, LA1913, LA448, LA1626, LA1984, LA1396, LA2152, LA441, LA392, LA2744, 0046Chi; AY875626.1, AY875624.1, AY875620.1, AY875616.1, AY875612.1, AY875610.1, AY875608.1, AY875606.1, AY875604.1, AY875602.1, AY875600.1, AY875598.1, AY875596.1, AY875594.1, AY875592.1, AY875590.1, AY875611.1, AY875609.1, AY875607.1, AY875605.1, AY875603.1, AY875601.1, AY875599.1, AY875597.1, AY875595.1, AY875593.1, AY875413.1, AB515430.1	Flower	NIJ894750235
S. physalifolium	USA, Bohs 2467 (UT); U47421, EF068253, DQ169041.	Herbarium	Herbarium of Utah 48437
		Herbarium	MELU (no number)
		Flower	Dr. Mario Vallejo-Marin (School of Biological and Environmental Sciences, University of Stirling, UK).
		Seed	Sandy Knapp (Natural History Museum, London, UK)
S. pinnatisectum	Mexico, Tarn 205A (PTIS); AF500850, DQ180453, DQ169042.	Herbarium	BM 000543887
S. prinophyllum	NIJ 904750171, Bohs 2725 (UT); AF500852, DQ180407, AY996456.	Herbarium	MELU 17740
		Flower	Dr. Mario Vallejo-Marin (School of Biological and Environmental Sciences, University of Stirling, UK).
S. pseudocapsicum	BIRM S.0870, no voucher; U47422, DQ180436, AY562963.	Flower	Dr. Mario Vallejo-Marin (School of Biological and Environmental Sciences, University of Stirling, UK).
S. ptychanthum	USA, Olmstead S-94 (WTU); U47423, DQ180454, AY996457.		
S. pubigerum	NIJ 904750104, no voucher; AF500853, DQ180455, DQ169043.	Herbarium	BM 000848306
		Seed	NIJ814750041
S. pyracanthos	USA (cultivated), Olmstead S-95 (WTU); AF500854, DQ180408, AY996459.	Seed	NIJ804750195

S. quitoense	trnT-F: Ecuador, Heiser s.n., LN996, AY266243; waxy: Costa Rica, Bohs 2873 UT, AY562965.1	Flower	NIJ924750016
S. riojense	Argentina, Nee & Bohs 50843 (NY); AF500856, DQ180456, DQ169044.	Seed	Sandy Knapp (Natural History Museum, London, UK)
S. rostratum	USA, no voucher; U47424, DQ180489, AY996463.	Flower	Dr. Mario Vallejo-Marin (School of Biological and Environmental Sciences, University of Stirling, UK).
S. rovirosanum	Costa Rica, Bohs 2919 (UT); AF500857, DQ180437, DQ169045.	Herbarium	BM 000894031
S. rugosum	Costa Rica, Bohs 3011 (UT); AF500858, DQ180490, DQ169046.	Herbarium	BM 000579852
		Seed	NIJ944750197
S. sandwicense	Hawaii, Bohs 2992 (UT); AF500859, DQ180409, AY996464.		
S. schimperianum	BIRM S.1538, Olmstead S-97 (WTU); AF500860, DQ180410, AY996465.	Herbarium	BM 000942693
S. schlechtendalianum	Costa Rica, Bohs 2915 (UT); AF500861, DQ180491, DQ169047.	Herbarium	BM 000579863
S. seaforthianum	BIRM S.0051, no voucher; U47425, DQ180438, DQ169048.	Herbarium	BM 000849300
		Herbarium	CGE [collector unknown]
		Seed	NIJ914750023
		Seed	Botanic Garden and Botanical Museum Berlin-Dahlem (Freie Universität, Berlin).
S. semiarmatum	Bohs 3560 UT; trnT-F: GQ163559, waxy: GQ163696.1		
S. shirleyanum	Australia; Bohs 3577; NIJA74750024*	Flower	NIJA74750024
S. sisymbriifolium	Argentina, Bohs 2533 (UT); AF500862, AY266235, AY562967.	Seed	Cambridge Botanic Gardens
		Herbarium	CGE [collector unknown]
S. stramonifolium	Peru, Whalen 860 (HUT); AF500863, AY266263, AY562970.		
S. tetrathecum	trnT-F: Bohs 3550 UT, ASP057, ASP033, GQ163566.1, DQ855052.1, DQ855051.1, waxy: Bohs 3550 UT; GQ163702.1	Flower	NIJA74750011
S. thelopodium	Bolivia, Nee & Bohs 50858 (NY); AF500865, DQ180470, AY996471.		
S. toliaraea	Madagascar, Bohs 2574 (UT); AF500866, DQ180411, AY996472.		
S. torvum	BIRM S.0839, Olmstead S-101 (WTU); L76286, AY266246, AY562972.	Herbarium	BM 000579928
		Herbarium	CGE A.T Gage 5
		Herbarium	CGE Jamaica, Mafsen 5106
		Seed	NIJ814750073
S. tridynamum	BIRM S.1831, Olmstead S-102 (WTU); AF500867, DQ180412, AY996474.		
S. triflorum	USA, Bohs 3062 (UT); AF500868, DQ180457, DQ169049.	Herbarium	CGE US, Kansas, K.K. Mackenzie
		Seed	NIJ924750074
S. tripartitum	BIRM S.0708, 71, Bohs 2465 (UT); U72750, DQ180458, DQ169050.	Herbarium	CGE CB 2/114
		Seed	NIJ884750218
S. trisectum	France, Bohs 2718 (UT); AF224063, DQ180471, AY996475.	Herbarium	CGE [collector unknown]
S. turneroides	Bolivia, Nee et al. 51716 (NY); AF500869, DQ180439, DQ169051.	-	-
S. uleanum	D'Arcy collection, Bohs 2720 (UT); AF500870, DQ180472, DQ169052.	-	-
	BIRM S.2091, Olmstead S-103 (WTU); AF224070, DQ180413, AY996476.	Herbarium	CGE [collector unknown]

S. vespertilio		Seed	www.rareplants.de (Am Parkfeld 14 E, D-65203 Wiesbaden, Germany).
		Seed	www.rareplants.de (Am Parkfeld 14 E, D-65203 Wiesbaden, Germany).
S. villosum	Iran, Bohs 2553 (UT); AF224066, DQ180459, DQ169053.	Herbarium	CGE [collector unknown]
S. violaceum	Bohs 3277 (UT), Bohs 3093 UT, Bloomfield sn (BM), Knapp 10110 (BM); trnT-F: HQ721955.1, EU176159.1, HQ721957.1, HQ721956.1, waxy: HQ722017.1, HQ722018.1, HQ722016.1, AY996478.1	Flower	NIJ814750077
S. wendlandii	BIRM S.0488, no voucher; U47427, DQ180440, AY562974.	Herbarium	BM (no number)
Withania somnifera	ndhF: Canary Is., (no voucher) in cult. at U. Connecticut Greenhouse (#199200148), EU580952; T. Tu 0650 (KUN) FJ914033.1; trnT-F: Canary Is., (no voucher) in cult. at U. Connecticut Greenhouse (#199200148), EU581069.1	Seed	NIJ894750106
Witheringia solanacea	ndhF: Costa Rica; Bohs 2416 UT, WSU72755; trnT-F: LB 790; waxy: Bohs 2427 UT, D'Arcy 16399 MO., AY665926.1 , DQ309474.1	Seed	NIJ814750082

Voucher list for species in *Solanum* phylogeny, including sources of morphological data. Numbers beginning NIJ indicate Nijmegen accession numbers.

* Species for which ndhF, trnT-F and waxy were isolated and sequenced by this lab and have not yet been assigned GenBank numbers